2004

Avalanche photodiodes arrays

Daniel Ma

Avalanche Photodiodes Arrays

By

Daniel Ma

B.S. College of Engineering, Rochester Institute of Technology (1998)

A thesis submitted in partial fulfillment of the
requirements for the degree of Master of Science
in the Chester F. Carlson Center for Imaging
Science of the College of Science
Rochester Institute of Technology

August 2004

Signature of the Author Daniel Ma

Accepted by Harvey E. Rhody 4/1/2005

Coordinator, M.S. Degree Program Date

CHESTER F. CARLSON
CENTER FOR IMAGING SCIENCE
COLLEGE OF SCIENCE
ROCHESTER INSTITUTE OF TECHNOLOGY
ROCHESTER, NEW YORK

CERTIFICATE OF APPROVAL

M.S. DEGREE THESIS

The M.S. Degree Thesis of Daniel Ma has been examined and approved by the thesis committee as satisfactory for the thesis requirement for the Master of Science degree

Zoran Ninkov

Dr. Zoran Ninkov, Thesis Advisor

Lynn Fuller

Dr. Lynn Fuller

Jonathan S. Arney

Dr. Jon Arney

4/1/2005

Date

THESIS RELEASE PERMISSION

ROCHESTER INSTITUTE OF TECHNOLOGY
COLLEGE OF SCIENCE
CHESTER F. CARLSON
CENTER FOR IMAGING SCIENCE

Title of Thesis: Avalanche Photodiode Arrays

I, Daniel Ma, hereby grant permission to the Wallace Memorial Library of R.I.T. to reproduce my thesis in whole or in part. Any reproduction will not be for commercial use or profit.

Avalanche Photodiode Arrays

By

Daniel Ma

Submitted to the Chester F. Carlson Center for Imaging Science College of Science in partial fulfillment of the requirements for the Master of Science Degree at the Rochester Institute of Technology

Abstract

This research investigates the performance of avalanche photodiode (APD) arrays that were designed, fabricated, and tested at Rochester Institute of Technology. The APD devices, based on the "reach-through" structure, were designed with various array sizes and dimensions in order to investigate the optimal design. An explanation of the operating principle and device theory is presented, along with the testing methods used in determining the performance of the APD arrays. The results and the reasons behind the performance of the devices are discussed. Suggestions and solutions to problems found are presented as a guide for any future research.

Table of Contents

Table of Figures

Table of Equations

1. Introduction

1.1. Scope of Work / Objectives

The primary objective of this research is to design, fabricate, and test avalanche photodiode (APD) arrays. The design is an array of planar reach-through APD structures on a single wafer. The performance of the photodiodes and photodiode arrays are investigated using figures of merit calculations. The feasibility of fabricating APD arrays in an academic lab environment is determined by comparing the performance of the devices in this research to other commercially available APDs. An analysis of improving the devices is discussed. The devices were designed and fabricated in Rochester Institute of Technology's Microelectronic Department using semiconductor processes.

1.2. APD History and Background

An avalanche photodiode (APD) is a solid-state photodetector that is typically fabricated using silicon (Si), germanium (Ge), or combinations of III-V materials from the periodic table such as gallium arsenide (GaAs), indium gallium arsenide (InGaAs), and InGaAs/InP. The device is commonly described as being similar to a p-n junction photodiode with a multiplication region.

Known as a device that has an own internal gain, caused by operating in high reverse bias and utilizing the avalanche mechanism within the semiconductor. The internal multiplication gives the PD a high signal to noise ratio, giving signal amplification without amplification of the noise.

Because of its sensitivity, APDs are used in low light level applications such astronomy, optical fiber communication, spectrometry, laser radar, or where photon counting and/or correlation information is needed [MacGregor, 1991]. Also, because an APD's gain is a function of the reverse bias voltage, it can be gain modulated by adjusting the reverse bias voltage.

The first publication of avalanche photodiodes was in 1966 by R. J. McIntyre, using silicon as the device material [McIntyre, 1966]. Research into using other materials, such as Ge, GaAs, InGaAs, and InGaAs/InP has been performed since. Different structures such as the planar reach-through and the MESA structure have been studied. Other areas of research include improving performance and uniformity of APDs. Since APDs have been popular due to their small size and high sensitivity, APDs of different varieties are also commercially available.

Although avalanche photodetectors (APD) have existed for many years, arrays of APD on a single chip are not widely commercially available. Arrays of APD present unique problems, such as preventing cross-talk between pixels and controlling the uniformity of the device. The applications for APD arrays are similar to single APDs such as astronomy, optical fiber communication, etc. Its usage can be comparable to CCD arrays, but with a higher sensitivity due to using APD technology as its photosensing mechanism.

One interesting application in using APD arrays versus a single APD is for the reception of optical communications from space. Signals suffer degradation of the optical phase front due to atmospheric turbulence, leading to random fluctuations of the point-spread function in the focal plane. To simply have a larger detector area to collect the entire signal would also increase background radiation noise, decreasing the noise to signal ratio. An optical detector array would

be able to adaptively select areas of higher signal while ignoring areas with high background noises [McIntyre, 1966].

1.2.1 Advantages of APDs Compared to Other Detectors

Compared to similar devices such as PIN photodiodes and photomultiplier tubes (PMT), APDs are more sensitive, robust, and compact. APDs are a derivative of PIN diodes and are similar in structure. PIN diodes have an intrinsic region sandwiched between a heavily doped p+ and n+ layers, creating a depletion region where electron-hole pairs are generated from incident photons:

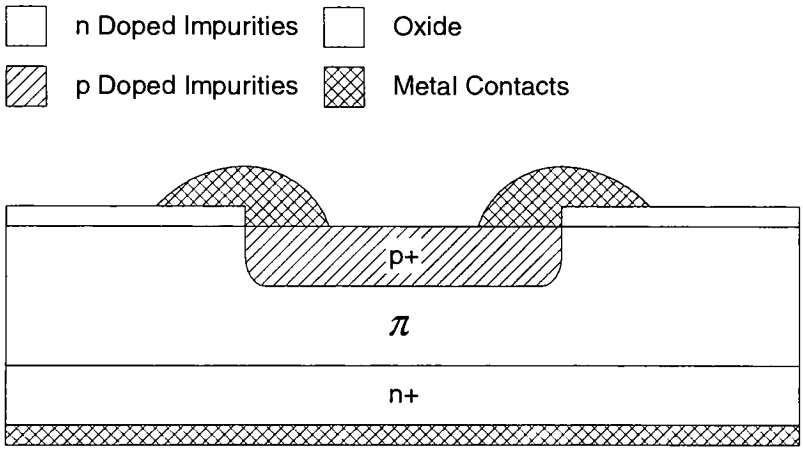

Figure 1.2.1: Cross-Section of a PIN Photodiode

The advantages of PINs over most photodetectors are that they are highly customizable in terms of spectral response and have a greatly enhanced frequency response. Because photons are absorbed in the intrinsic region (π-region) of the PIN, the peak wavelength response can be tailored by changing the thickness of the π-region. This is done by making the π-layer thickness equal to the inverse of the absorption coefficient ($1/\alpha$) for the desired wavelength. PINs have a

higher frequency response also due to the π-region. The high electric field within the depleted π-region leads to rapid collection of the photogenerated carriers [Pierret, 1996]

The major difference between PIN diodes and APDs are that APDs have an additional avalanching multiplication region. Consequently, PIN diodes are not as sensitive.

There are other devices that are as sensitive to photon detection as APDs. Photomultiplier tubes (PMT) are very sensitive and have a fast response, but the quantum efficiency drops significantly at wavelengths longer than 400nm [MacGregor, 1991]. Also, PMTs are susceptible to moisture, have a high dark current, and delicate, making it unsuitable for portability [Proudfoot, 1997]. In addition, trying to collect spatial information by having an array of PMTs is simply not possible or feasible due to its bulk size. A Multi-Anode Microchannel Array (MAMA) detector is possibly the closest equivalent to APD arrays, where MAMA detectors have the high sensitivity and can collect spatial information. Unfortunately their physical size and operation, where a photocathode, microchannel plate, anode array, and supporting electronics are needed, is still too delicate for portability.

Silicon APDs have useable quantum efficiency between wavelengths from around 200nm to 1100nm and hence, are sensitive between those wavelengths. Other materials have been investigated, especially III-V compounds such as GaAs, InGaAs, Ge, etc. which have better quantum efficiencies at higher wavelengths. Although III-IV compounds can have a higher sensitivity beyond 1100nm up to 1300nm, the advantage of silicon APDs is that it has a much lower noise due to having only one carrier, namely electrons, which initiate the avalanche process. The electron/hole ionization rate (α/β) of silicon is around 50, compared to α/β ratios of near unity for other III-IV compounds [Ridley, 1985].

1.3. Thesis Background

The original scope of work was to design and fabricate APD arrays along with onboard discriminator circuits. The array would be read in by a computer via a multi-channel I/O card, with the intended application is to have this device somewhat portable for in-the-field use. The devices were to be designed and fabricated at Rochester Institute of Technology's Microelectronic Department.

In order to achieve that final goal, several successful steps were needed: have working individual APDs, working APD arrays, working discriminator circuits onboard, and a practical interface to the computer.

Because avalanche photodiodes have never been fabricated at the Microelectronic Department, knowledge of the design and fabrication needed to be gained. In doing so, successful individual APDs, especially with uniform characteristics, were difficult to fabricate. The result is that only a handful of arrays (array sizes of only four pixels) were able to exhibit successfully working characteristics.

This thesis will discuss the theory and design of the avalanche photodiode, fabrication process, and test results. It will also discuss the problems of the devices and provide an analysis of improving the design and fabrication.

2. Device Theory and Design

APDs are solid-state devices that are fabricated using silicon (Si), germanium (Ge), and combinations of III-V materials from the periodic table such as gallium arsenide (GaAs), indium gallium arsenide (InGaAs), and InGaAs/InP.

APDs are essentially a p-n junction photodiode with a multiplication region. Common to most optoelectronic devices, there is a lightly doped layer that serves as a photo absorption region. What is unique to the avalanche photodiode is an extra multiplication region, giving the device its internal signal gain.

III-V compounds are sensitive up to wavelengths approximately 1600nm versus about 1100nm for silicon. But silicon APDs are much less noisy due to the high electron-hole ionization rate of about 50 versus close to unity for the other materials. This mechanism is important for the device operation and will be described in detail later. Also, another reason silicon technology is used is because it is much more widely used and therefore has more advanced fabrication techniques, which leads to better uniformity and control that is critical to device performance.

2.1. Device Structure and Operating Principles

The standard design of an avalanche photodiode consists of an intrinsically doped region for photo-absorption, a multiplication region that has a high electric field presence, and a guard ring

to minimize edge breakdown voltage problems. Here is a cross-sectional diagram of the standard design, and it's known as the planar reach-through structure:

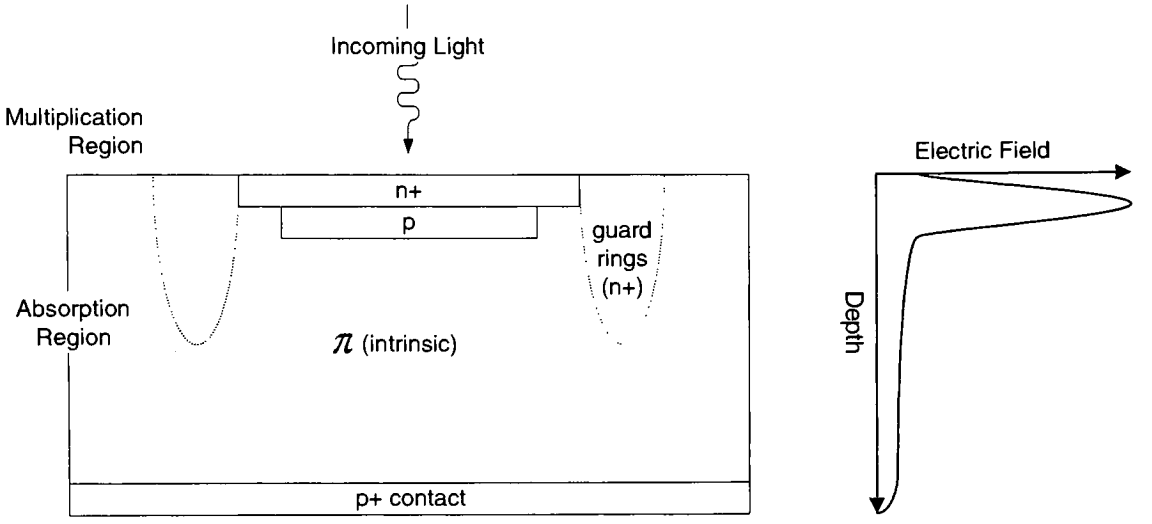

Figure 2.1.1: Cross-Section of a Reach-Through Avalanche Photodiode and Corresponding Electric Field Strength

The pixel shape of an APD is round, to achieve a uniform edge junction and preventing current crowding. That can lead to early voltage breakdown.

2.1.1 Depletion Region Concept

Because the planar reach-through APD structure consists of several layers of elements, combined with the criticalness of the APD of needing a high internal electric field for carrier multiplication, the doping of the device along with the concept of the depletion region is critical.

Avalanche multiplication of the carriers happens that the point of the highest electric field within the device. Ideally, this should occur in the designed multiplication area, around the top p-n junction area. As a review, the following is the conceptual idea of how the electric field is affected by the charge density and doping profile:

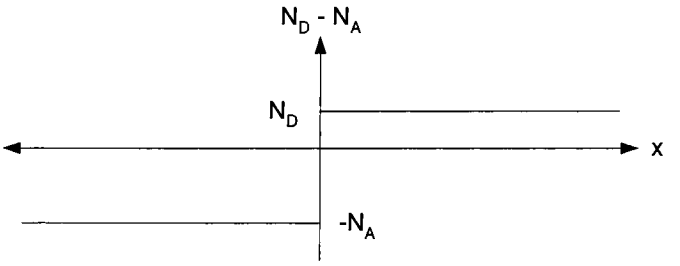

Figure 2.1.2: Doping Profile of a P-N Step Junction

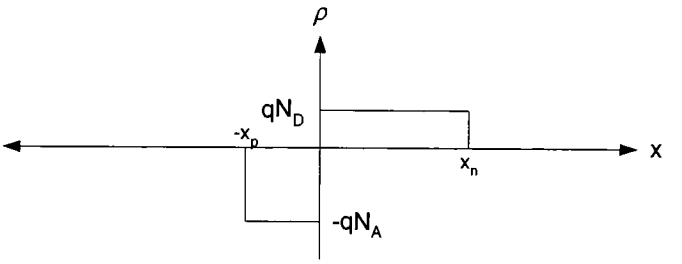

Figure 2.1.3: Charge Density Profile of a P-N Step Junction

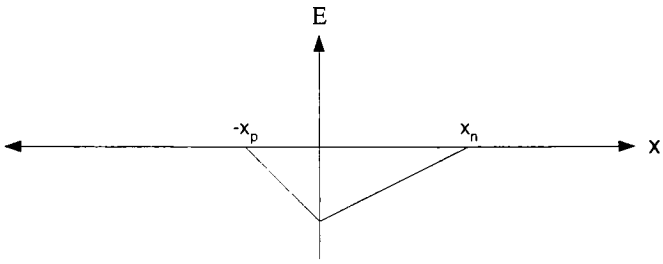

Figure 2.1.4: Electric Field Profile of a P-N Step Junction

For the purpose of the review, a step junction approximation is used for simplicity.

The following are equations that help form the above graphs. The charge density equation is given by:

$$\rho = \begin{cases} -qN_A & \ldots \quad -x_p \le x \le 0 \\ qN_D & \ldots \quad 0 \le x \le x_n \\ 0 & \ldots \quad x \le -x_p \text{ and } x \ge x_n \end{cases}$$

Equation 2.1: Charge Density Equation [Pierret, 1996]

Where q is the electron charge, N_A and N_D are the acceptor and donor doping concentration, respectively. x_n and x_p are the n-side and p-side width of the depletion region, respectively.

The electric field is given by:

$$E(x) = \begin{cases} -\frac{qN_A}{K_S \varepsilon_0}(x_p + x) & \ldots \quad -x_p \le x \le 0 \\ -\frac{qN_D}{K_S \varepsilon_0}(x_n + x) & \ldots \quad 0 \le x \le x_n \end{cases}$$

Equation 2.2: Electric Field Equation [Pierret, 1996]

Where K_S is the dielectric constant and ε_0 is the permittivity of free space. To determine x_p and x_n:

$$x_n = \left[\frac{2K_S \varepsilon_0 N_A}{qN_D (N_A + N_D)} V_{bi} \right]^{\frac{1}{2}}$$

$$x_p = \left[\frac{2K_S \varepsilon_0 N_D}{qN_A (N_A + N_D)} V_{bi} \right]^{\frac{1}{2}}$$

Equation 2.3: n-side / p-side Depletion Width [Pierret, 1996]

Where V_{bi} is the built-in potential, determined by:

$$V_{bi} = \frac{kT}{q} \ln\left(\frac{N_A N_D}{n_i^2} \right)$$

Equation 2.4: Built-in Potential Equation [Pierret, 1996]

Applying the above concept to the structure of the reach-through APD, the doping profile, charge density, and corresponding electric field is:

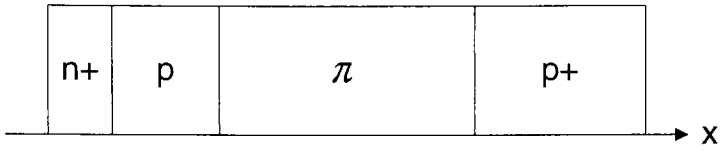

Figure 2.1.5: Layer Profile of a Reach-Through APD

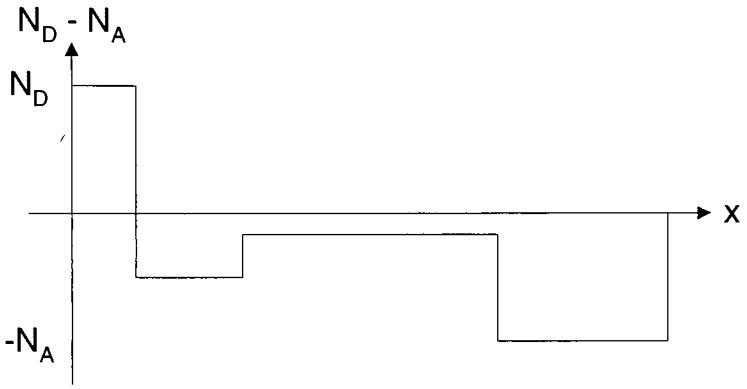

Figure 2.1.6: Doping Profile of a Reach-Through APD

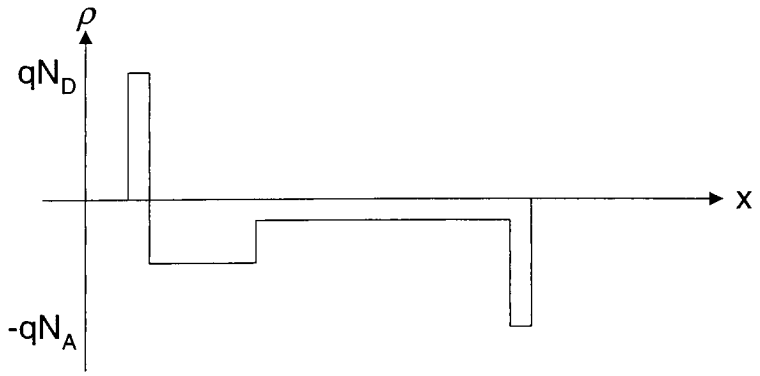

Figure 2.1.7: Charge Density Profile of a Reach-Through APD

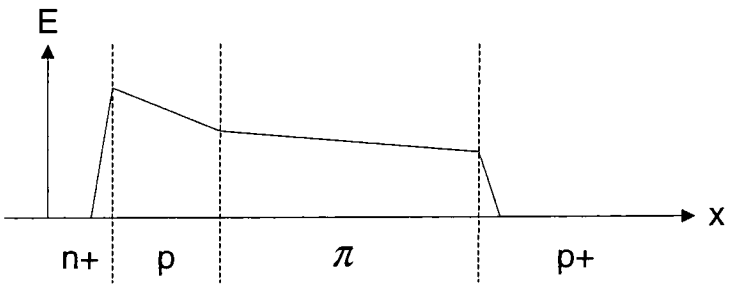

Figure 2.1.8: Electric Field Profile of a Reach-Through APD

Because of the unique shape of the electric field throughout the device, there are two regions of interest, the Absorption region, which is essentially the intrinsic (*i*) region of the device, and the Multiplication region, which is the p-n junction with the high electric field.

It is also pointed out here that, since it is desired to have the depletion region be extended into the intrinsic region and stop at the p+ layer, the middle p and i layers should be doped accordingly.

2.1.2 Absorption Region

As the name implies, the purpose of this region is to absorb the incoming photons. As photons are collected, electron-hole pairs are generated from the photon energy via photogeneration. Photogeneration is when electrons in the valence band are directly excited into the conduction band from the energy of the incoming photon [Pierret, 1996]. The mechanism of photogeneration is discussed in detail in Section 2.1.2.1. Once electron-hole pairs are generated, the mild electric field present in this region sweeps one carrier, either holes or electrons depending on device design, into the multiplication region.

Another characteristic of this region is in having a light doping to facilitate high carrier mobility. Since the goal of the absorption region is to collect photons and generate electron-hole pairs, recombination of carriers or collisions between the free carriers and the lattice is not desired. At the weak electric field that is present in the absorption region, any collisions with the lattice would not result in impact ionization and would in fact, impede the sensitivity of the device by the scattering of the carriers from the lattice vibration. Instead, this layer is to have a weak electric field sweep the carriers into the multiplication region, where the high electric field there would create the desired impact ionization.

The relationship between doping density and mobility is:

$$\mu = \mu_{min} + \frac{\mu_o}{1 + \left(\frac{N}{N_{ref}}\right)^{\alpha}}$$

Equation 2.5: Majority Carrier Mobility Equation [Pierret, 1996]

Where:

Parameter	*Values at 300°K*	
	Electron Carrier	**Hole Carrier**
N_{ref} [cm^{-3}]	$1.3 * 10^{17}$	$2.35 * 10^{17}$
μ_{min} [cm^3/V-sec]	92	54.3
μ_0 [cm^3/V-sec]	1268	406.9
α	0.91	0.88

[Pierret, 1996]

The graph is:

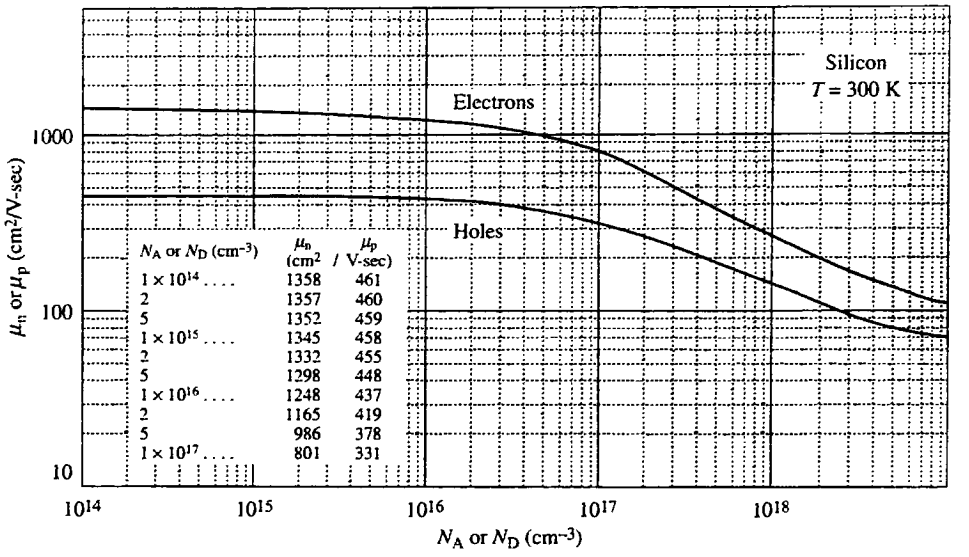

Figure 2.1.9: Carrier Mobilities as a Function of Dopant Concentration in Silicon [Pierret, 1996]

2.1.2.1 Photon Absorption / Electron-Hole Generation

When light is transmitted into semiconductor material, electron-hole pairs are generated if the incident photon energy is greater than the band gap energy. These generated electron-hole pairs in turn generate current. This is known as photogeneration and the current from this process is the photocurrent.

To understand how an absorbed photon generates electron-hole pairs, E-k plots (electron-energy band vs. electron crystal momentum) are used to visualize the process. There are two general categories of E-k plots in regards to semiconductor materials, direct semiconductor and indirect

semiconductor. The difference being that direct semiconductors have the minimum conduction band energy and the maximum valence band energy both at k=0, while indirect semiconductors have the conduction band minimum shifted off from k=0:

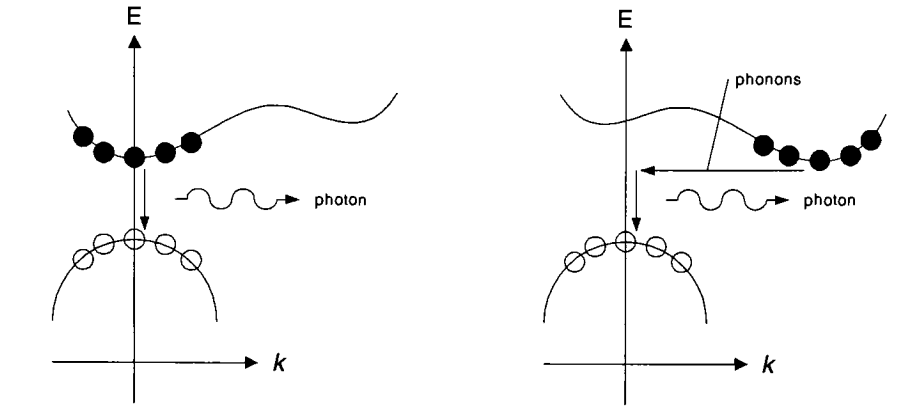

Direct Semiconductor Indirect Semiconductor

Figure 2.1.10: E-k Plots of Recombination of Direct and Indirect Semiconductor

Silicon is an indirect semiconductor. When a photon with certain energy (hv) is absorbed into the silicon, it is essentially a vertical transition of an electron on the E-k plot, since photons are massless entities and carry no momentum. In contrast, momentum generated from lattice vibrations, known as phonons, translate to a horizontal movement on the E-k plot [Pierret, 1996]. To generate an electron-hole pair from an incident photon, the photon need to have energy greater than the band gap energy and have some assistance from lattice vibrations in order to make the electron jump from valence to conduction band.

Because of the polarity of the electric field of the absorption region and the depletion region it creates, the photogenerated electron-hole pairs add a reverse current to the overall reverse

current generated from the avalanching mechanism. Hence, the reverse current increase when light is present.

To determine the current generated from the incident light, the photogeneration rate (G_L) needs to be determined first:

$$G_L = \frac{\alpha P_I}{A h\upsilon}$$

Equation 2.6: Photogeneration Rate [Pierret, 1996]

Where α is the absorption coefficient in [1/cm], P_I is the incident optical power in [W], A is the illuminated area in [cm^2], and $h\nu$ is the photon energy in [eV]. Photogeneration rate G_L is in [$cm^{3}*sec^{-1}$] units. The absorption coefficient is a function of wavelength and temperature and is different for each type of semiconductor:

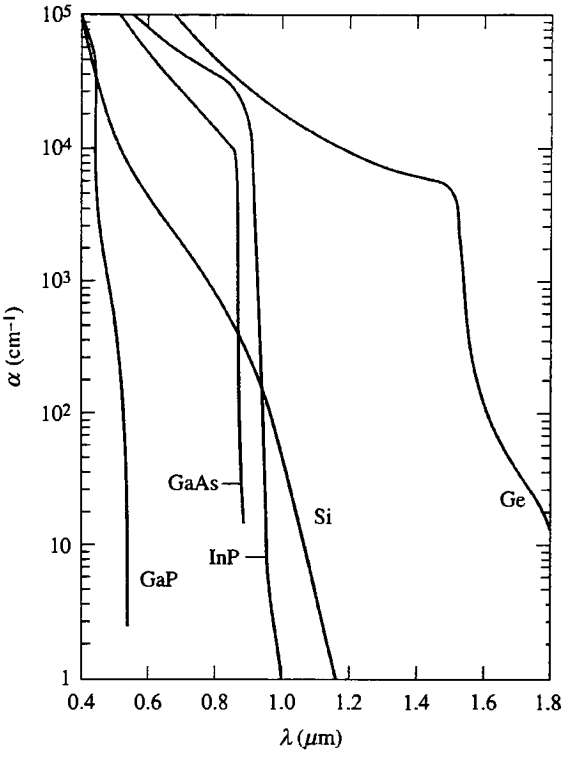

Figure 2.1.11: Absorption Coefficient as a Function of Wavelength at 300°K [Schroder, 1990]

Assuming a constant photogeneration rate throughout the semiconductor, the photocurrent due to incident light (I_L) is:

$$I_L = -qA\int_{x_1}^{x_2} G_L\, dx$$

Equation 2.7: Photocurrent Due to Incident Light

Where A is the illuminated area, x_1 and x_2 are the boundary locations of the thickness of the illuminated area.

The photocurrent generated from a semiconductor is also dependent on the wavelength, or spectral response. At the same incident optical power across all wavelengths, the photocurrent is expected to be:

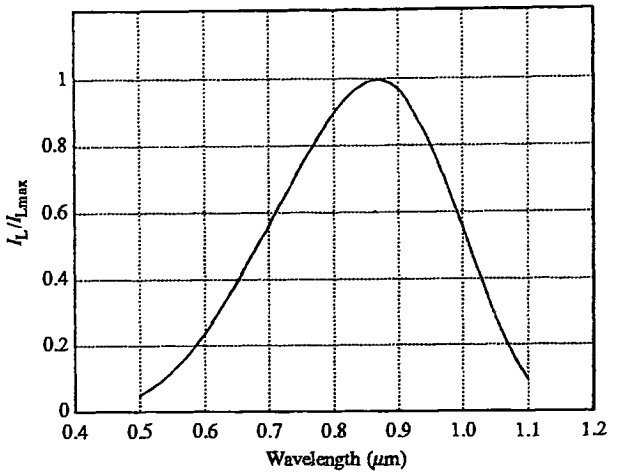

Figure 2.1.12: Spectral Response of Silicon P-N Junction Photodiode [Pierret, 1996]

The decrease in the longer wavelength region of the spectral response graph is due to the band gap of the silicon material. Since electron-hole pairs are generated only when the incident photons have more energy than the band gap, the upper wavelength limit essentially cuts off at:

$$\lambda_G = \frac{1.24}{E_G}$$

Equation 2.8: Wavelength Energy at Band Gap Energy

Where E_G is the energy band gap of the material. For silicon, the E_G is 1.12eV at 300°K and the effective wavelength limit is about 1.1μm.

The decrease of the spectral response at shorter wavelengths is due to two reasons. First, photon energy increases at shorter wavelengths. Since the incident optical power is held constant, the flux of the incident photon decreases as compared to longer wavelengths. Therefore, the decrease in spectral response is partially due to the decrease of the number of incident photons absorbed. Second, as shown in Figure 2.1.11, the absorption coefficient increases rapidly at shorter wavelengths. Taking the inverse of the absorption coefficient ($1/\alpha$), the light being absorbed in the material, on average, takes place increasingly closer to the surface at shorter wavelengths. Since the p-n junction is at a set depth into the material, the photogenerated carriers from the light absorption recombine before they can diffuse into the depletion region. It is noted that Figure 2.1.12 is a typical representation of spectral response; the peak can be tailored by changing the depth of the p-n junction in the device.

2.1.3 Multiplication Region / P-N Junction

The first two layers of the "front" side of an APD are the n+ and p layers. Together they form a p-n junction and its characteristics behave exactly as a classical p-n junction diode. In the case of the APD device, the p-n junction serves as the multiplication region. As photons are collected in the absorption region and electron-hole pairs are generated, the electron or hole carriers, depending on the device design, are swept into this multiplication region. The carriers are then multiplied via the avalanche mechanism, a condition created by applying a high reverse voltage bias on the p-n junction.

As a review, the doping profile, energy band, electrostatic potential, and electric field diagrams of a p-n junction under equilibrium, forward bias ($V_A>0$), and reverse bias ($V_A<0$) are [Pierret, 1996]:

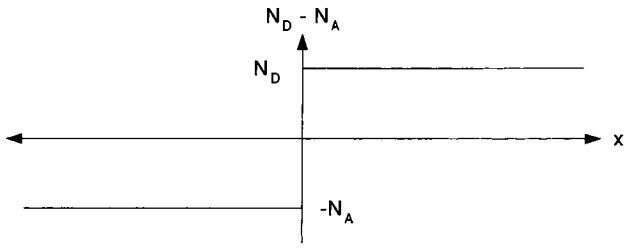

Figure 2.1.13: Doping Profile of a P-N Junction

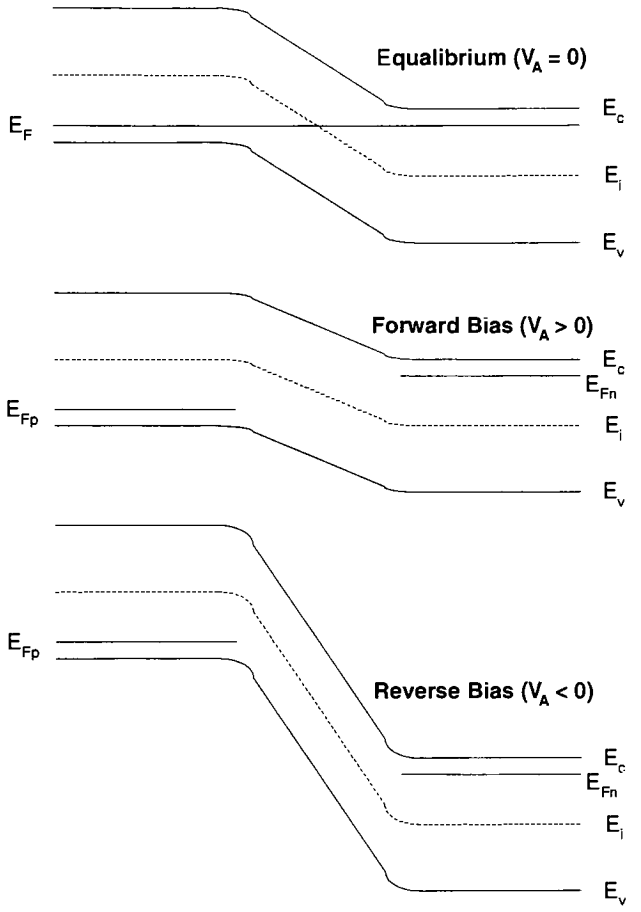

Figure 2.1.14: Energy Band Diagram of a P-N Junction

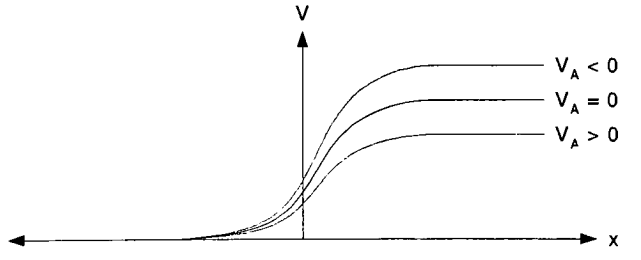

Figure 2.1.15: Electrostatic Potential of a P-N Junction

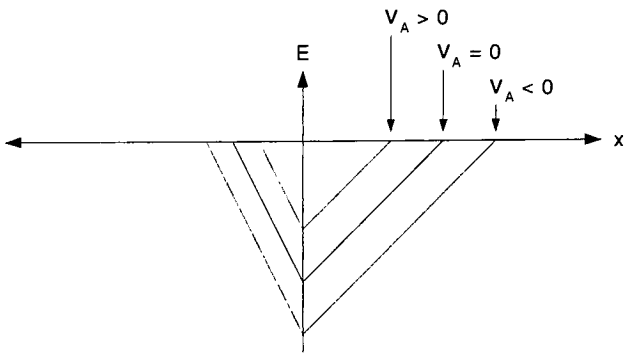

Figure 2.1.16: Electric Field of a P-N Junction

It is noted that the above diagrams are using a step junction profile for simplicity.

Notice in Figure 2.1.14 the energy band diagrams have a section where the bands are "bent", or band bending. Band bending is due to a connection made between the p-type and n-type materials. Charge carriers from both materials diffuse from regions of high concentration to low concentrations. Specifically, holes from the higher p-doped side would diffuse into the n region and electrons from the heavier n-doped side would diffuse into the p region. When the carriers diffuse away from their original location, they leave behind an unbalance of charges, or ionization. The p-side would have ionized acceptors and the n-side would have an equal number of ionized donors [Torres, et. al., 2002]. This section of the diode, where the p-doped and n-doped layers meet, is known as the depletion region.

The width of this depletion region is mainly a function of doping concentrations and is calculated by:

$$W = \left[\frac{2K_s \varepsilon_0}{q} \left(\frac{N_A + N_D}{N_A N_D} \right) V_{bi} \right]^{\frac{1}{2}}$$

Equation 2.9: Depletion Width at Zero Bias [Pierret, 1996]

Where Ks is the semiconductor dielectric constant, ε_o is the permittivity of free space ($8.85 * 10^{-14}$ [farad/cm]), q is the electronic charge ($1.6 * 10^{-19}$ [coul]), N_A and N_D is the acceptor and donor doping concentration in [cm^{-3}] respectively, and V_{bi} is the voltage breakdown in [V]. This equation is assuming that the junction is a perfect step function and no voltage bias is applied.

As suggested by Figure 2.1.15 and Figure 2.1.16, an increase of the electrostatic potential by having a reverse voltage bias can increase the magnitude of the electric field. As discussed in Section 2.1.3.1, a "good" avalanche mechanism is mainly dependent on having a high electric field.

2.1.3.1 Avalanche Mechanism

When reverse biasing a p-n junction, where current is flowing from the n-doped region of the semiconductor to the p-doped region, current flow is limited to a few milliamps and is independent to the magnitude of the reverse bias. If the reverse bias is continually increased beyond a certain point, known as the breakdown voltage, a large current will flow. This is a completely reversible process and does not damage the diode, except for overheating concerns if there is excessive current flow.

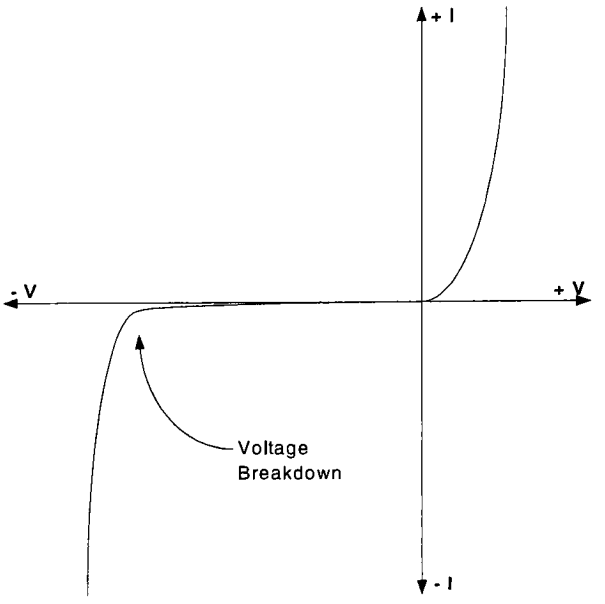

Figure 2.1.17: Typical Diode I-V Curve

Two processes cause this large current flow occurring beyond the voltage breakdown. One is the Zener process and the other more predominant process is the avalanche mechanism [Pierret, 1996].

The Zener process is where the particle, instead of gaining enough kinetic energy to overcome the potential energy barrier to move, tunnels through the barrier without any change in the particle energy. This phenomenon is rare compared to the avalanche process. It happens when the width of the potential energy barrier is very thin (less than 100Å) and can only happen when there are filled states on one side of the barrier and empty states on the other side of the barrier [Pierret, 1996].

The dominant process in contributing to the breakdown current is the avalanche process. When the diode is in reverse bias past the breakdown voltage, the current flow is due to minority carriers entering the depletion region and accelerated to the other side of the junction. The movement of the minority carriers is caused by the internal electric field. When minority carriers cross the depletion region, it collides with the semiconductor lattice. The mean free path is about ~10nm between collisions and depletion widths are around the order of magnitude of microns. At small reverse biases the energy losses from the collisions are small and only cause lattice vibrations. The result is just localized heating from friction vibrations.

At high reverse biases, beyond the reverse breakdown voltage, impact ionization occurs. The minority carriers accelerate through the depletion region with enough energy that when it collides with the lattice, it ionizes a semiconductor atom, freeing a valence electron from the atom and giving it enough energy to jump into the conduction band. This creates an electron-hole pair. Because of the high electric field present, these newly generated carriers are then immediately accelerated and consequently collide with the lattice for more impact ionization. The result is a multiplication of carriers and the reverse current essentially peaks off into infinity [Pierret, 1996].

As a note, the avalanche mechanism does not occur sharply at the breakdown voltage. Because collisions, mean free path, and energy of each carrier is a random variable distributed around a mean value, there are avalanching events happening far below breakdown and conversely, not all free carriers participate in the avalanche effect at voltages beyond breakdown. Below breakdown, there may be a few free carriers that have enough energy to cause impact ionization to start, but because of the low electric field, it does not permeate. It is only at higher reverse biases that this phenomenon becomes significant and leads to high reverse current [Pierret, 1996]. The result of this statistical distribution is that there is not a sharp edge at the voltage

breakdown, but a sloping approach and a slightly gentle bend to the curve as depicted in Figure 2.1.17.

When the device is in avalanche breakdown, the increase in current is expressed by a carrier multiplication factor, or gain:

$$M = \frac{1}{1 - \int_{x_1}^{x_2} \alpha \, dx}$$

Equation 2.10: Gain, M, Theoretical [Zeghbroeck, 2001]

Where x_1 and x_2 are the boundaries of the depletion layer region and α is the ionization coefficient. This theoretical equation assumes that the electrical field is constant between the depletion boundaries.

Empirically, the multiplication factor is expressed as:

$$M = \frac{1}{1 - \left(\frac{|V_a|}{V_{br}} \right)^m}$$

Equation 2.11: Gain, M, Empirical [McKay and Chynoweth, 1956]

Where V_a is the voltage applied, V_{br} is the breakdown voltage, and m is between 3 and 6 depending on the semiconductor material used.

As a note, the voltage breakdown value is can be designed by controlling the doping level of the lighter doped side of the junction. At lighter dopings, approximately below $10^{17}/cm^3$, the breakdown voltage is proportional to the doping level:

$$V_{BR} \propto \frac{1}{N_B^{0.75}}$$

Equation 2.12: Voltage Breakdown Proportion to Doping

Where N_B is the doping concentration on the lighter doped side of the junction [Pierret, 1996]. Figure 2.1.18 shows the V_{BR} and doping relationship for Si, Ge, and GaAs semiconductors [Sze, 1981]. At heavier dopings beyond $10^{17}/cm^3$, as indicated by the dashed line in the figure, the relationship does not follow Equation 2.12.

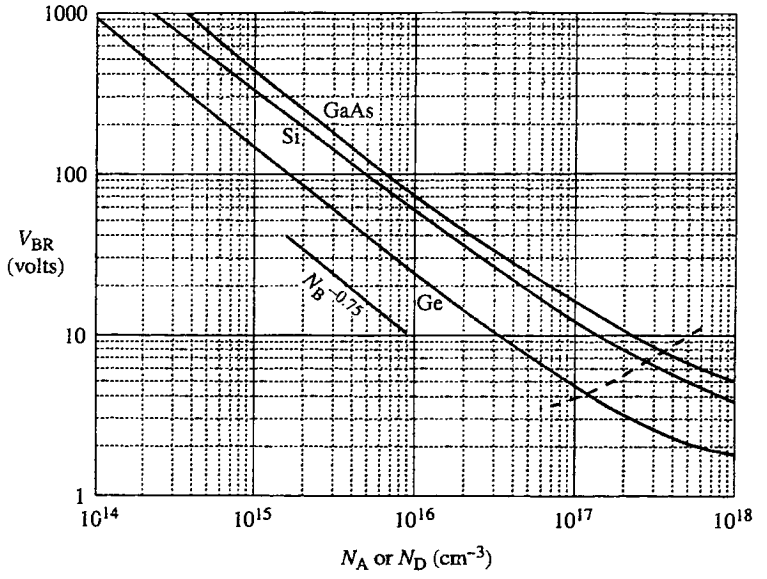

Figure 2.1.18: Breakdown Voltage Versus Nondegenerate-side Doping Concentration for Ge, Si, and GaAs semiconductors [Pierret, 1996]

2.1.4 Guard Ring

The purpose of the guard ring around the main avalanche photodiode structure is to minimize edge breakdown and achieve a more uniform breakdown across the photodiode [Pierret, 1996].

Because planar reach-through structures are fabricated using diffusion and ion-implantation through a mask, it always creates a curved edge from the bulk of the substrate to the edge:

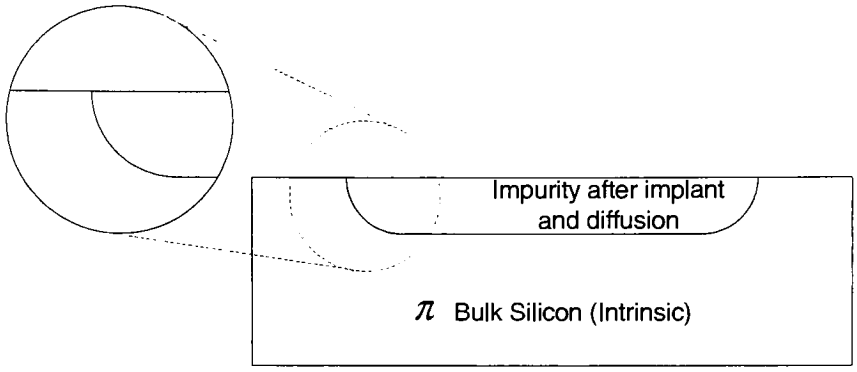

Figure 2.1.19: Exaggerated Detail of the Curvature Effect

This is known as a "curvature effect" [Sze, 1966]. It is due to the fact that when impurities diffuse, it diffuses in all direction; vertically and horizontally:

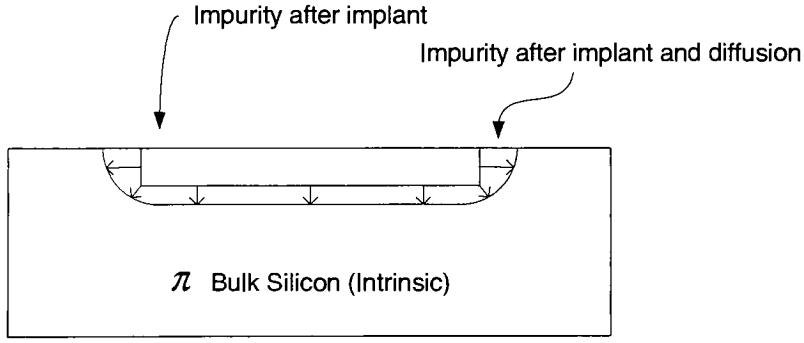

Figure 2.1.20: Curvature Effect - Implant and Diffusion Spread

Since the "curvature effect" presents a non-uniform edge shape between the heavily doped multiplication region and the lightly doped absorption region, it results in a premature low voltage breakdown at the junction periphery.

One approach to eliminate this problem is to create a guard ring at the junction periphery to reduce the electric field and minimize edge voltage breakdown. It can be thought of as a buffer zone between the multiplication and absorption region. The guard ring is lighter doped than the multiplication region, but is not as light as the absorption region [Matsushima, et. al., 1984].

2.2. Supporting Electronics

A complete APD array system requires supporting electronics in order for it to be functional. The two major components are a quenching circuit and a transimpedance amplifier.

2.2.1 Quenching Circuit

A quenching circuit is needed in order to prevent pixels to latch indefinitely in the avalanche mode. There are two main categories of quenching circuits: passive quenching and active quenching. Both of them operate on a principle based by lowering the bias voltage when extra current flows and restoring the voltage bias soon after to enable the photodetector to detect another signal. Passive quenching circuits are easier to implement, but are slow in recovery from the avalanche pulses [Cova, et. al., 1996].

Passive quenching circuits operate by developing a voltage drop on a high impedance load. It uses resistors in a voltage divider configuration to prevent latching [Cova, et. al., 1996]:

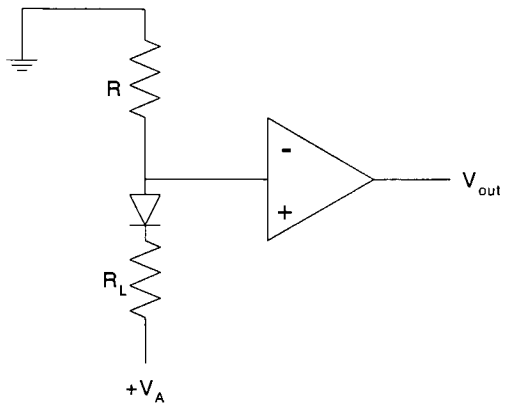

Figure 2.2.1: Passive Quenching Circuit

By selecting the right resistor values, the APD, depicted by the diode symbol in Figure 2.1.1, is at the desired bias in dark conditions (no signal light input).

Because the APD is a current sourcing device, when as incoming photon triggers the APD into avalanche and extra current is sourced, the biased voltage at the V_{bias} point drops, changing the reverse bias level of the APD itself and unlatching the avalanche mechanism. Therefore the voltage seen at V_{out} is at first negative (the detector is reverse biased) and spikes in the positive direction when there is incoming light, and drops back down to starting level when it is dark again. The passive quenching circuit is best using the APD in Geiger mode, counting photons and requiring the output to be binary in reporting if photons are present or not.

2.2.2 Transimpedance Amplifier

Since most solid-state devices are essentially current sourcing devices, a transimpedance amplifier is necessary for the operation of these devices. The role of a transimpedance amplifier

is to both amplify the signal of the detector and convert it from a current to a voltage signal. It utilizes an operational amplifier (op amp) circuitry with a feedback resistor:

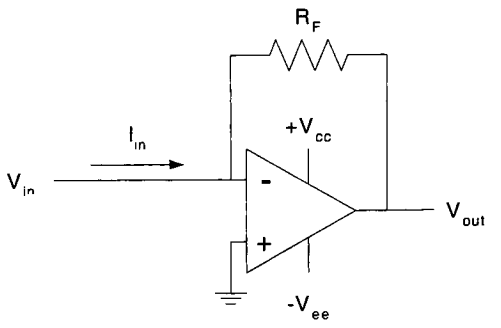

Figure 2.2.2: Transimpedance Amplifier Circuit

The value of the feedback resistor adjusts the voltage gain of the amplifier by using the classic formula:

$$V_{out} = -I_{in} R_F$$

Equation 2.13: Transimpedance Amplifier Voltage Output

A common mistake to avoid is in selecting a high gain such that the voltage output is higher than the $+V_{cc}$ and $-V_{ee}$ rail voltage used to power the op amp; the output will be clipped.

To utilize the transimpedance amplifier along with the quenching circuit to read from an APD, the circuit is:

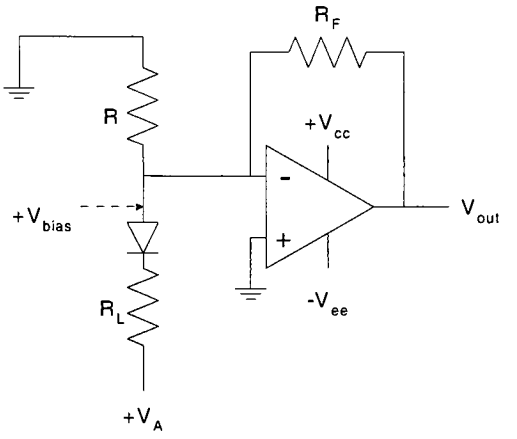

Figure 2.2.3: Quench and Transimpedance Amplifier Circuit

2.3. Problems with Arrays of APDs

Due to the nature of how an APD operate, creating an array of APDs has certain obstacles. The problems involved are in having optical and electrical cross-talk, the significance of non-uniformity within pixel and from pixel-to-pixel, and the possibility of having a pixel latched in the avalanching state after photon detection.

2.3.1 Cross-Talk

It was first reported in the 1950's that photons were emitted from avalanche breakdown in silicon. During a reverse bias voltage breakdown, photon emission occurs at the p-n junction and is due to both avalanche and Zener mechanism [McKay and Chynoweth, 1956]. Optical cross-talk describes the condition when the diode itself is emitting secondary photons from the avalanche and Zener mechanism as triggered by the primary incoming photons. These photons can then be

detected by surrounding pixels. In an experiment by Franco Zappa et. al., the secondary photons emitted are proportional to the current flowing through the diode [Zappa, 1996].

Electrical cross-talk can either arise from a readout circuit, consisting of a quenching circuit and an amplifier, or from the avalanche mechanism. The avalanche source of cross-talk is due to the relatively high electric field and impact ionization taking place. It is possible for the ionizing carrier to scatter into adjacent pixel and produce a false trigger. Because this is a random event, as the pixel-to-pixel distance gets closer, the probability of having a carrier wander into adjacent pixels is higher. Therefore, to minimize or eliminate electrical cross-talk, pixels need to be spaced out. The tradeoff of this is that the dead space, the region between pixels where it would not sense incoming photons, increases.

2.3.2 Non-Uniformity

The gain of an APD is dependent on the strength of the electric field across the depletion region. The uniformity of the electric field is dictated by the doping uniformity of the n and p regions of the ADP. Therefore, the gain of the device is dependent on the doping uniformity, which is dependent on the fabrication process technology.

To illustrate the importance of controlling the fabrication process to control the uniformity of diode performance, the equation of the photocurrent output of a diode is used:

$$I_p = \frac{P_o\, q(1-r)}{h\upsilon}(1-e^{-\alpha d})$$

Figure 2.3.1: Photocurrent Output of a Diode

Where P_o is the incident optical power, q is the charge, r is the optical reflection loss, hν is the photon energy, α is the absorption coefficient, and d is the depletion layer width. Since d is an exponential term, small changes in the depletion width would result in a significant change in the photocurrent of the diode.

2.3.3 Pixel Latching

There are problems associated with single APDs in general. Besides cross-talk that generates false triggers, thermally generated electron-hole pairs can also have the same effect. This is known as the dark current. At relatively higher temperatures, a carrier may be able to receive enough energy to ionize and cause the avalanche process, since the high electric field is already present.

A second problem is that when an electron-hole pair is generated, either thermally or optically from a photon, the device discharges and if it exceeds a certain latch current, would remain in the avalanche state. A quenching circuit is needed to momentary lower the electric field to stop the avalanche effect and quickly raise the electric field back in order to detect further photons.

3. Implementation

3.1. Design

APD arrays were fabricated at the Rochester Institute of Technology Microelectronics Department. Several APD array designs were fabricated and tested to see how certain design element changes would affect performance.

3.1.1 Wafer Variations

One wafer was used for each design variation. The variations included using either polysilicon or aluminum as the metal connection, having a guard ring, or eliminating the middle p layer. There were five designs:

Wafer ID	Description
APD02-01	Regular NiP structure
APD02-02	NiP structure with polysilicon contacts
APD02-03	NiP with no Guard Ring
APD02-04	NPiP Structure with no Guard Ring
APD02-05	NPiP Structure with Guard Ring

Table 3.1: Wafer Design Variations

To find how pixel dimensions change the performance of the device, several pixel dimensions were fabricated on the same die. Pixel diameter varied from 100 to 1500um. The guard ring

lateral width was from 10 to 50um. Most pixels were replicated and placed in an array fashion at various distances. The following table shows the different pixel dimensions available in the die:

Pixel (Active Area) Diameter	Guard Ring Lateral Width	Pixel to Pixel Distance (Center to Center)	Ring Material
100μm	10μm	100μm	Polysilicon
100μm	10μm	200μm	Polysilicon
100μm	10μm	400μm	Polysilicon
200μm	10μm	400μm	Polysilicon
200μm	20μm	250μm	Polysilicon
200μm	20μm	300μm	Polysilicon
200μm	20μm	300μm	Aluminum
200μm	20μm	400μm	Polysilicon
200μm	30μm	400μm	Polysilicon
400μm	20μm	500μm	Polysilicon
400μm	20μm	750μm	Polysilicon
1500μm	50μm	N/A	Aluminum

Table 3.2: Pixel Geometry Variations in Die Design

3.1.2 Die Layout

Several pixel sizes along with a few other devices were fabricated in each die. The following illustration shows the layout of the die:

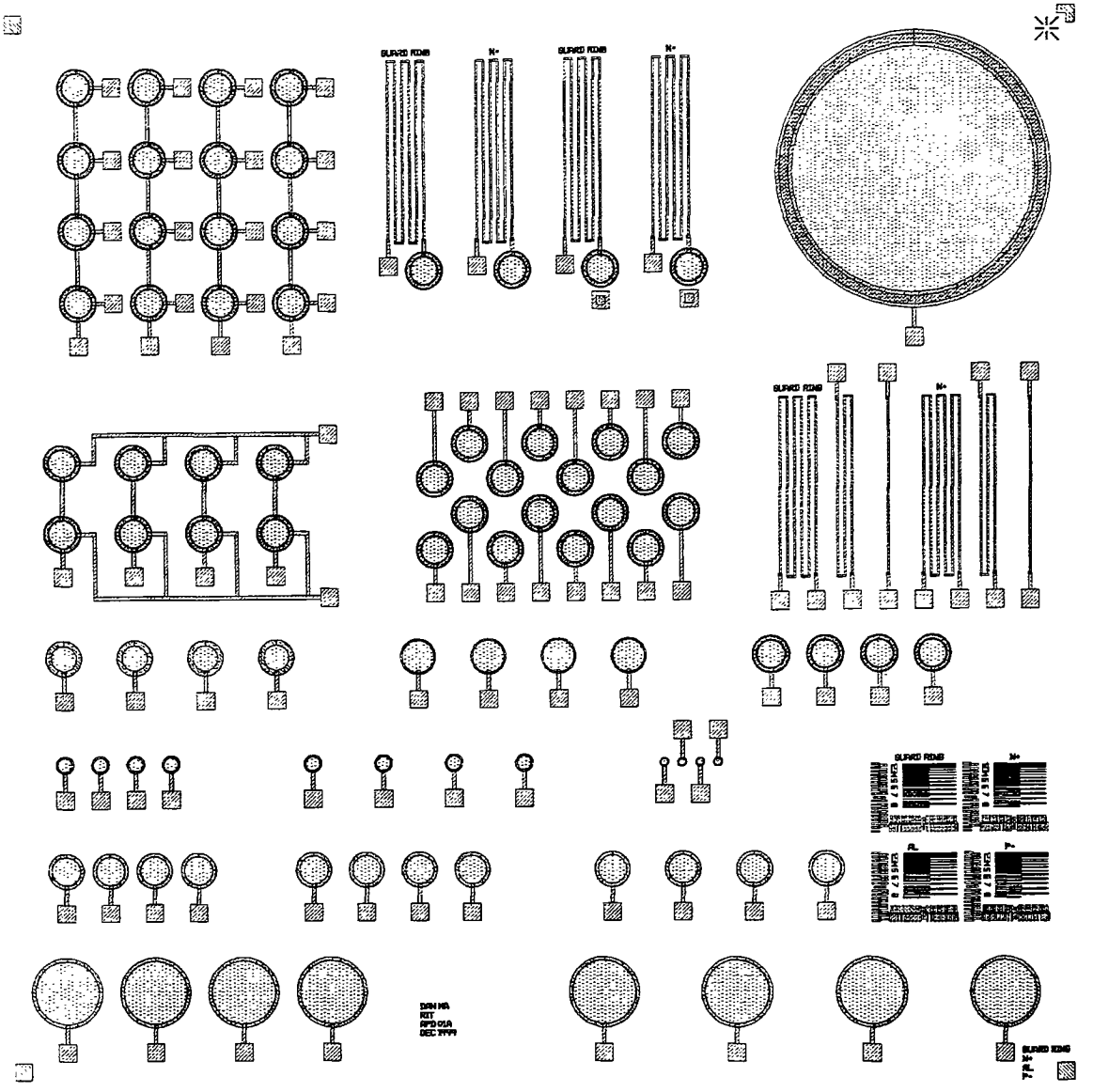

Figure 3.1.1: Die Layout

As a reference to the size of the die, all the contact pads are 100x100 µm. The die layout is shown again but with labels to indicate each area:

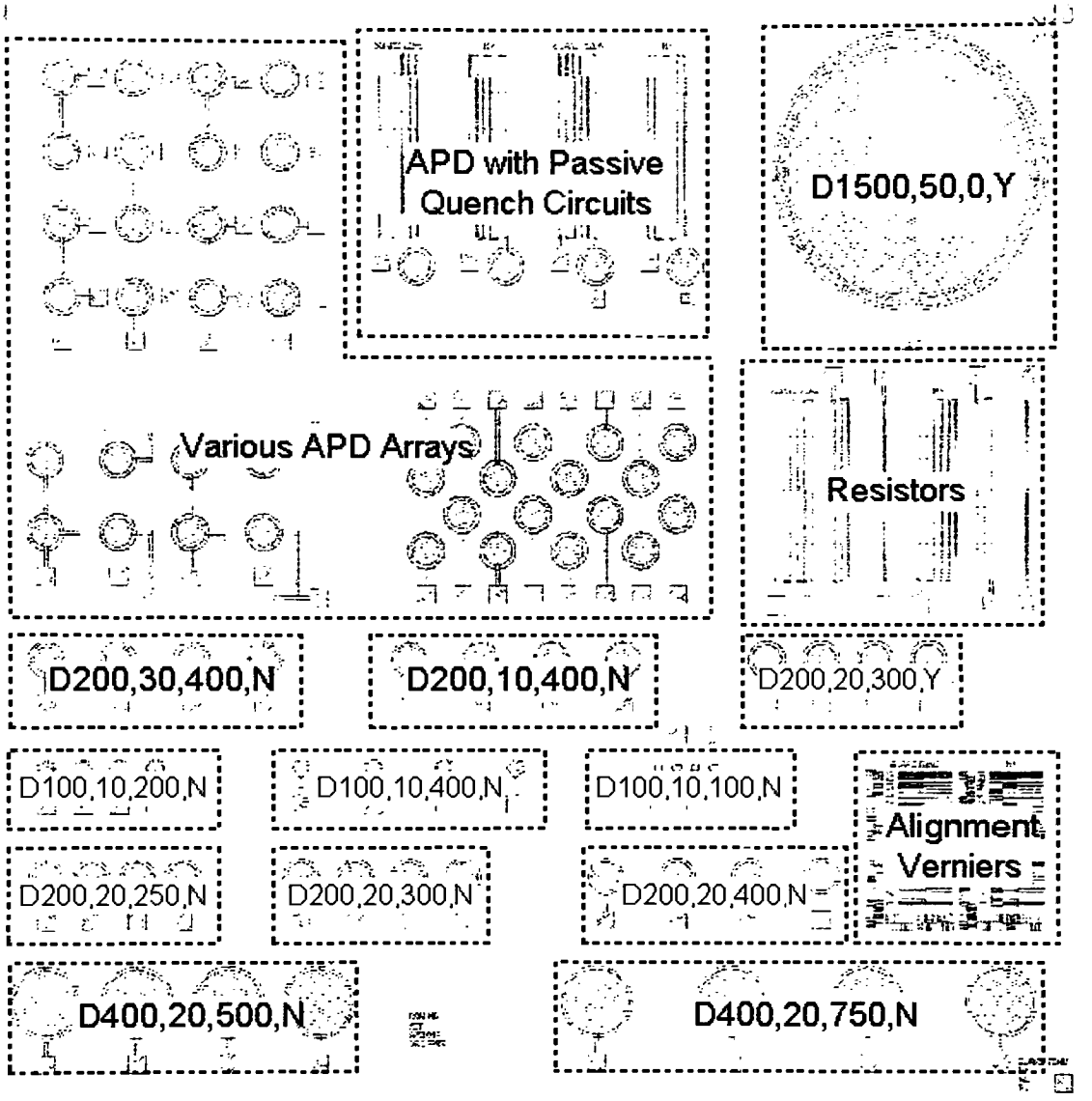

Figure 3.1.2: Die Layout with Labeled Areas

Photodiodes [D*ddd,gg,ppp,Y/N*]:

The arrays of photodiodes arranged in sets of fours are labeled with the following designation:

ddd	Active diameter of the photodiodes.
gg	Width of the guard ring.
ppp	Pixel to pixel distance measured from center to center.
Y/N	If the guard ring is fabricated of aluminum (Y) or from polysilicon (N).

Table 3.3: Photodiode Nomeclature

Various APD Arrays:

Various APD arrays in different configurations and connections.

APD with Passive Quench Circuits:

Individual APD pixels with connected resistor as quenching mechanism.

Resistors:

Various resistors with different resist values.

Alignment Verniers:

Used for aligning the Guard Ring, N+ Region, P+ Region, and Aluminum mask levels.

3.1.3 Device Cross-Section

The general device structure used was the planar reach-through structure as described in Section 2.1. The following figure shows the final cross-section of the device:

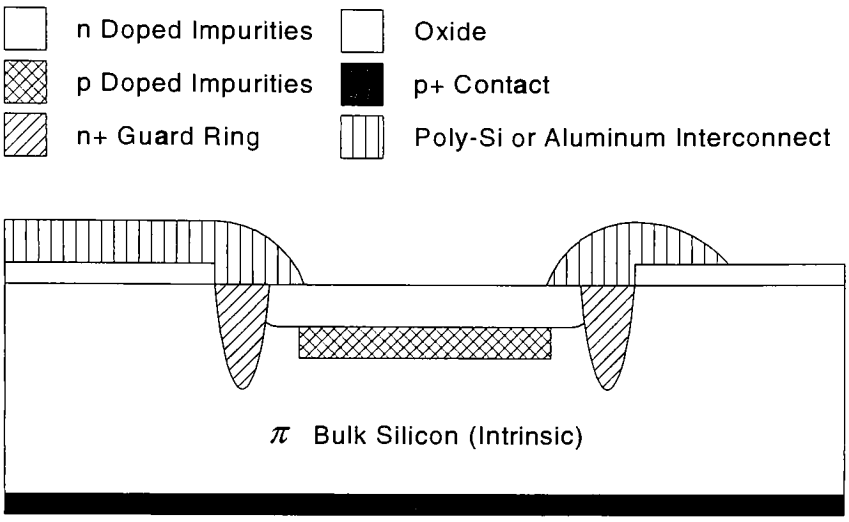

Figure 3.1.3: Cross-Section of a Reach-Through APD with Contacts

The type of wafer used was a heavily doped p-type (boron) substrate with a 28μm thick epitaxial layer. The substrate had a resistivity of 0.0163 Ω-cm while the epitaxial layer was around 18Ω-cm. The substrate served as the p+ contact layer while the remaining device features were in the epitaxial layer. The impurity layers are fabricated using ion implantation at various species and doses. The drive-in steps are done via diffusion furnaces. Traditional g-line optical lithography was used for masking and defining device layouts.

3.2. Calculations

Three specific calculations are needed in order to fabricate the device properly: oxide growth thickness, ion implant dose, and drive-in time.

3.2.1 Oxide Thickness

The following equation is used in order to determine the oxide thickness growth:

$$x = \frac{A}{2}\left(\sqrt{1+\frac{4tB}{A^2}}-1\right)$$

Equation 3.1: Oxide Thickness Calculation

Where:

$$A = K_1 e^{\frac{E_1}{kT}}$$

$$B = K_2 e^{\frac{E_2}{kT}}$$

B/A is known as the linear rate constant and B as the parabolic rate constant. T is the process temperature in Kelvin, t is the oxidation time in hours, and k is the Boltzmann constant in [eV/K]. Oxide thickness x is in microns. Exact values of K_1, K_2, E_1, and E_2 are shown in Appendix 6.1. Note that the equation used is for diffusion-rate limited regime in wet oxidation on bare silicon, which is applicable for the devices in this research. It is also noted that approximately 46% of the oxide grown is "consumed" from the silicon:

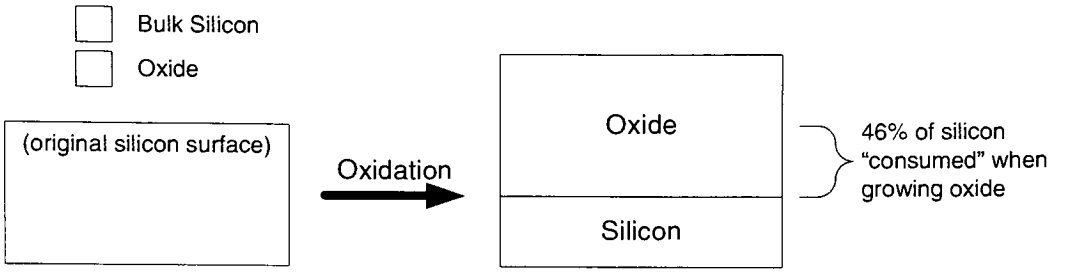

Figure 3.2.1: Silicon Consumption from Oxide Growth

Algebraic manipulation is all that is needed in order to determine the process parameters for a desired oxide thickness. Actual oxide calculations performed for this research are shown in Appendix 6.1.

3.2.2 Ion Implant

To determine the implanted ion concentration as a function of depth into the wafer, the following formula is used [Wolf and Tauber, 1986]:

$$N_i(x) = \frac{N'}{\sqrt{2\pi}\, dR_P} e^{\frac{-(x - R_P)^2}{2\, dR_P^2}}$$

Equation 3.2: Implanted Ion Concentration

Where x is the depth into the wafer, N' is the implant dose, R_P is the implant projected range, and dR_P the implant projected straggle. This calculation was needed for the guard ring, n+, and p+ device structures. Graphs and calculations of implant ion concentration are shown in detail in Appendix 6.2.

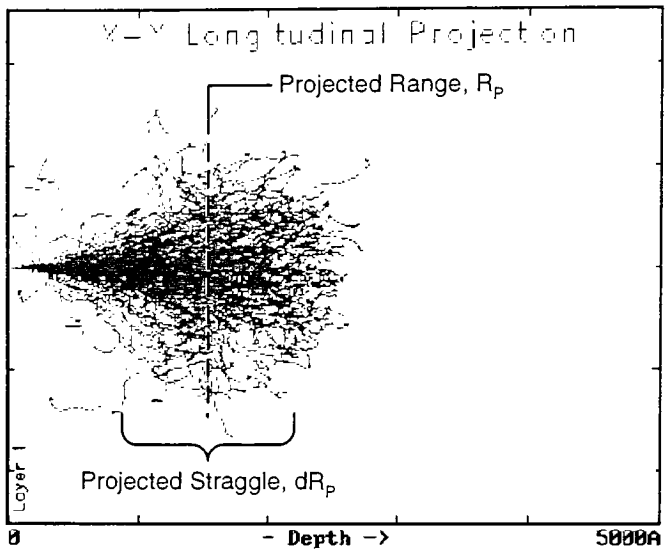

Figure 3.2.2: Ion Implant Range and Straggle - Longitudinal Axis [Cheung, 2003]

3.2.3 Drive-In

To determine the doping profile for a diffusion step (drive-in) at a specific process parameter, Fick's law of diffusion is used [Wolf and Tauber, 1986]:

$$C(x,t) = \frac{Q_o}{\sqrt{\pi D t}} e^{\frac{-x^2}{4Dt}}$$

Equation 3.3: Fick's Second Law of Diffusion

Where x is the depth into the wafer, t is the time of diffusion, Q_o is the total quantity of impurity present, and D is the diffusion coefficient.

Since all impurity drive-in performed on the devices in this research is after ion implantation, a simplified equation combining Equation 3.2 and Equation 3.3 can be used:

$$N_d(x) = \frac{N'}{\sqrt{2\pi}\sqrt{dR_P^{\,2} + 2Dt}} e^{\frac{-(x-R_P)^2}{2(dR_P^{\,2}+2Dt)}}$$

Equation 3.4: Impurity Profile after Implant and Diffusion

Details of this equation are shown in detail in Appendix 6.2.

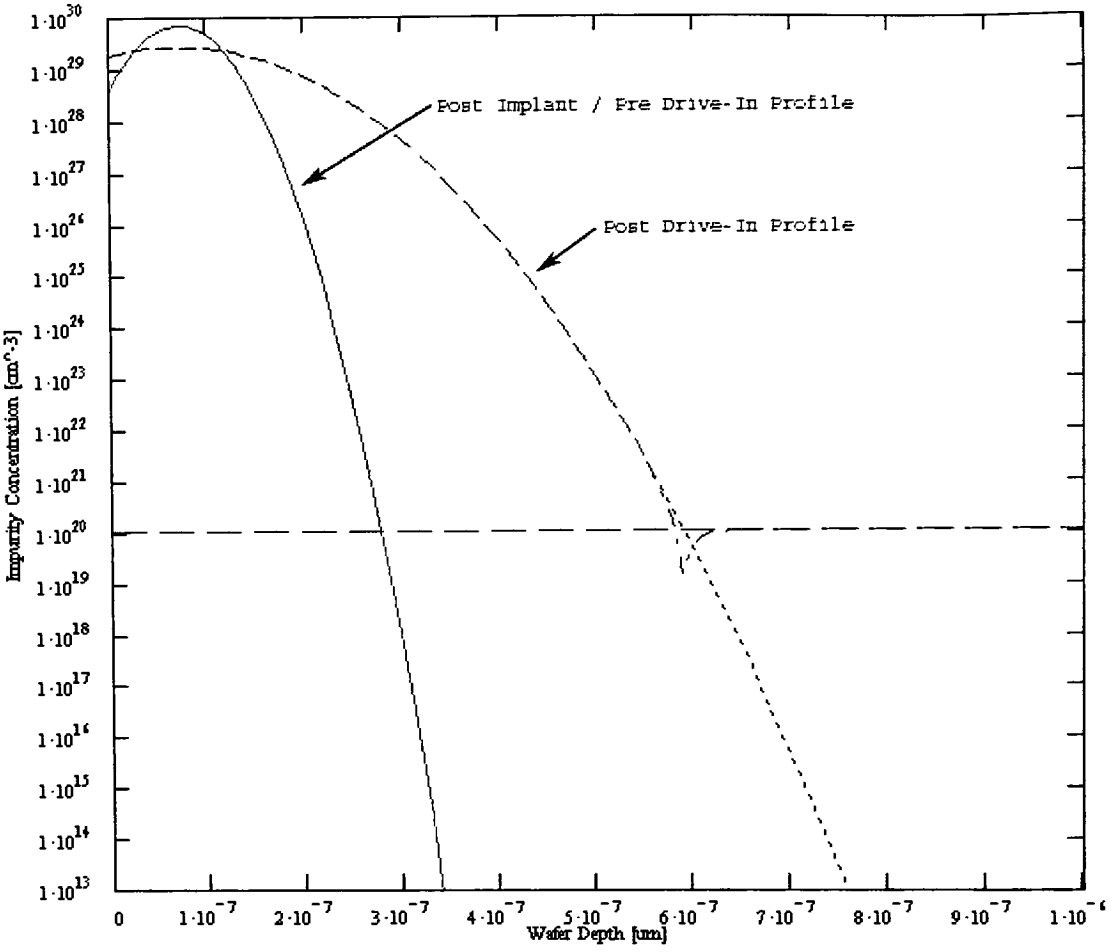

Figure 3.2.3: Ion Implant Drive-In

3.3. Fabrication

Appendix 6.3 outlines each step of the fabrication process and show the device profile for that process. As mentioned in Section 3.1.1, there were five wafers each with a slightly different

design variation. Next to each process description lists the wafers that were used for that particular step.

3.4. Test Set-up

The following diagram illustrates the test-up:

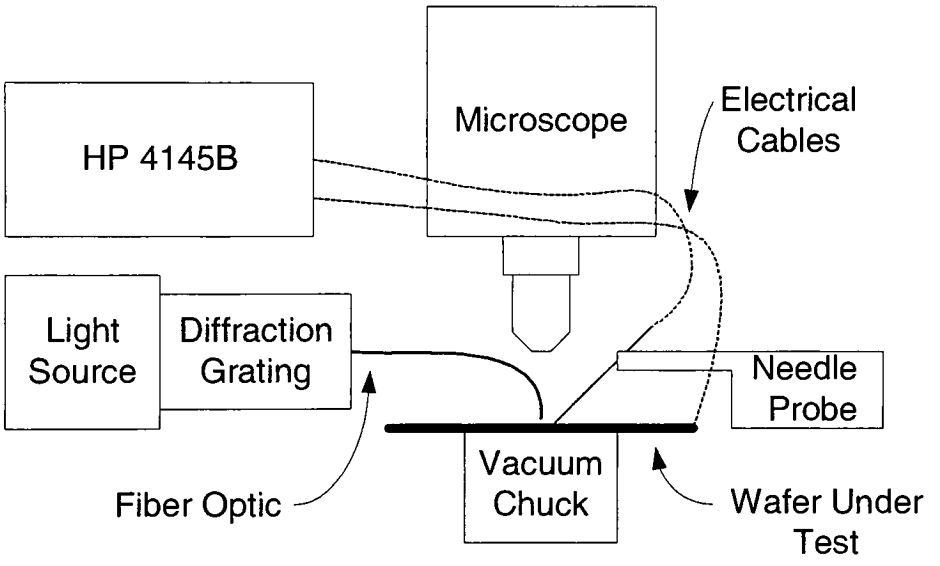

Figure 3.4.1: Test Set-Up Diagram

Here is a picture of the set-up:

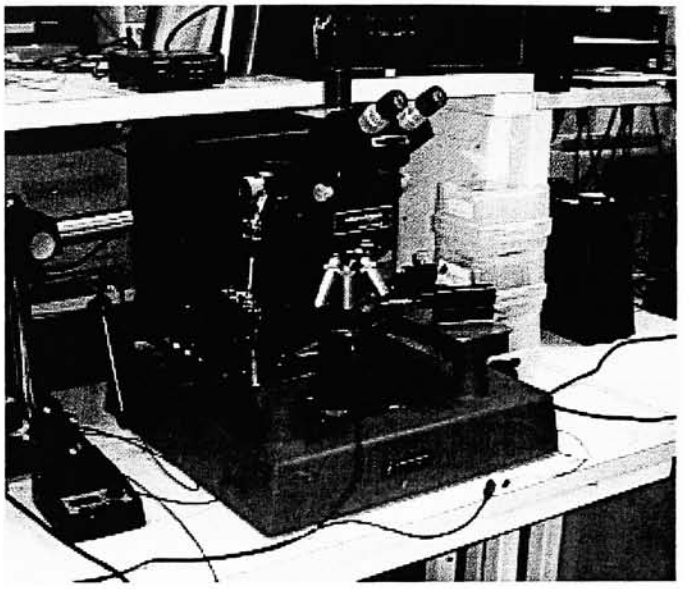

Figure 3.4.2: Test Set-Up Picture

The microscope used featured a shelf for the needle probe to rest on and is capable of moving independently from the wafer and vacuum chuck. The microscope head also has an independent range of movement.

A halogen light source is used as illumination, into a diffraction grating with the ability to select the desired wavelength. The light is piped into the photodiode tested. The fiber optic has an exit angle of approximately 30° FWHM (full width half-maximum intensity).

All I-V measurements were obtained on the HP4145B parametric analyzer.

3.5. Deviation of Fabricated Devices from Ideal

As mentioned in Section 2, "Device Theory and Design", of this paper, the main key in designing a successful APD is to have the doping levels correct for each of the layers such that the depletion region (and hence, the electric field) extends into the intrinsic layer when under sufficient reverse bias:

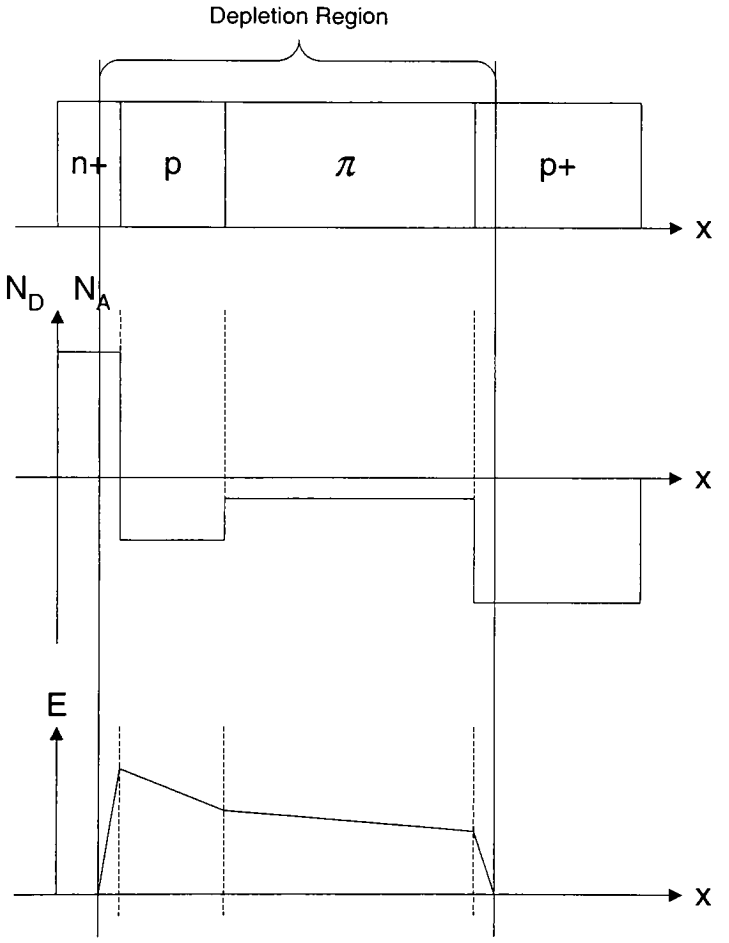

Figure 3.5.1: Doping, Depletion, and Electric Field Diagram of a Standard APD

Also, a more appropriate depth for each layer is usually less than 0.5μm for n+, to minimize the participation of holes in the detection process, and around a few microns for the middle p layer [Wêgrzecka, et. al., 2004]. The depth and thickness of the intrinsic *i* layer can be varied to adjust the spectral characteristics of the device.

Instead, the devices fabricated in this research had incorrect doping levels. The p layer had too high of a doping level such that the depletion region existed only between the n and p layers:

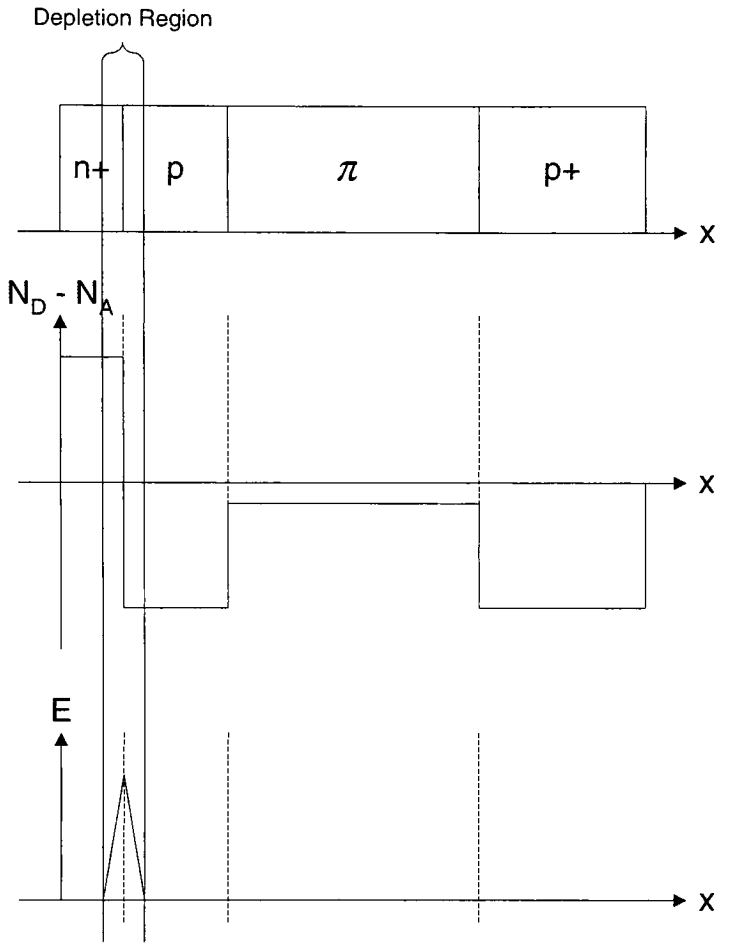

Figure 3.5.2: Doping, Depletion, and Electric Field Diagram of Fabricated Reach-Through APD

It is stated again that the above depletion and electric field characteristics are for the device in reverse bias state.

4. Test Results

4.1. Figures of Merit

To compare the performance of the avalanche photodiodes both within this research and with other manufactured photodiodes, four figures of merit are used: voltage breakdown, dark current, gain, and spectral responsitivity. Two independent plots of each photodiode are needed in order to calculate those figures of merit. A third plot is used specifically for photodiode arrays; to compare cross-talk between photodiodes.

The following explains how each figure of merit is obtained and calculated.

4.1.1 Breakdown Voltage

The breakdown voltage is the reverse voltage at which the current flow increases dramatically due to avalanche mechanism and Zener process (see Section 2.1.3.1 and Figure 2.1.17).

In the case of the photodiodes that tested here, the "knee" of where voltage breakdown occurs is not sharp enough to quote a definite number. Because of that, three definitions that are commonly practiced within the industry were used. Human judgment was then applied to determine which method reported the most sensible number, as some methods reported an erroneous or illogical voltage breakdown number. The three techniques used were:

1. Third-Order Polynomial Fit Method
2. Interpolation Method
3. Current Threshold Method

The Third-Order Polynomial Fit Method defines the voltage breakdown by first fitting a third-order polynomial to the data, finding the derivative, and determining where the maximum gradient occurs. This method worked best when the data did not exhibit a very sharp knee at the voltage breakdown point. Although a higher order polynomial fit would have fit that type of data better, there were too many inflection points around the linear region of the I-V curve of a photodiode (area between reverse bias (0V) and breakdown voltage). The computer algorithm performing the third-order polynomial fit method was coded in Microsoft Visual Basic 6.0. The code is reprinted in Appendix 6.4.

The Interpolation Method takes the avalanche regime of the photodiode I-V curve and interpolates a straight line towards the voltage axis. The intercept is the breakdown voltage:

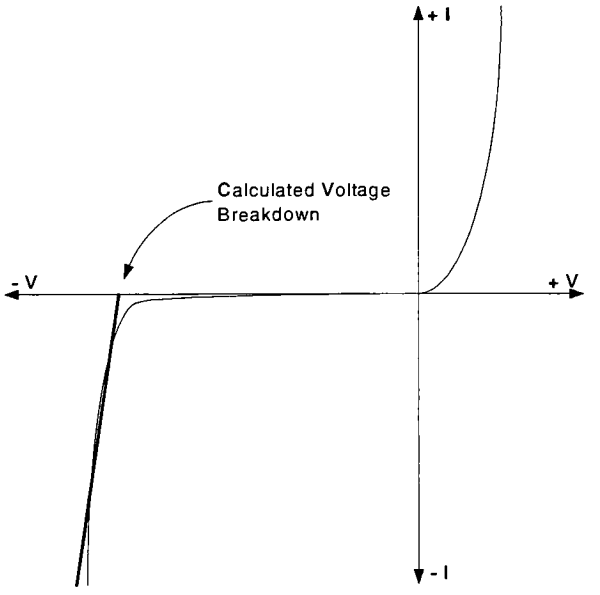

Figure 4.1.1: Breakdown Voltage via Interpolation Method

The Current Threshold Method defines the breakdown voltage by setting a certain current threshold. Because this research deals with different variations of device designs, this method is only useful if comparing photodiodes that has similar magnitudes on the I-V graph:

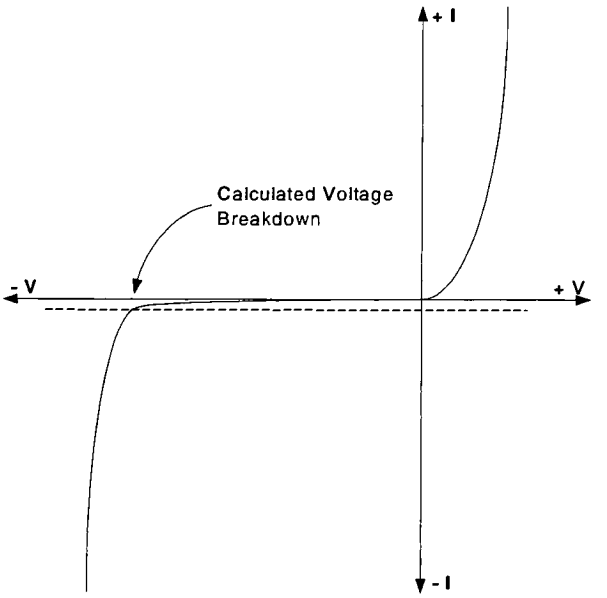

Figure 4.1.2: Breakdown Voltage via Threshold Method

4.1.2 Dark Current

Dark current is the current that flows in the photodiode when no incident light is present. Intrinsically, dark current is a function of temperature and the amount of reverse voltage. Dark current arises due to electrons having enough energy from thermal and lattice vibrations to jump from the valence band to the conduction band. If the reverse bias is high enough, these jumps result in a cascading avalanche situation.

Dark current can also be controlled using special device designs. One simple way to reduce dark current is to merely reduce the size of the active area of the photodiode, reducing the number of electrons jumping bands.

In this research, dark current is determined from the current-voltage (I-V) plot. For the I-V plot of each photodiode tested, a voltage sweep was done with no incident light. Dark current is usually specified at a certain reverse voltage, typically at the designed operating voltage. Since this research consists of different designs and sizes, a dark current number will be quoted at the defined breakdown voltage.

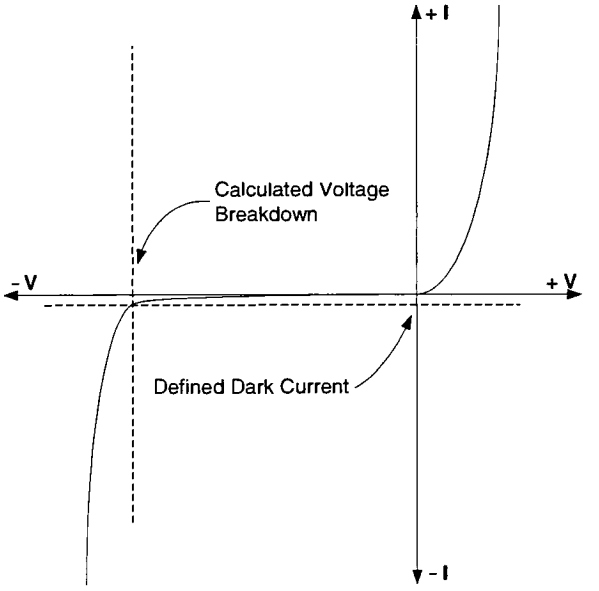

Figure 4.1.3: Defined Dark Current

4.1.3 Gain

The definition of gain for a photodiode is the ratio of the total multiplied output current to the primary unmultiplied photocurrent:

$$M = \frac{I}{I_P}$$

Equation 4.1: Photodiode Gain, M

I is the multiplied current that is output from the detector. Ip is the photocurrent that is generated during the absorption of photons into the device. Where:

$$I_P = \left(\frac{q}{h\upsilon}\right) P_O \left[1 - e^{(-\alpha_s w)}\right](1 - R_f)$$

Equation 4.2: Primary Photocurrent, I_P

Where q is the electronic charge in [C], h is Planck's constant [J*s], υ is the photon momentum [Hz], P_O is the incident optical power [W], α is the absorption coefficient of the photodiode material [1/m], w is the depletion width [m] inside the semiconductor, and R_f is the surface reflectivity percentage.

In examining Equation 4.2, I_P is already taking into account the reflectivity of the photodiode surface, incident optical power, wavelength, and absorption into the device. Therefore, Equation 4.1, M, only deals with the gain that is produced internally inside the photodiode.

Since gain is also a function of bias voltage, the gain at breakdown voltage will be used to quote a gain specification.

4.1.4 Responsitivity

Responsitivity is a measure of how well the photodiode converts incident light into current. A higher responsitivity means that the photodiode is more sensitive to light and would yield a higher electrical output than one with a lower responsitivity. Responsitivity is defined as:

$$R = \frac{I_P}{P_O}$$

Equation 4.3: Responsitivity, R

Where I_P is the primary photocurrent (same as Equation 4.2) and P_O is the incident optical power. If the equation was written out to the basic properties, responsitivity is a function of photon energy, absorption coefficient of the material, depletion width of the p-n junction, and the optical power loss due to reflection:

$$R = \left(\frac{q}{h\upsilon}\right)\left[1 - e^{(-\alpha_s w)}\right](1 - R_f)$$

Equation 4.4: Functions of Responsitivity

Responsitivity is a function of wavelength. As mentioned in Section 2.1.2.1, different semiconductor materials would have different absorption coefficients of wavelengths. For silicon,

it stops absorbing light beyond 1100nm due to the incident photons not having enough energy to excite an electron to jump the 1.12eV band gap. Responsitivity will be quoted at 600nm.

4.1.5 Crosstalk Plot

The arrays of four photodiodes were used to test for crosstalk. The first photodiode was connected to the measurement equipment while each photodiode was individually illuminated one at a time (i.e. one through four). The current output, defined at a specific voltage bias that is particular to the arrays tested, was compared at each illumination. Knowing the distance between the four photodiodes, a signal output versus distance plot was obtained (see Figure 4.3.1). To have the plot meaningful, the output signals are normalized to the first photodiode.

The following figure illustrates how a perfectly isolated crosstalk and a poorly isolated crosstalk plot should look like:

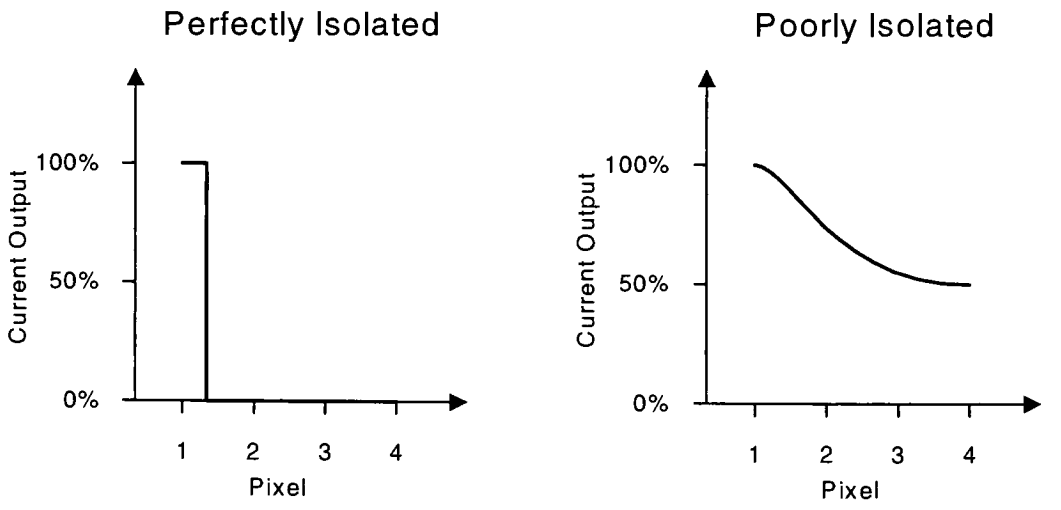

Figure 4.1.4: Theoretical Crosstalk Plots

4.2. Single APD Results and Comparison to Commercial Devices

Typical to both research and manufacturing, some of the devices fabricated performed as expected and some did not. Most of the devices suffered at least one of the following problems: no signal, uncontrolled voltage breakdown, and low responsitivity. Those issues are discussed in detail in Section 4.4.

Because of the number of imperfect photodiodes, a judgment needed to be made in order to determine which photodiodes to test. Ideally, the current-voltage (I-V) plot should look similar to the one as shown in Figure 4.2.1. That figure also shows how most photodiodes look like, where the transition into the avalanche breakdown regime is not sharp but a gradual slope:

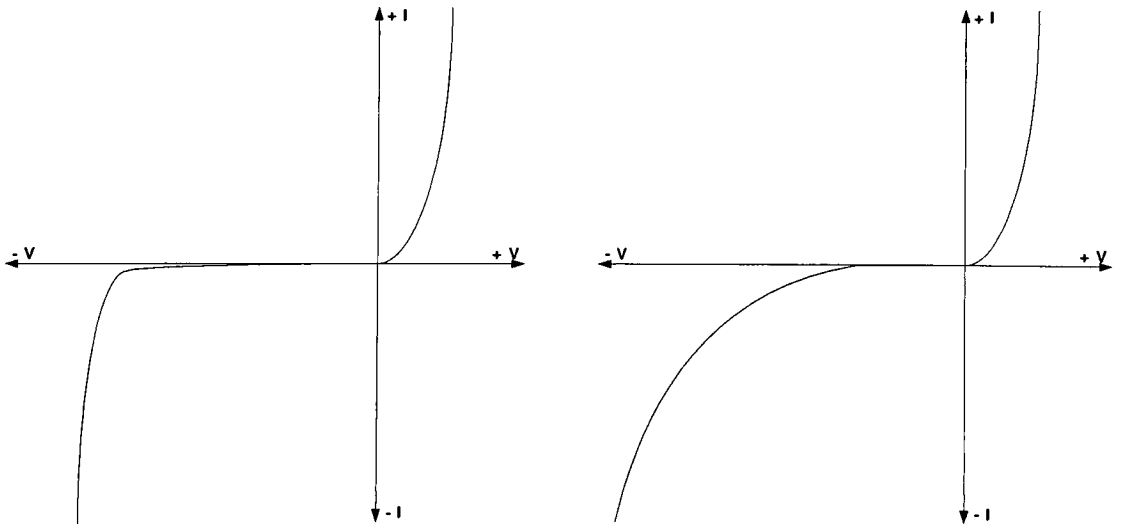

Acceptable I-V Curve

Unacceptable I-V Curve

Figure 4.2.1: Acceptable and Unacceptable APD Current-Voltage Curves

With each wafer containing more than 121 dies, two dies were chosen to be tested. Within each die, five different photodiode sizes were tested, with each photodiode being randomly selected within each size.

Of the five different device structure variations (APD02-1 through APD02-5), the fourth wafer (APD02-4) represents the standard planar reach-through structure. Photodiode [W4 C7,3 D200,20,300,Y] will be used to discuss the analysis in detail. In addition, specifics of other photodiodes will be shown as appropriate. Appendix 6.5 contains the complete graphs of all 42 photodiodes tested. Using the figures of merit as defined in Section 4.1 as a metric for comparison, six photodiodes were considered acceptable. Here is the summary of the results:

Cell	Breakdown Voltage [V]	Dark Current [μA]	Gain	Responsitivity [A/W]	NEP [μW]
W1 C5,6 D1500,50,0,Y	-1.244	-38.7	1513	0.199	0.195
W2 C6,8 C1500,50,0,Y	-1.346	-73.8	2413	0.199	0.371
W3 C11,10 D200,20,300,Y	-0.451	-3.4	1332	0.199	0.017
W4 C7,3 D200,20,300,Y	-7.624	-2484	22677	0.280	8.870
W4 C7,3 D200,30,400,N	-5.2	-10.4	188	0.272	0.038
W5 C9,10 D400,20,500,N	-50.43	-63	19053	0.307	0.205

Table 4.1: Tested Photodiodes Results

4.2.1 I-V Curve

Photodiode [W4 C7,3 D200,20,300,Y] has a diameter of 200μm and a 20μm width aluminum guard ring, located on wafer 4 on die 7,3. Its I-V curve is:

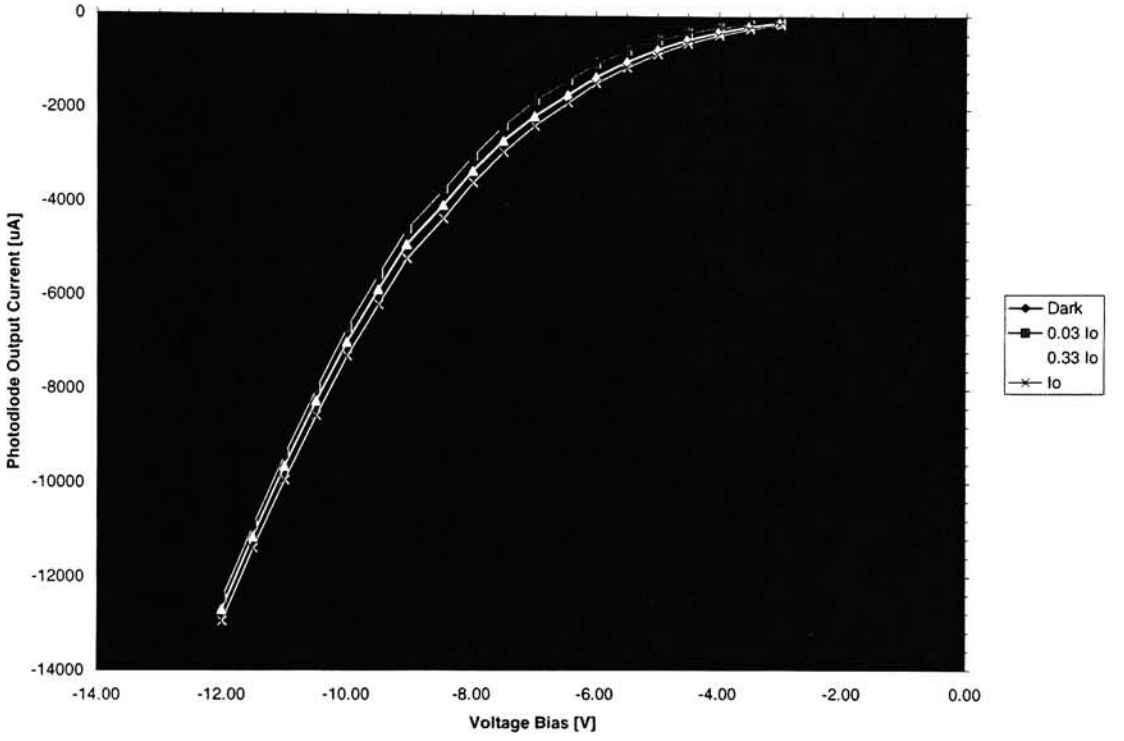

Figure 4.2.2: I-V Plot (W4 C7,3 D200,20,300,Y)

Denoting Io as the full optical power used in the test set-up, it shows the curves at no light (dark), 3% light (0.03 Io), 33% light (0.33 Io), and full power (Io) as described in test set-up in Section 3.4. Full optical power (Io) was approximately 486nW/cm^2.

Coincidentally, this photodiode exhibited the highest current output of all tested photodiodes. The high current output is most likely due to non-uniformity issues during fabrication and is not due to design. This is proven because a similar photodiode on the same wafer with roughly the same device geometry [W4 C7,3 D200,30,400,N] happen to exhibit the lowest current output of the group.

The typical output of an APD that is commercially fabricated has the following I-V curve:

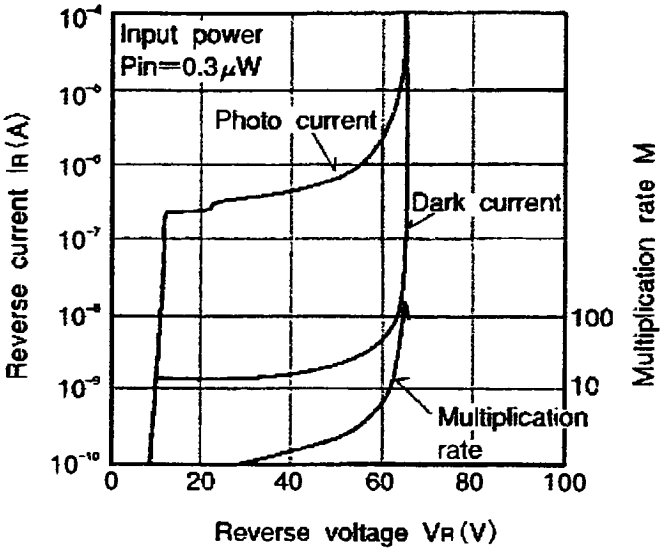

Figure 4.2.3: I-V Plot (Mitsubishi PD8XX2 Series Photodiode) [Mitsubishi, 1997]

Note that this graph shows the reverse voltage and reverse current as a positive scale. Of the tested photodiodes in this research, one photodiode [W4 C7,3 D200,30,400,N] exhibited the closest response:

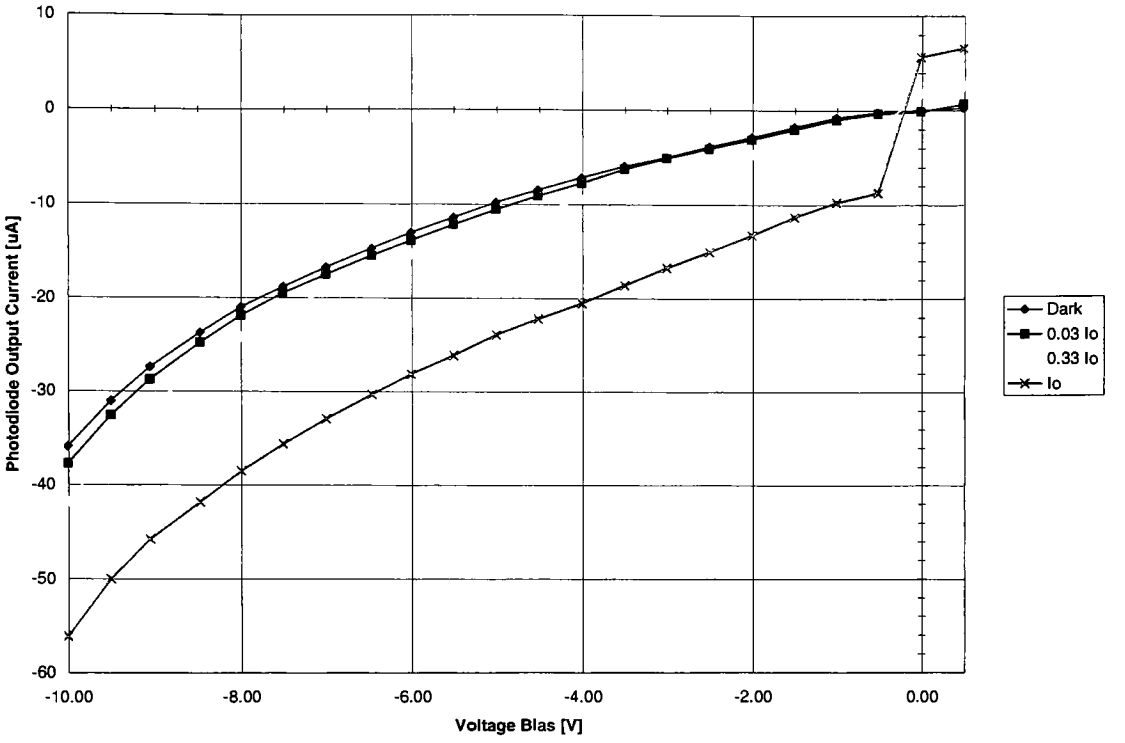

Figure 4.2.4: I-V Plot (W4 C7,3 D200,30,400,N)

4.2.2 Breakdown Voltage

For [W4 C7,3 D200,30,400,N], the voltage breakdown (V_{br}) was determined by using the Interpolation Method:

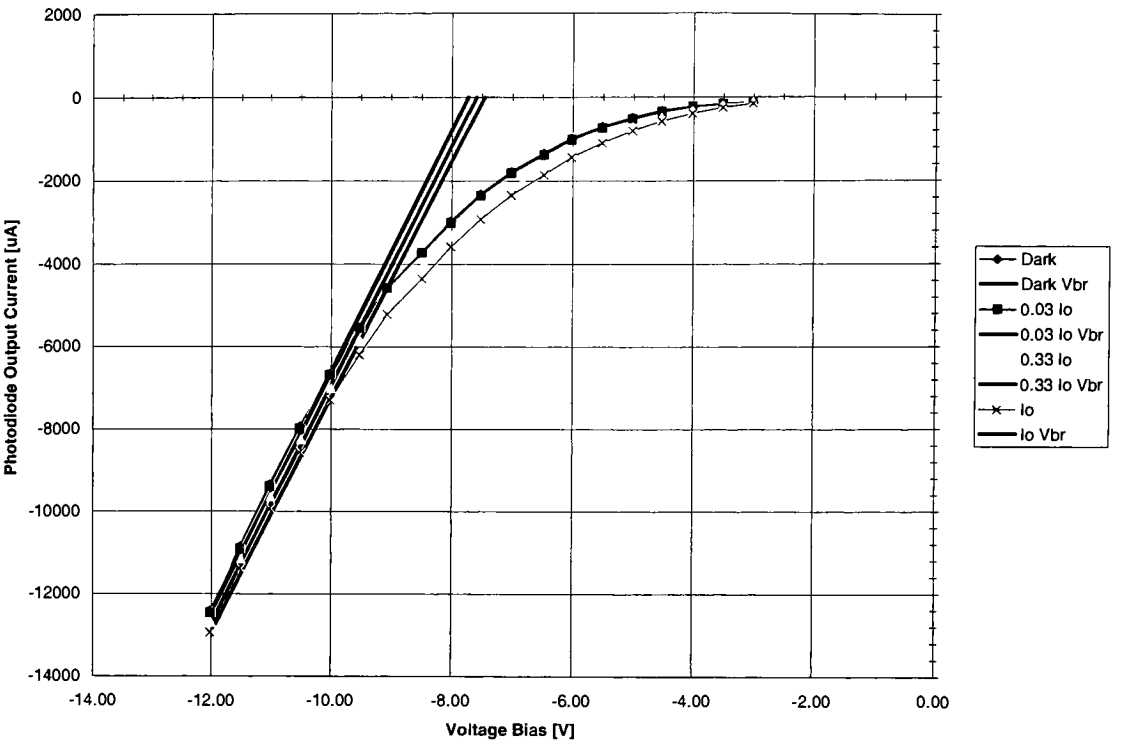

Figure 4.2.5: I-V Plot with Breakdown Voltage Interpolation Lines (W4 C7,3 D200,20,300,Y)

Because V_{br} is slightly different depending on the light intensity, the overall V_{br} number was obtained by averaging the four curves. Ideally, V_{br} should be the same at all light intensities. The V_{br} for this photodiode is at -7.624V.

As mentioned earlier that a typical diode should have a sharp transition into the avalanche regime, of all the photodiodes tested [W5 C9,10 D400,20,500,N], showed the most defined transition:

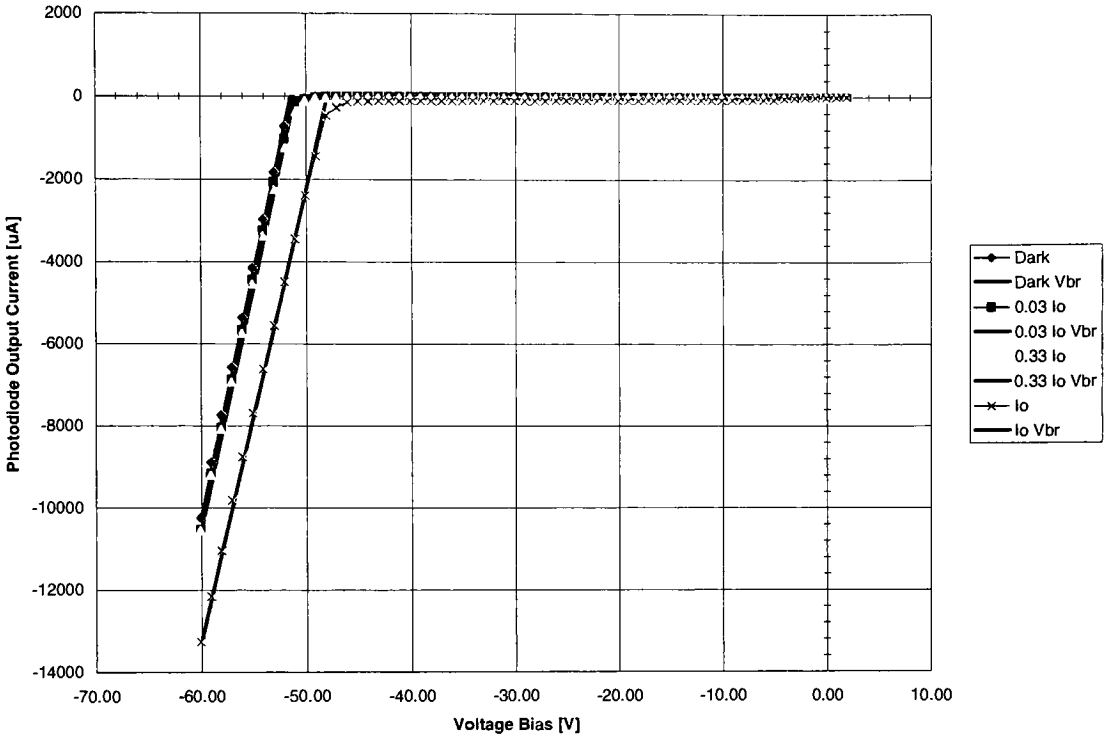

Figure 4.2.6: I-V Plot with Breakdown Voltage Interpolation Lines (W5 C9,10 D400,20,500,N)

It's also noted that [W5 C9,10 D400,20,500,N], and wafer 5 in general, showed devices with the highest breakdown voltage. Although wafer 5 devices do not have the advantage of having a guard ring, which prevents a premature low voltage breakdown at the junction periphery, it benefits from having a simpler design. It's also possible that wafer 5 unintentionally had a lower doping concentration; a result of processing non-uniformity.

Commercial avalanche photodiode devices have a much higher breakdown voltage, typically over 80V. The devices in this research were designed to have low breakdown voltages, but at a

tradeoff of making the photodiodes perform more like a Zener diode, which is explained in Section 4.4.2.

4.2.3 Dark Current

Using the V_{br} as the operating voltage, the dark current (I_{dark}) at V_{br} is -2484μA for [W4 C7,3 D200,30,400,N]:

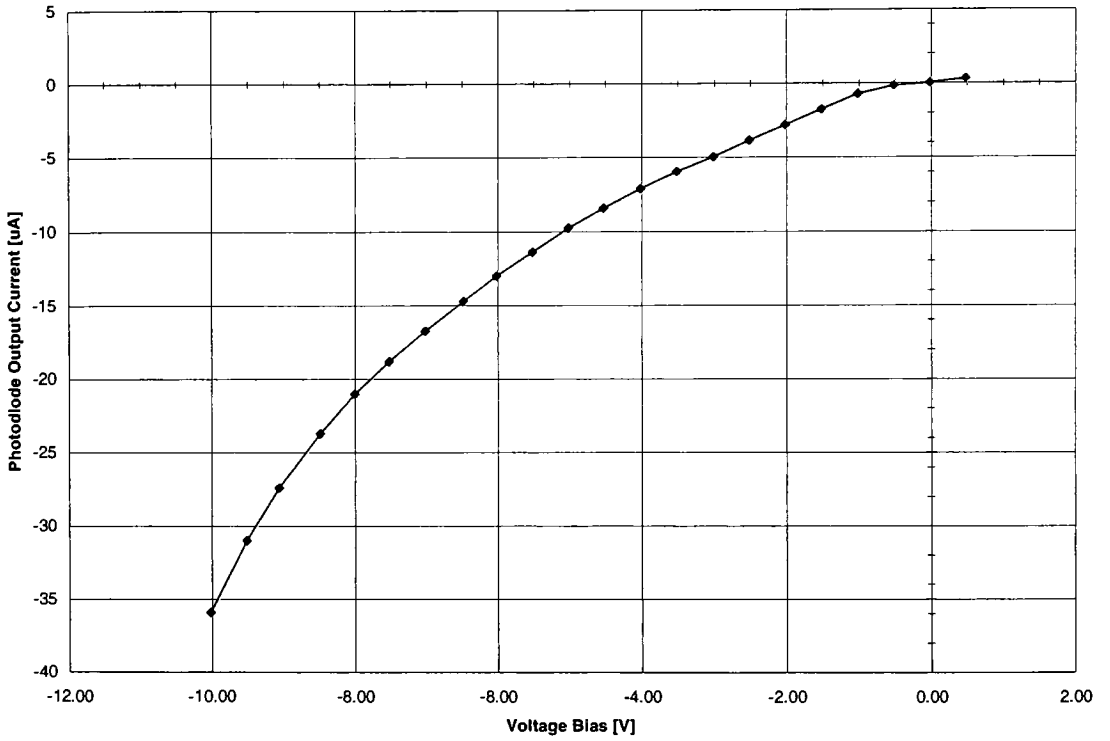

Figure 4.2.7: Dark Current (W4 C7,3 D200,30,400,N)

The expected trend of dark current is that the higher the reverse bias voltage, more dark current will be present. Since dark current arises from mobile electrons gaining energy from lattice vibrations, at higher reverse bias voltages, these electrons might initiate a cascading avalanche situation.

4.2.4 Gain

Quoting gain (M) at V_{br} as the operating voltage, the gain of [W4 C7,3 D200,30,400,N] is 22677:

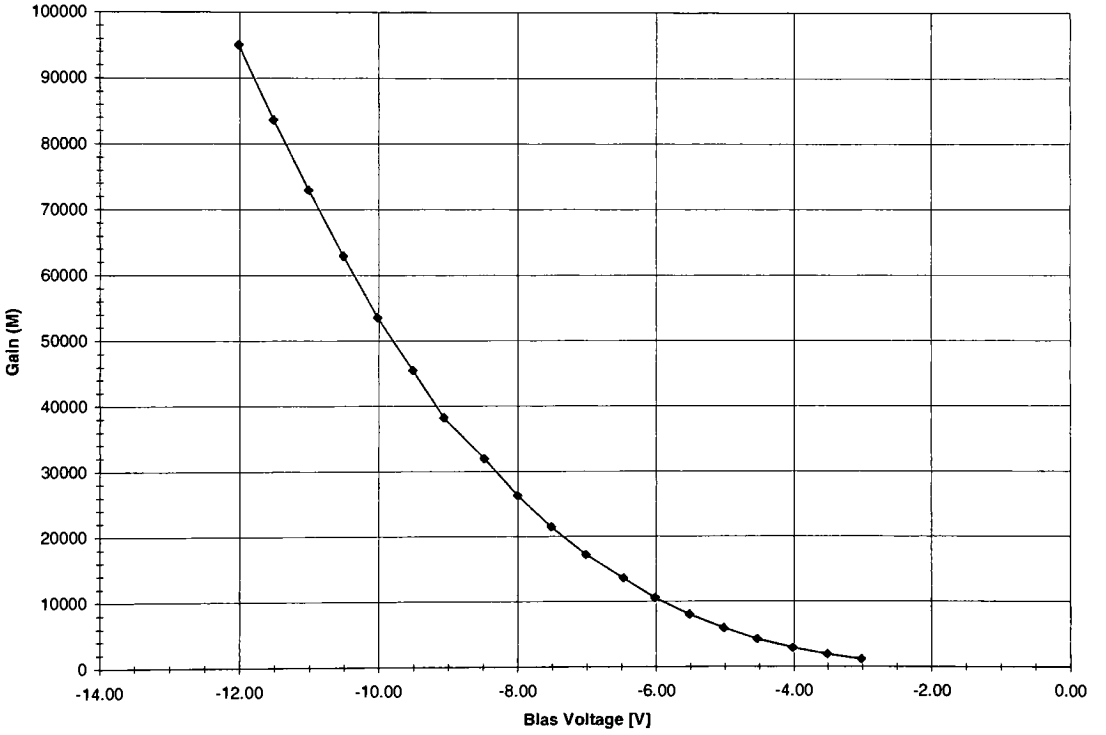

Figure 4.2.8: Gain (W4 C7,3 D200,20,300,Y)

The general trend of this gain curve is similar in all the photodiodes tested. Comparing to gain curves as released by Perkin Elmer, photodiode [W4 C7,3 D200,30,400,N] comes closest to their data:

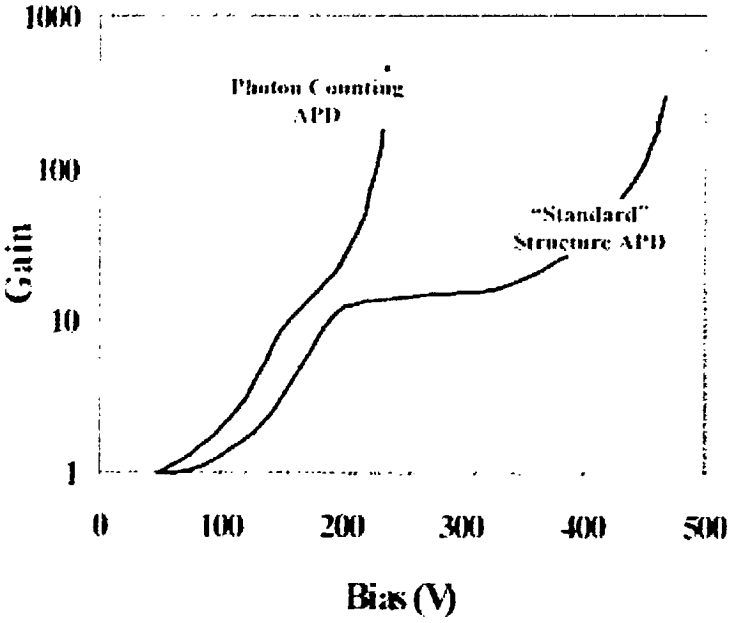

Figure 4.2.9: Gain (Perkin Elmer)

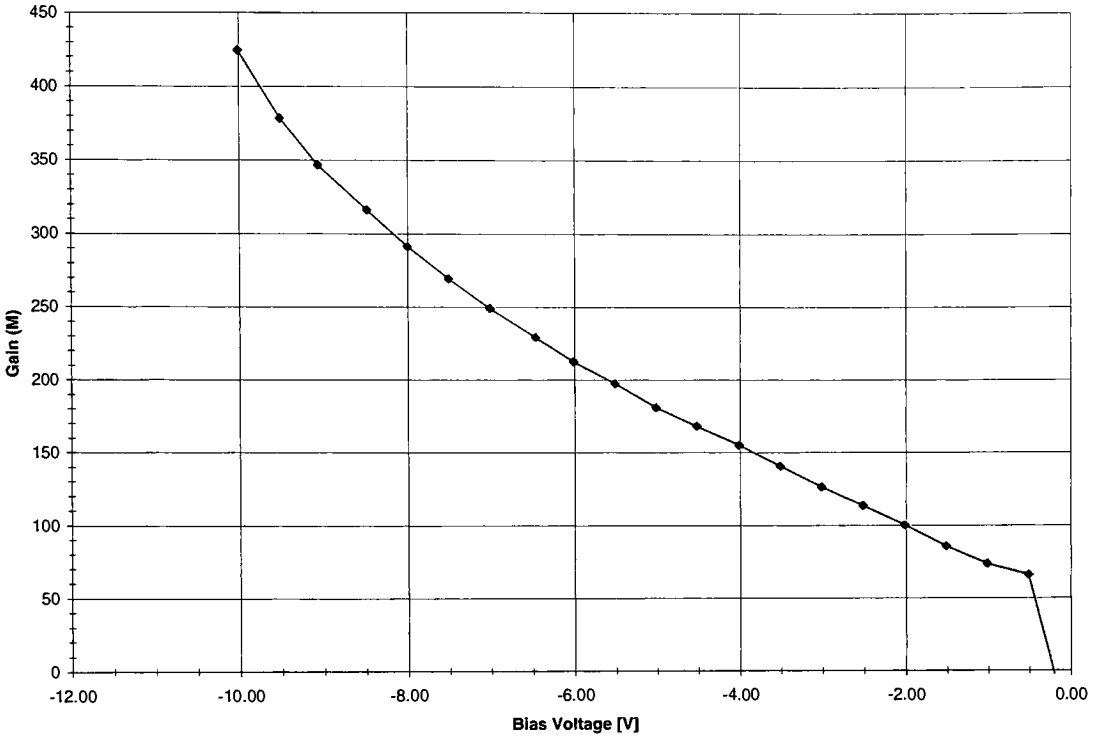

Figure 4.2.10: Gain (W4 C7,3 D200,30,400,N)

It is noted here again that Figure 4.2.9 shows the reverse bias voltage as a positive scale while data generated from this research uses the convention of plotting the reverse bias voltage as a negative scale.

The fabricated devices have higher gain output than commercial devices. This is due to the high doping level used, which resulted in a high electric field around the p-n junction region.

4.2.5 Spectral Response

Plotting the spectral response curve of photodiode [W4 C7,3 D200,20,300,Y], its peak is around 500nm:

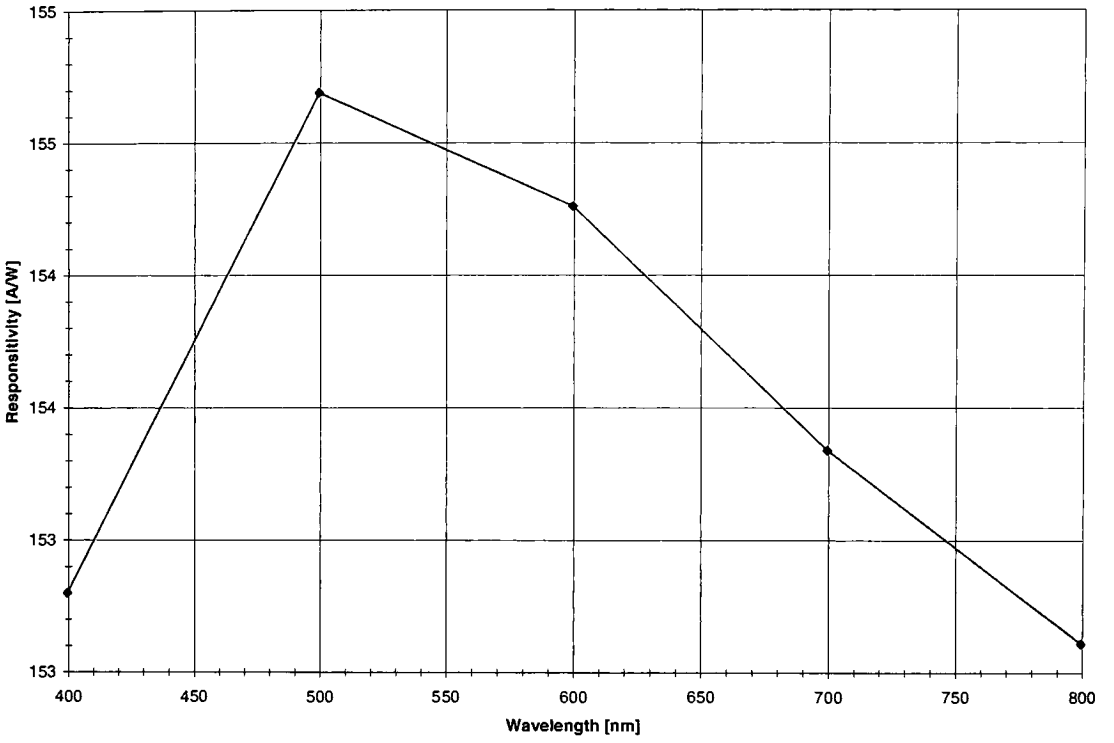

Figure 4.2.11: Responsitivity vs. Wavelength (W4 C7,3 D200,20,300,Y)

The peak of this photodiode is lower than typically measured in the rest of the photodiodes tested. The typical response of the photodiodes are closer to photodiode [W5 C9,10 D400,20,500,N], where the peak is around 600nm:

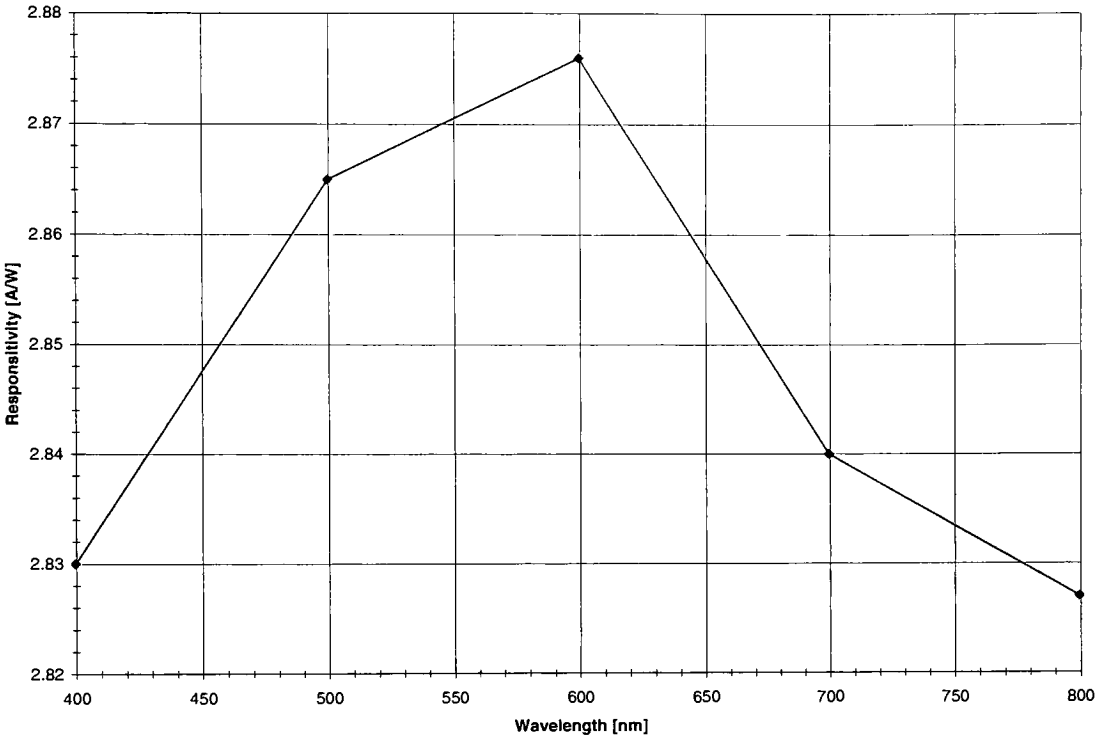

Figure 4.2.12: Responsitivity vs. Wavelength (W5 C9,10 D400,20,500,N)

The peak of the spectral response can be tailored by changing the impurity junction depth into the device. As explained in Section 2.1.2.1, longer wavelengths are absorbed deeper into the silicon. If the long wavelengths are absorbed beyond the depletion region, the electron-hole pair has a much higher chance to recombine before it is swept into the depletion region.

In comparing to commercial devices, the fabricated devices in this research tend to have the spectral peak at a lower wavelength. Most commercial devices are around 800nm.

4.2.6 Responsitivity

The responsitivity is calculated at unity gain (M = 1) is 0.2801A/W, which is equivalent to a quantum efficiency (QE) of 0.580 electrons per photon. See Appendix 6.5 for responsitivity to QE conversion details. The responsitivity is quoted at 600nm wavelength:

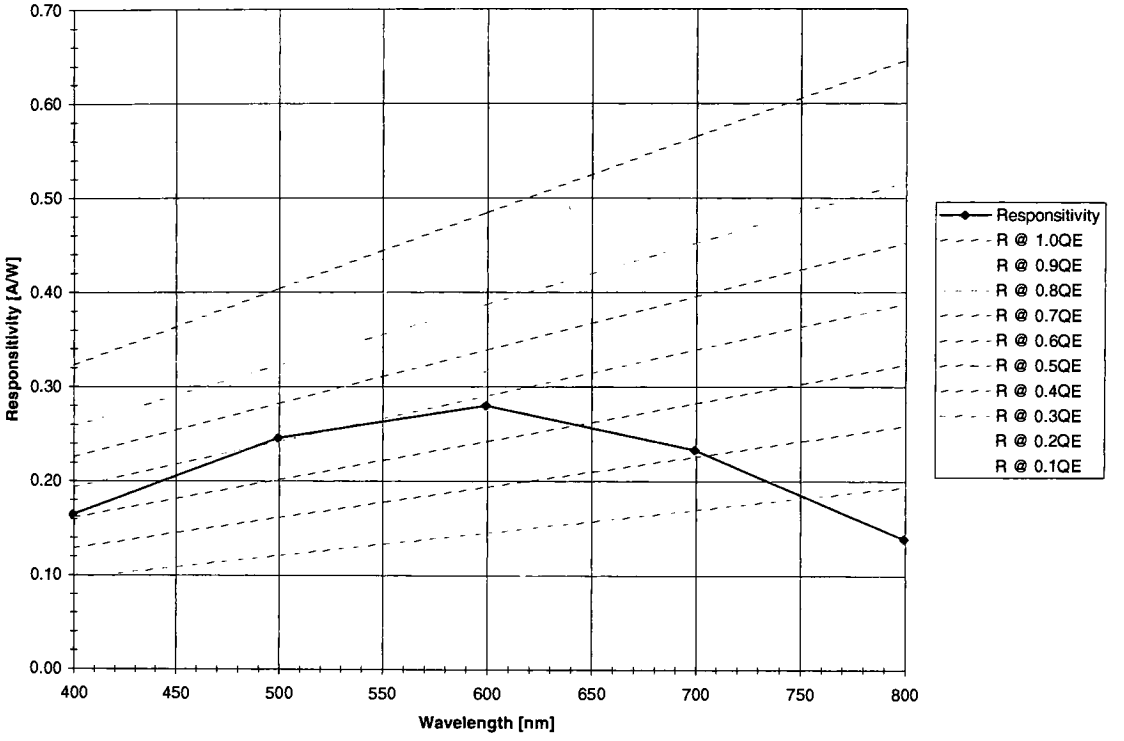

Figure 4.2.13: Responsitivity @ M=1 (W4 C7,3 D200,20,300,Y)

Examining the responsitivity of commercially available photodiodes, the responsitivity should peak close to 1000nm, near the energy band gap of silicon:

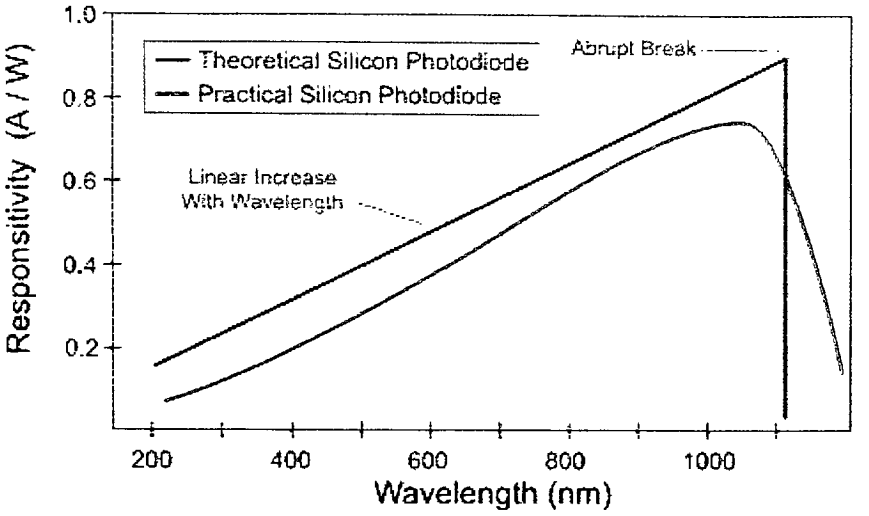

Figure 4.2.14: Practical Silicon Photodiode Responsitivity [Kruger, 2002]

Section 4.4.3 will discuss the details of why the photodiodes tested have low responsitivity.

4.2.7 Noise Equivalent Power

Noise Equivalent Power (NEP) is defined as the signal power required to achieve a unity signal-to-noise ratio within a one second integration. For this research, the equation is:

$$NEP = \frac{-I_{dark}}{R}$$

Equation 4.5: Noise Equivalent Power (NEP)

Where I_{dark} is the dark current [A] and R is the responsitivity [A/W].

The noise equivalent power (NEP) of [W4 C7,3 D200,20,300,Y] at V_{br} is 0.00887W. As expected, note that as the gain of the photodiode increases, the NEP increases somewhat linearly:

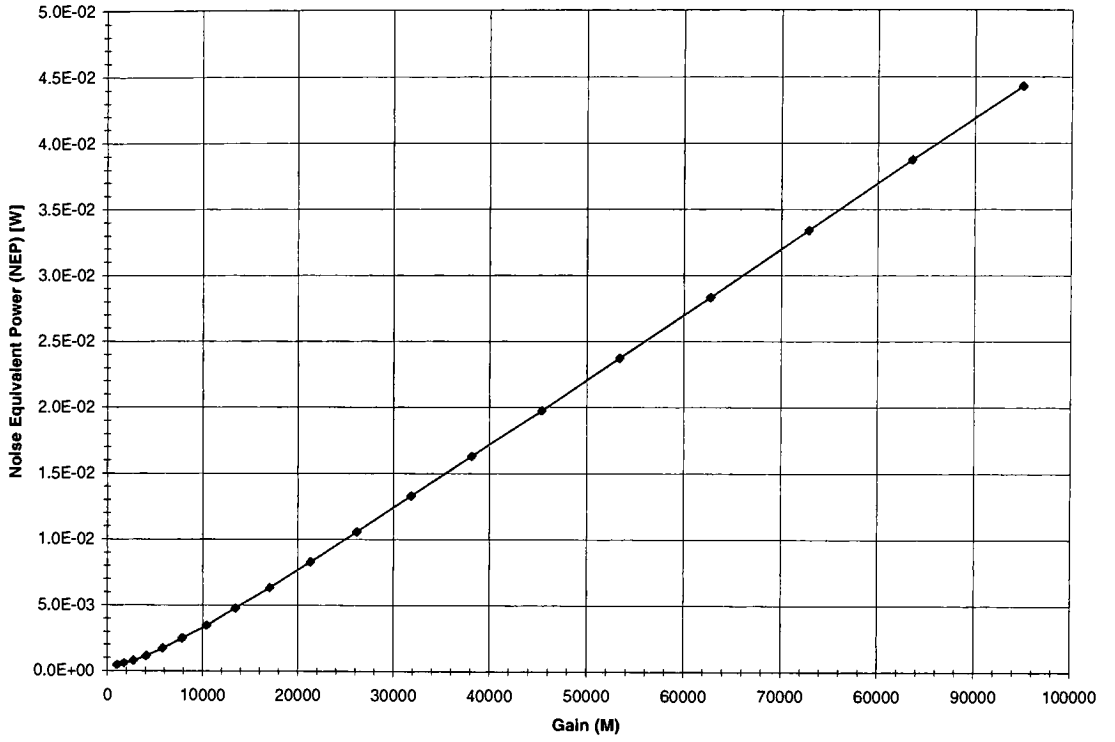

Figure 4.2.15: Noise Equivalent Power (NEP) (W4 C7,3 D200,20,300,Y)

4.3. APD Array Results

In designing APD arrays, one area of concern is the crosstalk between individual elements. Because APDs operate on the nature of internal gain, there is a higher chance of crosstalk between pixels than compared to, as an example, regular PIN photodiode arrays. The random

paths of the electrons during the avalanche mechanism may possibly wander into the adjacent pixel and trigger a signal there instead.

The simplest solution to the problem would be to increase the distance between pixels as far as possible. Unfortunately, this would decrease the spatial resolution of the array. Another solution, which is beyond the scope of this research, is to use device structures that would minimize the lateral fields of a photodiode, possibly by having the same equipotential as the pixels themselves [Webb and McIntyre, 1984].

From just spatially spacing the arrays of photodiodes, this research shows that the signal is not perfectly isolated and that there is a certain level of crosstalk as a function of distance.

Since only a few arrays were found to be fully successful, data was not complete in characterizing the APD array design. The following arrays were found to be successfully working:

Array 1:[W1 C11,10 D400,20,750,N]

Array 2:[W3 C5,8 D400,20,750,N]

Array 3:[W4 C5,6 D400,20,750,N]

Array 4:[W4 C10,9 D200,20,300,N]

In mapping the crosstalk plot as described in Section 4.1.5, this is the result:

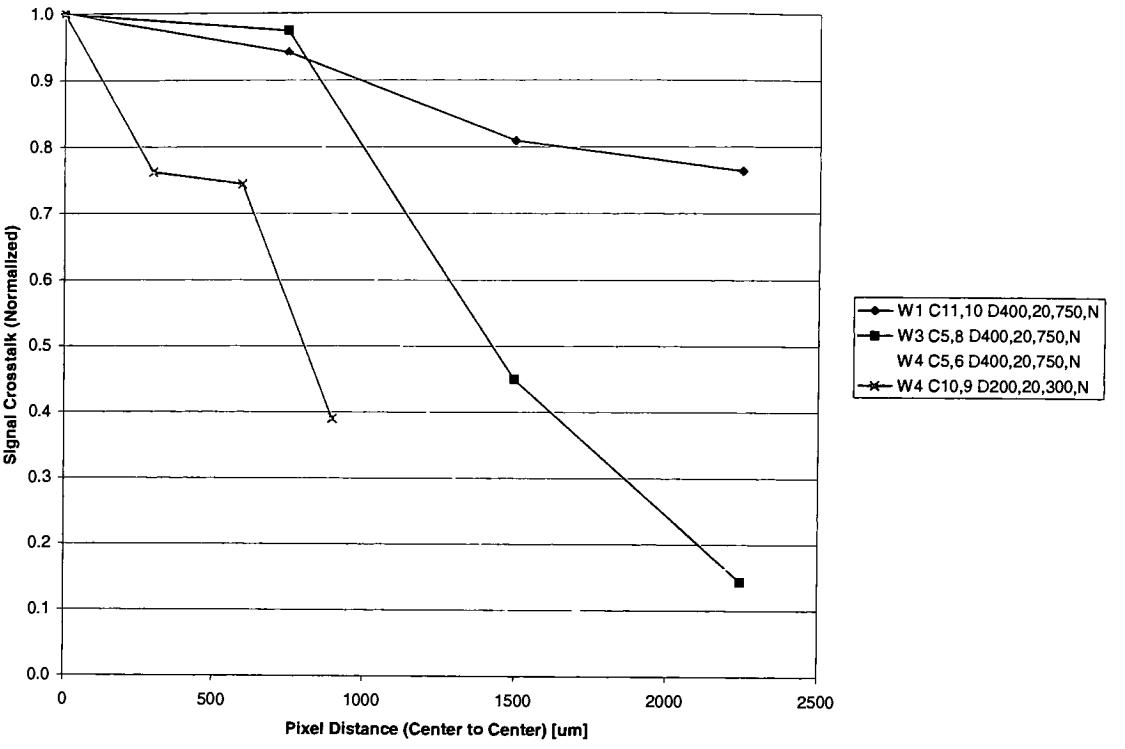

Figure 4.3.1: Crosstalk Plot

Arrays 1 to 3 have the same pixel to pixel distance, 750μm. Array 4 has a pixel to pixel distance of 300μm. Arrays 1 to 3 exhibit the same general response and are somewhat in agreement at a distance of 750μm. The plot also suggests that the guard ring features do lower crosstalk and minimize lateral fields as Array 4 shows.

4.4. Problems of Non-Working Devices

The major challenge of this research was to have working, uniform photodiodes to test. As discussed in Section 3.5, the basis for the lack of performance from the fabricated devices were due to wrong doping levels, namely for the p layer. The effect was that, although it performed somewhat similar to true APDs, it had many "characteristics" that were not favorable.

Specifically, the avalanche photodiodes did not perform as expected for at least one of the following reasons:

1. No signal.
2. Low sensitivity.
3. Uncontrolled voltage breakdown.
4. Low responsitivity.
5. Performance uniformity.

4.4.1 No Signal

In order to connect to the photodiodes, the needle probes make contact to the metal pads, which are 100μm x 100μm in size. When trying to connect to some photodiodes, it is apparent that the connection could not be made, as there was no current flow at any voltage level.

The reason is simple; the metal interconnect from the metal pad to the photodiode has discontinuities. The most likely places of discontinuities are either along the thin interconnect from the pad to the photodiode (Figure 4.4.1), or at the junction near the photodiode edge (Figure 4.4.2):

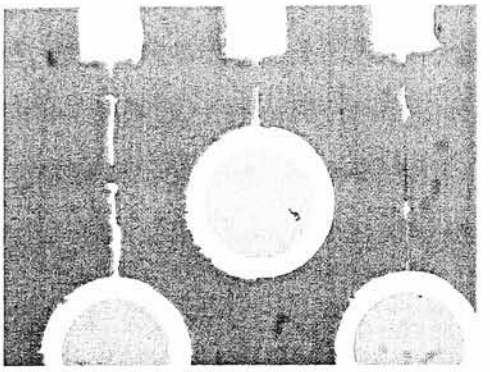

Figure 4.4.1: Metal Discontinuity Example A

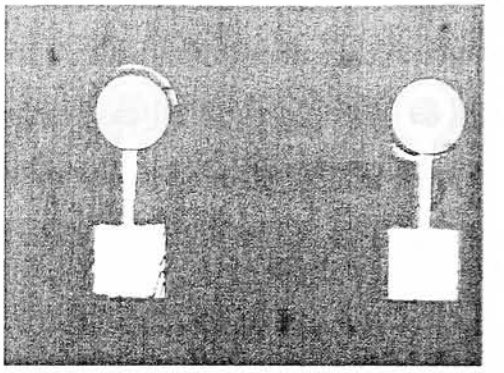

Figure 4.4.2: Metal Discontinuity Example B

The metal layer, fabricated using aluminum, was wet etched. Although both discontinuities are a result of overetching, the break in the thin interconnect is a result from having too small of a geometry in width and the junction break is from step height differences between the layers.

Referring to the cross-section of the device (Figure 3.1.3), there is a large step height from the top of the oxide to the photodiode edge. When depositing the aluminum layer via sputtering, it is subject to step coverage problems, where the aspect ratio from the top of the oxide to the top of the silicon bulk may be too great. This leads to thinning of the aluminum at the edge and it would be etched faster than the rest of the layer [Wolf and Tauber, 1986]. The oxide thickness in these wafers was approximately ~4950Å thick.

4.4.2 Uncontrolled Voltage Breakdown

Most APDs tested exhibited a very soft knee during transition into the avalanche regime, as illustrated in Figure 4.2.1. This makes determining the breakdown voltage difficult and uncertain.

This characteristic is typically known as "soft" breakdown and is an indication that there is a presence of tunneling current occurring [Forrest, et. al., 1980], [Laifer and Gilad, 2002]. Tunneling current occurs in a diode when both sides of the p-n junction are so heavily doped that the depletion width is less than 10^{-6}cm. To have such small depletion widths, the lighter doped side of the p-n junction would still be in excess of approximately $10^{17}/cm^3$. This causes the width of the potential energy barrier to become very thin. As Section 2.1.3.1 described, another way for current to flow in reverse bias besides the avalanche mechanism is by the Zener process, where the particle tunnels through the energy barrier instead of gaining additional energy to overcome it. This is a quantum mechanical phenomenon and doesn't have a classical equivalent.

One device that utilizes the tunneling current mechanism is the Zener diode. It was found that the devices in this research were inadvertently designed similarly to Zener diodes; the p-n junction was degenerately doped. A low breakdown voltage was desired, which is typical of Zener diodes. In order to achieve low breakdown voltages, heavily doped p-n junctions are needed, which triggered the whole tunneling current situation and resulting in the "soft" breakdown found in the I-V curves of the devices of this research.

4.4.3 Low responsitivity

Responsitivity values are obtained indirectly through calculations from measured values of the photodiodes. Compared to commercial devices, the photodiodes in this research have a much lower responsitivity, especially at the longer wavelengths.

In this research, the depletion width of the p-n junction is what causes the low responsitivity. Here is the responsitivity equation reprinted:

$$R = \left(\frac{q}{h\upsilon}\right)\left[1 - e^{(-\alpha_s w)}\right](1 - R_f)$$

Equation 4.6: Reprint of Equation 4.4

The equation used to calculate the depletion width (w) is based on a linearly degraded junction model:

$$W = \left[\frac{12 K_s \varepsilon_o}{q a}(V_{bi} - V_A)\right]^{\frac{1}{3}}$$

Equation 4.7: Depletion Width, Linearly Graded Junction

The built-in voltage, V_{bi}, is solved by iteration using the following equation:

$$V_{bi} = \frac{2kT}{q} \ln\left[\frac{a}{2n_i}\left(\frac{12 K_s \varepsilon_o}{q a} V_{bi}\right)^{\frac{1}{3}}\right]$$

Equation 4.8: Built-in Voltage, Linearly Graded Junction

Where a is the grading constant. Details of Equation 4.7 and Equation 4.8 are shown in Appendix 6.6. With the photodiodes in this research having a peak doping of $2.635*10^{23}/cm^3$ at a junction depth of 0.0731μm for n+ implant, and a peak doping of $1.975*10^{23}/cm^3$ at a junction depth of 0.2801μm for p+ implant (see Section 3.2.2), the typical grading constant is $3.188*10^{27}/cm^4$. Because of the heavy doping levels of the multiplication region (namely the p layer that was too heavily doped), the depletion width is a thin 0.00542μm at an applied voltage of 5.2V, making the responsitivity of the devices very low.

A chip designer has only two parameters to control, without changing the material used, in order to control responsitivity: depletion width and surface reflectivity of light (R_f). A designer can improve responsitivity by merely getting more light into the silicon. Or rather, decrease the surface reflectivity of the light. This involves fabricating an anti-reflection coating on top of the photodiodes and other standard practices that are not concentrated by this research.

The other is to increase the depletion width. As the depletion width is increased in Equation 4.4, responsitivity increases. The effect is more pronounced at longer wavelengths, due to increased absorption coefficient, lower reflectivity and higher photon energy at the longer wavelengths.

As an example, if diode [W5 C9,10 D400,20,500,N] had a depletion width of 0.108μm instead of 0.0108μm (biased at the breakdown voltage of –50.43V), the responsitivity would have increased as such:

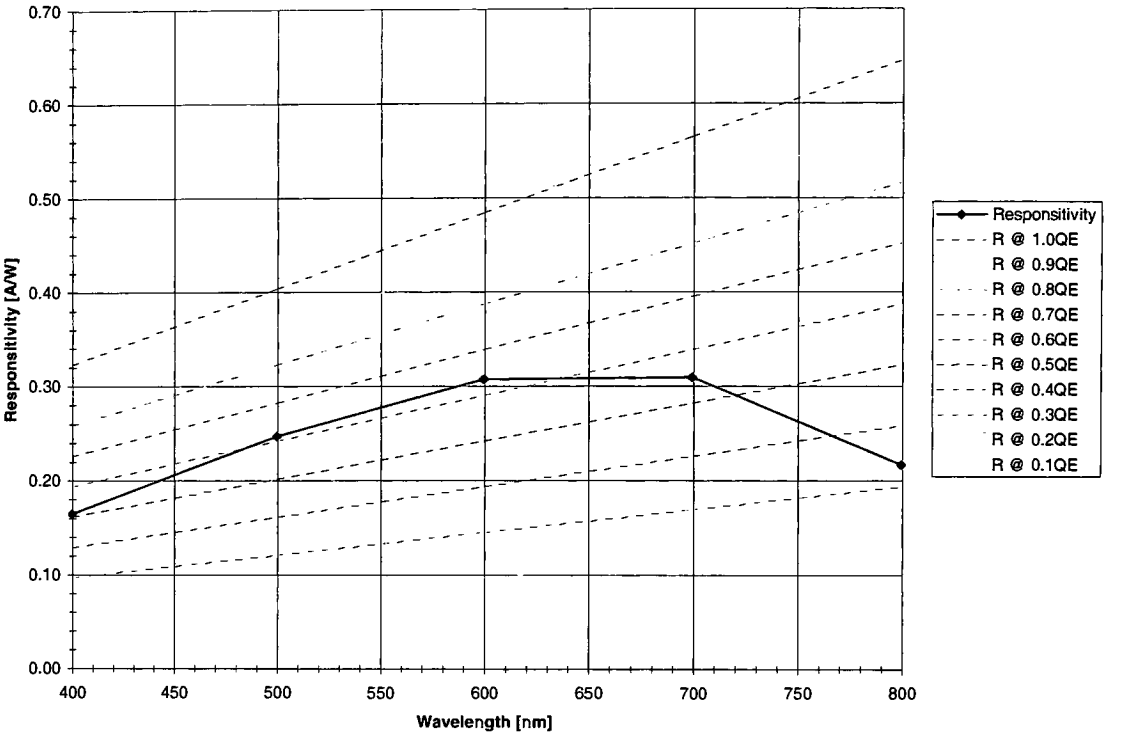

Figure 4.4.3: Responsitivity @ M=1 (W5 C9,10 D400,20,500,N) (@ 0.01μm Depletion Width)

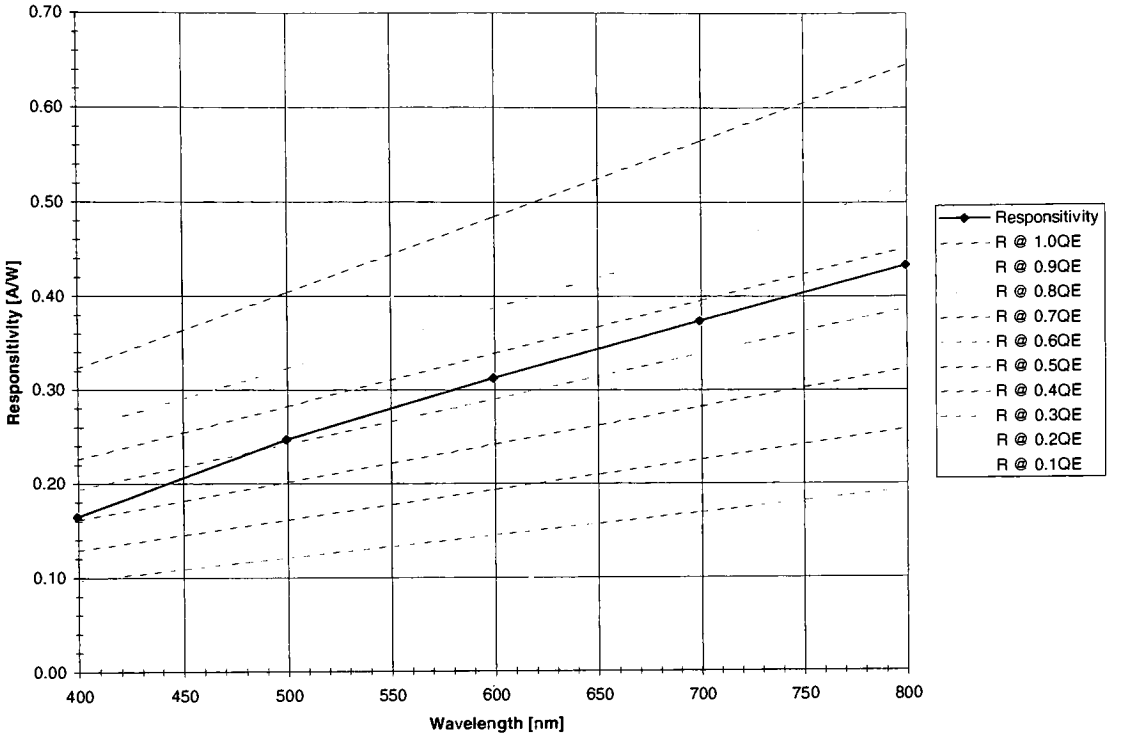

Figure 4.4.4: Responsitivity @ M=1 (W5 C9,10 D400,20,500,N) (@ 0.1μm Depletion Width)

The depletion width is controlled by the amount of doping used.

4.4.4 Performance Uniformity

Even when the devices exhibited a general I-V curve of a photodiode, there was an issue of having the devices perform uniformly. As an example, photodiodes [W4 C7,3 D200, 20, 300, N] and [W4 C10,9 D200, 20, 300, N] are of the same dimensions on the same wafer. Their I-V curve is widely different:

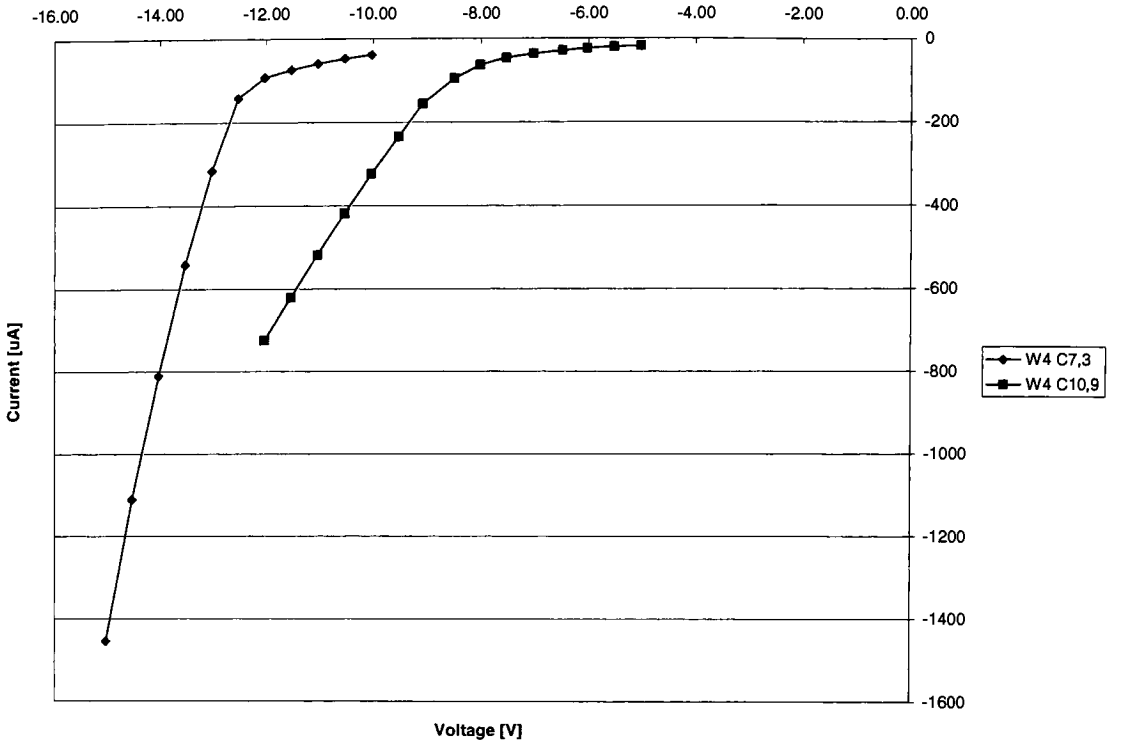

Figure 4.4.5: [W4 C7,3 D200,20,300,N] and [W4 C10,9 D200,20,300,N] Comparison @ 100% Illumination

By just looking at the differences in the breakdown voltage suggests that implant doping levels in the p-n junction are very different. Figure 2.1.18 shows how doping levels affect the breakdown voltage. At breakdown voltages of a few volts, as in the case of [W4 C7,3 D200,20,300,N] and [W4 C10,9 D200,20,300,N], a significant change in doping is needed in order for a small amount of voltage change.

As previous sections have described, the doping level is an integral part of the device characteristic as it affects an avalanche photodiodes' responsitivity, gain, photon absorption, etc.

4.5. Solutions for Improvement

The following are solutions that rectify the problems outlined in the previous sections and improve on the design. These steps are follow-up suggestions for any future research.

4.5.1 Lower Doping Levels / Correct P Layer Doping

In order to have correct working APDs, the doping levels should be lower. Specifically, the fabricated devices had too high of a doping for the p layer. As mentioned in Section 3.5, the highly doped p layer had effectively contained the depletion layer to just between the n+ and p layers. If the p layer was doped lighter, then the depletion layer could extend into the intrinsic layer when under sufficient reverse bias. Beyond the incorrect device designed, the high doping also made the devices exhibit a "soft" breakdown voltage and have a low responsitivity.

The devices exhibit "soft" breakdown due to excessive tunneling current taking place. If the doping levels are lowered, the depletion width would increase and the width of the energy barrier would be wider, decreasing the chance of tunneling and breakdown would occur more due to avalanching. A wider depletion width would also increase responsitivity. As discussed in Section 4.4.3, the depletion width would be the only factor that a device designer would have easy control over.

The original intention of the design was to have an avalanche photodiode with a low breakdown voltage for portability reasons. In order to have low breakdown voltages high doping levels are

needed. Unfortunately, a design tradeoff exists between low voltage breakdown and having the occurrence of tunneling current.

4.5.2 Fabrication Control and Uniformity

To realize a design of an avalanche photodiode array, good fabrication control is needed. The performance of the devices in this research was subject to fabrication problems, mainly uniformity problems. The two fabrication processes that would improve the current devices dramatically would be the aluminum etch process and implant process.

Devices that did not work because of no signal showed obvious problems with the aluminum interconnect (see Figure 4.4.1 and Figure 4.4.2). The process used to etch the aluminum was a wet etch. Because wet etch is an isotropic etch, where it etches uniformly in all directions, sharp corners of the interconnects erode quicker due to a larger exposed surface area. A more suitable etch to use in future research is an aluminum etch that is anisotropic.

The design variations between the five wafers are not extreme in differences. As Table 3.1 listed out, the variations are either to have a guard ring, an extra P layer, or a different metal layer. The only element that would affect an individual photodiode's performance would be the extra P layer. In testing the devices, it was found that device characteristics varied widely from wafer to wafer and even within wafer. As an example, Wafer 5 exhibited the highest breakdown voltages in general. Yet, with the exception of having a guard ring, it is identical to Wafer 4. Figure 4.4.5 illustrates the variability within wafer. The differences in breakdown voltage indicate that the doping levels are different. The breakdown voltage change between ~8V and ~12V are significant, where the doping levels are almost an order of magnitude in difference.

5. Conclusion

The original direction of this research was to realize an avalanche photodiode array device with an onboard discriminator circuit for readouts. The array would be controlled via computer I/O and possibly be portable for in-the-field use.

To reach that stage, several intermediate steps were needed. The first step is to have working individual APDs since that has not been designed or fabricated at the RIT Microelectronic Fab. As this research shows, the first attempt in the design and fabrication needed improvement, as it has been found that the doping levels were incorrect.

Individual devices did not function mainly due to design error problems. In the pursuit of designing the devices to be usable in portable applications, low breakdown voltages were needed. To achieve the low breakdown voltages, high doping levels were needed for the p-n junction. In doing that, the devices ran into two major problems, current tunneling and low responsitivity. Both problems are attributed to having too high of a doping for the p layer, resulting in a too small of a depletion width that didn't extend into the intrinsic region. As the device is put under increased reverse bias, current tunneling occurs, where reverse current started trickling before the actual breakdown. This decreased the ability for the device to have a clear on/off current output. Low responsitivity, especially at higher wavelengths, is also mainly caused by the small depletion width.

Once individual photodiodes are properly designed, fabricating arrays of working photodiodes present another hurdle. During testing of the photodiodes in this research, it was concluded that process uniformity, especially within wafer, need to be better controlled. The two main areas to concentrate for improvement is the aluminum etch and implant processes.

In order to reach the ultimate goal of having an APD array with onboard discriminators, device design and fabrication control need to be improved. After the design and fabrication issues of the above are addressed, the next steps of research would be to either integrate the onboard discriminators and/or enhance the performance of the APD array by increasing the spatial density of the photodiodes.

6. Appendix

6.1. Oxide Thickness Calculation

Oxide Growth Calculation [44]
(For Diffusion-Rate Limited Regime in Wet Oxidation on Bare Silicon)

Constants are for (100) silicon in wet oxidation.

$K1 := 4.02 \cdot 10^{-6}$ [um]

$E1 := 1.29$ [eV]

$K2 := 214$ [um2/hr]

$E2 := 0.71$ [eV]

$k := 8.617 \cdot 10^{-5}$ [eV/K]

Process parameters.

$t := 1.53$ [hr]

$T := 1273$ [K]

$$A := K1 \cdot e^{\frac{E1}{k \cdot T}}$$

$$B := K2 \cdot e^{\frac{-E2}{k \cdot T}}$$

$$x := \left(\frac{A}{2}\right) \cdot \left(\sqrt{1 + \frac{t}{\frac{A^2}{4 \cdot B}}} - 1\right)$$

$x = 0.4991$ [um]

6.2. Ion Implant and Drive-In Calculation

Guard Ring Impurity Profile

Constants:

$eV := 1.6 \cdot 10^{-19} J$ Electron Volt

$k := 8.617 \cdot 10^{-5} \cdot \frac{eV}{K}$ Boltzmann Constant

$x := 0, 0.01 \cdot 10^{-6} m .. 1.5 \cdot 10^{-6} m$ Depth

Wafer Parameters:

$Nb(x) := 1 \cdot 10^{14} \cdot cm^{-3}$ Background Doping

Implant Parameters:

$R_p := 0.073 \, 10^{-6} m$ Projected Range

$dR_p := 0.0305 \, 10^{-6} m$ Projected Straggle

$N' := 1.6 \cdot 10^{18} \cdot cm^{-2}$ Implant Dose

Diffusion Parameters:

$D_o := 03.85 \cdot \frac{cm^2}{s}$ Frequency Factor [Boron(0.76), Phos(3.85)]

$E_a := 3.66 \cdot eV$ Activation Energy [Boron(3.46), Phos(3.66)]

$T1 := 1273K$ Diffusion Temperature 1

$t1 := 4.5hr$ Diffusion Time 1

$T2 := 1223K$ Diffusion Temperature 2

$t2 := 2.3hr$ Diffusion Time 2

Implant Calculation:

$$N_{xrp} := \frac{N'}{\sqrt{2\pi}\cdot dR_p}$$

$N_{xrp} = 2.093\times 10^{23}\ \frac{1}{cm^3}$ Peak Concentration [N(x=Rp)]

$$Ni(x) := N_{xrp}\cdot e^{\frac{-(x-R_p)^2}{2\cdot dR_p^{\,2}}}$$ Impurity Profile After Implant

Drive-in Calculation:

$$D1 := D_o\cdot e^{\frac{-E_a}{k\cdot T1}}$$ Diffusion Coefficient

$$D2 := D_o\cdot e^{\frac{-E_a}{k\cdot T2}}$$

$$Nd(x) := \frac{N'}{\sqrt{2\cdot\pi}\cdot\sqrt{dR_p^{\,2} + 2\cdot(D1\cdot t1 + D2\cdot t2)}}\cdot e^{\left[\frac{-(x-R_p)^2}{2\left[dR_p^{\,2}+2\cdot(D1\cdot t1+D2\cdot t2)\right]}\right]}$$ Impurity Profile After Drive-in

$N_d(0) = 2.795\times 10^{22}\ \frac{1}{cm^3}$ Surface Doping Concentration

$$xj := \left| \begin{array}{l} i \leftarrow 0m \\ \text{while } \left|Nd(i) - Nb(i)\right| > 1\cdot 10^{19}\cdot m^{-3} \\ \quad i \leftarrow i + 1\cdot 10^{-9}m \end{array} \right.$$

$xj = 1.417\times 10^{-6}\ m$ Junction Depth

Profile Graph:

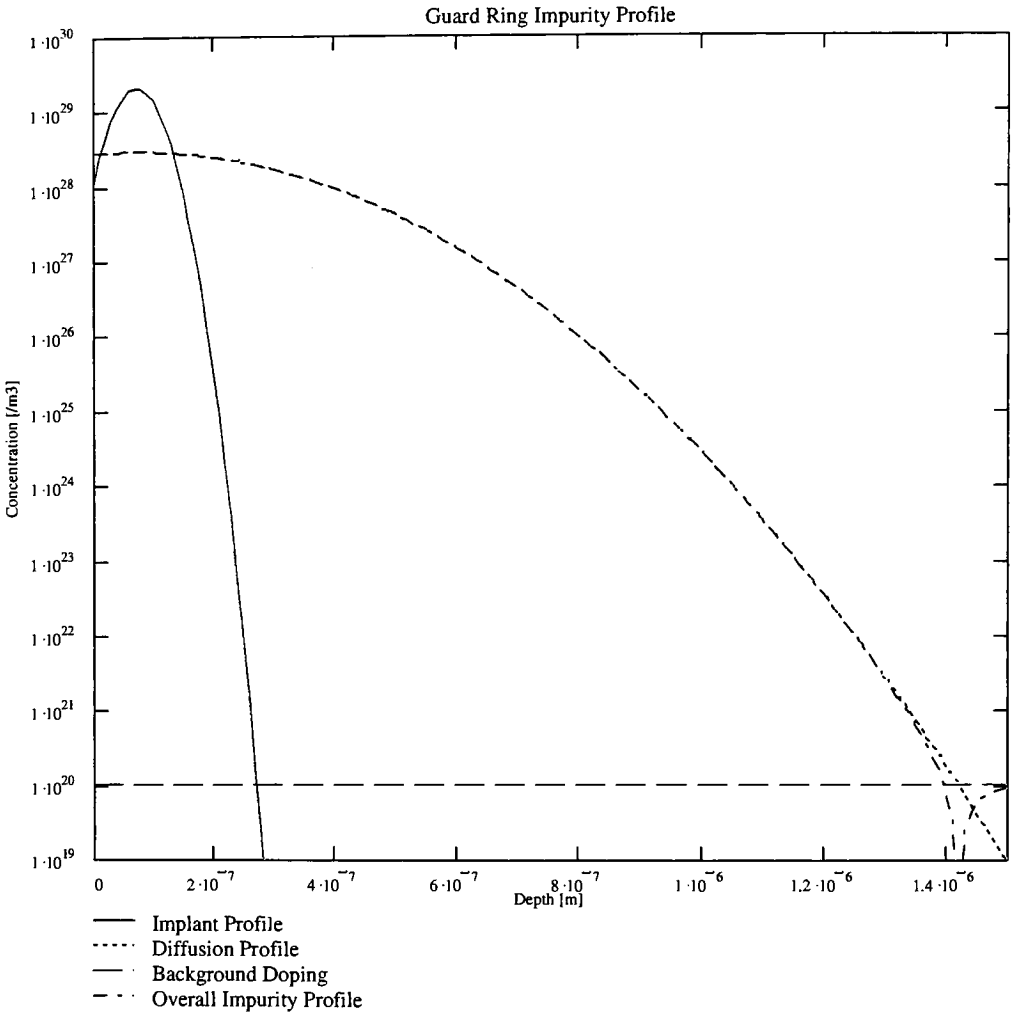

N+ / P+ Impurity Profile

Constants:

$eV := 1.6 \cdot 10^{-19} J$	Electron Volt
$k := 8.617 \cdot 10^{-5} \cdot \frac{eV}{K}$	Boltzmann Constant
$x := 0, 0.01 \cdot 10^{-6} m .. 1.5 \cdot 10^{-6} m$	Depth

Wafer Parameters:

$Nb(x) := 1 \cdot 10^{14} \cdot cm^{-3}$	Background Doping

Implant Parameters:

$R_{p1} := 0.073 \cdot 10^{-6} m$	Projected Range
$dR_{p1} := 0.0305 \cdot 10^{-6} m$	Projected Straggle
$N'1 := 5.2 \cdot 10^{18} \cdot cm^{-2}$	Implant Dose

Diffusion Parameters:

$D_{o1} := 03.85 \frac{cm^2}{s}$	Frequency Factor [Boron(0.76), Phos(3.85)]
$E_{a1} := 3.66 \cdot eV$	Activation Energy [Boron(3.46), Phos(3.66)]
$T1 := 1223K$	Diffusion Temperature
$t1 := 2.3hr$	Diffusion Time

Implant Calculation:

$$N_{xrp1} := \frac{N'1}{\sqrt{2\pi}\cdot dR_{p1}}$$

$N_{xrp1} = 6.802\times 10^{23}\ \frac{1}{cm^3}$ Peak Concentration [N(x=Rp)]

$$Ni1(x) := N_{xrp1}\cdot e^{\frac{-(x-R_{p1})^2}{2\cdot dR_{p1}^{\ 2}}}$$ Impurity Profile After Implant

Drive-in Calculation:

$$D1 := D_{o1}\cdot e^{\frac{-E_{a1}}{k\cdot T1}}$$ Diffusion Coefficient

$D1 = 3.181\times 10^{-15}\ \frac{cm^2}{s}$

$$Nd1(x) := \frac{N'1}{\sqrt{2\cdot\pi}\cdot\sqrt{dR_{p1}^{\ 2} + 2\cdot D1\cdot t1}}\cdot e^{\left[\frac{-(x-R_{p1})^2}{2\cdot\left(dR_{p1}^{\ 2}+2\cdot D1\cdot t1\right)}\right]}$$ Impurity Profile After Drive-in

$Nd1(0) = 1.714\times 10^{23}\ \frac{1}{cm^3}$ Surface Doping Concentration

$$xj1 := \left| \begin{array}{l} i \leftarrow 0m \\ \text{while } \left|Nd1(i) - Nb(i)\right| > 1\cdot 10^{19}\cdot m^{-3} \\ \quad i \leftarrow i + 1\cdot 10^{-9}m \end{array} \right.$$

$xj1 = 5.91\times 10^{-7}\ m$ Junction Depth

P+ Impurity Profile

Implant Parameters:

$R_{p2} := 0.28 \cdot 10^{-6} m$ Projected Range

$dR_{p2} := 0.064 \, 10^{-6} m$ Projected Straggle

$N'2 := 5.2 \cdot 10^{18} \cdot cm^{-2}$ Implant Dose

Diffusion Parameters:

$D_{o2} := 0.76 \cdot \frac{cm^2}{s}$ Frequency Factor [Boron(0.76), Phos(3.85)]

$E_{a2} := 3.46 \cdot eV$ Activation Energy [Boron(3.46), Phos(3.66)]

$T2 := 1223K$ Diffusion Temperature

$t2 := 2.3hr$ Diffusion Time

Implant Calculation:

$$N_{xrp2} := \frac{N'2}{\sqrt{2\pi}\cdot dR_{p2}}$$

$$N_{xrp2} = 3.241\times 10^{23}\,\frac{1}{cm^3}$$ Peak Concentration [N(x=Rp)]

$$Ni2(x) := N_{xrp2}\cdot e^{\frac{-(x-R_{p2})^2}{2\cdot dR_{p2}^{\,2}}}$$ Impurity Profile After Implant

Drive-in Calculation:

$$D2 := D_{o2}\cdot e^{\frac{-E_{a2}}{k\cdot T2}}$$ Diffusion Coefficient

$$D2 = 4.19\times 10^{-15}\,\frac{cm^2}{s}$$

$$Nd2(x) := \frac{N'2}{\sqrt{2\cdot\pi}\cdot\sqrt{dR_{p2}^{\,2} + 2\cdot D2\cdot t2}}\cdot e^{\left[\frac{-(x-R_{p2})^2}{2\cdot\left(dR_{p2}^{\,2}+2\cdot D2\cdot t2\right)}\right]}$$ Impurity Profile After Drive-in

$$Nd2(0) = 5.658\times 10^{21}\,\frac{1}{cm^3}$$ Surface Doping Concentration

$$xj2:= \left|\begin{array}{l} i \leftarrow 0m \\ \text{while } \left|Nd2(i) - Nb(i)\right| > 1\cdot 10^{19}\cdot m^{-3} \\ \quad i \leftarrow i + 1\cdot 10^{-9}m \end{array}\right.$$

$$xj2 = 9.66\times 10^{-7}\,m$$ Junction Depth

N+ / P+ Profile Calculations

$$\text{PNJuncDepth} := \left| \begin{array}{l} i \leftarrow 0 \cdot m \\ \text{while } Nd1(i) > (1.001 \cdot Nd2(i)) \vee Nd1(i) < (0.999\, Nd2(i)) \\ \quad i \leftarrow i + 1 \cdot 10^{-10} \cdot m \end{array} \right.$$

$$\text{PNJuncDepth} = 1.73 \times 10^{-7}\, m$$

$$Nd1(\text{PNJuncDepth}) = 1.176 \times 10^{29}\, \frac{1}{m^3}$$

$$Nd2(\text{PNJuncDepth}) = 1.176 \times 10^{29}\, \frac{1}{m^3}$$

$$\text{Nd1Peak} := \left| \begin{array}{l} i \leftarrow 0 \\ \text{while } Nd1(i) > Nd1\left(i - 10^{-10} m\right) \\ \quad i \leftarrow i + 10^{-10} m \end{array} \right.$$

$$\text{Nd1Peak} = 7.31 \times 10^{-8}\, m$$

$$\text{Nd2Peak} := \left| \begin{array}{l} i \leftarrow 0 \\ \text{while } Nd2(i) > Nd2\left(i - 10^{-10} m\right) \\ \quad i \leftarrow i + 10^{-10} m \end{array} \right.$$

$$\text{Nd2Peak} = 2.801 \times 10^{-7}\, m$$

$$Nd1(\text{Nd1Peak}) = 2.635 \times 10^{29}\, \frac{1}{m^3}$$

$$Nd2(\text{Nd2Peak}) = 1.975 \times 10^{29}\, \frac{1}{m^3}$$

$$a := \frac{(Nd1(\text{Nd1Peak}) - Nd2(\text{Nd2Peak}))}{\text{Nd1Peak} - \text{Nd2Peak}}$$

$$a = -3.188 \times 10^{35}\, \frac{1}{m^4}$$ Grading Constant

Profile Graph:

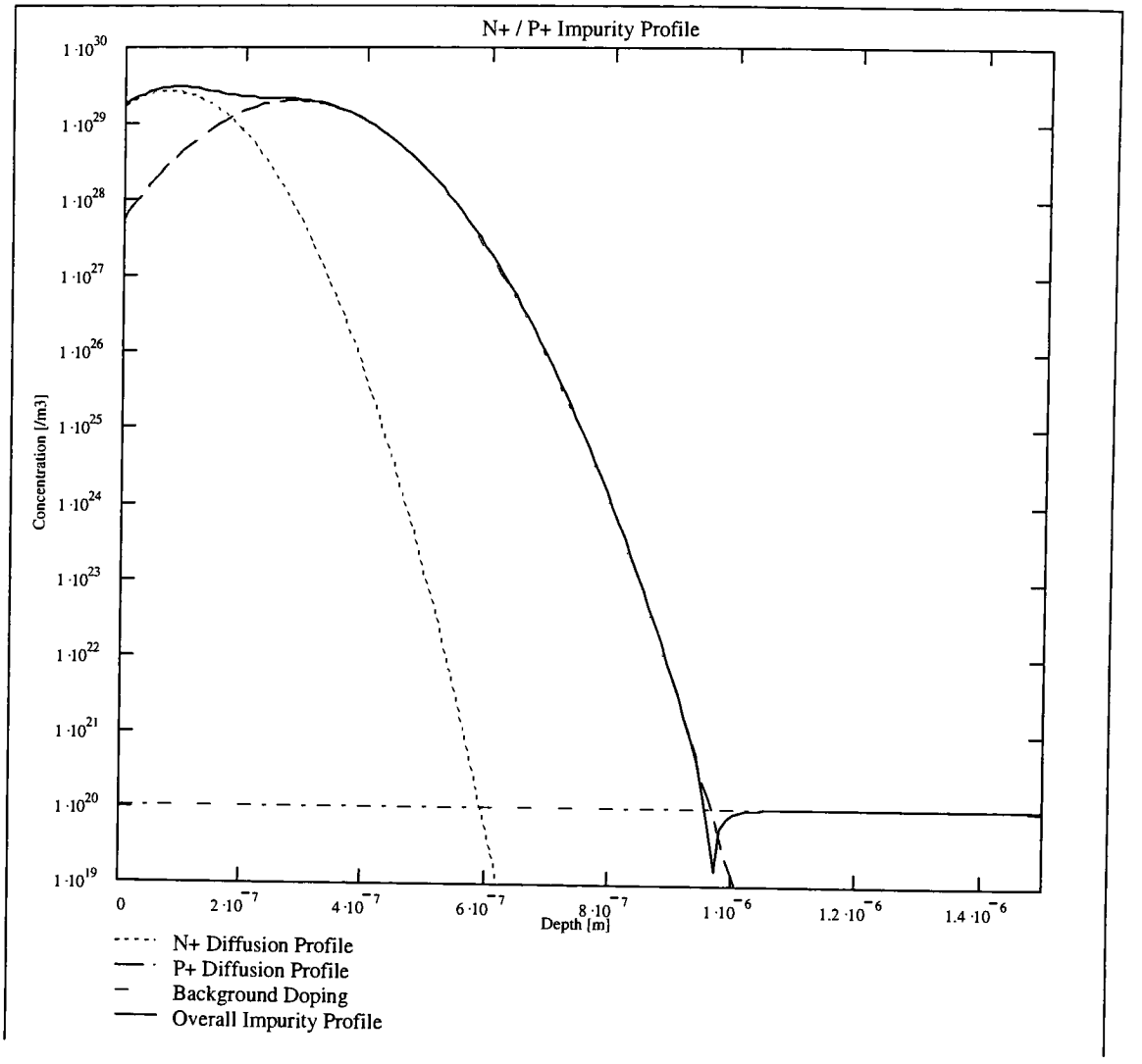

6.3. Fabrication Steps

1. Scribe (APD02-x)
   1.1. APD02-1
   1.2. APD02-2
   1.3. APD02-3
   1.4. APD02-4
   1.5. APD02-5

2. RCA Clean (APD02-x)

3. Field Oxide (APD02-x)
   3.1. Target thickness: 5kÅ
   3.2. Recipe #350 on Bruce Furnace
      3.2.1. Push @ 800C°, 12in/min., N_2
      3.2.2. Ramp up to 1100C°, dry O_2
      3.2.3. Soak 210min, wet O_2
      3.2.4. Ramp down to 800C°, N_2
      3.2.5. Pull @ 12in/min.

4. Photolithography – Guard Ring (APD02-1,2,4)

5. Etch – Oxide (APD02-1,2,4)
   5.1. Expected oxide thickness to etch: 5kÅ
   5.2. Etch in BHF
   5.3. Etch rate: ~1kÅ/min.
   5.4. Etch time: ~5 min.

6. Implant – Guard Ring (APD02-1,2,4)
   6.1. Target x_j: 1.4μm
      6.1.1. Energy: 60keV
      6.1.2. Dose: $1.6 * 10^{18}/cm^2$
      6.1.3. Species: P_{31}

7. Resist Strip (APD02-1,2,4)

8. Diffusion – Guard Ring Drive-In (APD02-1,2,4)
   8.1. Temp: 1000°C
   8.2. Time: 4.5 hours
      8.2.1. (6.5 hours would yield an x_j of 1μm, but there is a following thermal step of 1 hour @ 950°C)

9. Photolithography – N+ Region (APD02-x)

10. Etch – Oxide (APD02-x)

10.1. Expected oxide thickness to etch: 4.5kÅ
10.2. Etch in BHF
10.3. Etch rate: ~1kÅ/min.
10.4. Etch time: ~4.5 min.
10.4.1. Leave ~500Å oxide as sacrificial oxide during implant.

11. Implant – N+ (APD02-x)
11.1. Target x_j: 0.5μm
11.1.1. Energy: 60keV
11.1.2. Dose: 5.2 * $10^{18}/cm^2$
11.1.3. Species: P_{31}

12. Resist Strip (APD02-x)

13. Photolithography – P+ Region (APD02-4,5)

14. Implant – P+ (APD02-4,5)
14.1. Target x_j: 1μm
14.2. Energy: 90keV
14.3. Dose: 5.2 * $10^{18}/cm^2$
14.4. Species: B

15. Resist Strip (APD02-4,5)

16. Diffusion – N+/P+ Drive-In / Anneal (APD02-x)
16.1. Temp: 950°C
16.2. Time: 2.3 hours

17. Etch – Oxide (APD02-x)
17.1. Expected oxide thickness to etch: 0.5kÅ
17.2. Etch in BHF
17.3. Etch rate: ~1kÅ/min.
17.4. Etch time: ~0.5 min.

18. Aluminum Sputter (APD02-1,3,4,5)
18.1. Target thickness: 2kÅ
18.2. Material: Al / 1% Si
18.3. Power: 2kW
18.4. Time: 10min.

19. CVD – Polysilicon (APD02-2)
19.1. Target thickness: 1kÅ

20. Photolithography – Aluminum (APD02-x)

21. Etch – Aluminum (APD02-1,3,4,5)
21.1. Standard procedure

22. Plasma Etch – Polysilicon (APD02-2)

22.1. Gases: SF_6 @ 42sccm, O_2 @ 7.5sccm
22.2. Pressure: 400mT
22.3. Power: 40W
22.4. Time: 40 secs.

23. Resist Strip (APD02-x)

24. Aluminum Sinter (APD02-1,3,4,5)
    24.1. Standard Recipe
        24.1.1. Temp: 450C°
        24.1.2. Gas: N2/H2
        24.1.3. Time: 15-30min.

6.4. Third-Order Polynomial Fit Algorithm in Microsoft Visual Basic 6.0

```
Option Explicit
Option Base 1

Public sData() As Single
Public sCoeffArr() As Variant

Public Function ReadDataFile(strFileName As String)
Dim iFileNum As Integer
Dim strLineInput As String
Dim iRow As Integer
Dim iCol As Integer
Dim iRowUB As Integer
Dim iColUB As Integer
Dim sTempArr() As Single
Dim i, j

iFileNum   FreeFile
ReDim sData(50, 50)

Open strFileName For Input As #iFileNum
iRow   0
Do Until EOF(1)
    Line Input #iFileNum, strLineInput
    iRow   iRow + 1
    If iRow >= iRowUB Then iRowUB = iRow
    'Data file should be a comma delimited file.
    'Tagging line with a ',' to make string parsing MUCH easier in next section.
    strLineInput   strLineInput + ","
    iCol   0
    Do Until strLineInput   ""
        iCol   iCol + 1
        If iCol >= iColUB Then iColUB   iCol
        sData(iCol, iRow)   Val(Left(strLineInput, InStr(strLineInput, ",")   1))
        strLineInput   Mid(strLineInput, InStr(strLineInput, ",") + 1)
    Loop
Loop
Close #iFileNum

'Resize sData() array to streamline memory.  Swap with temp array to keep data.
ReDim Preserve sTempArr(iColUB, iRowUB)

For i   1 To iColUB
    For j   1 To iRowUB
        sTempArr(i, j)   sData(i, j)
    Next j
Next i

ReDim sData(iColUB, iRowUB)

For i   1 To iColUB
    For j   1 To iRowUB
        sData(i, j)   sTempArr(i, j)
    Next j
Next i

End Function

Public Function CalcData()
'First col are X values, following cols are Y values for each respective curve.
Dim RegObj As New RegressionObject
Dim sIThres As Single
Dim sCalcI As Single
Dim sPrevCalcI As Single
Dim sVoltStep As Single
```

```
Dim i, j, k

ReDim sCoeffArr(UBound(sData(), 1), 9)

sCoeffArr(1, 1)   "Poly Coeff A"
sCoeffArr(1, 2)   "Poly Coeff B"
sCoeffArr(1, 3)   "Poly Coeff C"
sCoeffArr(1, 4)   "Poly Coeff D"
sCoeffArr(1, 5)   "2nd Deriv Coeff A"
sCoeffArr(1, 6)   "2nd Deriv Coeff B"
sCoeffArr(1, 7) = "Max Grad Vbr"
sCoeffArr(1, 8)   "Thres Vbr"
sCoeffArr(1, 9) = "Vbr"

RegObj.Degree   3

'Calculate the coefficients of the 3rd order polynomial.
For i   2 To UBound(sData(), 1)
    RegObj.Init
    For j = 1 To UBound(sData(), 2)
        'Add data to RegObj.  When done grab coefficients from it.
        RegObj.XYAdd sData(1, j), sData(i, j)
    Next j
    'Grab coefficients from RegObj. Will be 4 coefficients.
    '[x^3 is sCoeffArr(i, 1) or RegObj.Coeff(3)]
    '[const is sCoeffArr(i, 4) or RegObj.Coeff(0)], etc.
    For k   1 To 4
        sCoeffArr(i, 1) = RegObj.Coeff(3)
        sCoeffArr(i, 2) = RegObj.Coeff(2)
        sCoeffArr(i, 3) = RegObj.Coeff(1)
        sCoeffArr(i, 4)   RegObj.Coeff(0)
    Next k
Next i

'Calculate the coefficients of 2nd derivative and voltage point of max gradient.
For i   2 To UBound(sData(), 1)
    sCoeffArr(i, 5)   6 * sCoeffArr(i, 1)
    sCoeffArr(i, 6)   2 * sCoeffArr(i, 2)
    sCoeffArr(i, 7)   -sCoeffArr(i, 6) / sCoeffArr(i, 5)
Next i

End Function

Public Function WriteOutputFile(strOutputFileName As String)
Dim iFileNum As Integer
Dim i, j

iFileNum   FreeFile

Open strOutputFileName For Output As #iFileNum
For j   1 To UBound(sCoeffArr(), 2)
    For i = 1 To UBound(sData(), 1)
        Print #iFileNum, sCoeffArr(i, j) & ", ";
    Next i
    Print #iFileNum, ""
Next j
Close #iFileNum

End Function
Option Explicit

Private Const MaxO&   25
Private Global0& '"Ordnung" = degree of the polynom expected
Private Finished As Boolean

Private SumX#(0 To 2 * MaxO)
Private SumYX#(0 To MaxO)
Private M#(0 To MaxO, 0 To MaxO + 1)
Private C#(0 To MaxO) 'coefficients in: Y   C(0)*X^0 + C(1)*X^1 + C(2)*X^2 + ...

Private Sub GaussSolve(O&)
'gauss algorithm implementation,
```

```
'following R.Sedgewick's "Algorithms in C", Addison-Wesley, with minor modifications
Dim i&, j&, k&, iMax&, T#, O1#
  O1   O + 1
  'first triangulize the matrix
  For i = 0 To O
    iMex = i: T   Abs(M(iMex, i))
    For j   i + 1 To O 'find the line with the largest absvalue in this row
      If T < Abs(M(j, i)) Then iMax   j: T   Abs(M(iMex, i))
    Next j
    If i < iMex Then 'exchange the two lines
      For k   i To O1
        T   M(i, k)
            M(i, k) = M(iMax, k)
                      M(iMax, k)   T
      Next k
    End If
    For j   i + 1 To O 'scale all following lines to have a leading zero
      T   M(j, i) / M(i, i)
      M(j, i)   0#
      For k : i + 1 To O1
        M(j, k)   M(j, k)   M(i, k) * T
      Next k
    Next j
  Next i
  'then substitute the coefficients
  For j   O To 0 Step -1
    T = M(j, O1)
    For k = j + 1 To O
      T   T   M(j, k) * C(k)
    Next k
    C(j)   T / M(j, j)
  Next j
  Finished   True
End Sub

Private Sub BuildMatrix(O&)
Dim i&, k&, O1&
  O1   O + 1
  For i = 0 To O
    For k   0 To O
      M(i, k) = SumX(i + k)
    Next k
    M(i, O1)   SumYX(i)
  Next i
End Sub

Private Sub FinalizeMatrix(O&)
Dim i&, O1&
  O1   O + 1
  For i   0 To O
    M(i, O1)   SumYX(i)
  Next i
End Sub

Private Sub Solve()
Dim O&
  O   GlobalO
  If XYCount <= O Then O = XYCount   1
  If O < 0 Then Exit Sub
  BuildMatrix O
  On Error Resume Next
    GaussSolve (O)
    While (Err.Number <> 0) And (1 < O)
      Err.Clear
      C(0)   0#
      O - O   1
      FinalizeMatrix (O)
    Wend
  On Error GoTo 0
End Sub

Private Sub Class_Initialize()
```

```
  Init
  Global0   2
End Sub

Public Sub Init()
Dim i&
  Finished   False
  For i = 0 To Max0
    SumX(i) = 0#
    SumX(i + Max0)   0#
    SumYX(i) = 0#
    C(i)   0#
  Next i
End Sub

Public Property Get Coeff#(Exponent&)
Dim Ex&, O&
  If Not Finished Then Solve
  Ex   Abs(Exponent)
  O = Global0
  If XYCount <= O Then O   XYCount   1
  If O < Ex Then Coeff   0# Else Coeff   C(Ex)
End Property

Public Property Get Degree&()
  Degree : Global0
End Property
Public Property Let Degree(NewVal&)
  If NewVal < 0 Or Max0 < NewVal Then
    Err.Raise 6000, "RegressionObject", NewVal & " is an invalid property value! Use 0<= Degree <= " &
Max0
    Exit Property
  End If
  Init
  Global0   NewVal
End Property

Public Property Get XYCount&()
  XYCount = CLng(SumX(0))
End Property

Public Function XYAdd(ByVal NewX#, ByVal NewY#)
Dim i&, j&, TX#, Max20&
  Finished - False
  Max20   2 * Global0
  TX   1#
  SumX(0)   SumX(0) + 1
  SumYX(0) = SumYX(0) + NewY
  For i   1 To Global0
    TX   TX * NewX
    SumX(i)   SumX(i) + TX
    SumYX(i) = SumYX(i) + NewY * TX
  Next i
  For i   Global0 + 1 To Max20
    TX   TX * NewX
    SumX(i)   SumX(i) + TX
  Next i
End Function

Public Function RegVal#(X#)
Dim i&, O&
  If Not Finished Then Solve
  RegVal   0#
  O = Global0
  If XYCount <= O Then O   XYCount   1
  For i   0 To O
    RegVal   RegVal + C(i) * X ^ i
  Next i
End Function
```

6.5. Responsitivity to Quantum Efficiency Conversion Calculation

Responsitivity to Electrons / Photon Conversion

Parameters:

$R := 0.2801 \cdot \frac{A}{W}$

$\lambda := 600 10^{-9} m$

Constants:

$h := 6.626 10^{-34} \cdot J \cdot s$

$c := 2.997924581 0^{8} \cdot \frac{m}{s}$

$eV := 1.6 \cdot 10^{-19} C$

$eV\_per\_sec := R \cdot \frac{C}{eV} \cdot W$

$eV\_per\_sec = 1.751 \times 10^{18} A$

$E := \frac{h \cdot c}{\lambda}$

$E = 3.311 \times 10^{-19} J$

$photons\_per\_sec := \frac{1}{E}$

$photons\_per\_sec = 3.021 \times 10^{18} \frac{s^2}{kg\, m^2}$

$x := \frac{eV\_per\_sec}{photons\_per\_sec}$

$x = 0.580 \frac{kg\, m^2 A}{s^2}$ [electrons / photon]

6.6. Depletion Width and Built-in Voltage Calculation

PN Junction Electrostatics of a Linearly Graded Junction

Constants:

$eV := 1.6 \cdot 10^{-19} J$ Electron Volt

$q := 1.6 \cdot 10^{-19} C$ Charge

$n_i := 1 \cdot 10^{10} \cdot cm^{-3}$ Intrinsic Carrier Concentration

$T := 300K$ Temperature

$k := 8.617 \cdot 10^{-5} \cdot \frac{eV}{K}$ Boltzmann Constant

$\mu_n := 801 \cdot \left(\frac{cm^2}{V \cdot s} \right)$ Electron Mobility (@ Nd = 10^17/cm3)

$\tau_n := 1 \cdot 10^{-6} s$ Electron Minority-Carrier Lifetime (Average)

$\mu_p := 331 \cdot \left(\frac{cm^2}{V \cdot s} \right)$ Hole Mobility (@ Na = 10^17/cm3)

$\tau_p := 1 \cdot 10^{-6} s$ Hole Minority-Carrier Lifetime (Average)

$Ks := 11.8$ Dielectric Constant of Silicon

$\varepsilon_o := 8.85 \cdot 10^{-14} \cdot \frac{F}{cm}$ Permittivity of Free Space

Sub-Calculations:

$D_n := \mu_n \cdot \left(\frac{k \cdot T}{q} \right)$ Electron Diffusion Coefficient

$L_n := \sqrt{D_n \cdot \tau_n}$ Electron Diffusion Length

$D_p := \mu_p \cdot \left(\frac{k \cdot T}{q} \right)$ Hole Diffusion Coefficient

$L_p := \sqrt{D_p \cdot \tau_p}$ Hole Diffusion Length

Device Parameters:

$N_a := 1.939 \, 10^{23} \cdot \frac{1}{cm^3}$ Acceptor Concentration

$N_d := 2.484 \, 10^{23} \cdot \frac{1}{cm^3}$ Donor Concentration

$V_A := -5.2V$ Applied Voltage

$a := 3.188 \, 10^{27} cm^{-4}$ Grading Constant

Calculations:

$Vguess_0 := 0.5V \qquad f := 0..10$

$$Vguess_{(f+1)} := \frac{2 \cdot k \cdot T}{q} \cdot \ln\left[\frac{a}{2 \cdot n_i} \cdot \left(\frac{12 \cdot Ks \cdot \varepsilon_o}{q \cdot a} \cdot Vguess_f\right)^{\frac{1}{3}}\right]$$

$V_{bi} := Vguess_{10}$

$V_{bi} = 1.2739V$ Built-in Voltage

$$W := \left[\frac{12 \cdot Ks \cdot \varepsilon_o}{q \cdot a} \cdot (V_{bi} - V_A)\right]^{\frac{1}{3}}$$

$W = 5.4181 \times 10^{-9} m$ Depletion Width

$$x := \frac{-W}{2}, \left(\frac{-W}{2} + \frac{W}{20}\right) .. \frac{W}{2}$$

$$V(x) := \frac{q \cdot a}{6 \cdot Ks \cdot \varepsilon_o} \cdot \left[2 \cdot \left(\frac{W}{2}\right)^3 + 3 \cdot \left(\frac{W}{2}\right)^2 \cdot x - x^3\right]$$ Electrostatic Potential

$$\xi(x) := \frac{q \cdot a}{2 \cdot Ks \cdot \varepsilon_o} \cdot \left[x^2 - \left(\frac{W}{2}\right)^2\right]$$ Electric Field

$\rho(x) := q \cdot a \cdot x$ Charge Density

6.7. Photodiode Test Data

6.7.1 Raw I-V Graphs

The following graphs are the raw I-V test results of the APD arrays constructed for this research.

****** GRAPHICS PLOT ******

W1 C7, 9 D200, 20, 300, N

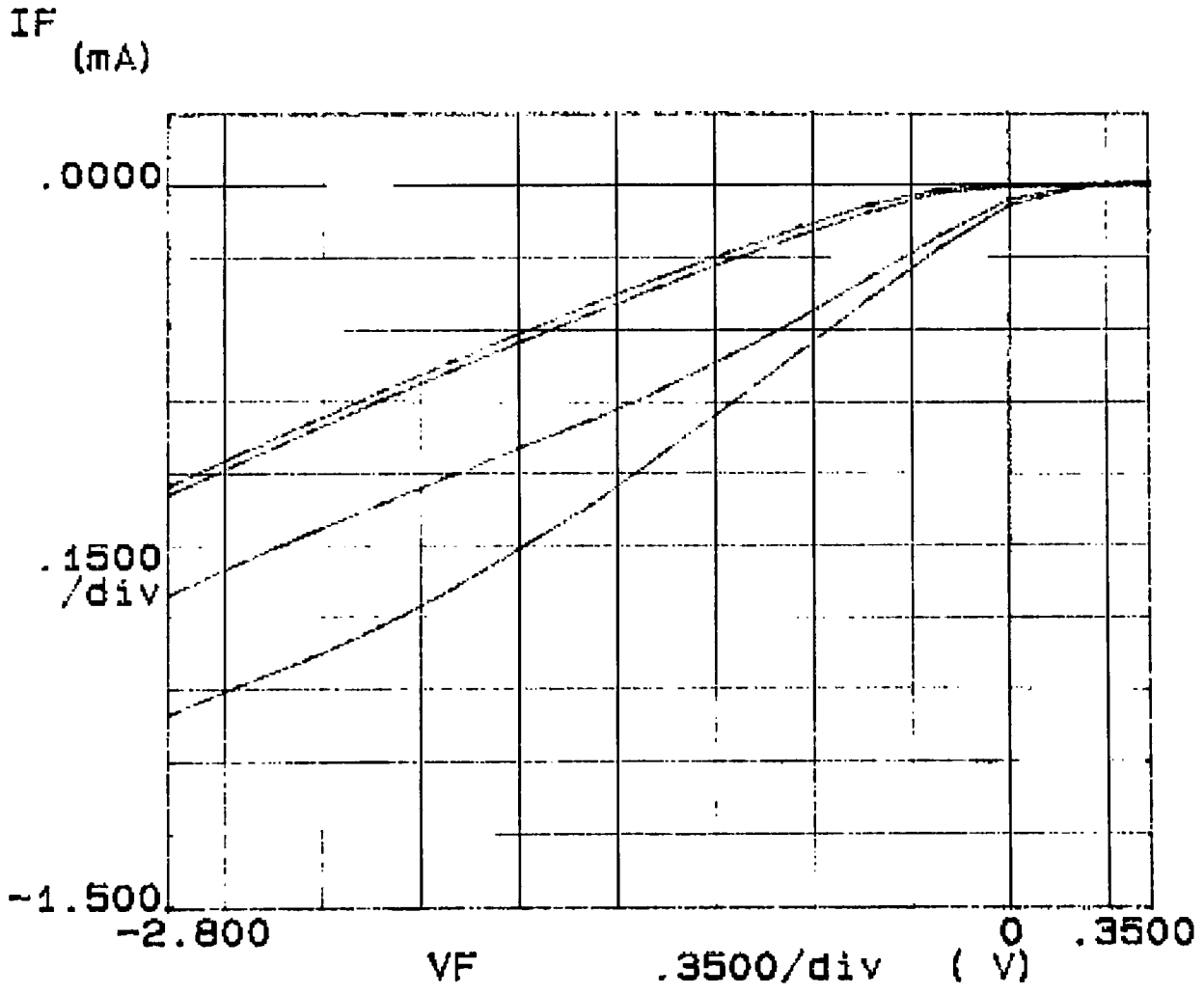

Variable1:
VF -Ch1
Linear sweep
Start -3.0000V
Stop .5000V
Step .2800V

Constants:
V -Ch3 .0000V

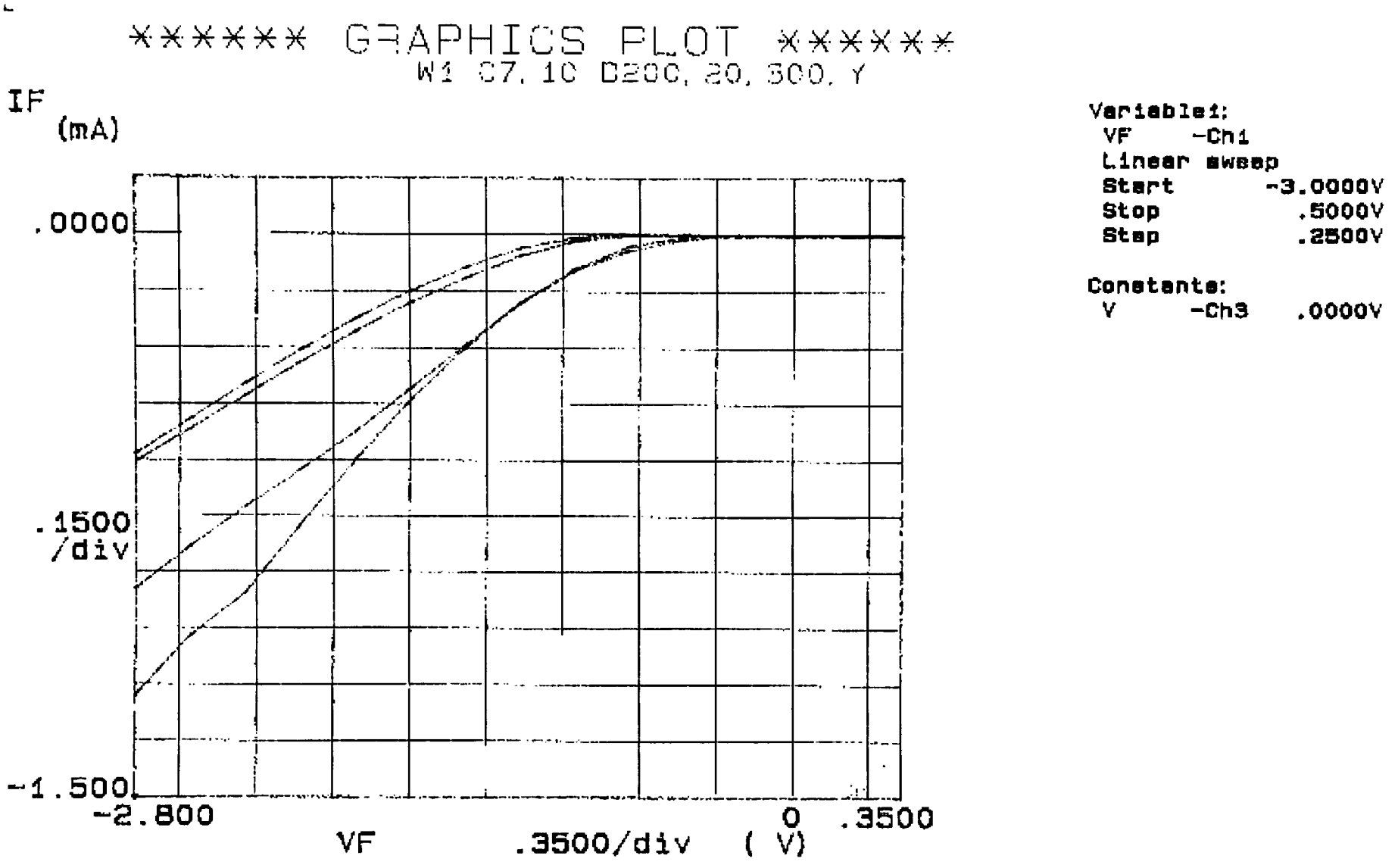
****** GRAPHICS PLOT ******
W1 C7, 1C D200, 20, 300, Y
IF
(mA)
.0000
.1500
/div
-1.500
-2.800
0
.3500
VF
.3500/div
(V)
Variable1:
VF -Ch1
Linear sweep
Start -3.0000V
Stop .5000V
Step .2500V
Constants:
V -Ch3 .0000V

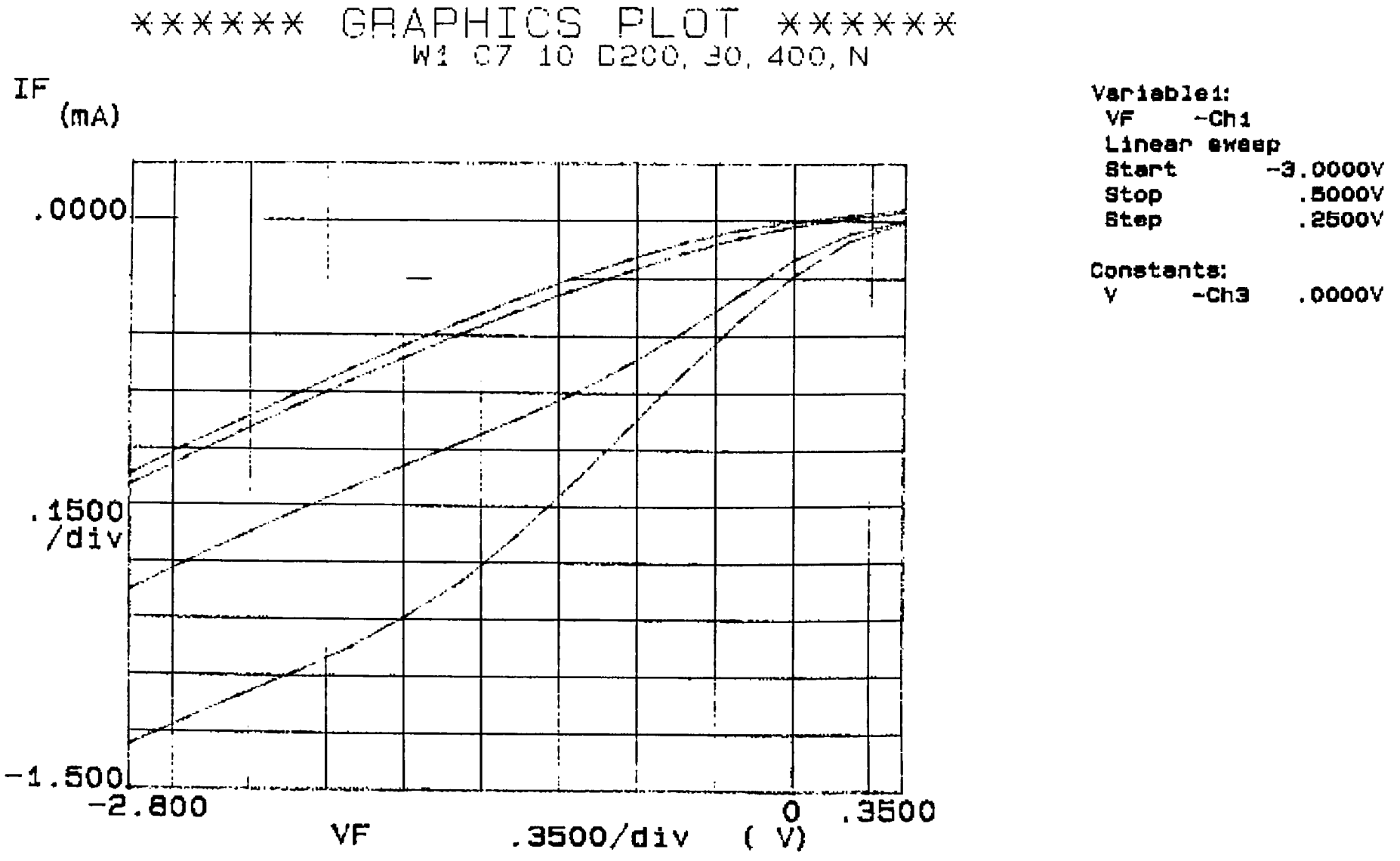
****** GRAPHICS PLOT ******
W1 C7 10 D200, 30, 400, N
IF
(mA)
.0000
.1500
/div
-1.500
-2.800
0
.3500
VF
.3500/div
(V)
Variable1:
VF -Ch1
Linear sweep
Start -3.0000V
Stop .5000V
Step .2500V
Constants:
V -Ch3 .0000V

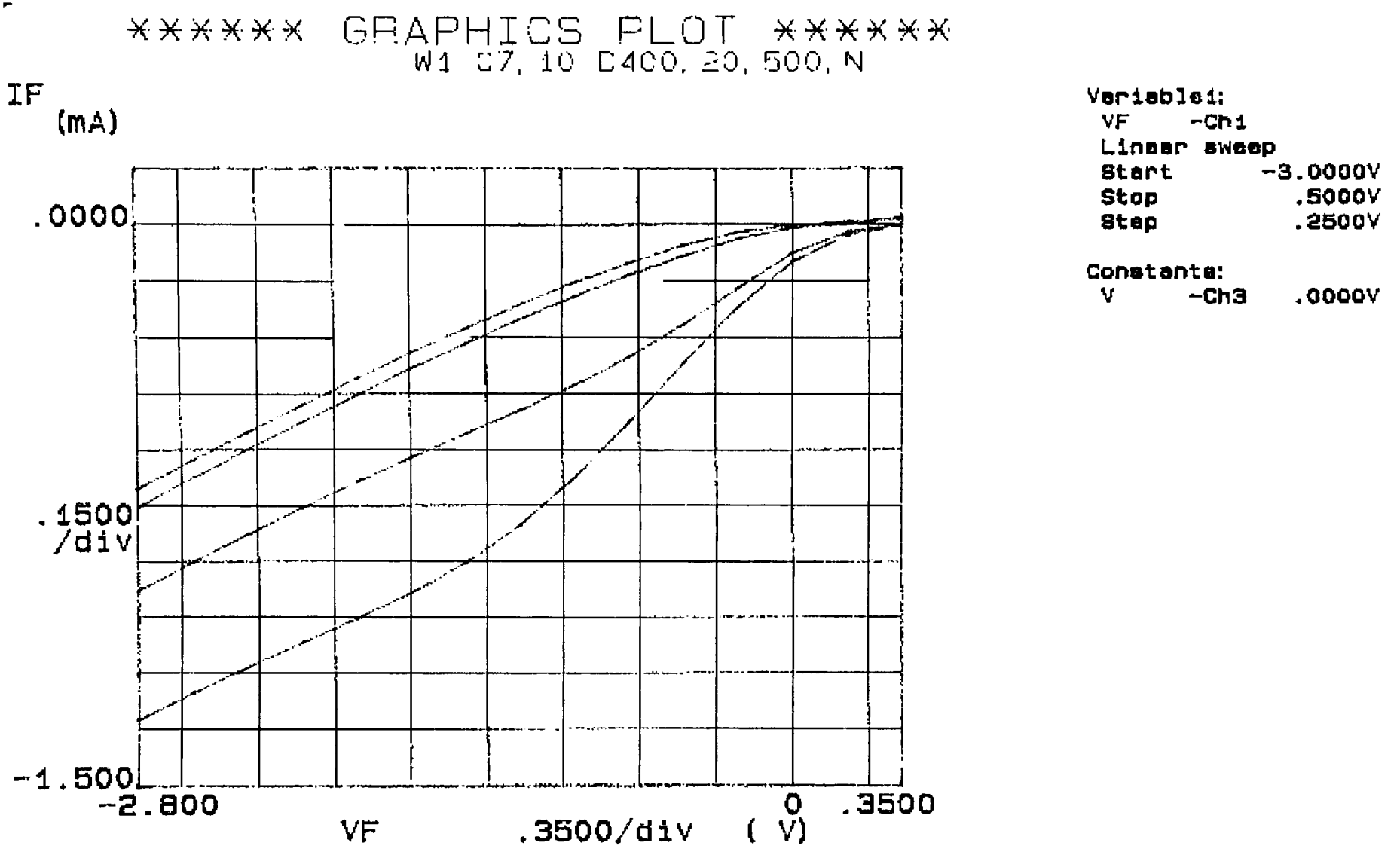
****** GRAPHICS PLOT ******
W1 S7, 10 D400, 20, 500, N
IF
(mA)
.0000
.1500
/div
-1.500
-2.800
0
.3500
VF
.3500/div
(V)
Variable1:
VF -Ch1
Linear sweep
Start -3.0000V
Stop .5000V
Step .2500V
Constante:
V -Ch3 .0000V

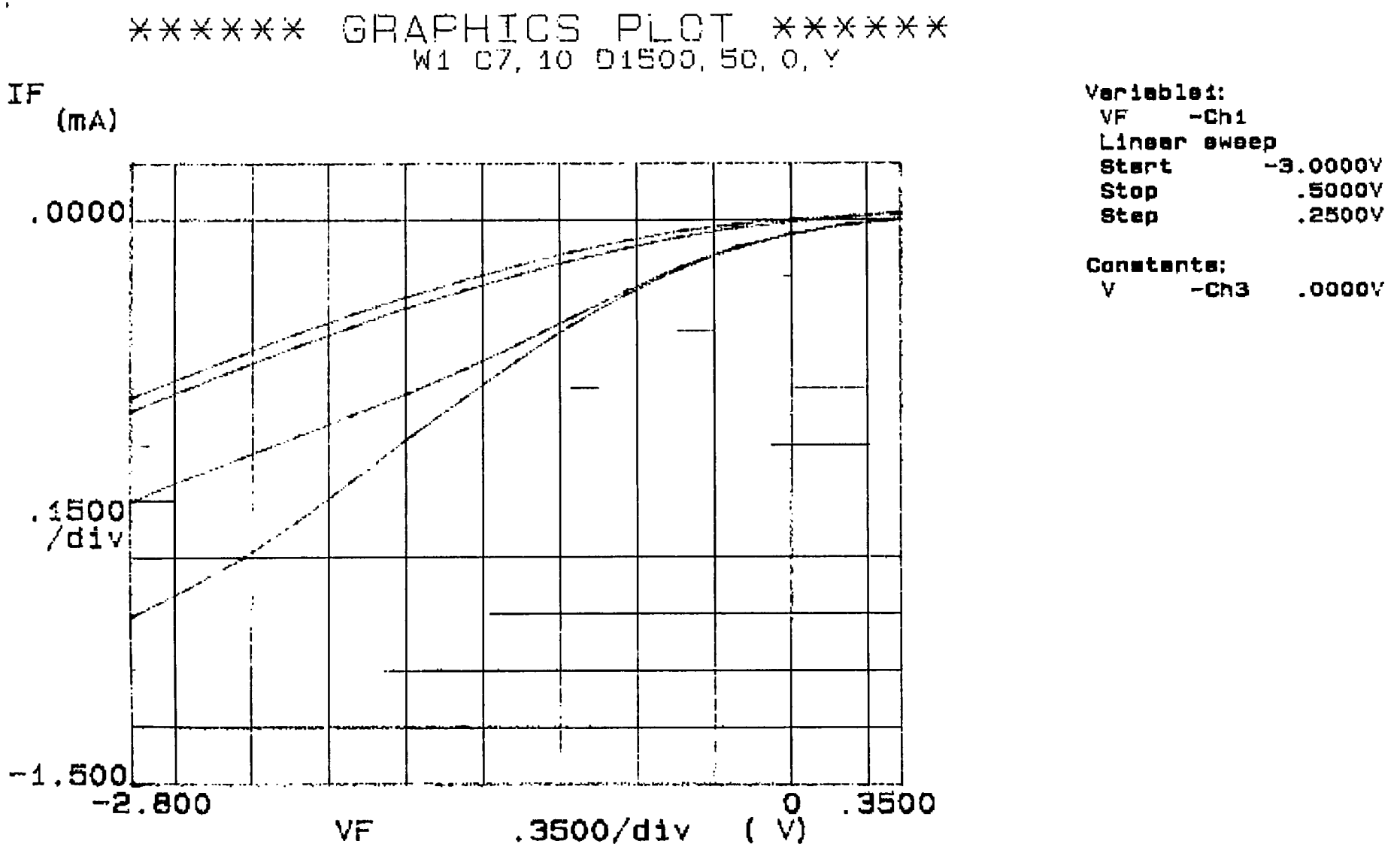
****** GRAPHICS PLOT ******
W1 C7, 10 D1500, 50, 0, Y
IF
(mA)
.0000
.1500
/div
-1.500
-2.800
0
.3500
VF
.3500/div
(V)
Variable1:
VF -Ch1
Linear sweep
Start -3.0000V
Stop .5000V
Step .2500V
Constants:
V -Ch3 .0000V

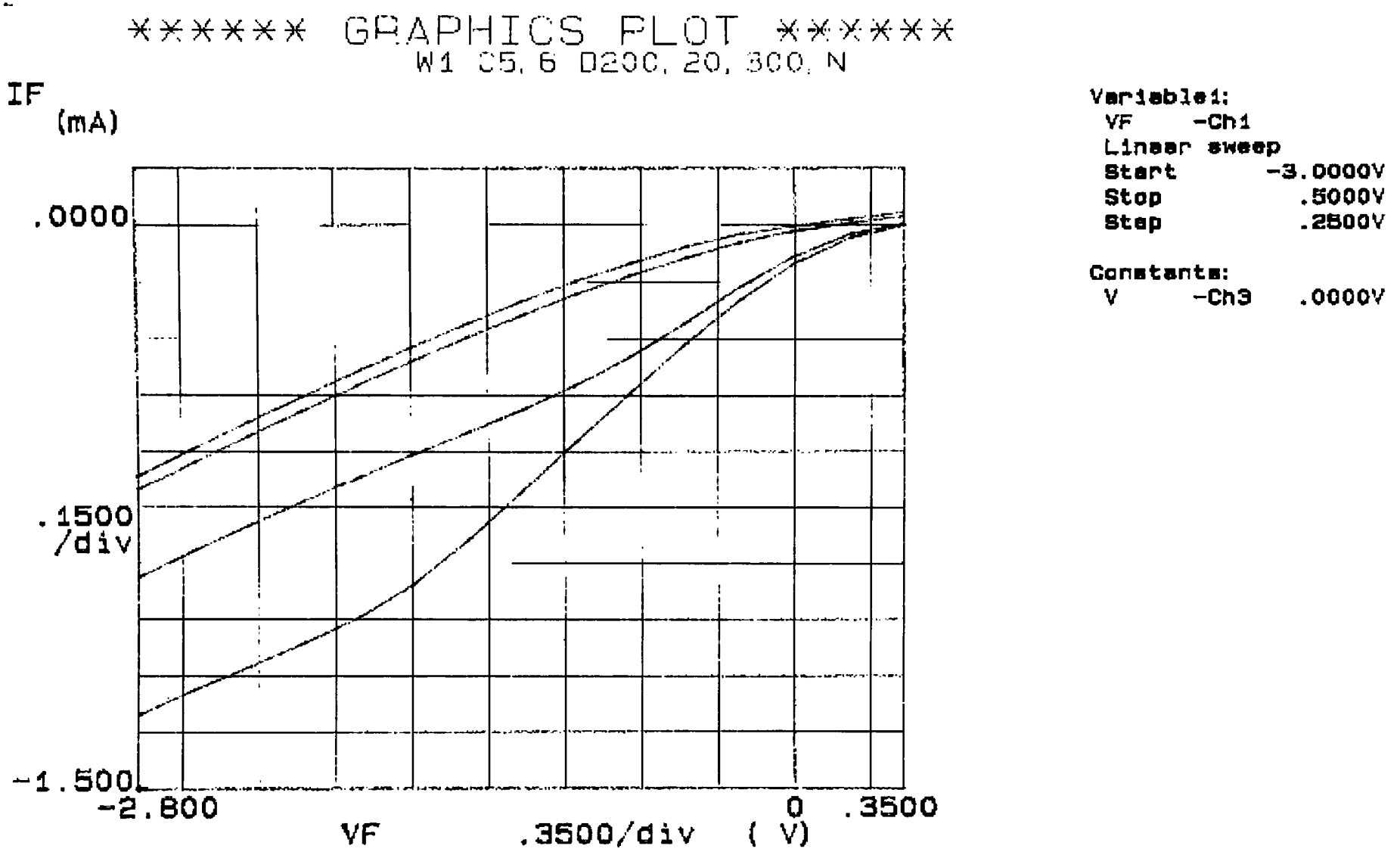
****** GRAPHICS PLOT ******
W1 C5,6 D20C,20,30C,N
IF
(mA)
.0000
.1500
/div
-1.500
-2.800
0
.3500
VF .3500/div (V)
Variable1:
VF -Ch1
Linear sweep
Start -3.0000V
Stop .5000V
Step .2500V
Constants:
V -Ch3 .0000V

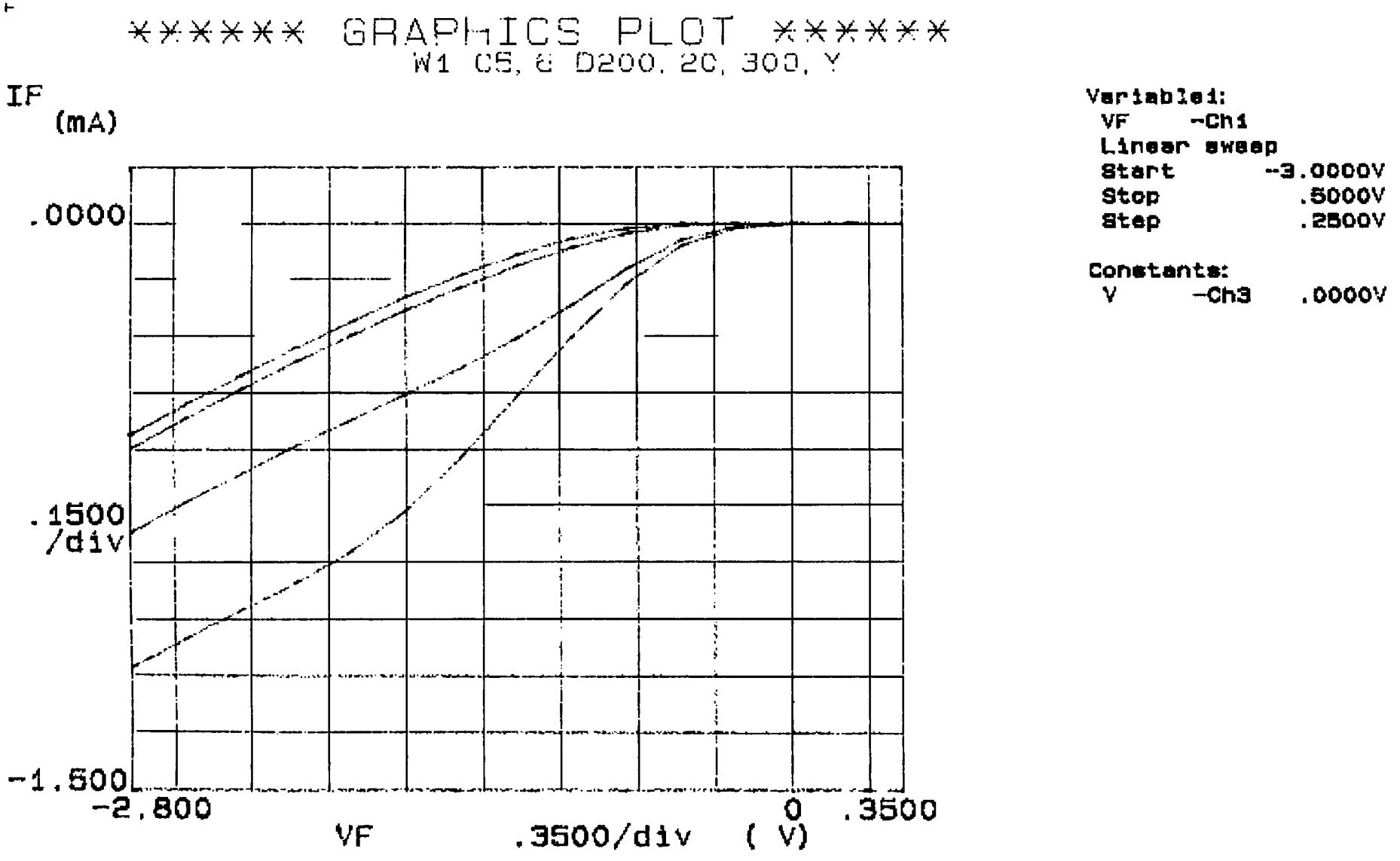
****** GRAPHICS PLOT ******
W1 C5, 6 D200, 20, 300, Y
IF
(mA)
.0000
.1500
/div
-1.500
-2.800
0
.3500
VF
.3500/div
(V)
Variable1:
VF -Ch1
Linear sweep
Start -3.0000V
Stop .5000V
Step .2500V
Constants:
V -Ch3 .0000V

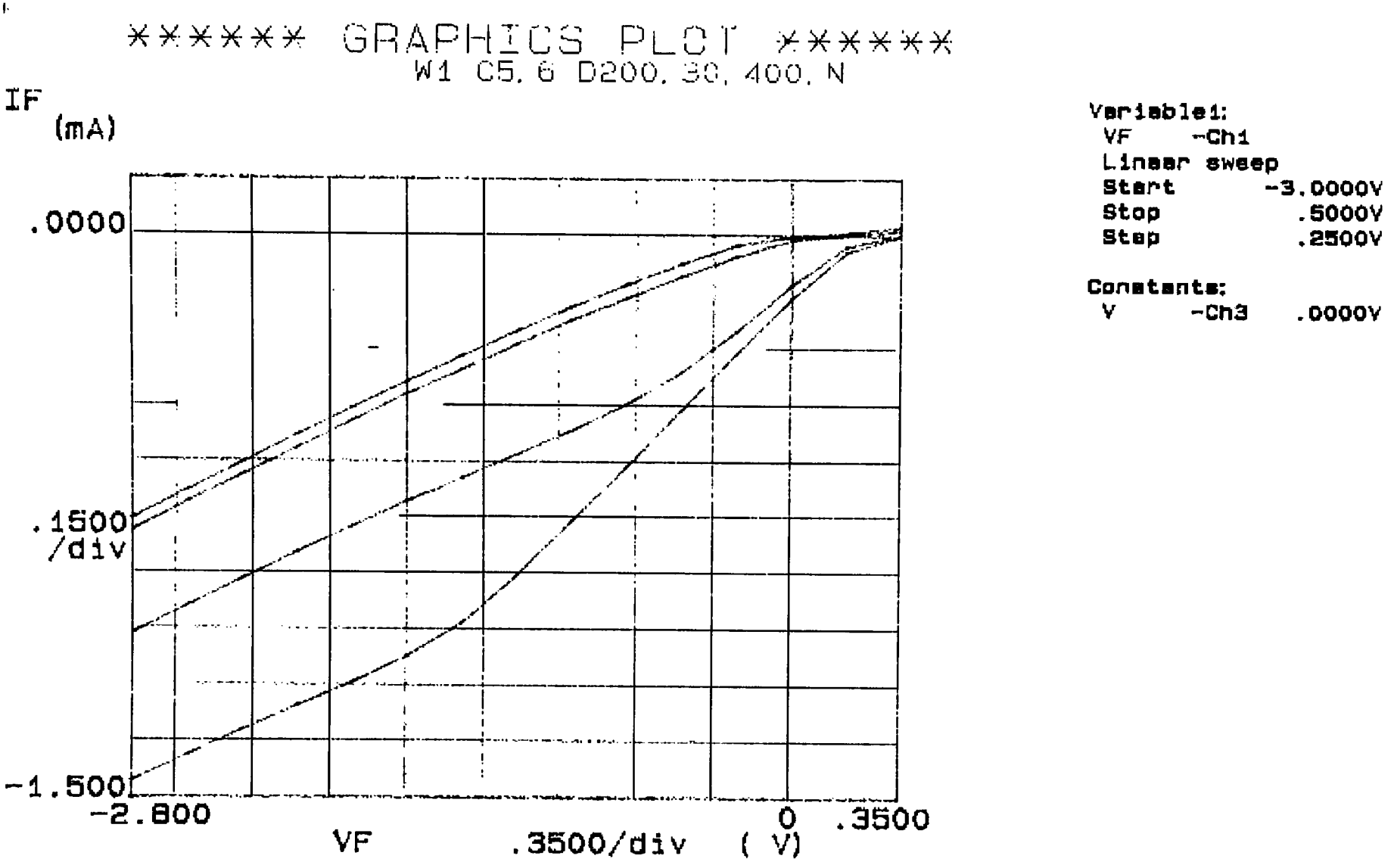
****** GRAPHICS PLOT ******
W1 C5.6 D200.30.400.N
IF
(mA)
.0000
.1500
/div
-1.500
-2.800
0
.3500
VF
.3500/div
(V)
Variable1:
VF -Ch1
Linear sweep
Start -3.0000V
Stop .5000V
Step .2500V
Constants:
V -Ch3 .0000V

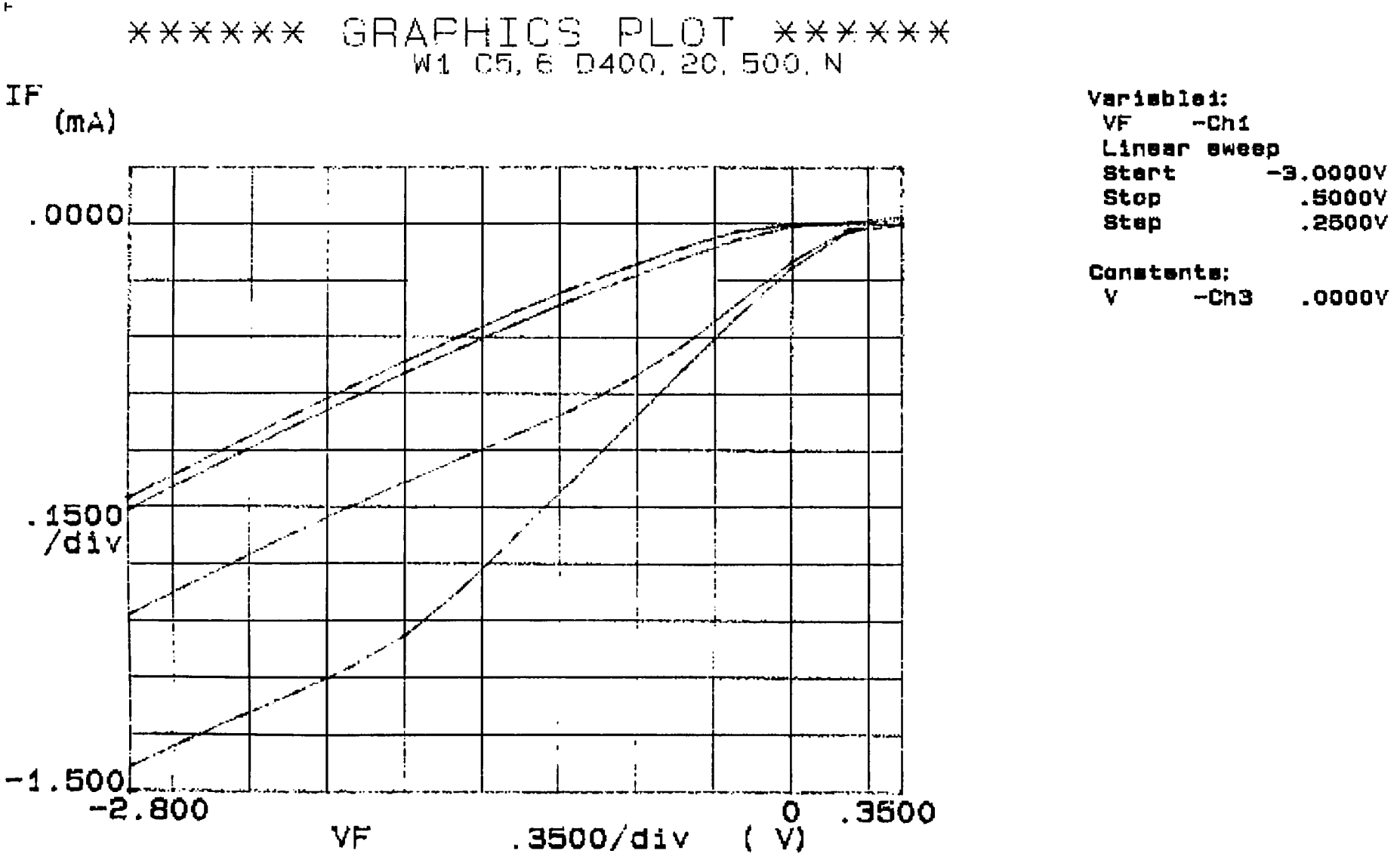
****** GRAPHICS PLOT ******
W1 C5, 6 D400, 20, 500, N
IF
(mA)
.0000
.1500
/div
-1.500
-2.800
0
.3500
VF
.3500/div
(V)
Variable1:
VF -Ch1
Linear sweep
Start -3.0000V
Stop .5000V
Step .2500V
Constants:
V -Ch3 .0000V

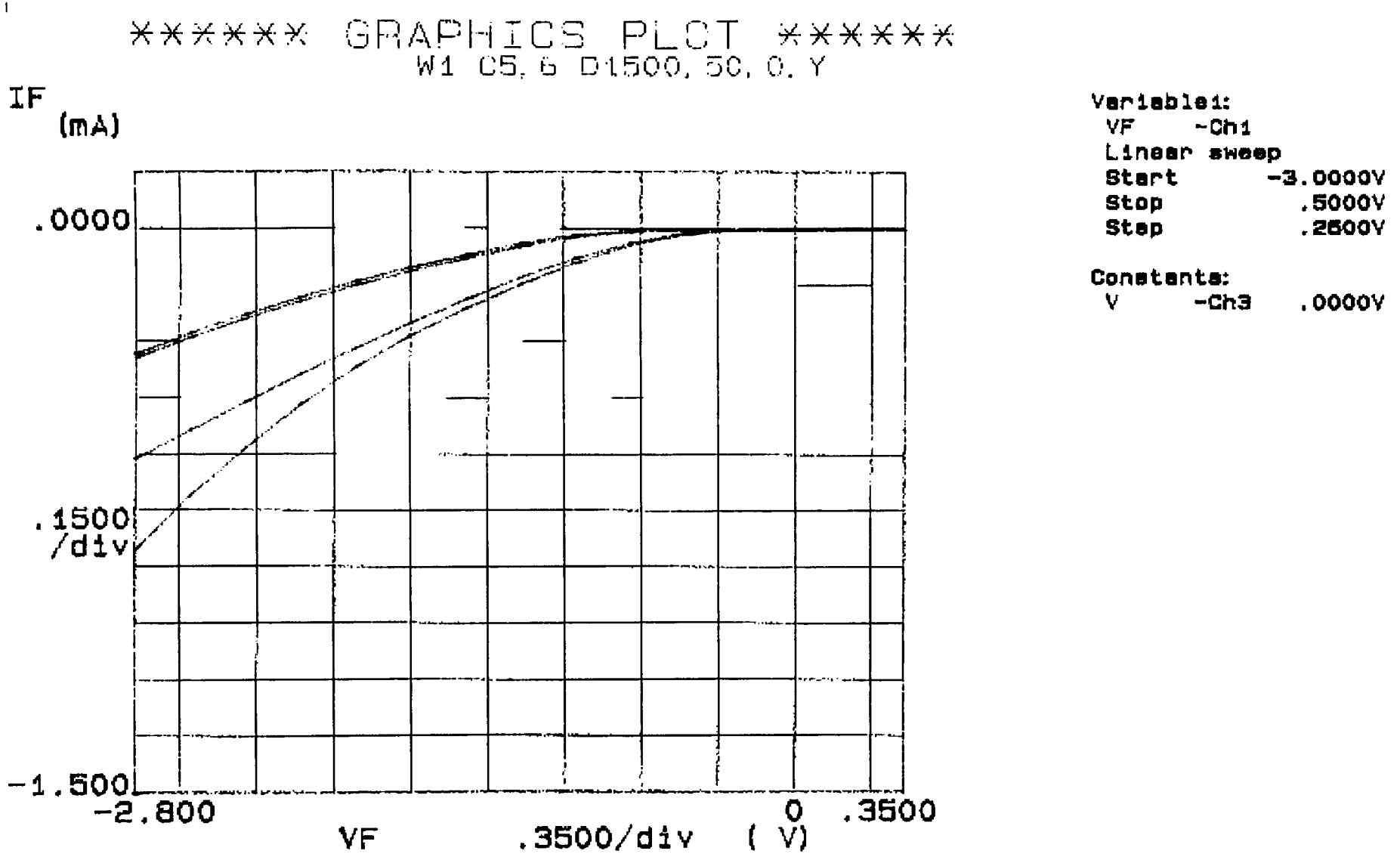
****** GRAPHICS PLOT ******
W1 C5,6 D1500,50,0,Y
IF
(mA)
.0000
.1500
/div
-1.500
-2.800
0
.3500
VF
.3500/div
(V)
Variable1:
VF -Ch1
Linear sweep
Start -3.0000V
Stop .5000V
Step .2500V
Constants:
V -Ch3 .0000V

****** GRAPHICS PLOT ******

W2 C9, 6 D200, 20, 300, N

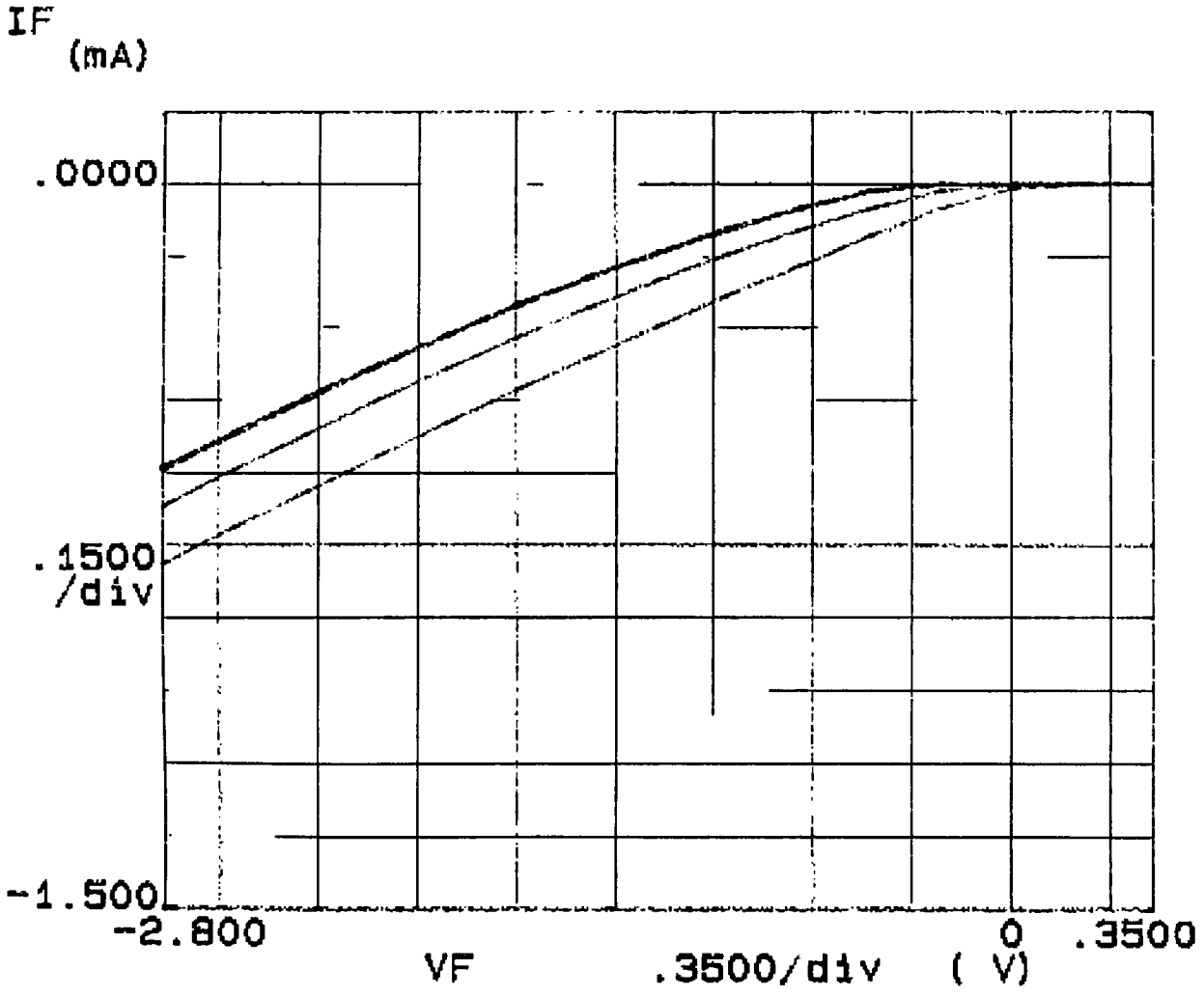

Variable1:
VF -Ch1
Linear sweep
Start -3.0000V
Stop .5000V
Step .2500V

Constants:
V -Ch3 .0000V

****** GRAPHICS PLOT ******

W2 C9, 6 D200, 20, 30C, Y

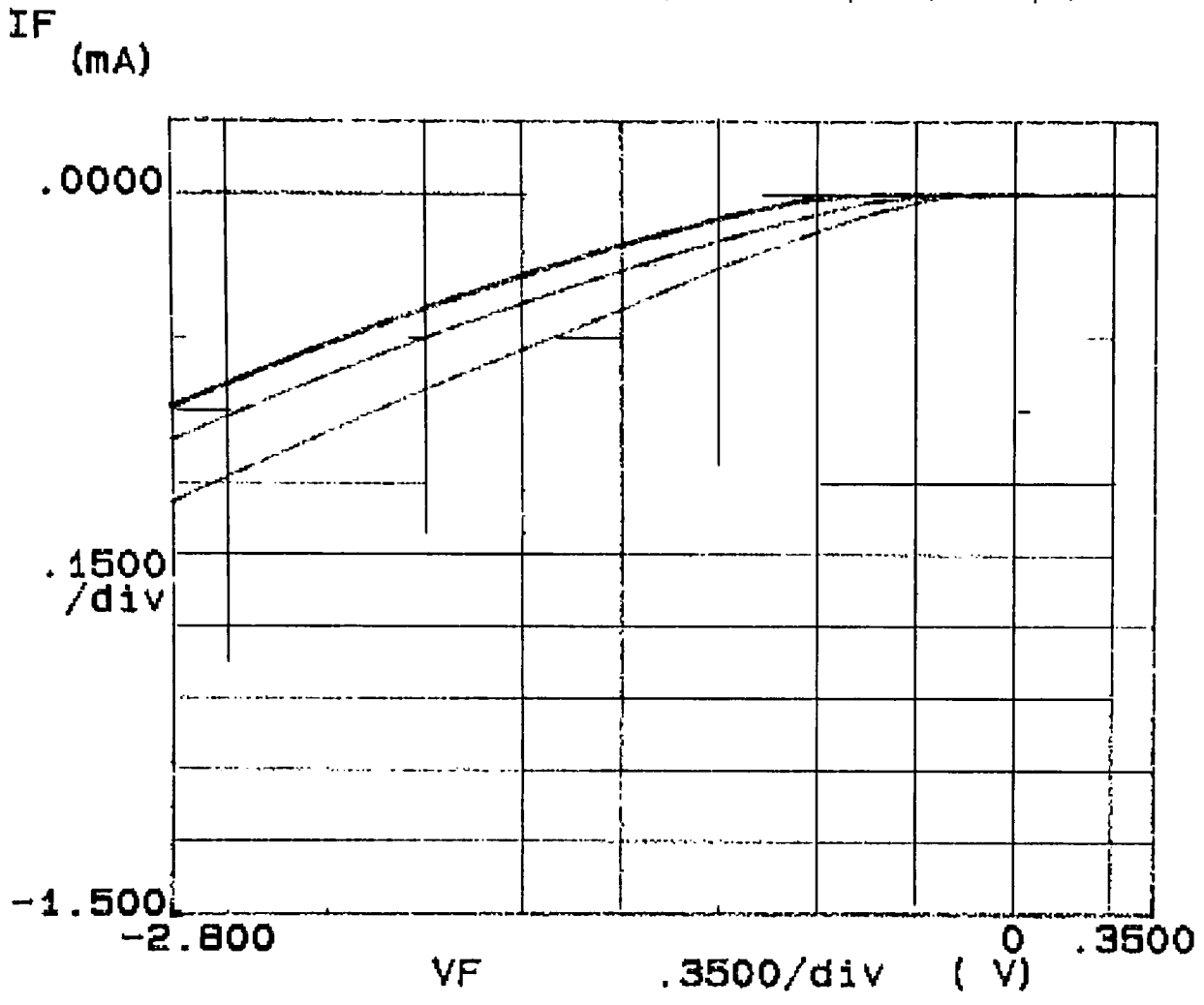

Variable1:
VF -Ch1
Linear sweep
Start -3.0000V
Stop .5000V
Step .2500V

Constants:
V -Ch3 .0000V

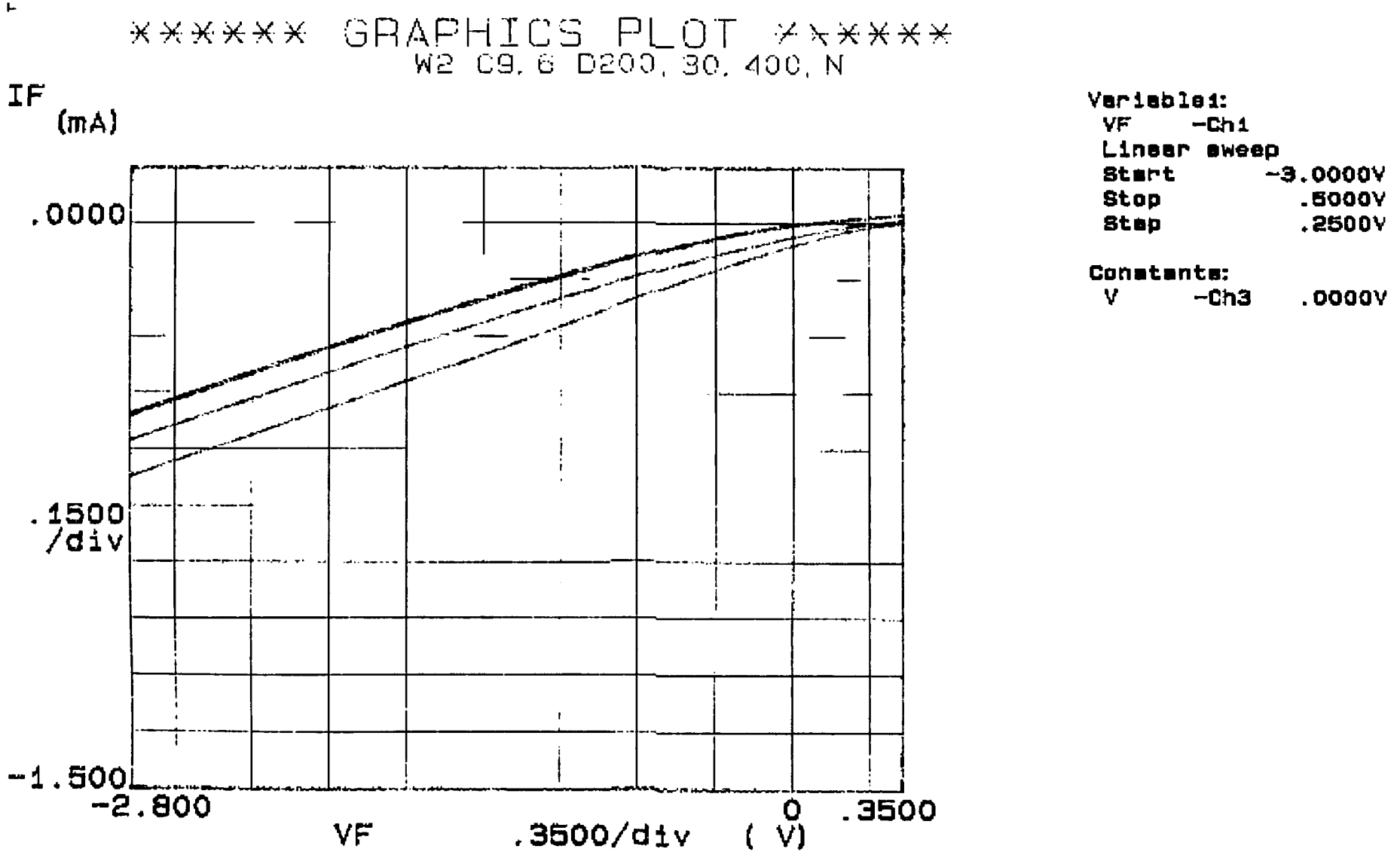
****** GRAPHICS PLOT ******
W2 C9.6 D200,30,400,N
IF
(mA)
.0000
.1500
/div
-1.500
-2.800
0
.3500
VF
.3500/div
(V)
Variable1:
VF -Ch1
Linear sweep
Start -3.0000V
Stop .5000V
Step .2500V
Constants:
V -Ch3 .0000V

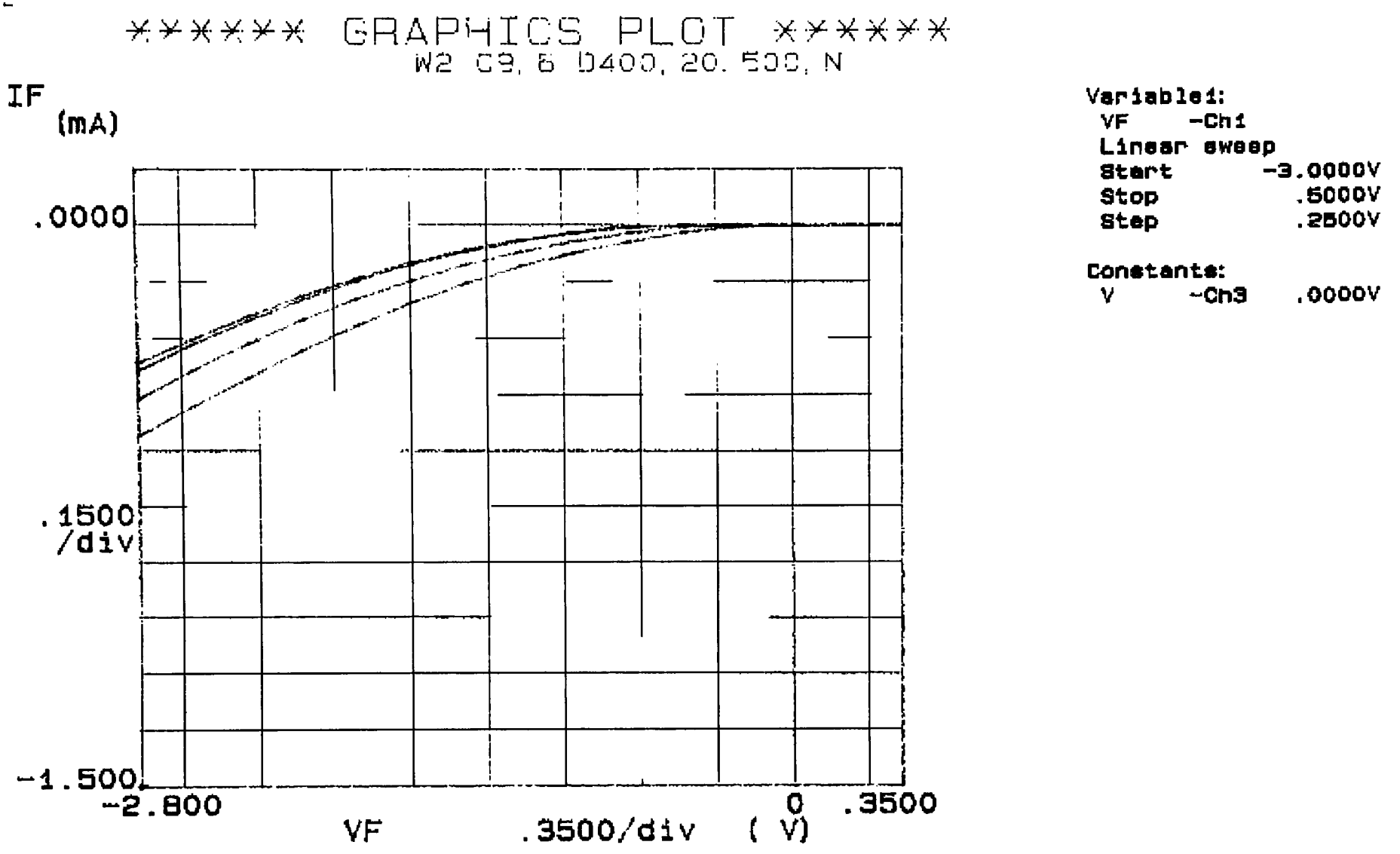
****** GRAPHICS PLOT ******
W2 C9, 6 D400, 20. 500, N
IF
(mA)
.0000
.1500
/div
-1.500
-2.800
0
.3500
VF
.3500/div
(V)
Variable1:
VF -Ch1
Linear sweep
Start -3.0000V
Stop .5000V
Step .2500V
Constants:
V -Ch3 .0000V

****** GRAPHICS PLOT ******

W2 C3,6 D150C,50,0,Y

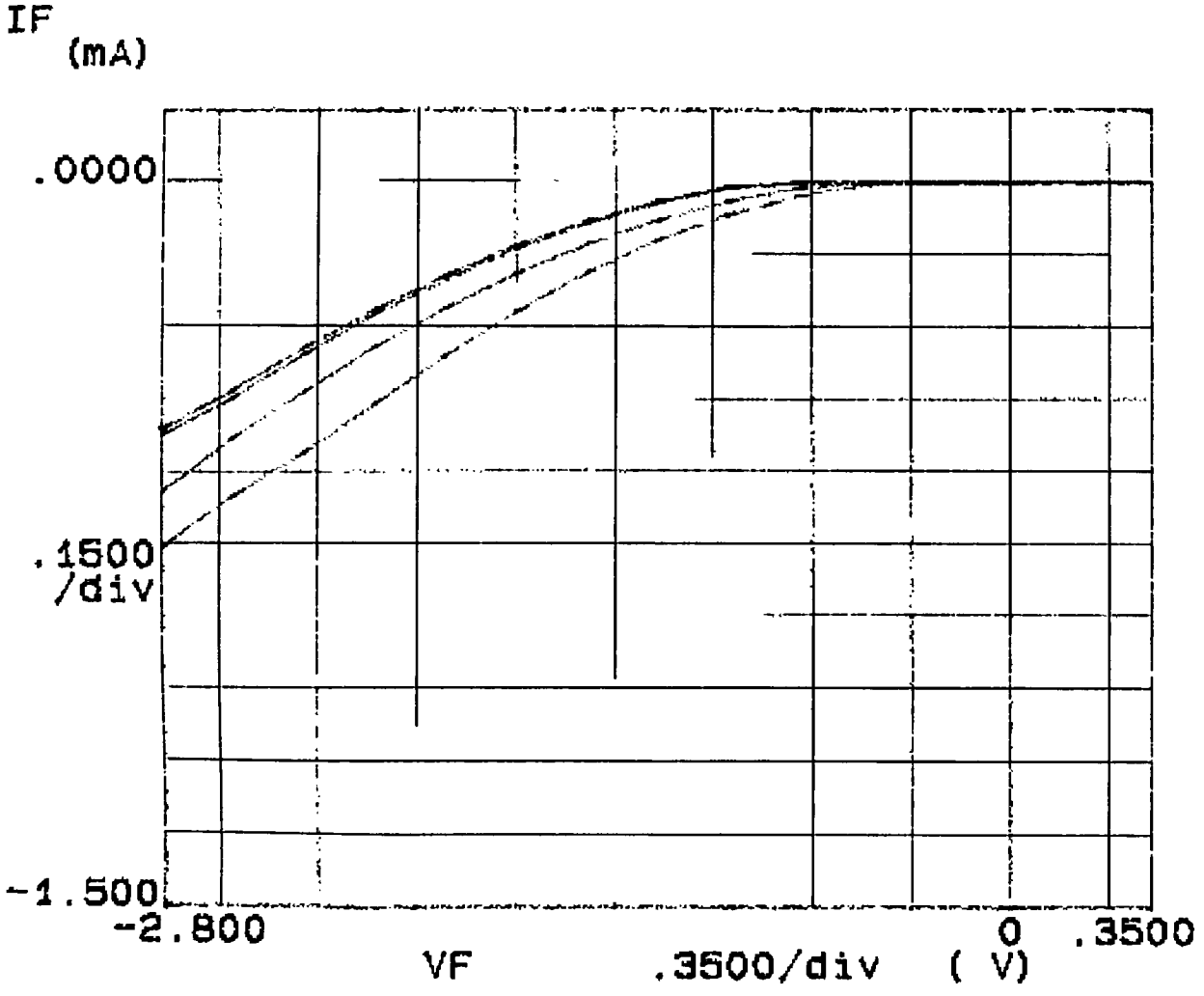

Variable1:
VF -Ch1
Linear sweep
Start -3.0000V
Stop .5000V
Step .2500V

Constants:
V -Ch3 .0000V

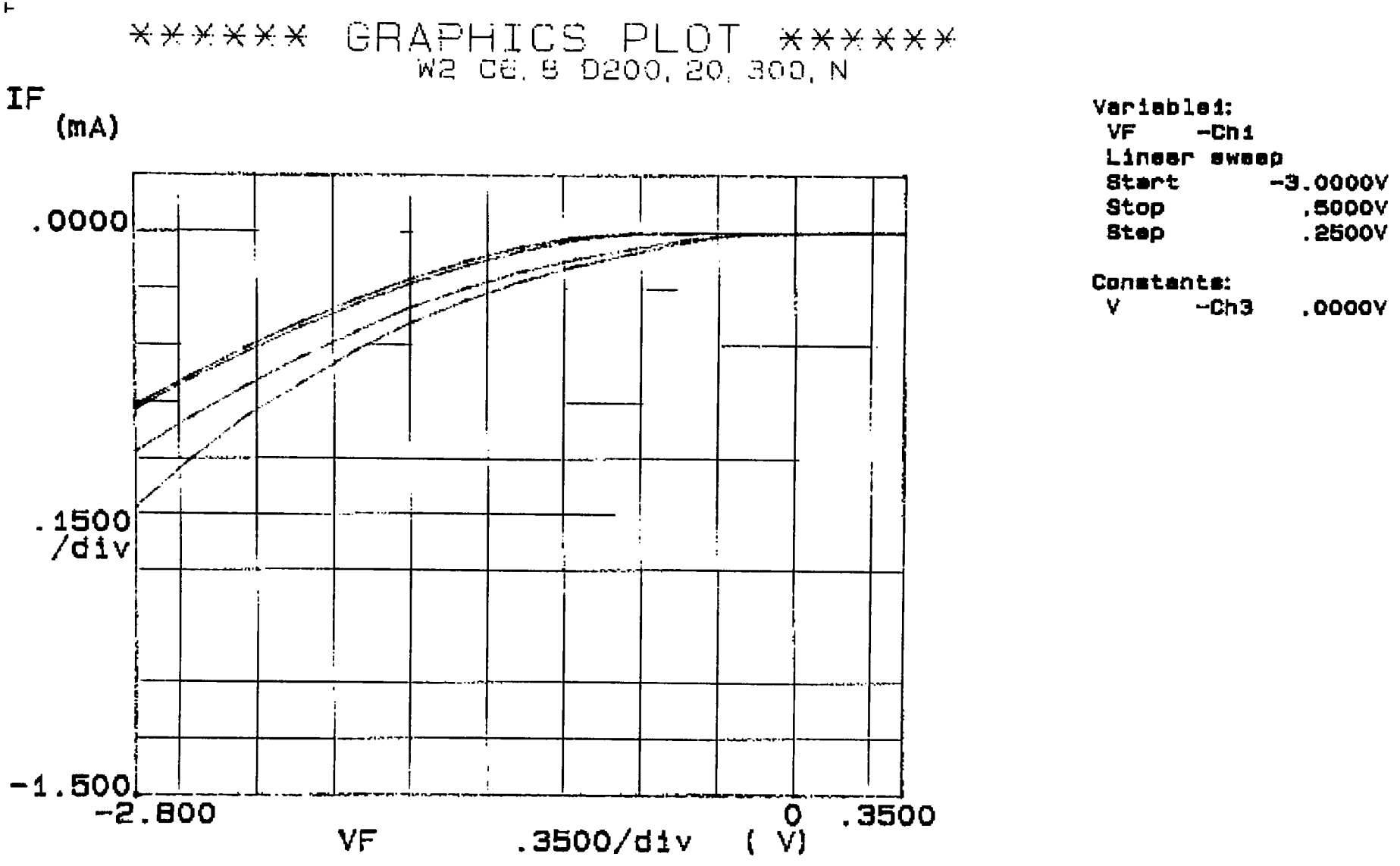
****** GRAPHICS PLOT ******
W2 C8, 8 D200, 20, 300, N
IF
(mA)
.0000
.1500
/div
-1.500
-2.800
0
.3500
VF
.3500/div
(V)
Variable1:
VF -Ch1
Linear sweep
Start -3.0000V
Stop .5000V
Step .2500V
Constants:
V -Ch3 .0000V

****** GRAPHICS PLOT ******

W2 C6.8 D200.20.300.Y

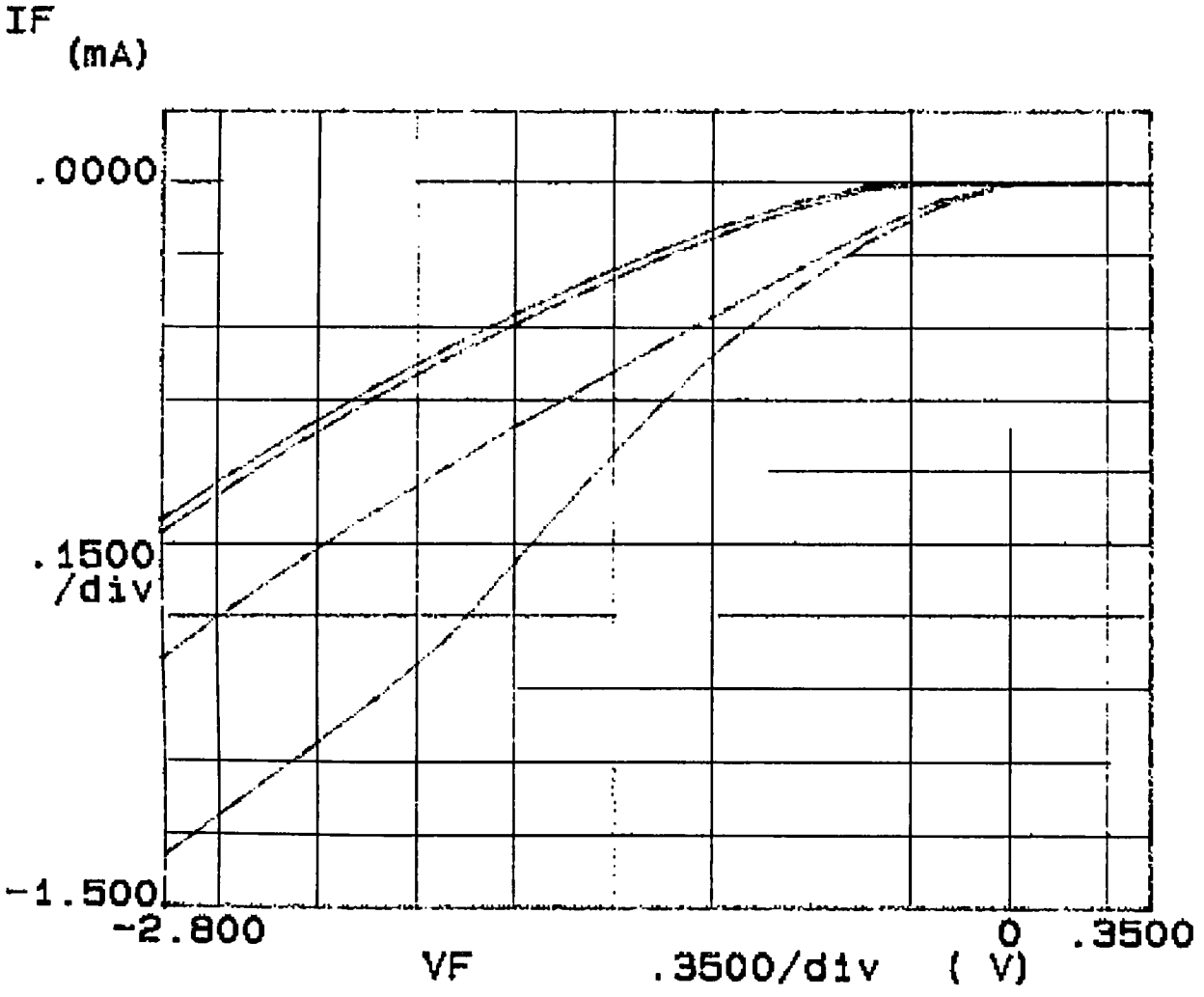

Variable1:
VF -Ch1
Linear sweep
Start -3.0000V
Stop .5000V
Step .2500V

Constants:
V -Ch3 .0000V

****** GRAPHICS PLOT ******

W2 C6, 8 D200, 30, 400, N

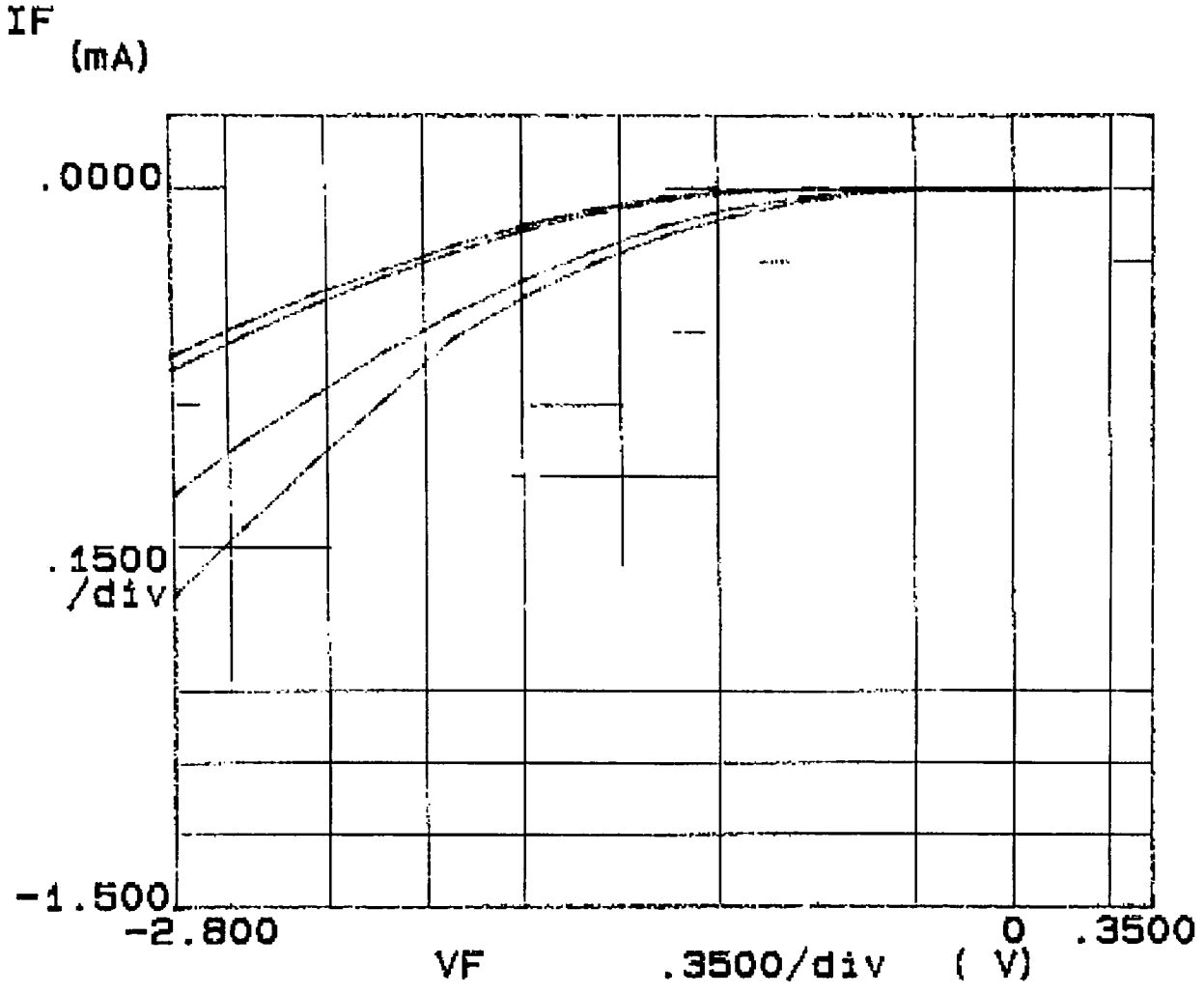

Variable1:
VF -Ch1
Linear sweep
Start -3.0000V
Stop .5000V
Step .2500V

Constants:
V -Ch3 .0000V

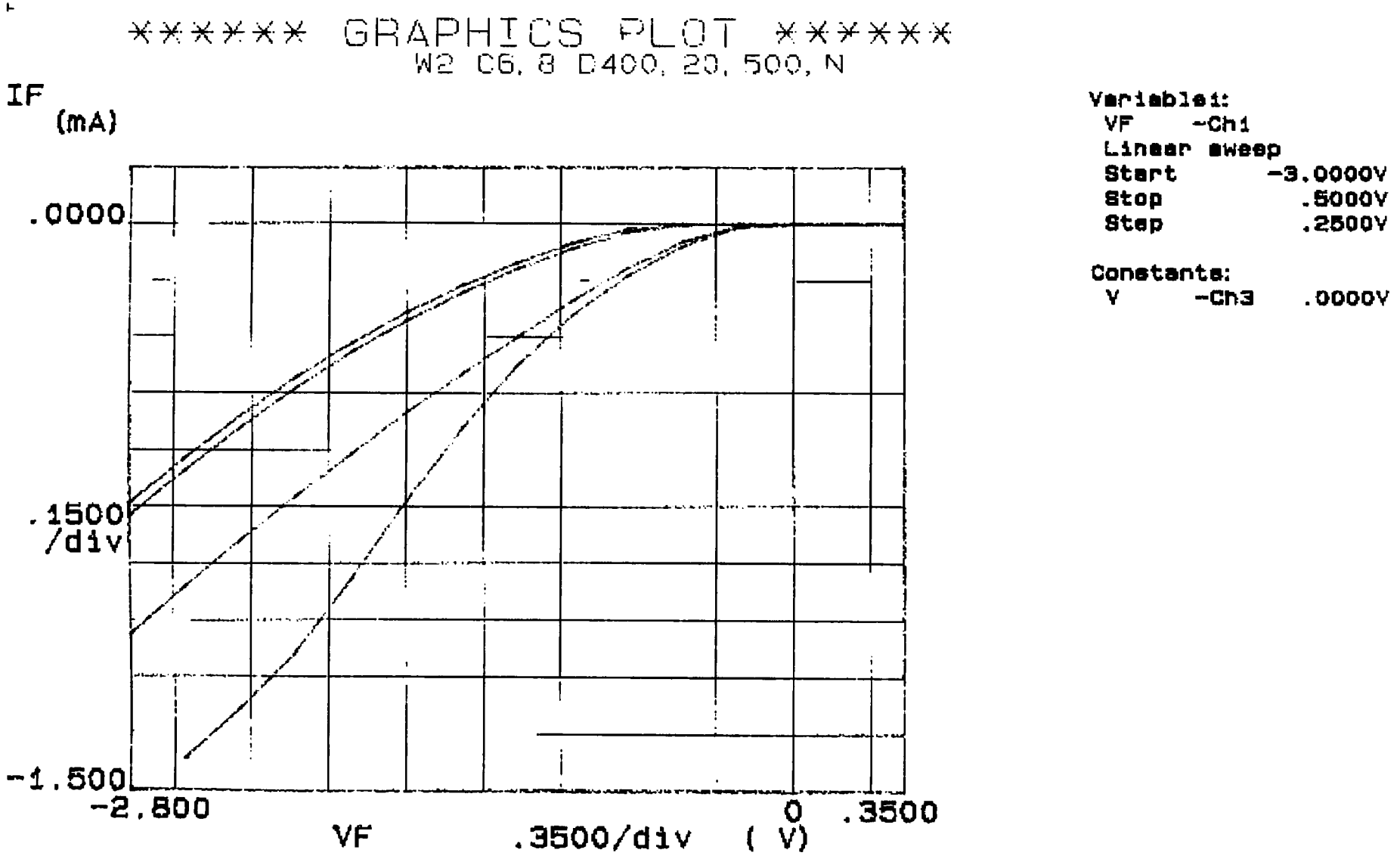
****** GRAPHICS PLOT ******
W2 C6, 8 D400, 20, 500, N
IF
(mA)
.0000
.1500
/div
-1.500
-2.800
0
.3500
VF
.3500/div
(V)
Variable1:
VF -Ch1
Linear sweep
Start -3.0000V
Stop .5000V
Step .2500V
Constants:
V -Ch3 .0000V

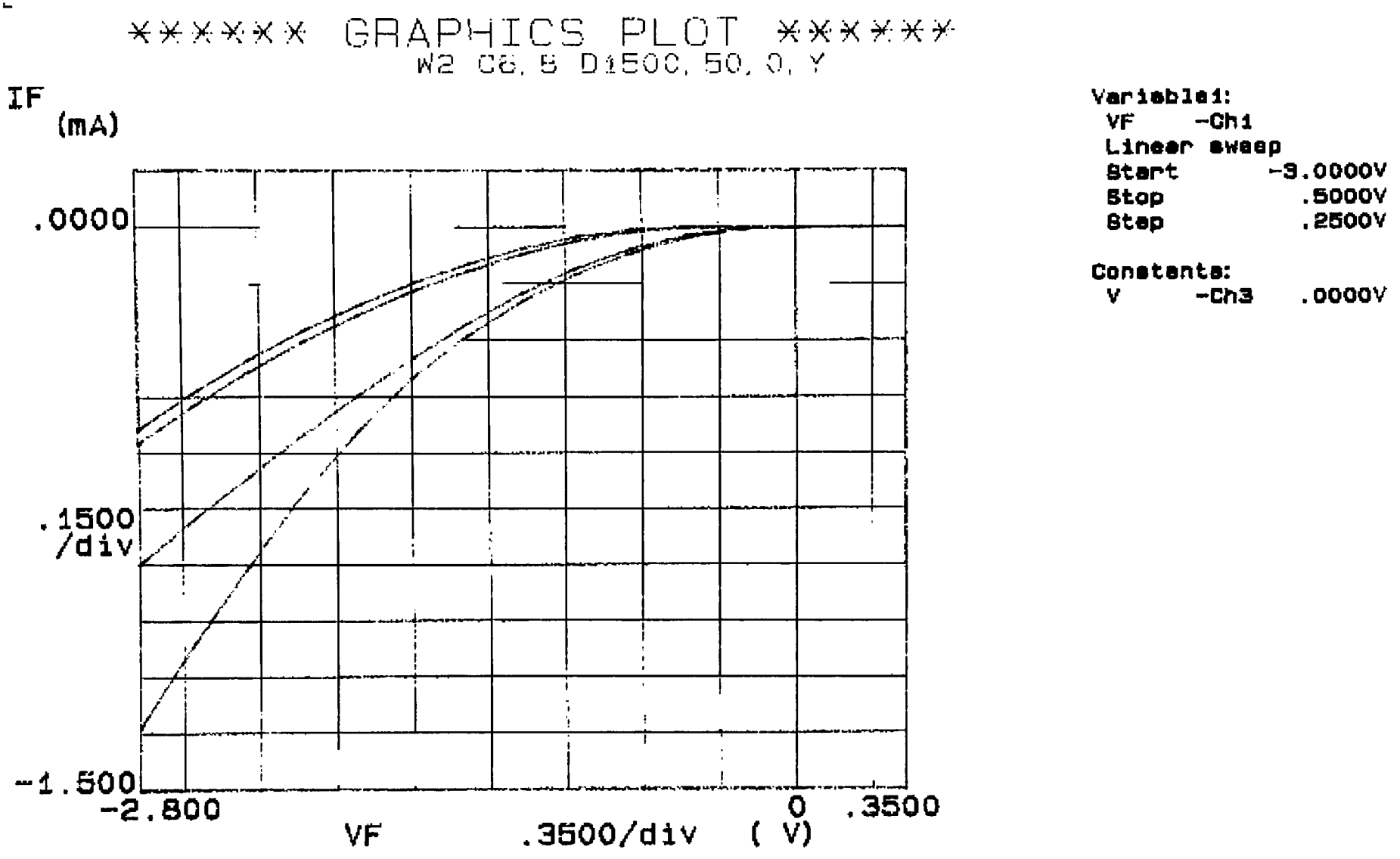
****** GRAPHICS PLOT ******
W2 C6,5 D150C,50,0,Y
IF
(mA)
.0000
.1500
/div
-1.500
-2.800
0
.3500
VF
.3500/div
(V)
Variable1:
VF -Ch1
Linear sweep
Start -3.0000V
Stop .5000V
Step .2500V
Constants:
V -Ch3 .0000V

****** GRAPHICS PLOT ******

W3 C5, 9 D200, 3C. 300. N

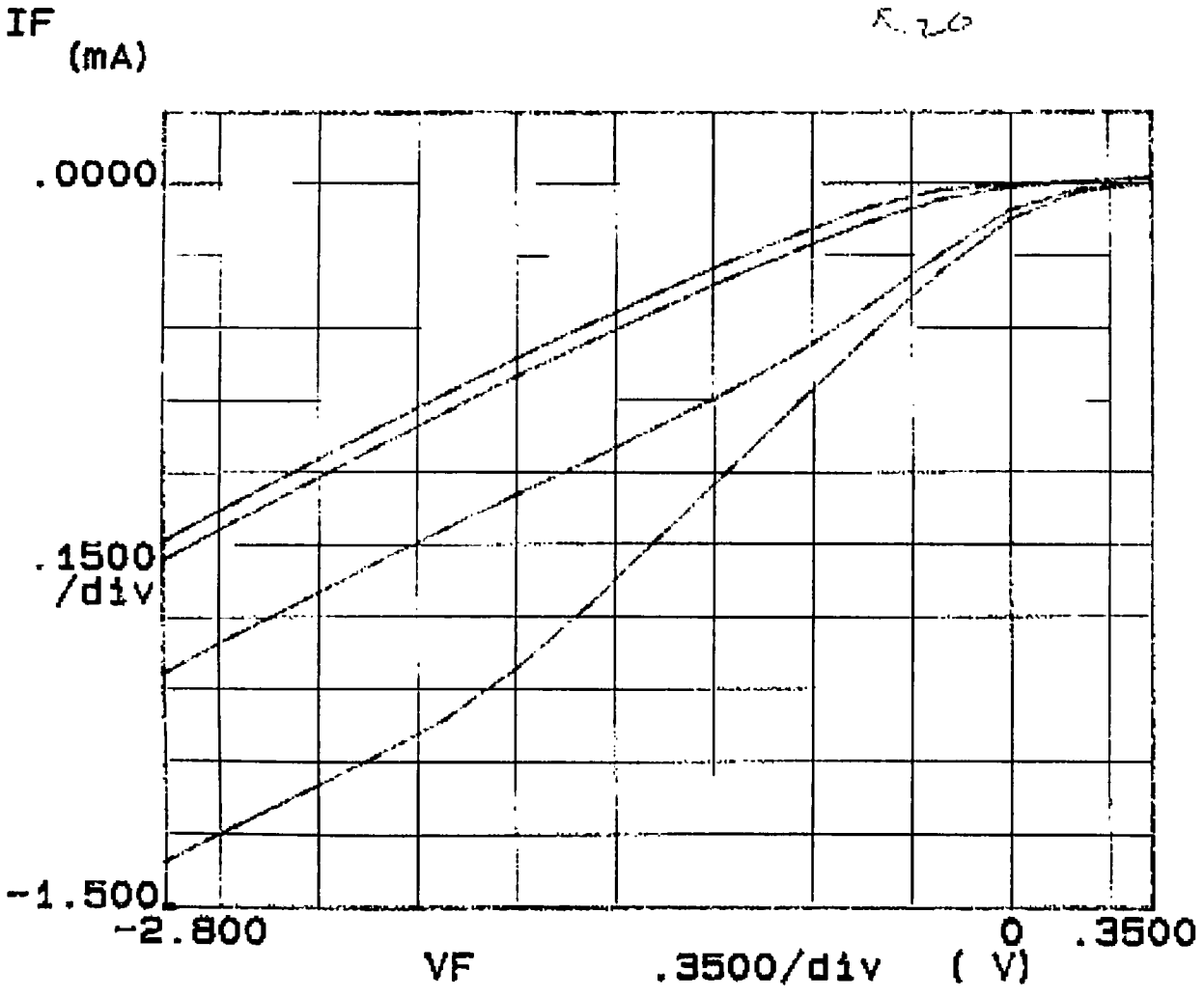

Variable1:
VF -Ch1
Linear sweep
Start -3.0000V
Stop .5000V
Step .2500V

Constants:
V -Ch3 .0000V

****** GRAPHICS PLOT ******

W3 C5, 9 C200, 30, 300, Y

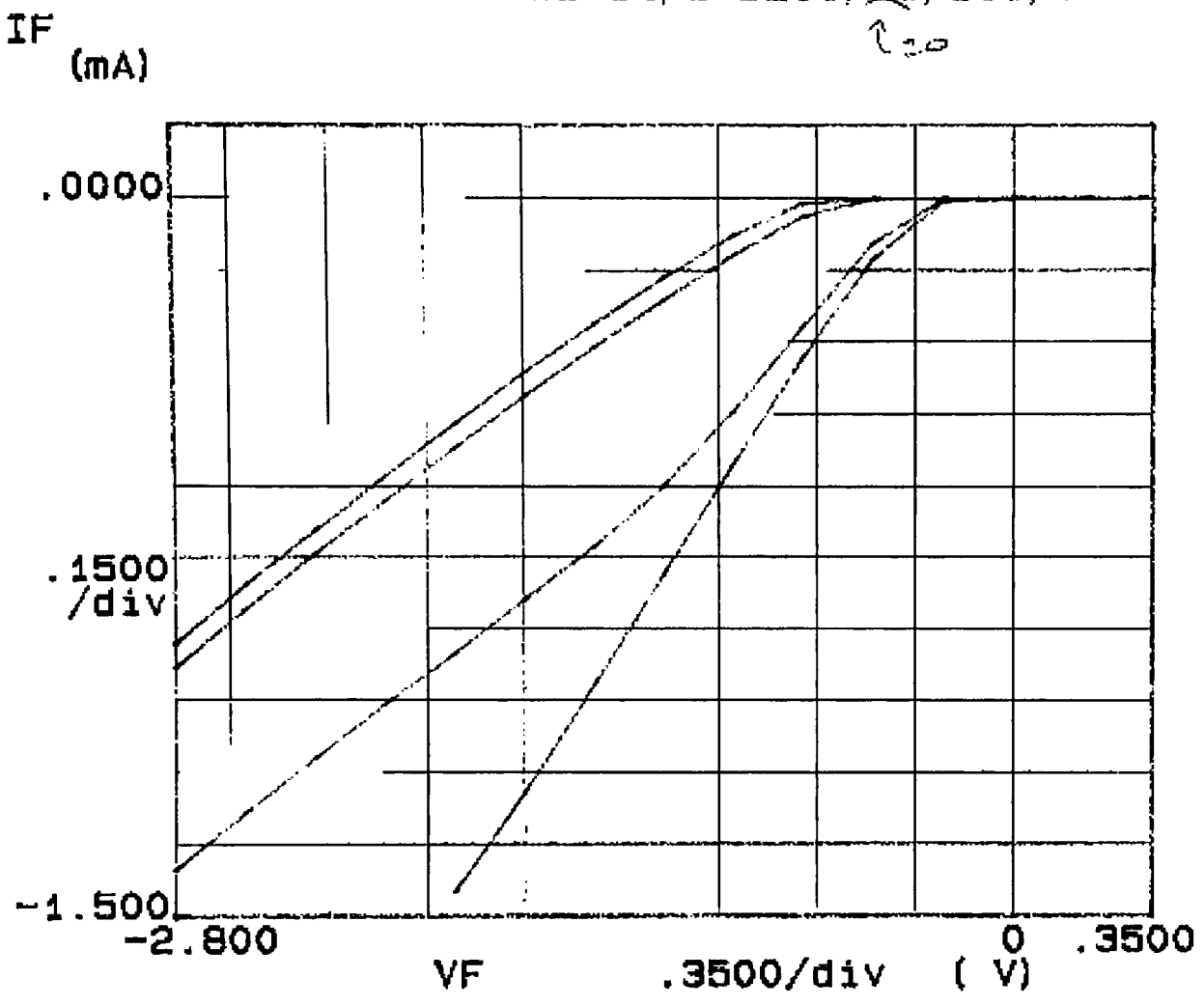

Variable1:
VF -Ch1
Linear sweep
Start -3.0000V
Stop .5000V
Step .2500V

Constante:
V -Ch3 .0000V

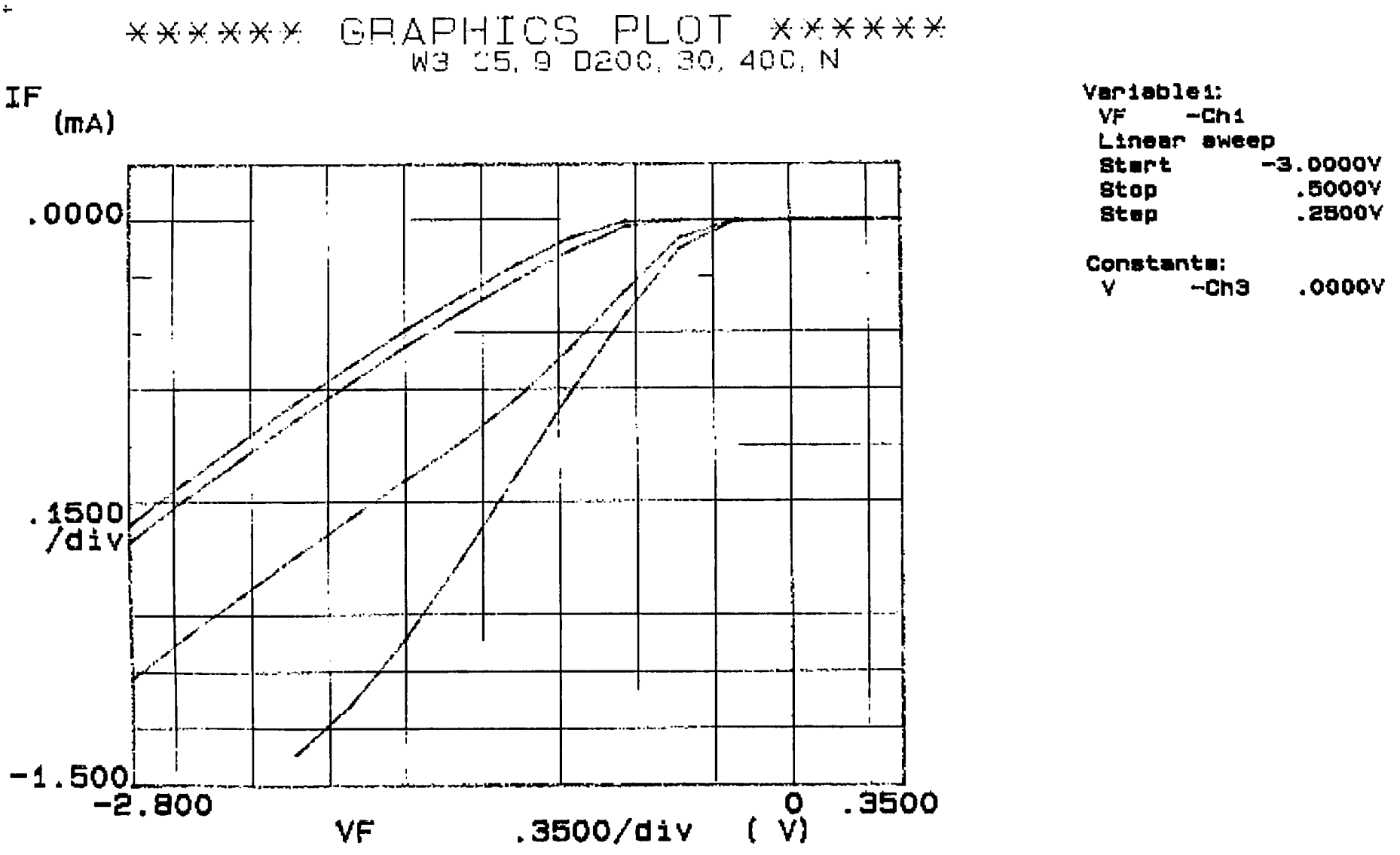
****** GRAPHICS PLOT ******
W3 C5, 9 D200, 30, 400, N
IF
(mA)
.0000
.1500
/div
-1.500
-2.800
0
.3500
VF
.3500/div
(V)
Variable1:
VF -Ch1
Linear sweep
Start -3.0000V
Stop .5000V
Step .2500V
Constants:
V -Ch3 .0000V

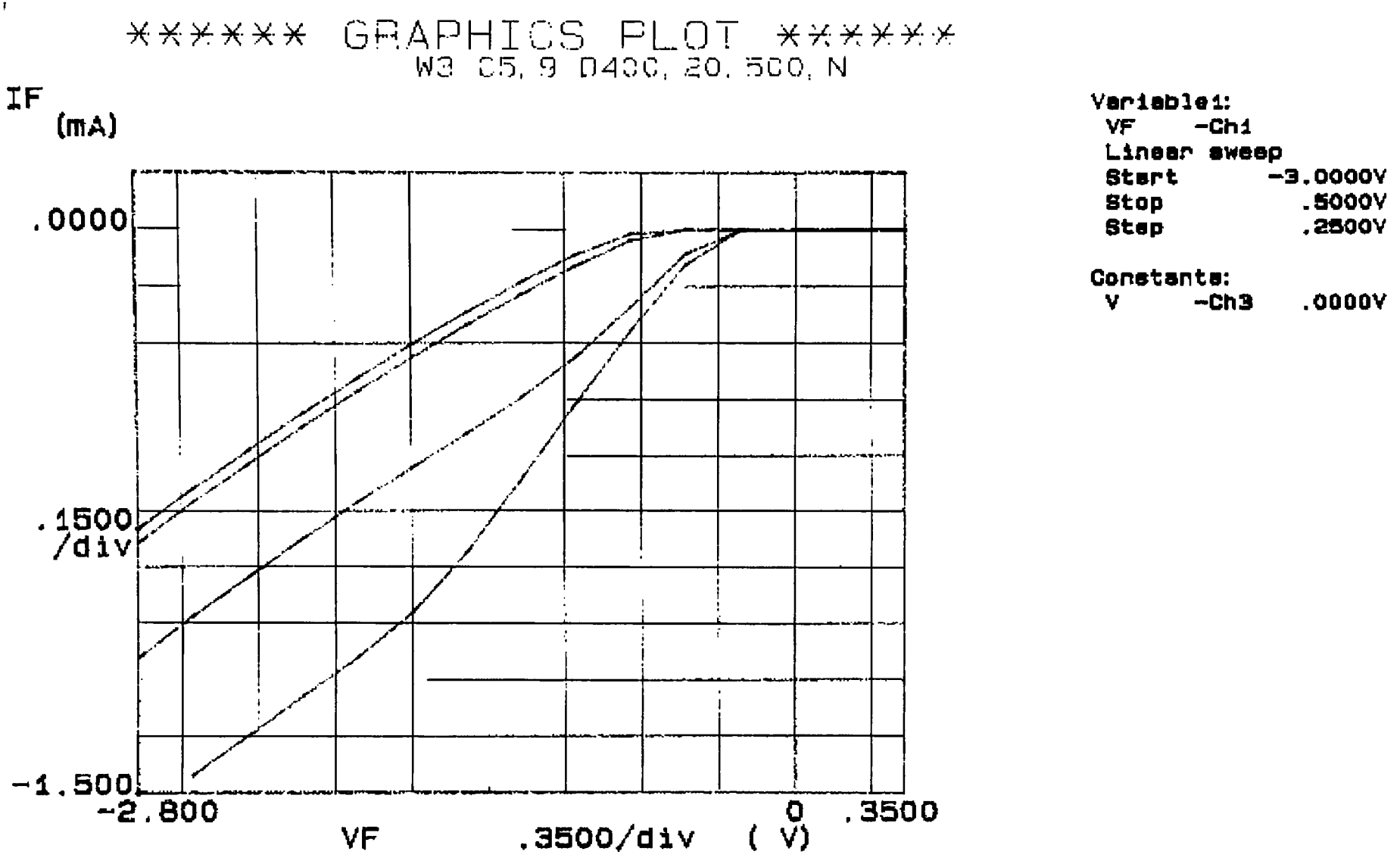
****** GRAPHICS PLOT ******
W3 C5, 9 D400, 20, 500, N
IF
(mA)
.0000
.1500
/div
-1.500
-2.800
0
.3500
VF
.3500/div
(V)
Variable1:
VF -Ch1
Linear sweep
Start -3.0000V
Stop .5000V
Step .2500V
Constants:
V -Ch3 .0000V

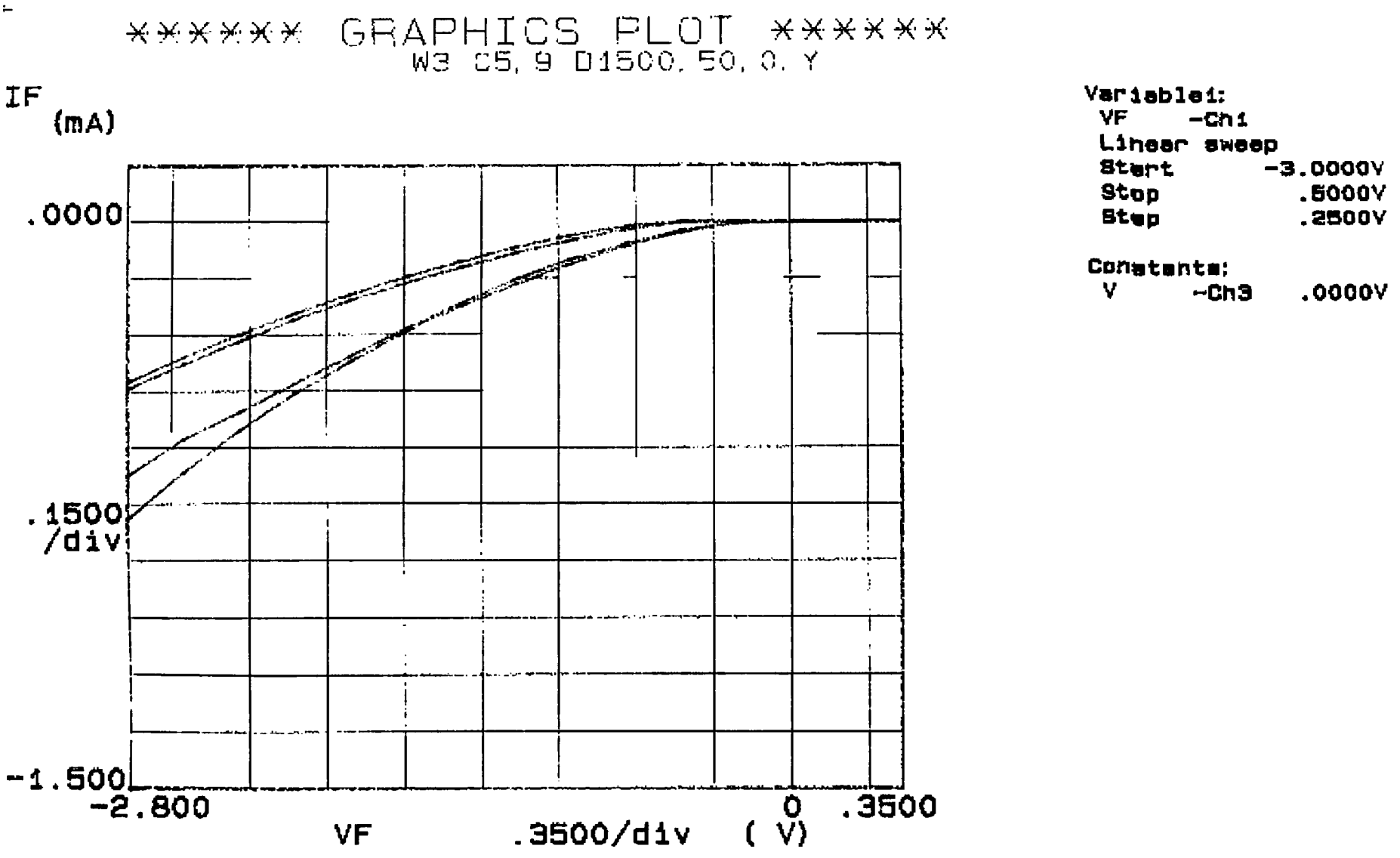
****** GRAPHICS PLOT ******
W3 C5, 9 D1500, 50, 0, Y
IF
(mA)
.0000
.1500
/div
-1.500
-2.800
0
.3500
VF
.3500/div
(V)
Variable1:
VF -Ch1
Linear sweep
Start -3.0000V
Stop .5000V
Step .2500V
Constants:
V -Ch3 .0000V

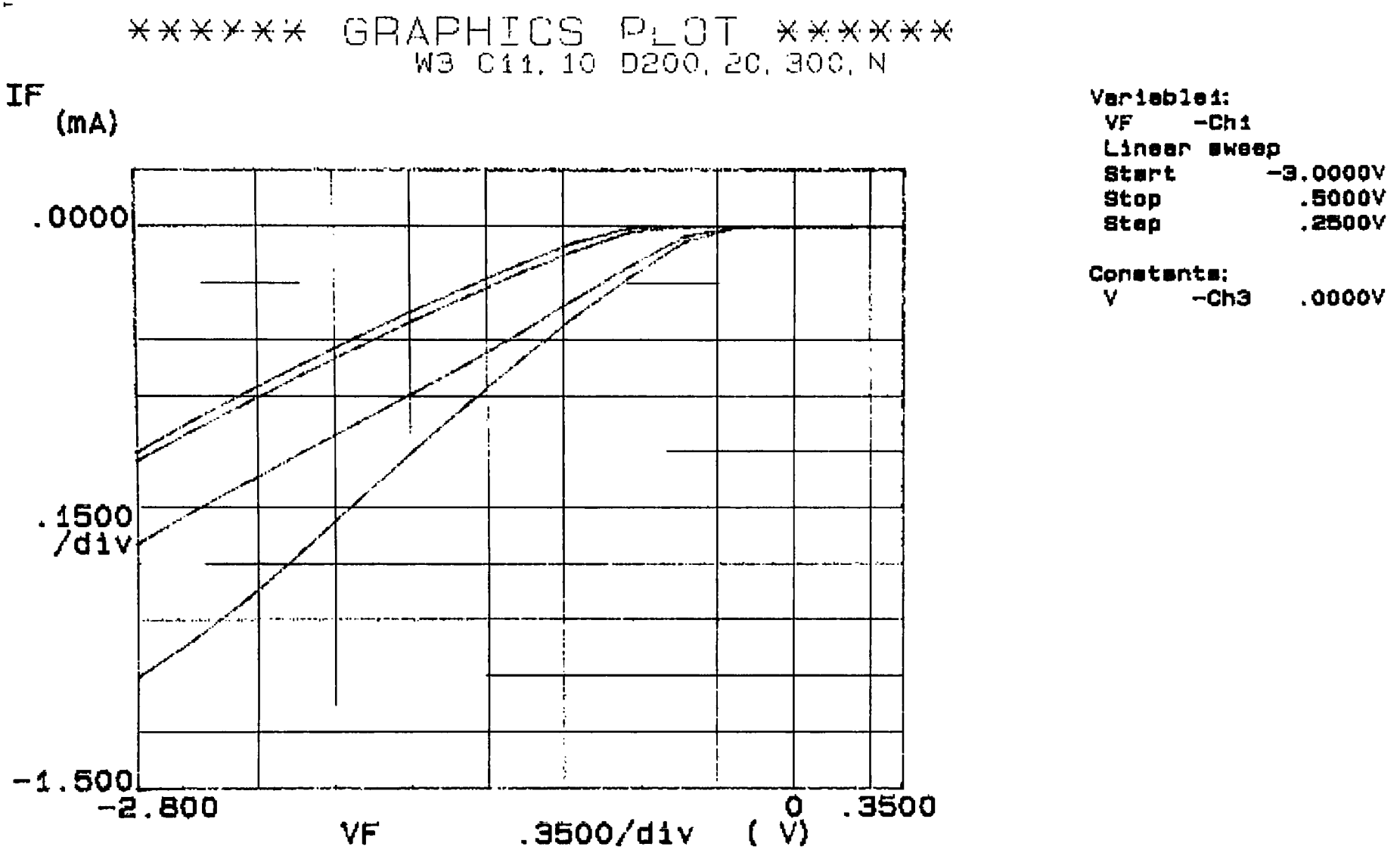
****** GRAPHICS PLOT ******
W3 C11, 10 D200, 20, 300, N
IF
(mA)
.0000
.1500
/div
-1.500
-2.800
0
.3500
VF
.3500/div
(V)
Variable1:
VF -Ch1
Linear sweep
Start -3.0000V
Stop .5000V
Step .2500V
Constants:
V -Ch3 .0000V

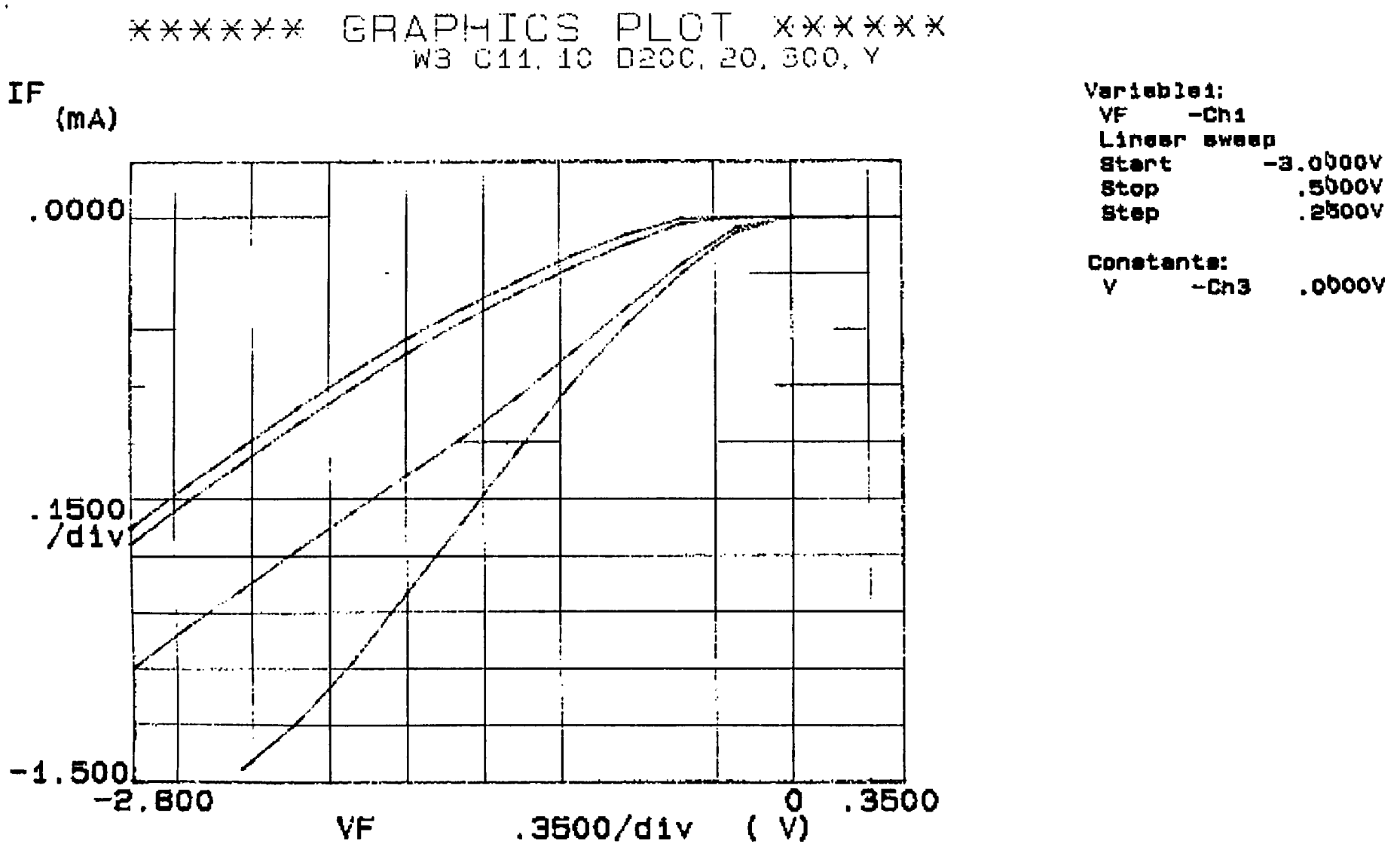
****** GRAPHICS PLOT ******
W3 C11, 10 D200, 20, 300, Y
IF
(mA)
.0000
.1500
/div
-1.500
-2.600
0
.3500
VF
.3500/div
(V)
Variable1:
VF -Ch1
Linear sweep
Start -3.0000V
Stop .5000V
Step .2500V
Constants:
V -Ch3 .0000V

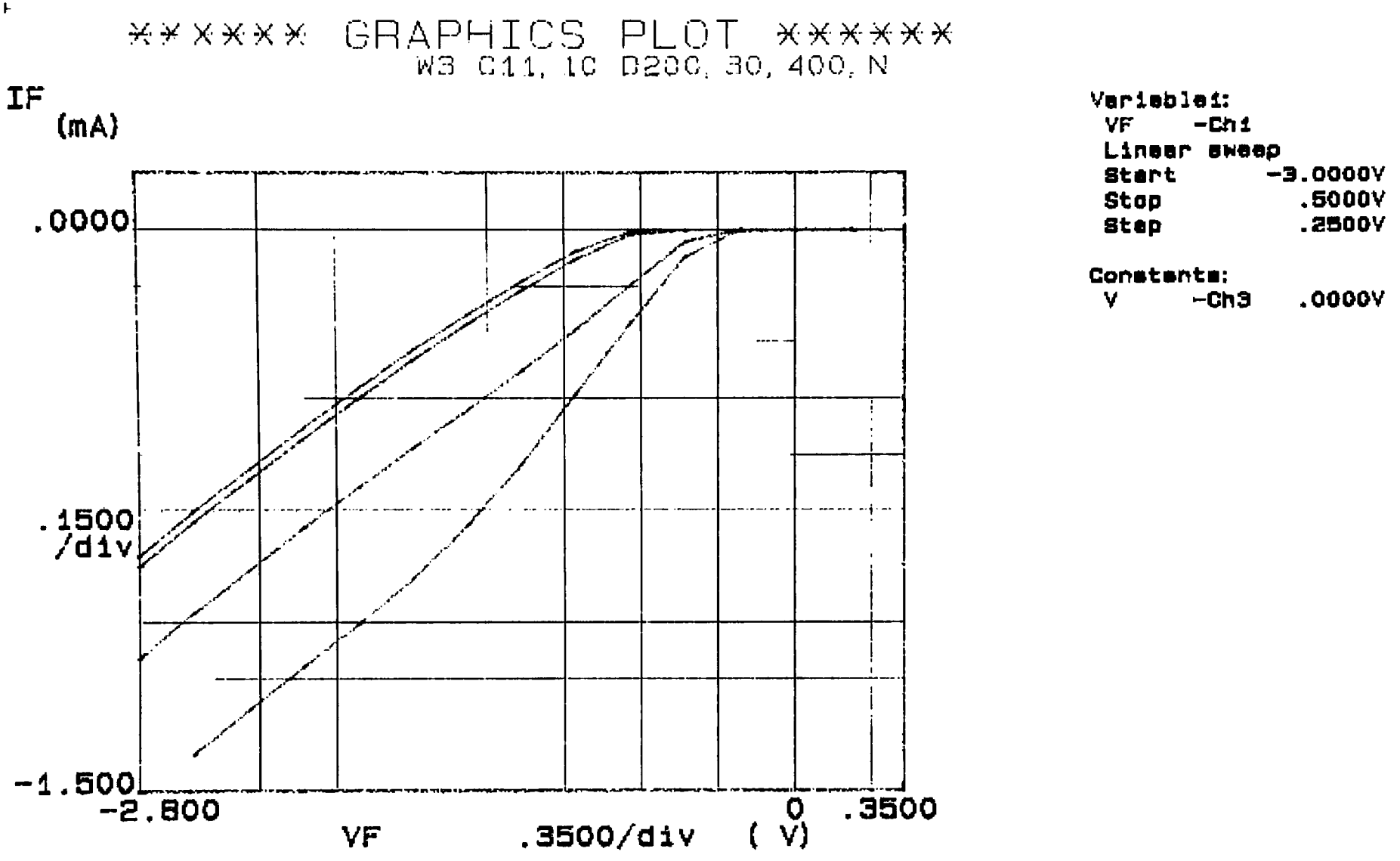
****** GRAPHICS PLOT ******
W3 C11, 1C D200, 30, 400, N
IF
(mA)
.0000
.1500
/div
-1.500
-2.800
0
.3500
VF
.3500/div
(V)
Variable1:
VF -Ch1
Linear sweep
Start -3.0000V
Stop .5000V
Step .2500V
Constants:
V -Ch3 .0000V

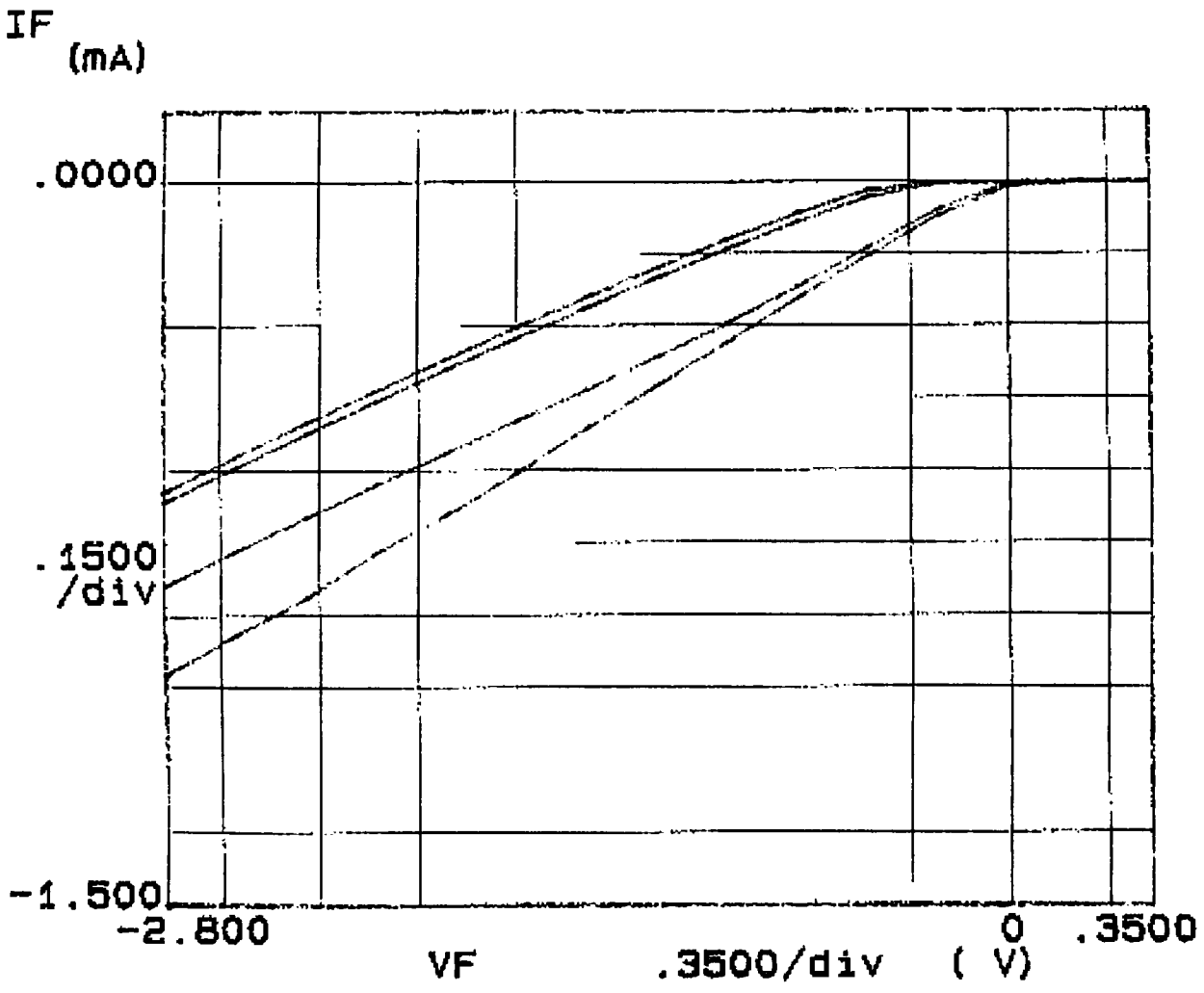

Variable1:
VF -Ch1
Linear sweep
Start -3.0000V
Stop .5000V
Step .2500V

Constants:
V -Ch3 .0000V

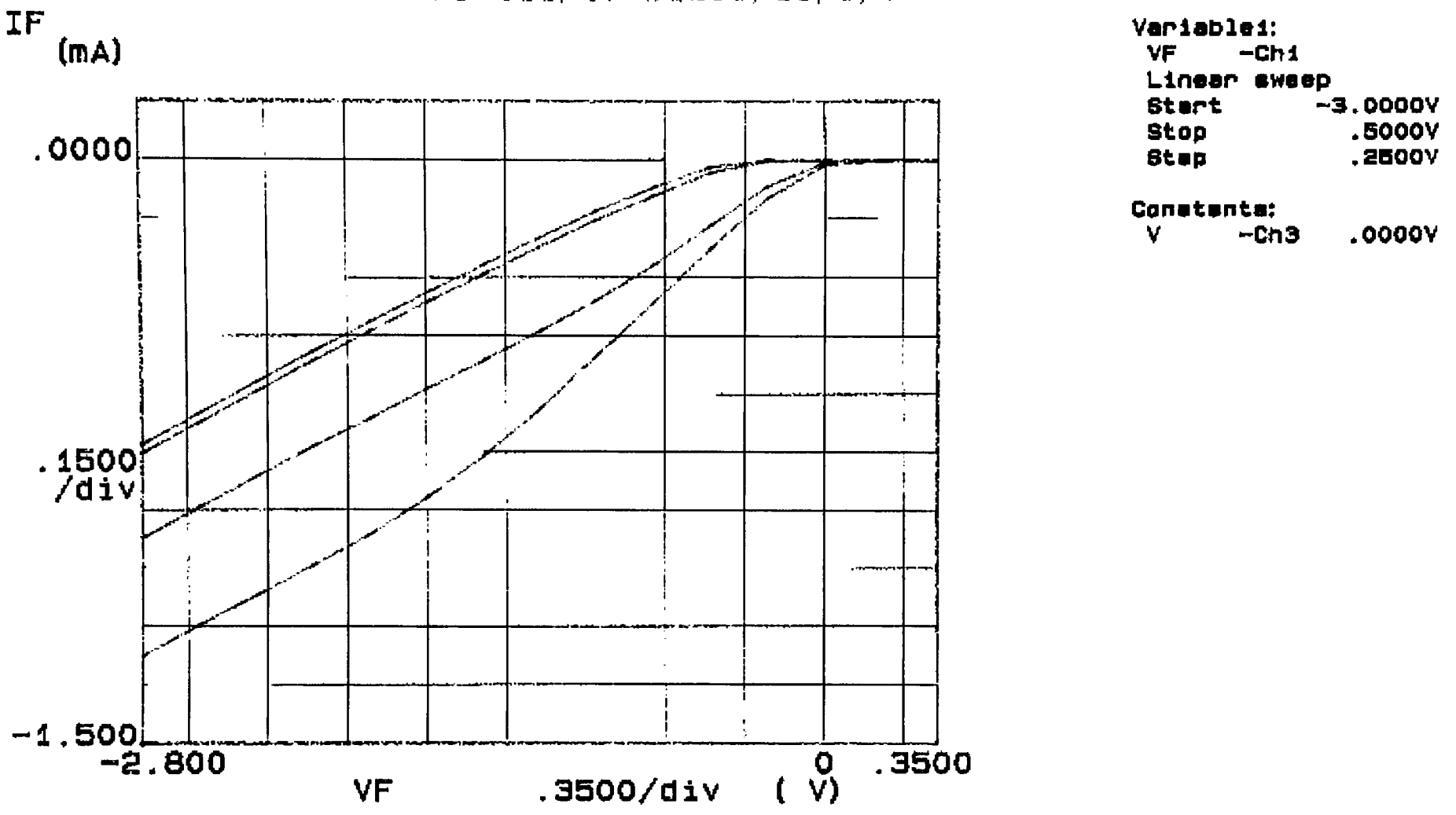
****** GRAPHICS PLOT ******
W3 C11, 10 D1500, 50, 0, Y
IF
(mA)
.0000
.1500
/div
-1.500
-2.800
0
.3500
VF
.3500/div
(V)
Variable1:
VF -Ch1
Linear sweep
Start -3.0000V
Stop .5000V
Step .2500V
Constants:
V -Ch3 .0000V

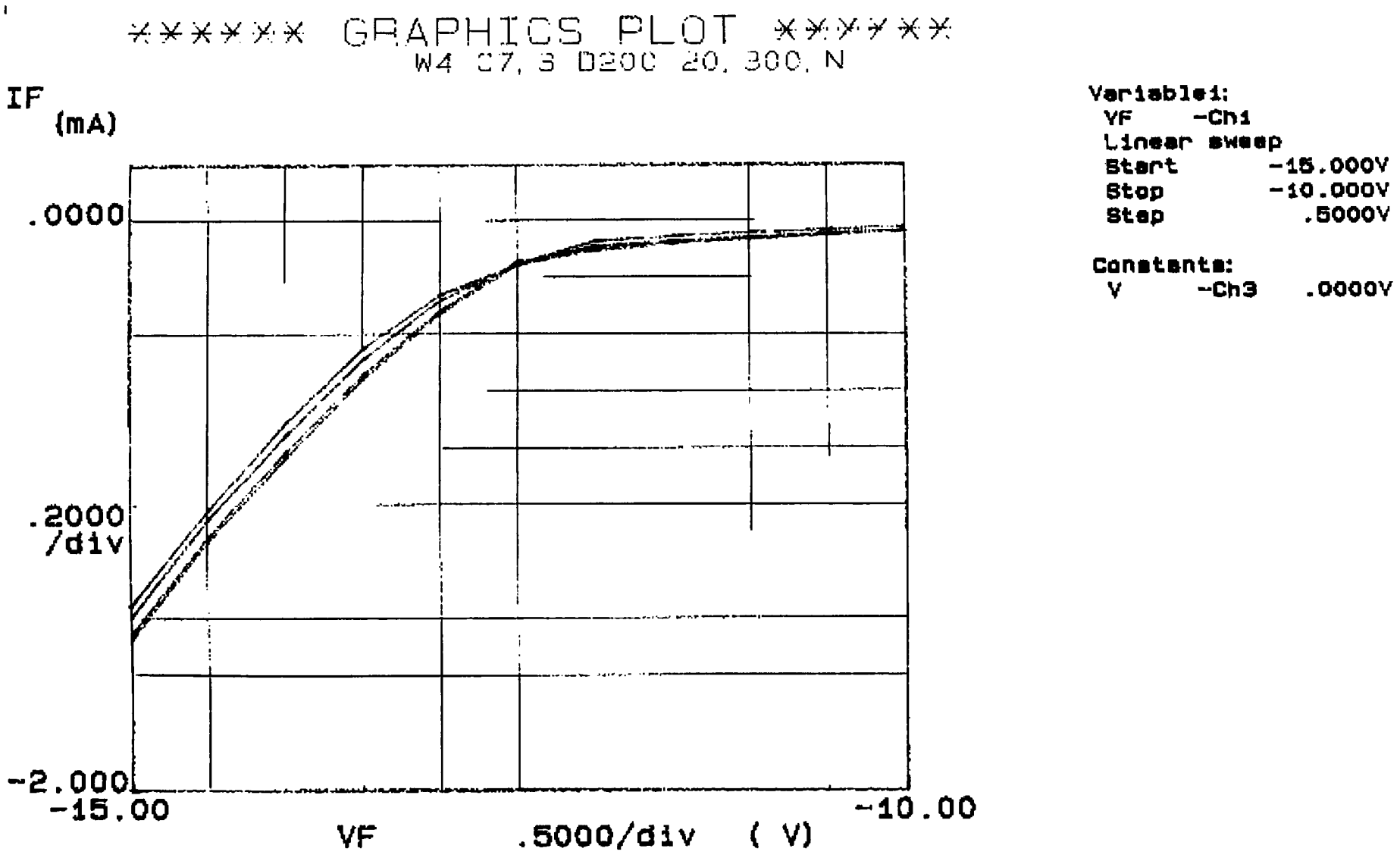
****** GRAPHICS PLOT ******
W4 C7, 3 D20C 20, 300, N
IF
(mA)
.0000
.2000
/div
-2.000
-15.00
-10.00
VF .5000/div (V)
Variable1:
VF -Ch1
Linear sweep
Start -15.000V
Stop -10.000V
Step .5000V
Constants:
V -Ch3 .0000V

****** GRAPHICS PLOT ******

W4 C7,3 D200,20,300,Y

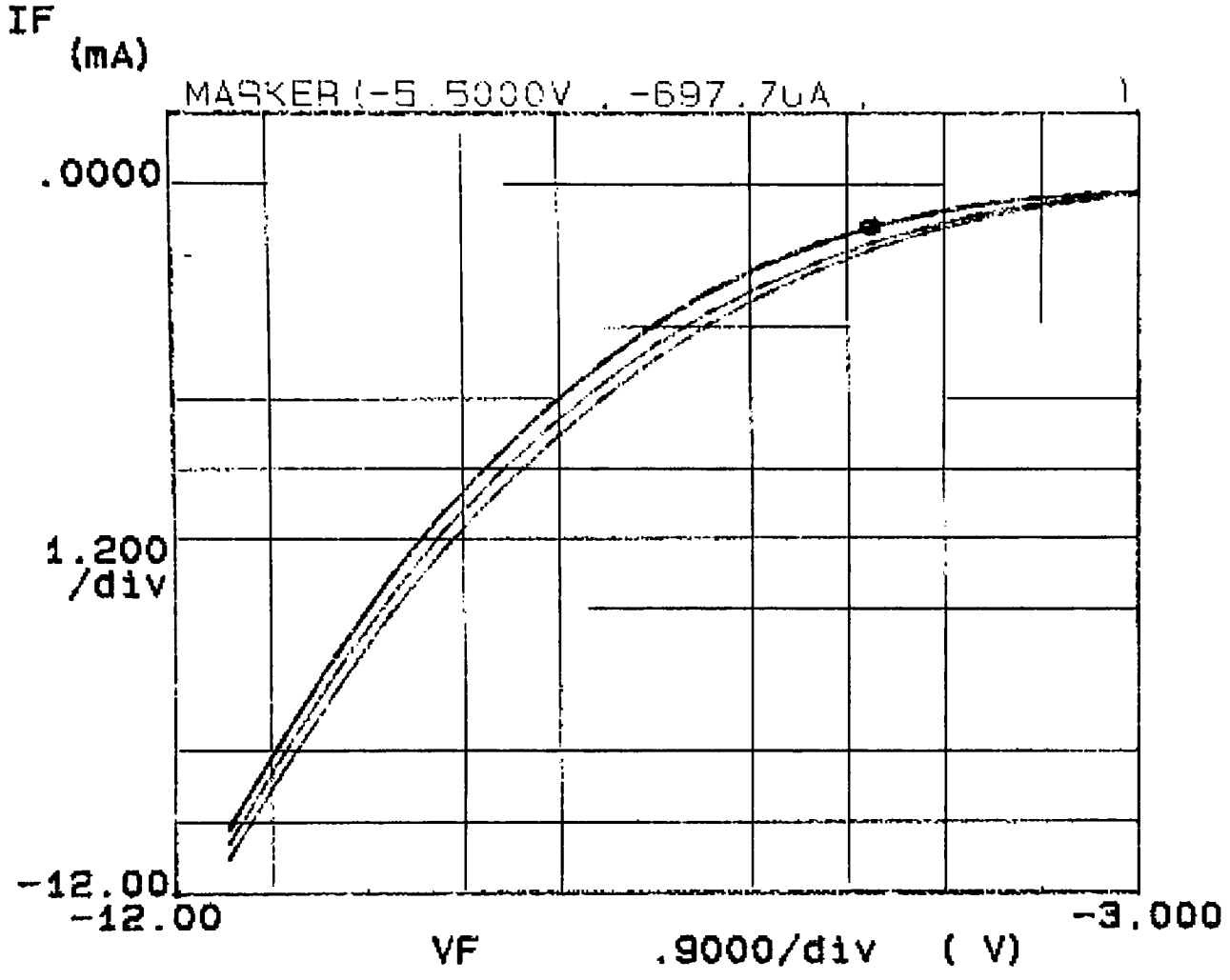

Variable1:
VF -Ch1
Linear sweep
Start -12.000V
Stop -3.0000V
Step .5000V

Constants:
Y -Ch3 .0000V

****** GRAPHICS PLOT ******

W4 C7, 3 D200, 30, 400, N

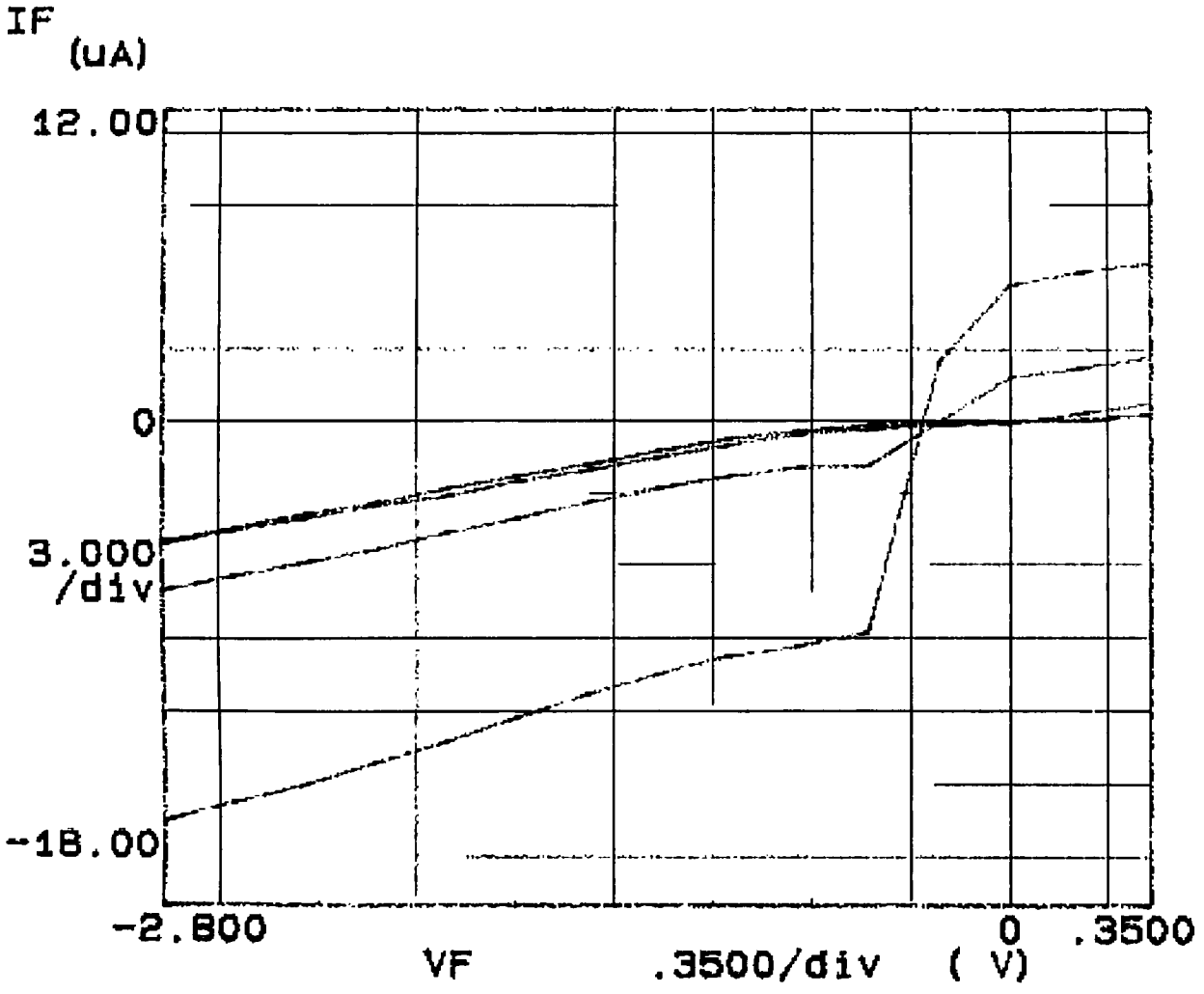

Variable1:
VF -Ch1
Linear sweep
Start -3.0000V
Stop .5000V
Step .2500V

Constants:
V -Ch3 .0000V

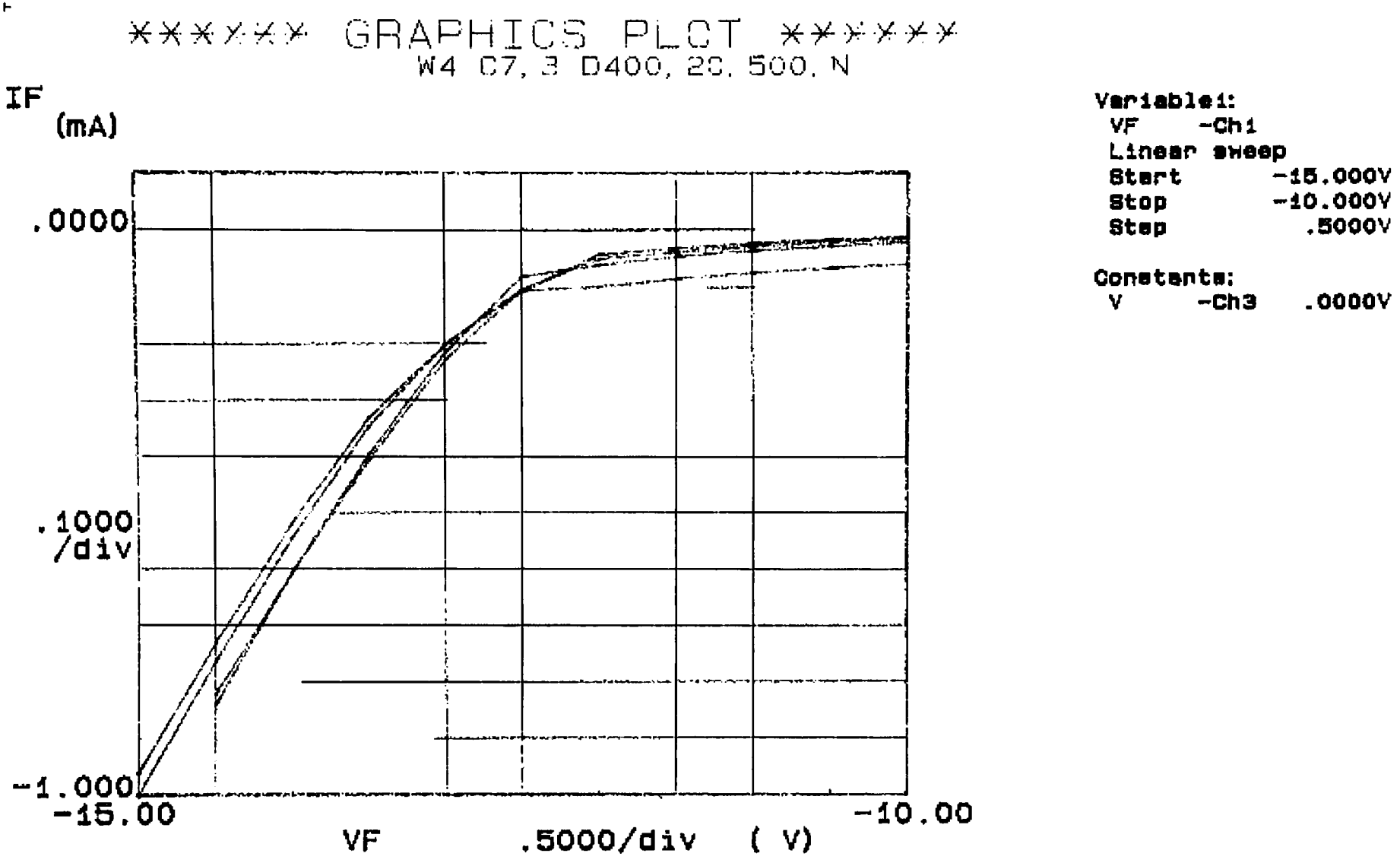
****** GRAPHICS PLOT ******
W4 C7, 3 D400, 20, 500, N
IF
(mA)
.0000
.1000
/div
-1.000
-15.00
-10.00
VF .5000/div (V)
Variable1:
VF -Ch1
Linear sweep
Start -15.000V
Stop -10.000V
Step .5000V
Constants:
V -Ch3 .0000V

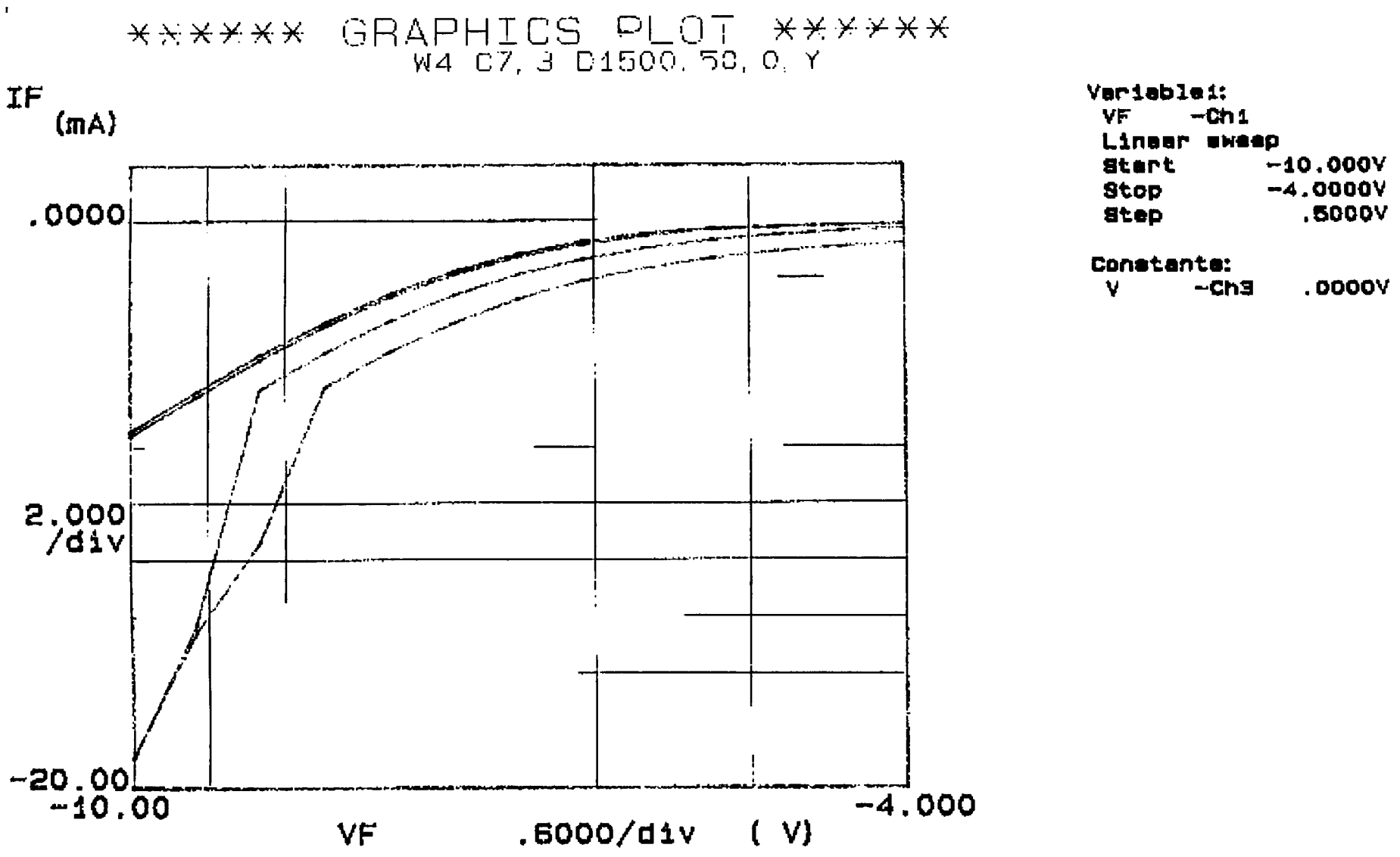
****** GRAPHICS PLOT ******
W4 C7,3 D1500,50,0,Y
IF
(mA)
.0000
2.000
/div
-20.00
-10.00
-4.000
VF .6000/div (V)
Variable1:
VF -Ch1
Linear sweep
Start -10.000V
Stop -4.0000V
Step .5000V
Constante:
V -Ch3 .0000V

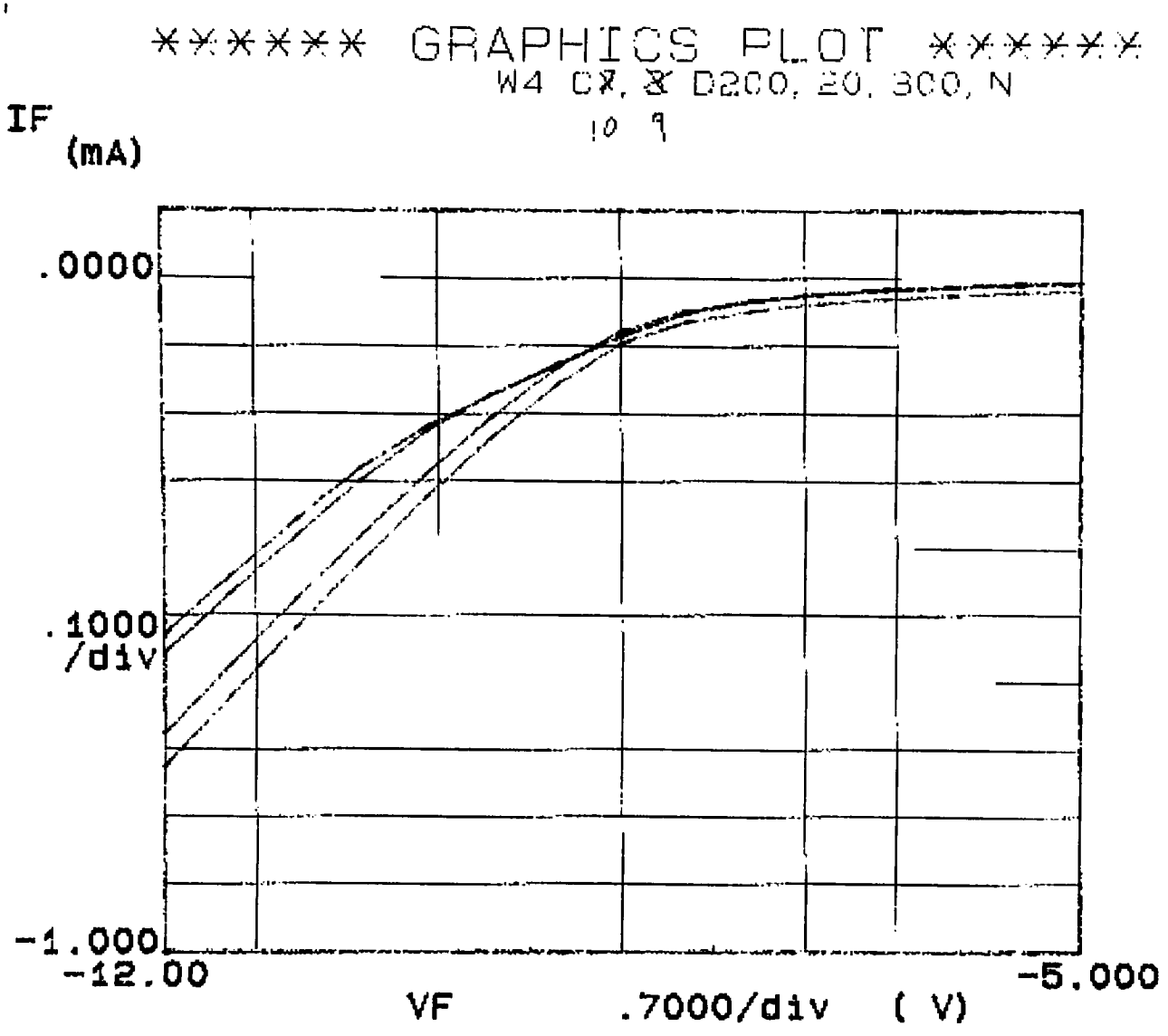

Variable1:
VF -Ch1
Linear sweep
Start -12.000V
Stop -5.0000V
Step .5000V

Constants:
V -Ch3 .0000V

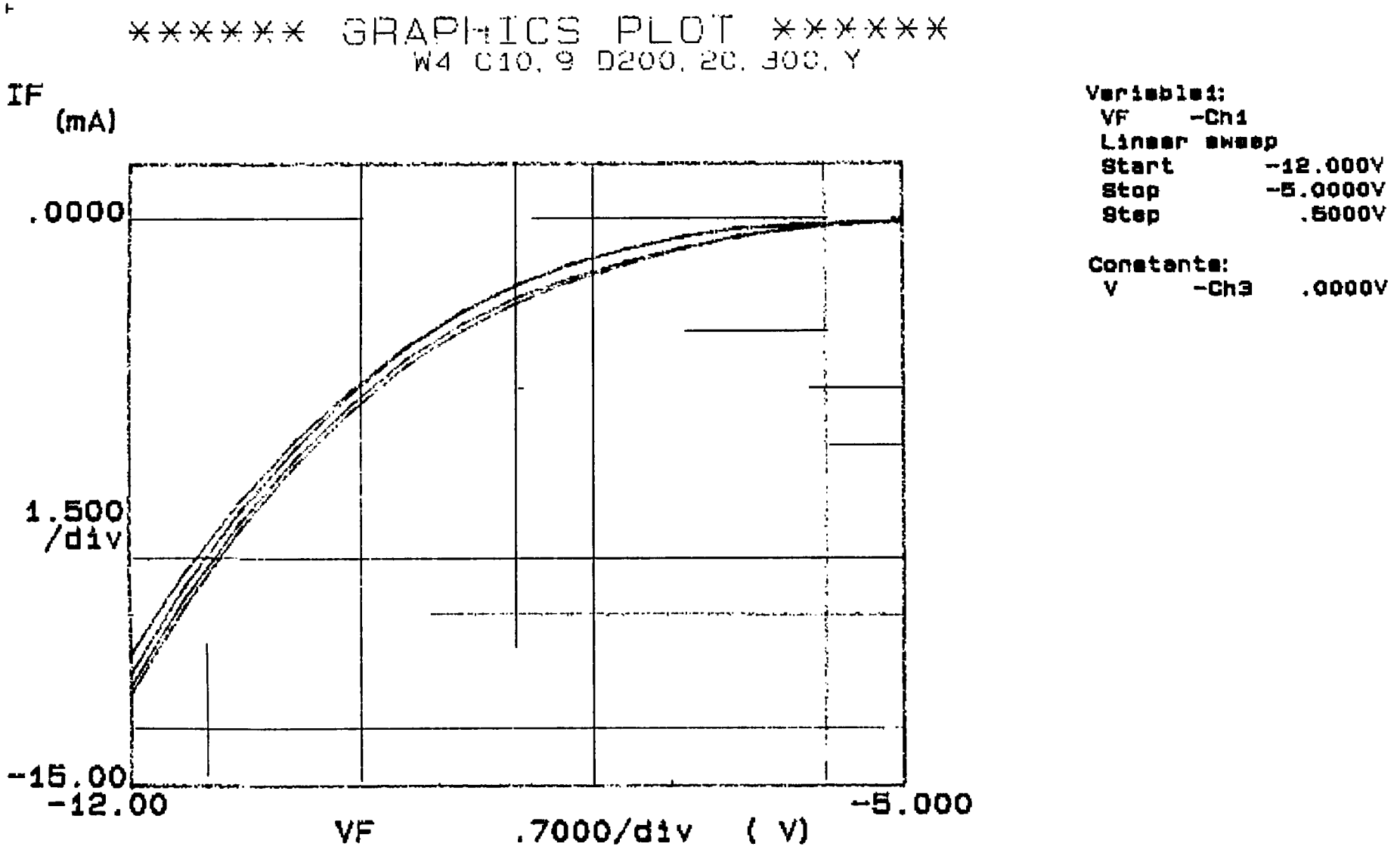
****** GRAPHICS PLOT ******
W4 C10,9 D200,20,300,Y
IF
(mA)
.0000
1.500
/div
-15.00
-12.00
-5.000
VF .7000/div (V)
Variable1:
VF -Ch1
Linear sweep
Start -12.000V
Stop -5.0000V
Step .5000V
Constante:
V -Ch3 .0000V

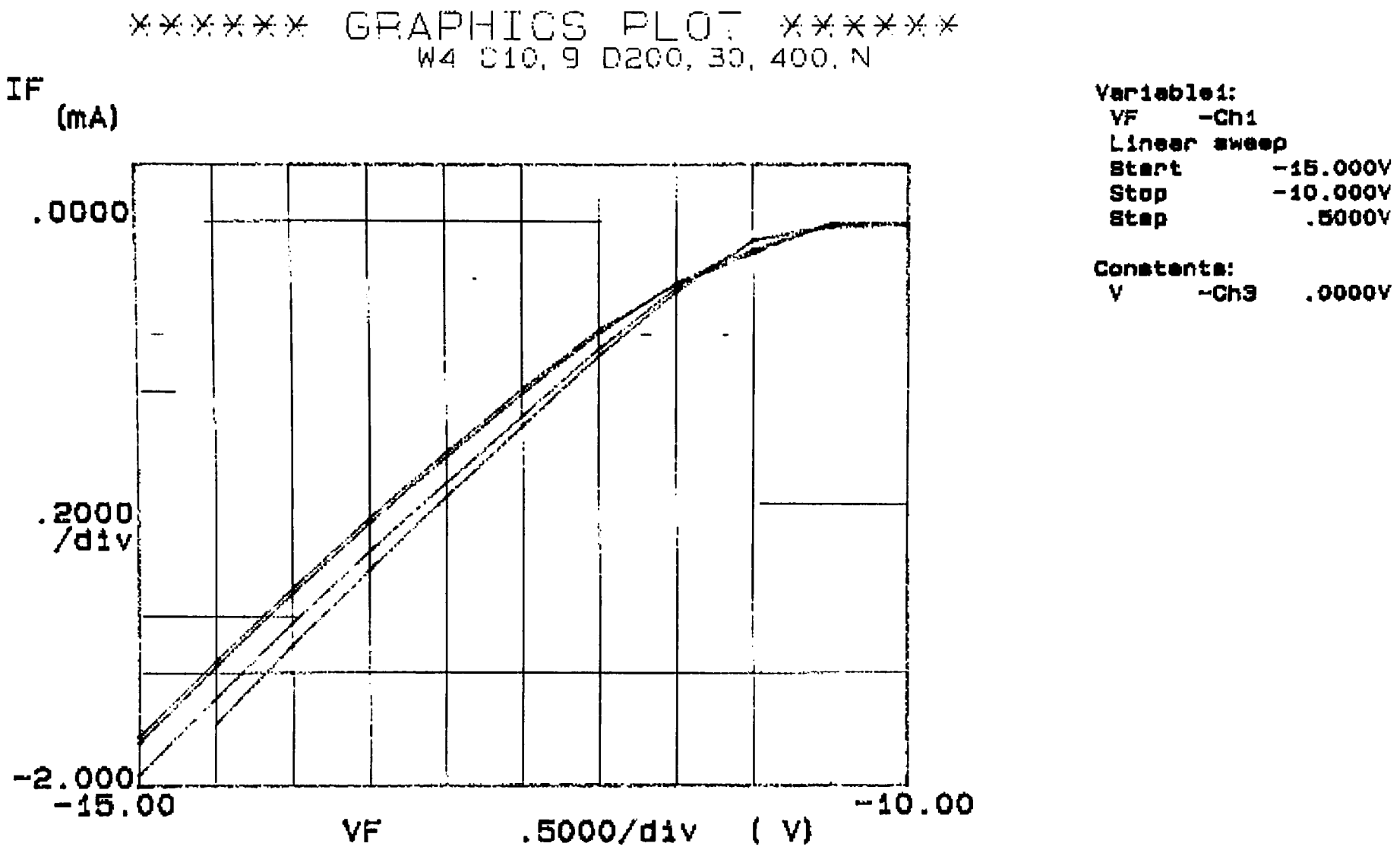
****** GRAPHICS PLOT ******
W4 C10, 9 D200, 30, 400, N
IF
(mA)
.0000
.2000
/div
-2.000
-15.00
-10.00
VF .5000/div (V)
Variable1:
VF -Ch1
Linear sweep
Start -15.000V
Stop -10.000V
Step .5000V
Constants:
V -Ch3 .0000V

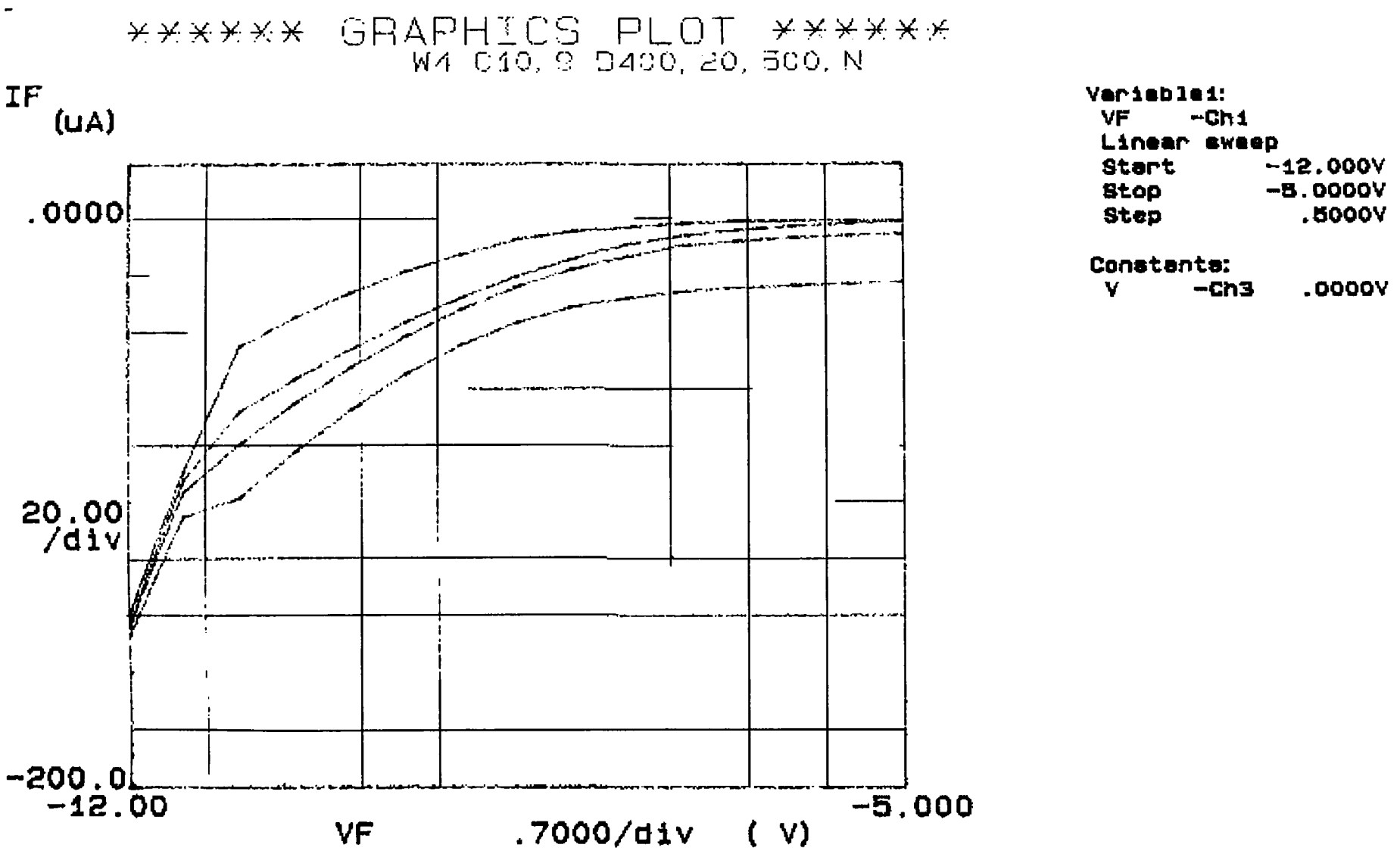
****** GRAPHICS PLOT ******
W1 C10,9 D400,20,500,N
IF
(uA)
.0000
20.00
/div
-200.0
-12.00
-5.000
VF .7000/div (V)
Variable1:
VF -Ch1
Linear sweep
Start -12.000V
Stop -5.0000V
Step .5000V
Constants:
V -Ch3 .0000V

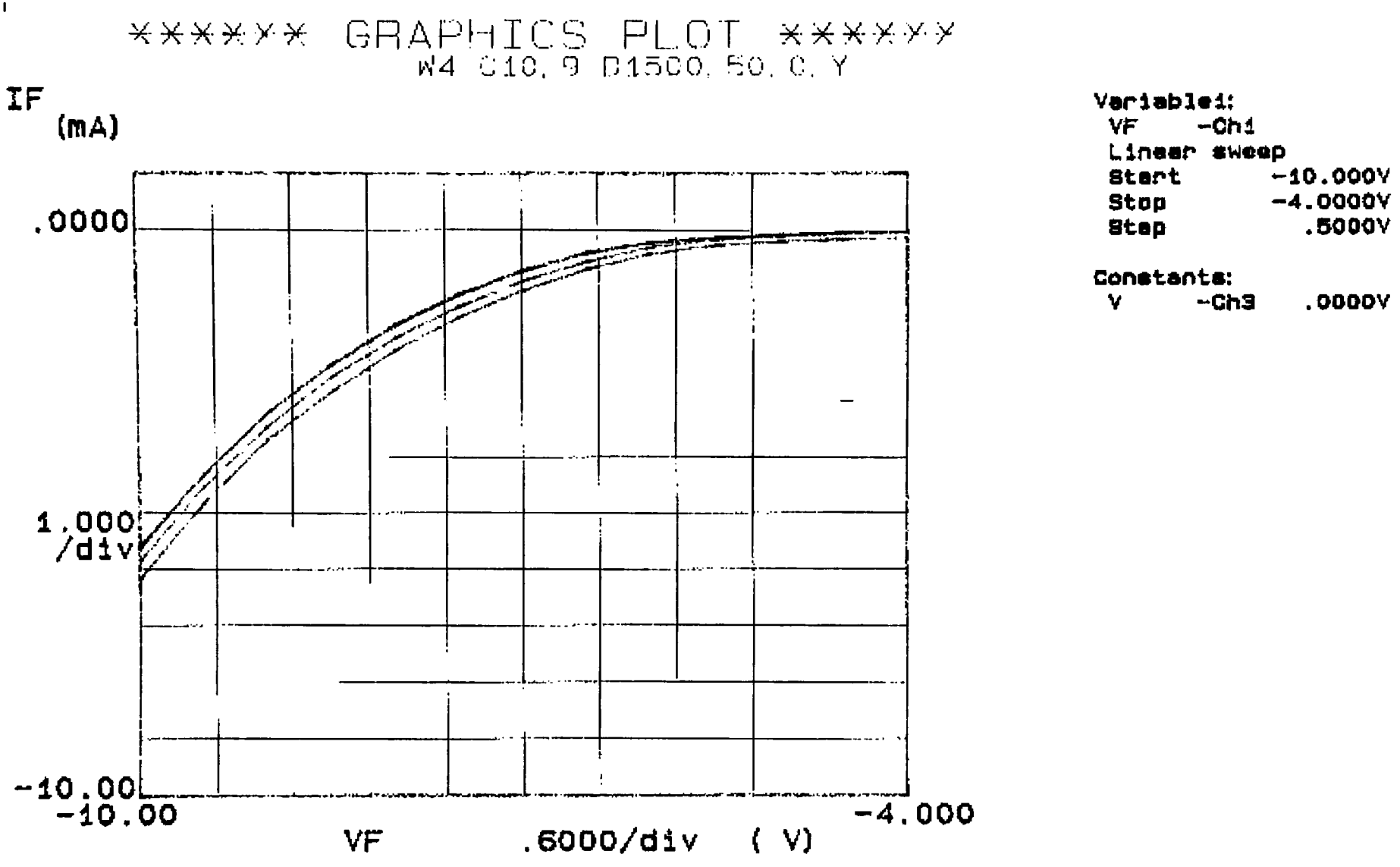
****** GRAPHICS PLOT ******
W4 C10.9 D1500.50.C.Y
IF
(mA)
.0000
1.000
/div
-10.00
-10.00
-4.000
VF .6000/div (V)
Variable1:
VF -Ch1
Linear sweep
Start -10.000V
Stop -4.0000V
Step .5000V
Constants:
V -Ch3 .0000V

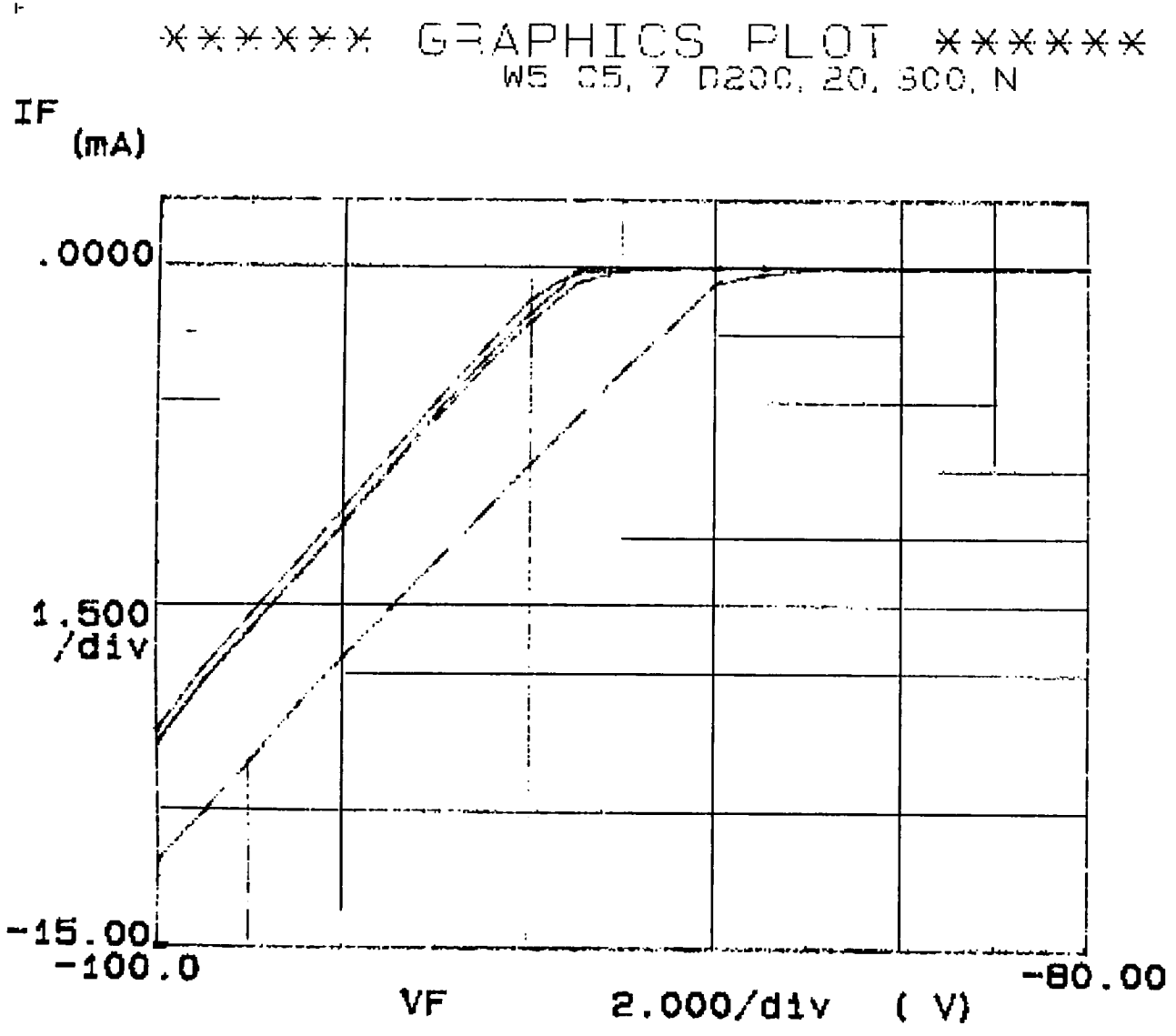

Variable1:
VF -Ch1
Linear sweep
Start -100.00V
Stop -80.000V
Step 1.0000V

Constants:
V -Ch3 .0000V

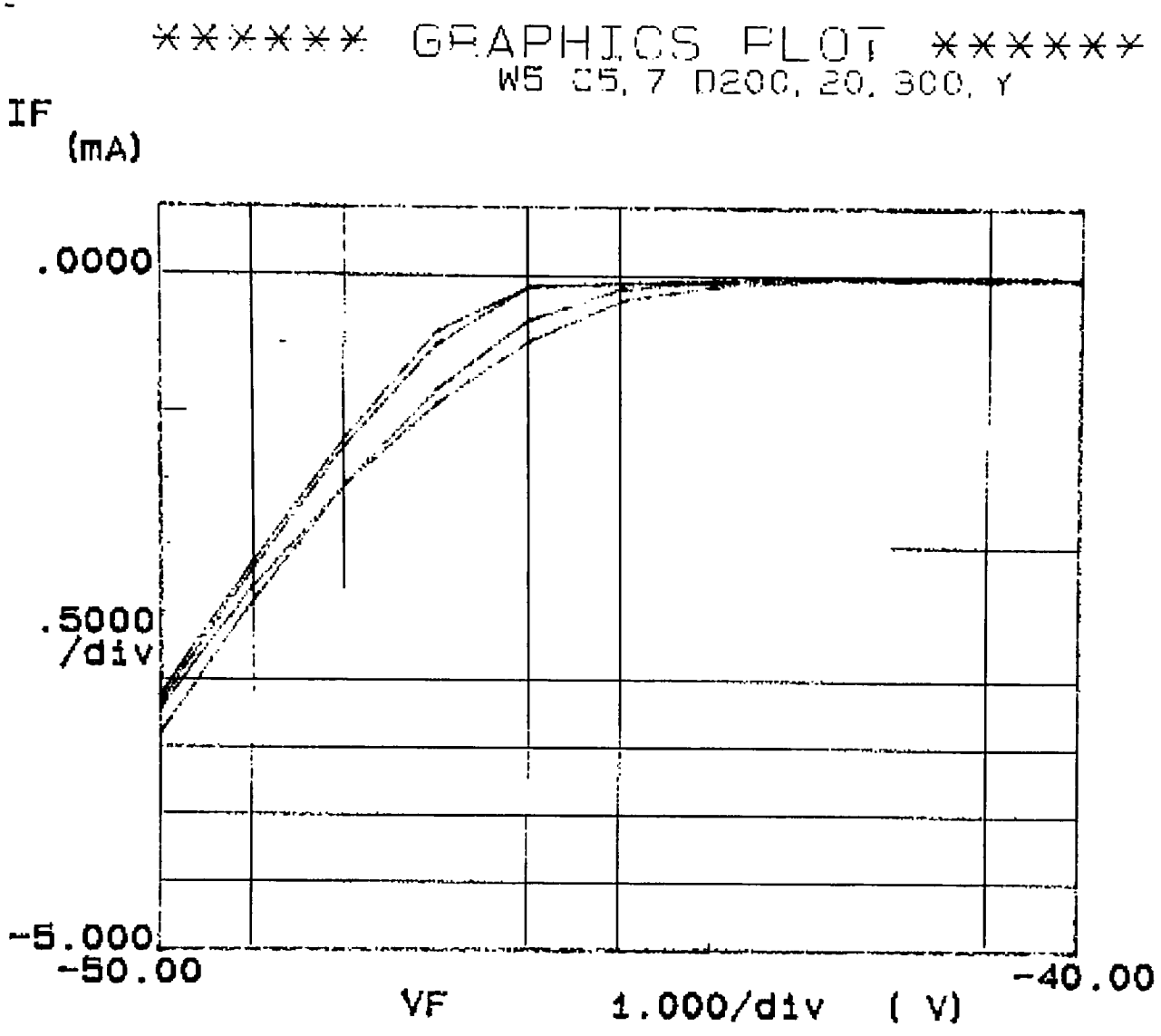

Variable1:
VF -Ch1
Linear sweep
Start -50.000V
Stop -40.000V
Step 1.0000V

Constants:
V -Ch3 .0000V

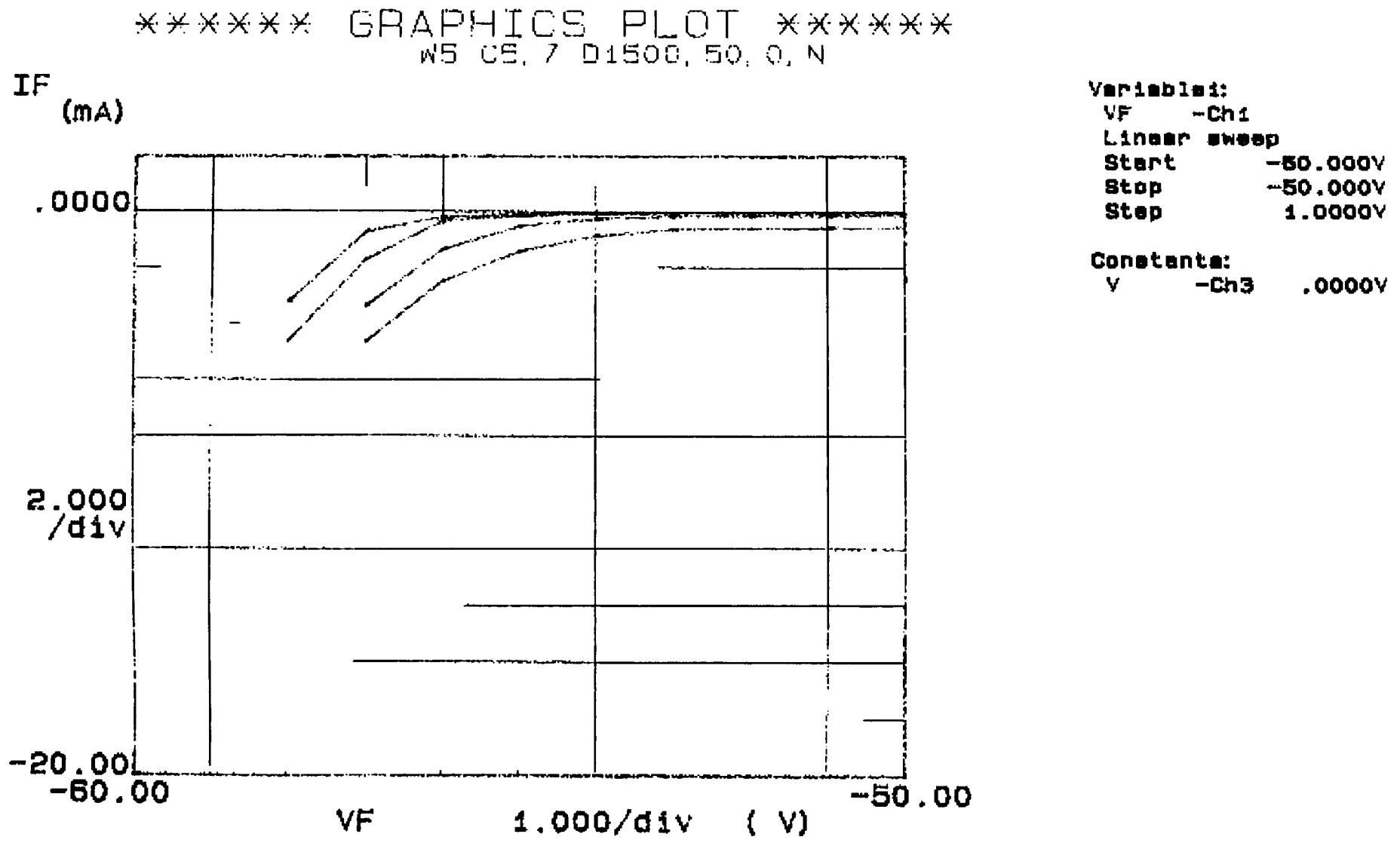
****** GRAPHICS PLOT ******
W5 CS, 7 D1500, 50, 0, N
IF
(mA)
.0000
2.000
/div
-20.00
-60.00
-50.00
VF
1.000/div
(V)
Variable1:
VF -Ch1
Linear sweep
Start -50.000V
Stop -50.000V
Step 1.0000V
Constants:
V -Ch3 .0000V

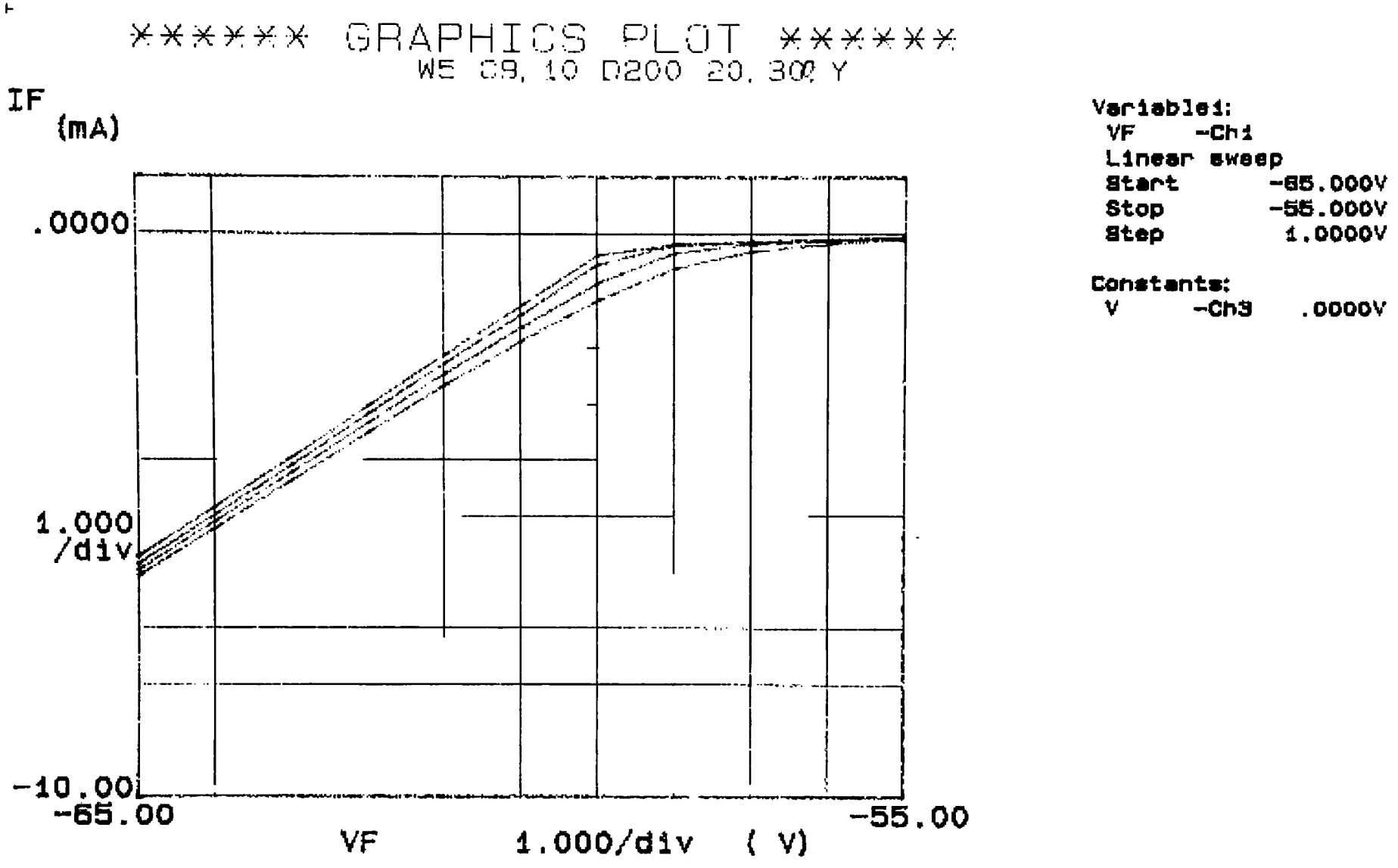
****** GRAPHICS PLOT ******
WE 09, 10 0200 20, 30 Y
IF
(mA)
.0000
1.000
/div
-10.00
-65.00
-55.00
VF
1.000/div
(V)
Variable1:
VF -Ch1
Linear sweep
Start -65.000V
Stop -55.000V
Step 1.0000V
Constants:
V -Ch3 .0000V

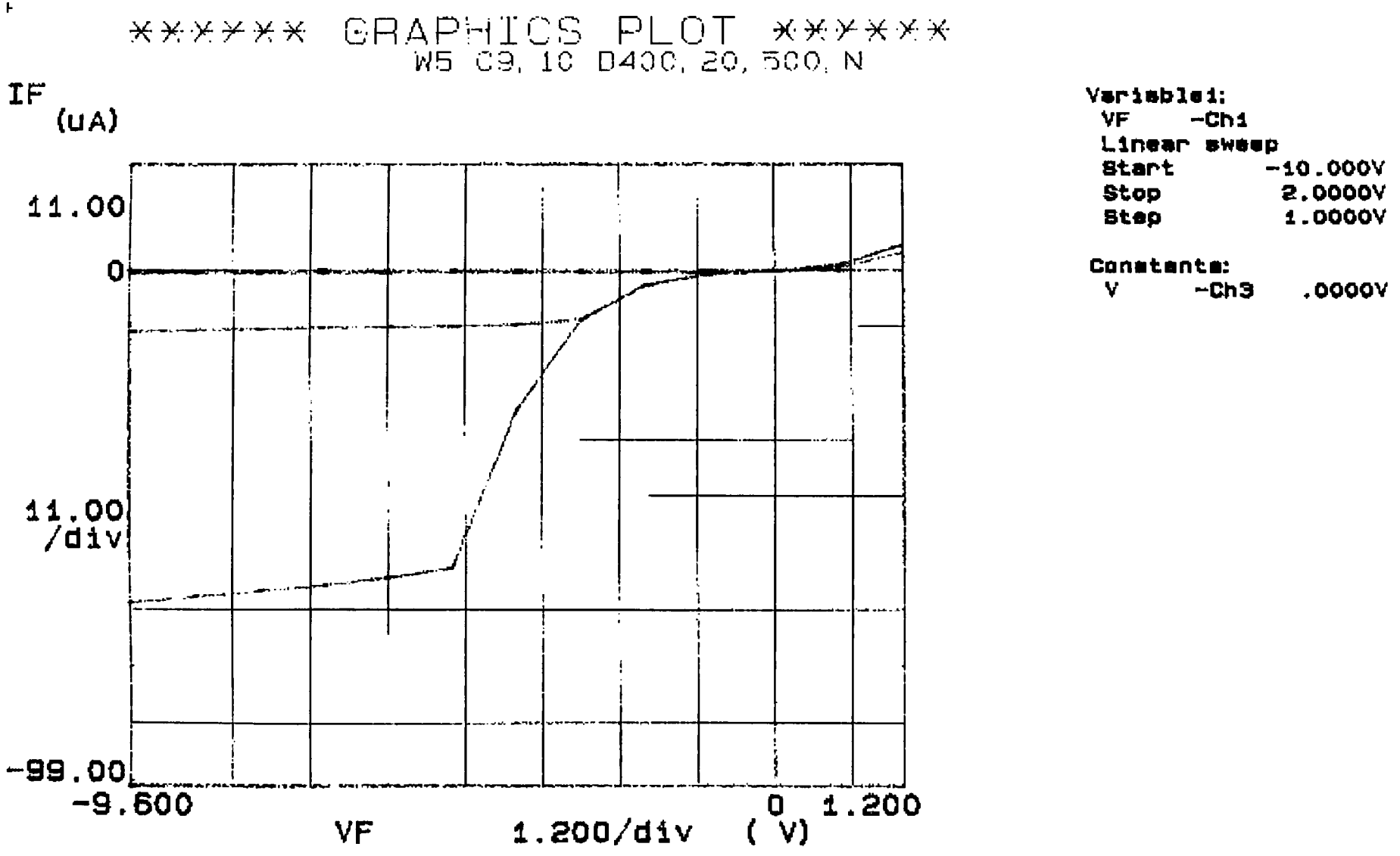
****** GRAPHICS PLOT ******
W5 C9, 10 D400, 20, 500, N
IF
(uA)
11.00
0
11.00
/div
-99.00
-9.600
0
1.200
VF
1.200/div
(V)
Variable1:
VF -Ch1
Linear sweep
Start -10.000V
Stop 2.0000V
Step 1.0000V
Constants:
V -Ch3 .0000V

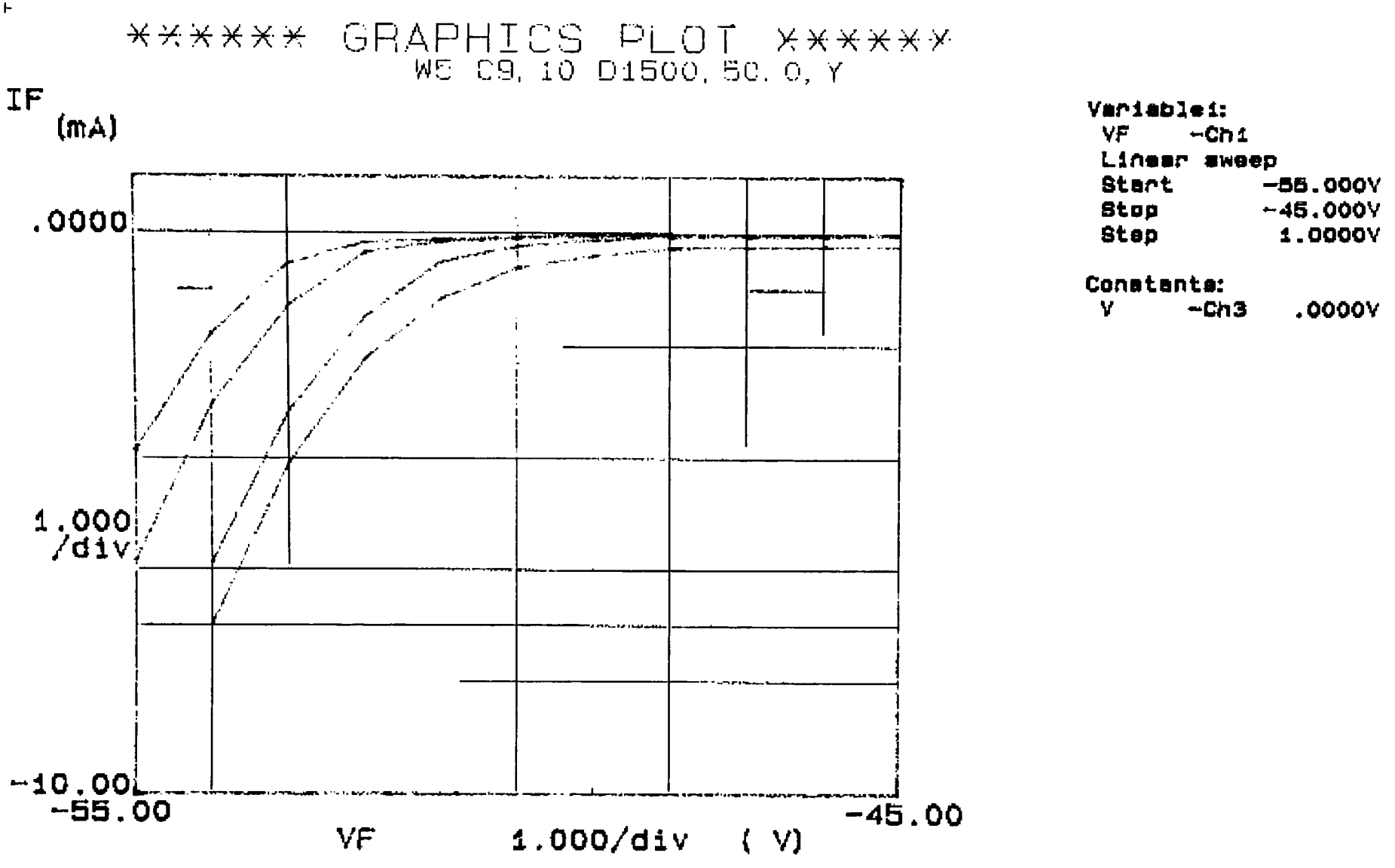
****** GRAPHICS PLOT ******
WS C9, 10 D1500, 50, 0, Y
IF
(mA)
.0000
1.000
/div
-10.00
-55.00
-45.00
VF 1.000/div (V)
Variable1:
VF -Ch1
Linear sweep
Start -55.000V
Stop -45.000V
Step 1.0000V
Constants:
V -Ch3 .0000V

6.7.2 Raw I-V Data

The following tables are the raw numerical data from the I-V graphs of Section 6.7.1

Wafer		1	1	1	1	1	1	1	1	1	1	1	1
Cell		7, 9	7, 9	7, 9	7, 9	7, 10	7, 10	7, 10	7, 10	7, 10	7, 10	7, 10	7, 10
Diameter [um]		200	200	200	200	200	200	200	200	200	200	200	200
Guard Ring [um]		20	20	20	20	20	20	20	20	30	30	30	30
Pixel Dist [um]		300	300	300	300	300	300	300	300	400	400	400	400
Metal Ring		N	N	N	N	Y	Y	Y	Y	N	N	N	N
Illumination [%]		0%	60%	80%	100%	0%	60%	80%	100%	0%	60%	80%	100%
Bias Voltage [V]	-3.00	-622.90	-641.70	-851.20	-1102.00	-583.60	-603.90	-945.10	-1228.00	-667.50	-696.90	-973.70	-1383.00
	-2.75	-557.20	-575.80	-786.40	-1042.00	-489.80	-516.70	-832.00	-1072.00	-595.30	-625.50	-903.20	-1316.00
	-2.50	-492.70	-511.10	-723.10	-984.00	-395.30	-427.10	-726.00	-955.90	-524.80	-555.40	-834.00	-1252.00
	-2.25	-429.20	-447.70	-661.80	-918.60	-305.40	-338.50	-625.80	-774.10	-456.20	-487.10	-767.10	-1190.00
	-2.00	-367.00	-385.60	-602.20	-842.40	-222.40	-256.00	-523.40	-598.80	-389.60	-420.90	-702.60	-1123.00
	-1.75	-306.30	-325.10	-544.50	-757.40	-148.70	-180.50	-409.60	-441.00	-325.20	-357.20	-640.20	-1043.00
	-1.50	-247.90	-266.50	-487.60	-663.70	-85.61	-113.50	-292.60	-300.60	-263.50	-295.90	-580.20	-950.40
	-1.25	-191.70	-209.90	-425.00	-561.60	-36.01	-56.72	-181.30	-183.40	-205.10	-237.50	-520.30	-832.20
	-1.00	-137.40	-155.50	-354.00	-454.80	-8.04	-17.44	-91.11	-96.05	-150.10	-182.40	-453.50	-693.40
	-0.75	-86.34	-103.70	-276.20	-345.60	-0.12	-1.42	-31.23	-41.05	-100.10	-131.10	-376.90	-546.60
	-0.50	-40.11	-55.41	-191.60	-236.30	0.00	0.00	-5.52	-11.49	-56.48	-84.77	-290.90	-400.60
	-0.25	-7.75	-14.70	-103.90	-130.50	0.01	-0.01	-0.18	-1.26	-22.62	-43.71	-193.00	-261.40
	0.00	-0.23	-1.20	-28.52	-40.47	-0.01	0.00	0.01	-0.08	0.02	-11.96	-98.44	-139.30
	0.25	2.74	1.66	-2.28	-3.44	0.03	0.01	0.00	0.00	15.43	7.72	-32.18	-51.56
	0.50	8.28	6.34	1.50	0.83	-0.04	-0.03	-0.01	0.01	30.88	22.98	1.44	-3.75
Curve Fit	a												
	b												
	c												
	d												
2nd Derivative	a												
	b												
Max Gradient	Vbr												
Threshold	Vbr												
Voltage Breakdown													

1	1	1	1	1	1	1	1	1	1	1	1	1	1	1
7, 10	7, 10	7, 10	7, 10	7, 10	7, 10	7, 10	7, 10	5, 6	5, 6	5, 6	5, 6	5, 6	5, 6	5, 6
400	400	400	400	1500	1500	1500	1500	200	200	200	200	200	200	200
20	20	20	20	50	50	50	50	20	20	20	20	20	20	20
500	500	500	500	0	0	0	0	300	300	300	300	300	300	300
N	N	N	N	Y	Y	Y	Y	N	N	N	N	Y	Y	Y
0%	60%	80%	100%	0%	60%	80%	100%	0%	60%	80%	100%	0%	60%	80%
-704.30	-753.60	-976.40	-1323.00	-474.80	-510.60	-750.30	-1058.00	-664.7	-702	-936.1	-1302	-559.8	-596.8	-820.8
-627.40	-675.50	-900.40	-1252.00	-416.40	-451.10	-690.80	-984.80	-592.1	-629.9	-866.9	-1238	-480	-516.7	-740.6
-552.20	-599.10	-626.70	-1183.00	-360.40	-393.50	-633.10	-902.80	-521.2	-559.1	-799.4	-1176	-403	-439.5	-663.8
-479.10	-524.50	-754.90	-1116.00	-305.60	-338.60	-576.60	-807.00	-452.4	-490.2	-733.8	-1114	-329.2	-365.6	-589.8
-408.10	-452.10	-685.50	-1051.00	-254.90	-286.60	-521.60	-697.30	-385.4	-423.3	-670.2	-1046	-259.4	-295.4	-519.1
-339.40	-381.90	-618.80	-983.30	-207.70	-237.50	-464.70	-585.90	-321	-356.4	-608.6	-958.6	-194.2	-229.2	-451.4
-273.90	-314.50	-554.30	-900.90	-163.60	-191.70	-401.80	-478.90	-259.4	-296.7	-549.2	-840.6	-135	-168.3	-382.3
-211.50	-250.50	-492.20	-802.40	-123.30	-149.20	-334.70	-377.40	-201.3	-237.9	-489.4	-709.7	-83	-113	-304.4
-153.20	-189.90	-427.00	-676.70	-86.64	-110.40	-263.70	-284.30	-147.5	-182.7	-422.7	-576.5	-40.24	-64.95	-216.4
-99.79	-133.30	-350.70	-526.70	-55.72	-76.28	-191.20	-201.40	-98.53	-131.5	-346.6	-442.8	-11.43	-25.79	-120.3
-53.12	-81.54	-264.70	-368.70	-31.05	-46.48	-125.90	-131.50	-56.17	-85.22	-258.2	-314.5	-0.471	-3.954	-42.82
-18.04	-36.09	-166.80	-218.90	-12.70	-22.85	-74.01	-77.20	-22.95	-43.96	-162.3	-196.6	-0.03828	-0.0579	-6.709
0.03	-6.70	-73.89	-95.83	0.06	-6.46	-37.77	-39.42	-0.01917	-12.88	-78.86	-98.17	0.03504	0.03466	-0.1016
9.23	4.66	-77.78	-25.62	9.57	4.74	-14.00	-15.19	16.75	7.174	-23.06	-31.69	0.01161	-0.0304	0.02348
20.33	14.48	1.24	-1.23	20.60	14.57	2.09	-0.37	34.37	23.65	4.783	0.001043	0.00189	0.005025	0.03656
								-7.54063	-7.24583	-4.23815	-45.3099	-4.45705	-8.17153	-30.1401
								-66.1251	-60.4759	-6.42492	-146.983	-81.8772	-92.7141	-152.862
								91.70101	112.1307	290.1429	352.3849	-12.1022	-0.39457	80.5786
								2.604762	-15.3694	-109.309	-114.781	13.74183	12.87909	3.280537
								-45.2438	-43.475	-25.4289	-271.859	-26.7423	-49.0292	-180.841
								-132.25	-120.952	-12.8498	-293.967	-163.754	-185.428	-305.724
								-2.92306	-2.7821	-0.50533	-1.08132	-6.12342	-3.782	-1.69057
								-0.74899	-0.584	-4.75E-11	-4.75E-11	-1.30501	-1.167	-0.627
								-0.74899	-0.584	-4.75E-11	-4.75E-11	-1.30501	-1.167	-0.627

1	1	1	1	1	1	1	1	1	1	1	1	1
5, 6	5, 6	5, 6	5, 6	5, 6	5, 6	5, 6	5, 6	5, 6	5, 6	5, 6	5, 6	5, 6
200	200	200	200	200	400	400	400	400	1500	1500	1500	1500
20	30	30	30	30	20	20	20	20	50	50	50	50
300	400	400	400	400	500	500	500	500	0	0	0	0
Y	N	N	N	N	N	N	N	N	Y	Y	Y	Y
100%	0%	60%	80%	100%	0%	60%	80%	100%	0%	60%	80%	100%
-1177	-754.6	-787.5	-1063	-1456	-724.5	-755.2	-1033	-1436	-331.9	-343.3	-610.8	-855.4
-1101	-678.4	-711.6	-989	-1388	-649.2	-679.7	-958.7	-1348	-276.4	-287.5	-535.6	-711.6
-1027	-603.2	-636.6	-915.9	-1320	-575.1	-605.9	-886.8	-1302	-226.2	-237.4	-460.9	-582.4
-953.7	-529.3	-563.3	-845.3	-1256	-502.6	-533.4	-816.7	-1239	-181.8	-191.9	-387.6	-467.4
-870.2	-457	-491.4	-776	-1191	-431.5	-462.5	-748.4	-1172	-139.1	-150.6	-317.6	-368.1
-763.6	-386.4	-421.1	-708.7	-1123	-362.7	-393.8	-682.6	-1089	-102.4	-112.9	-250.1	-284.4
-618.5	-317.9	-353	-644.4	-1034	-296.2	-327.5	-619.1	-967.2	-69.19	-78.32	-187.1	-211.6
-459.2	-254.8	-287.3	-581.3	-907.5	-232.2	-263.4	-557.2	-828	-39.24	-46.91	-129.1	-147.4
-302.4	-188.6	-224.3	-518.6	-764.4	-171.6	-202.5	-492.5	-683.9	-16.07	-21.87	-77.7	-89.96
-161.2	-128.6	-164.2	-447.2	-616.2	-114.6	-145	-416.5	-537.4	-3.657	-6.594	-36.33	-43.5
-58.77	-73.03	-107.4	-361.7	-464.3	-62.93	-91.37	-325.4	-389.7	-0.188	-0.9371	-11.34	-14.02
-11	-24.45	-53.71	-253.3	-312.6	-19.13	-41.45	-212	-246	-0.01516	0.02318	-2.021	-2.632
-0.244	0.007455	-9.484	-129.8	-165.5	0.00453	-5.184	-97.17	-113.5	-0.00445	-0.03432	-0.0167	0.0828
0.02096	8.949	3.852	-26.2	-41.1	5.994	2.786	-15.22	-21.75	-0.009	0.01149	-0.01705	0.03369
-0.03374	25.39	15.94	2.533	0.8484	18.57	11.66	1.457	0.6422	0.01121	0.01576	-0.00152	-0.03434
-76.079	-13.4398	-11.5011	8.242671	-28.8023	-13.4565	-12.2094	1.918655	-45.066	0.791497	-0.43243	-10.8056	4.100972
-329.261	-87.9636	-74.8662	53.75721	-45.622	-90.9314	-81.0325	26.11999	-125.212	-38.3977	-42.4428	-99.5635	-78.2265
88.06353	105.6637	131.9668	364.6308	528.0625	87.67628	111.1421	355.1129	444.6051	-8.39679	-6.0222	7.035659	15.1429
26.99502	-3.69724	-22.9007	-164.288	-200.26	-1.9052	-16.6813	-139.242	-145.89	6.895505	7.021514	11.72551	6.48461
-456.474	-80.6388	-69.0064	49.45603	-172.814	-80.7392	-73.2566	11.51193	-270.396	4.748983	-2.5946	-64.8338	24.60583
-658.522	-175.927	-149.736	107.5144	-91.2439	-181.863	-162.065	52.23999	-250.424	-76.7953	-84.8856	-199.127	-156.453
-1.44263	-2.18167	-2.16989	-2.17394	-0.52799	-2.25247	-2.21229	-4.5379	-0.92614	16.1709	-32.7162	-3.07135	6.358372
-0.528	-0.621	-0.469	-4.75E-11	-4.75E-11	-0.68299	-0.548	-4.75E-11	-4.75E-11	-1.74803	-1.67502	-1.08899	-1.04799
-0.528	-0.621	-0.469	-4.75E-11	-4.75E-11	-0.68299	-0.548	-4.75E-11	-4.75E-11	16.1709	-1.67502	-1.08899	6.358372

Wafer			2	2	2	2	2	2	2	2	2	2	2	2
Cell			9, 6	9, 6	9, 6	9, 6	9, 6	9, 6	9, 6	9, 6	9, 6	9, 6	9, 6	9, 6
Diameter [um]			200	200	200	200	200	200	200	200	200	200	200	200
Guard Ring [um]			20	20	20	20	20	20	20	20	30	30	30	30
Pixel Dist [um]			300	300	300	300	300	300	300	300	400	400	400	400
Metal Ring			N	N	N	N	Y	Y	Y	Y	N	N	N	N
Illumination [%]			0%	60%	80%	100%	0%	60%	80%	100%	0%	60%	80%	100%
Bias Voltage [V]		-3.00	-586.2	-593.2	-666.6	-787.7	-437.6	-444.2	-511.4	-639.6	-504	-510.8	-574.9	-669.9
		-2.75	-513.8	-520.6	-592.5	-712.2	-378.7	-384.1	-448.5	-573.1	-453.5	-460.6	-524.7	-620.2
		-2.50	-443.3	-449.9	-520.6	-638.4	-320.7	-326.3	-388.5	-507.6	-403.8	-410.6	-475	-570.1
		-2.25	-375.3	-381.6	-450.2	-566.1	-266.3	-271.6	-331.8	-443.8	-355.2	-361.8	-425.5	-520.3
		-2.00	-310.6	-316.5	-383	-495.9	-214.4	-219.9	-277.5	-382.3	-307.2	-314	-376.7	-469.8
		-1.75	-249.3	-254.8	-318.1	-427.1	-165.4	-170.8	-226	-322.8	-260.6	-267.1	-328.7	-419.3
		-1.50	-191.9	-197.2	-256.9	-359.7	-119.7	-125	-176.8	-263.2	-215.6	-222	-281.8	-369.1
		-1.25	-138.9	-143.8	-199.2	-294	-77.65	-82.44	-130	-201.8	-172	-178	-236.2	-317.6
		-1.00	-90.37	-95.01	-145.2	-230.8	-40.12	-44.41	-86.55	-141.2	-130.5	-136.2	-191.6	-264.2
		-0.75	-47.62	-51.66	-95.32	-169.6	-9.707	-12.73	-47.14	-85.66	-91.4	-96.9	-148.5	-208.5
		-0.50	-13.07	-15.91	-50.76	-107.4	-0.0975	-0.2371	-14.1	-37.71	-55.64	-60.48	-107.3	-153.9
		-0.25	-0.2337	-0.401	-14.68	-49.95	0.04143	0.00217	-0.225	-0.374	-24.24	-28.29	-68.81	-102.7
		0.00	-0.04131	-0.03082	-0.2458	-8.459	-0.04356	-0.01949	0.0425	-0.02817	-0.04529	-2.692	-34.22	-56.6
		0.25	-0.02746	-0.01603	-0.04131	-0.03868	0.02283	0.03744	-0.03723	-0.00574	0.01394	12.1	-6.066	-18.68
		0.50	-0.1086	-0.08335	-0.00255	-0.01837	0.005205	-0.04207	0.007275	0.02519	0.02667	24.64	10.58	5.516
Curve Fit	a													
	b													
	c													
	d													
2nd Derivative	a													
	b													
Max Gradient	delta													

2	2	2	2	2	2	2	2	2	2	2	2	2	2	2
9, 6	9, 6	9, 6	9, 6	9, 6	9, 6	9, 6	9, 6	6, 8	6, 8	6, 8	6, 8	6, 8	6, 8	6, 8
400	400	400	400	1500	1500	1500	1500	200	200	200	200	200	200	200
20	20	20	20	50	50	50	50	20	20	20	20	20	20	20
500	500	500	500	0	0	0	0	300	300	300	300	300	300	300
N	N	N	N	Y	Y	Y	Y	N	N	N	N	Y	Y	Y
0%	60%	80%	100%	0%	60%	80%	100%	0%	60%	80%	100%	0%	60%	80%
-364.5	-384.2	-460.5	-558.2	-511.6	-524	-641.5	-757.1	-458	-468.3	-581.7	-732.7	-699	-725.6	-985.2
-301.3	-315.4	-384.5	-479.2	-432.1	-449	-530.7	-651.2	-380.8	-387.9	-481.7	-601.6	-601.3	-627	-880.3
-240.8	-253.1	-313	-405.2	-344.1	-357.7	-434.7	-559.4	-305.4	-318.1	-407.3	-488.1	-509.3	-533.6	-779.5
-186.5	-196.4	-250.5	-331.4	-264.6	-274.6	-342.4	-460.8	-237.9	-250.8	-330.4	-398.8	-423.5	-446.6	-683.4
-138.8	-146.2	-194.5	-265.5	-193.5	-201.7	-261.2	-359.7	-176.9	-190	-263.6	-313	-344.2	-366	-592.1
-97.95	-103.7	-146.2	-205.1	-131.7	-137.9	-190.2	-269.8	-123.2	-135.4	-197.6	-240.2	-271.3	-291.7	-505.1
-64.53	-68.62	-103.7	-152.9	-80.51	-84.94	-128.9	-187.4	-76.68	-88.23	-147.4	-179.7	-203.9	-223.2	-421.3
-38.27	-40.75	-69.15	-108.7	-37.57	-42.96	-78.91	-120	-39.03	-47.08	-104.8	-130.2	-142.1	-159.9	-340.1
-17.74	-19.31	-41.97	-72.51	-10.39	-12.38	-39.65	-67.99	-11.66	-18.73	-70.5	-89.9	-86.59	-102.5	-261.2
-3.029	-3.919	-20.36	-43.03	-0.1383	-0.3357	-11.64	-29.34	-0.8494	-2.151	-42.42	-55.75	-39.34	-52.31	-179.8
0.01347	-0.08025	-4.319	-18.33	-0.01686	-0.01267	-0.4016	-4.98	-0.01075	0.0036	-18.8	-25.9	-5.547	-12.88	-100.3
-0.04187	0.04382	-0.0192	-2.187	-0.0378	0.00446	-0.04435	0.006395	-0.01977	-0.02746	-1.863	-4.14	0.009065	-0.1219	-36.14
0.01357	-0.04098	-0.00529	-0.07292	-0.04013	0.01586	0.04532	-0.04097	-0.03579	0.03733	-0.02929	-0.05311	-0.03649	0.03187	-1.82
0.00475	0.01624	-0.0043	0.04121	-0.04879	-0.02963	-0.00732	0.04821	-0.03574	-0.03541	0.002045	0.03523	0.04093	-0.00453	0.03034
-0.01651	-0.00654	0.02246	-0.02279	-0.00356	0.04845	0.00649	-0.01488	0.02477	0.01298	0.01473	-0.02585	0.02508	0.02022	-0.01215

2	2	2	2	2	2	2	2	2	2	2	2	2
6, 8	6, 8	6, 8	6, 8	6, 8	6, 8	6, 8	6, 8	6, 8	6, 8	6, 8	6, 8	6, 8
200	200	200	200	200	400	400	400	400	1500	1500	1500	1500
20	30	30	30	30	20	20	20	20	50	50	50	50
300	400	400	400	400	500	500	500	500	0	0	0	0
Y	N	N	N	N	N	N	N	N	Y	Y	Y	Y
100%	0%	60%	80%	100%	0%	60%	80%	100%	0%	60%	80%	100%
-1396	-346.4	-376.7	-637.3	-850.6	-740.1	-773.7	-1089	-1545	-535.5	-573.2	-897.9	-1336
-1288	-281.3	-306.1	-528.1	-708.1	-621.6	-653.6	-961.8	-1415	-436.5	-473.1	-777.5	-1110
-1181	-219.6	-241.2	-431.7	-569.3	-510.5	-540.6	-839.6	-1283	-351.5	-382.8	-661	-900.8
-1073	-167	-182.2	-340.7	-440.3	-408.6	-436.4	-722.7	-1136	-274.9	-303	-549.8	-706.9
-949.2	-117.3	-131.7	-260.1	-310.1	-317	-342.1	-610.8	-941.1	-207.4	-232.5	-445.8	-540.5
-787.7	-76.69	-86.77	-190	-224.7	-235.5	-258.1	-502.6	-736	-148.7	-170.6	-348.3	-400.9
-621.1	-42.94	-50.81	-127.9	-153.6	-163.4	-183.9	-398.9	-544	-98.99	-117.6	-257	-288.8
-468.9	-18.4	-24.28	-78.83	-99.73	-102.5	-119.4	-300.8	-378.1	-58.03	-72.86	-176.8	-198.1
-332.7	-4.637	-7.729	-42.02	-57.3	-51.5	-65.16	-204.4	-244.2	-27.03	-37.69	-110.6	-125.5
-218.5	-0.1527	-0.8095	-16.83	-26.5	-13.01	-22.07	-116.5	-138.1	-7.197	-13.53	-58.94	-69.58
-122.2	0.03422	-0.03171	-3.421	-7.602	-0.2355	-0.8864	-47.49	-58.98	-0.1097	-0.8989	-23.24	-30.07
-47.75	-0.03546	-0.03516	0.00001	-0.3939	0.02633	-0.04154	-5.287	-9.024	-0.03668	-0.03785	-3.783	-6.599
-4.143	0.01184	0.01041	-0.0354	-0.03707	-0.03816	0.03411	-0.06643	-0.06755	0.01482	0.01709	-0.01475	-0.08139
-0.04039	0.003895	0.00697	0.03084	-0.02597	0.03712	-0.02543	0.03568	0.0263	-0.00971	-0.01285	0.002555	0.04026
0.03502	-0.00929	-0.01211	-0.0046	-0.00396	-0.00442	0.006105	-0.0357	-0.03599	0.00502	-0.00071	-0.01521	-0.0094

Wafer		3	3	3	3	3	3	3	3	3	3	3	3
Cell		5, 9	5, 9	5, 9	5, 9	5, 9	5, 9	5, 9	5, 9	5, 9	5, 9	5, 9	5, 9
Diameter [um]		200	200	200	200	200	200	200	200	200	200	200	200
Guard Ring [um]		20	20	20	20	20	20	20	20	30	30	30	30
Pixel Dist [um]		300	300	300	300	300	300	300	300	400	400	400	400
Metal Ring		N	N	N	N	Y	Y	Y	Y	N	N	N	N
Illumination [%]		0%	60%	80%	100%	0%	60%	80%	100%	0%	60%	80%	100%
Bias Voltage [V]	-3.00	-741.7	-781	-1016	-1406	-930.4	-980.7	-1404	-1976	-807	-853.5	-1217	-1749
	-2.75	-662.3	-701.4	-937.9	-1333	-809.2	-859.6	-1284	-1859	-696	-742	-1106	-1639
	-2.50	-584.7	-623.5	-862.1	-1260	-692.2	-742.5	-1169	-1743	-589	-635	-999.2	-1530
	-2.25	-509	-547.6	-788	-1188	-578.8	-628.7	-1060	-1610	-486.1	-531.4	-893.6	-1416
	-2.00	-435.2	-473.3	-715.1	-1110	-469.3	-519.2	-949.3	-1447	-387.3	-432	-791.4	-1283
	-1.75	-363.2	-400.8	-643.8	-1008	-363.6	-413.1	-839	-1243	-292.7	-336.6	-691.4	-1110
	-1.50	-293.7	-330.6	-574.1	-877.1	-262.2	-310.9	-726.3	-1017	-203.3	-245.7	-589.5	-899.8
	-1.25	-226.5	-262.5	-504.2	-738.3	-165.6	-212.8	-598.3	-785.5	-120.3	-160.3	-476.7	-678.7
	-1.00	-161.9	-197	-432	-597.3	-78.47	-119.9	-445.4	-555.6	-48.04	-83.22	-343.1	-460.5
	-0.75	-102.6	-135.2	-350.6	-455.9	-10.89	-39.08	-268.8	-332.5	-3.852	-17.55	-189.1	-253.2
	-0.50	-48.7	-79.64	-253.6	-315.8	-0.04244	-0.8063	-93.62	-127.2	-0.0765	-0.4545	-46.53	-74.45
	-0.25	-12.39	-32.32	-145.7	-182.4	0.0212	0.011	-2.936	-6.778	0.02332	-0.00616	-0.8595	-1.851
	0.00	0.00072	5.834	-53.53	-71.85	-0.03089	0.00251	-0.00794	-0.03412	-0.03311	-0.01423	0.00024	-0.04298
	0.25	5.304	5.124	-8.728	-14.09	0.03385	-0.00422	-0.00313	0.03475	0.03438	0.02759	-0.02998	0.02201
	0.50	13.71	16.29	3.302	1.922	-0.01779	0.01063	0.01095	-0.02922	0.01009	-0.02764	0.03311	-0.03524

3	3	3	3	3	3	3	3	3	3	3	3	3	3	3
5, 9	5, 9	5, 9	5, 9	5, 9	5, 9	5, 9	5, 9	11, 10	11, 10	11, 10	11, 10	11, 10	11, 10	11, 10
400	400	400	400	1500	1500	1500	1500	200	200	200	200	200	200	200
20	20	20	20	50	50	50	50	20	20	20	20	20	20	20
500	500	500	500	0	0	0	0	300	300	300	300	300	300	300
N	N	N	N	Y	Y	Y	Y	N	N	N	N	Y	Y	Y
0%	60%	80%	100%	0%	60%	80%	100%	0%	60%	80%	100%	0%	60%	80%
-798.7	-835.9	-1141	-1564	-425.1	-443.7	-673.6	-790.7	-549.9	-623.9	-845.8	-1203	-824.7	-866.9	-1198
-690	-726.7	-1031	-1454	-359.7	-378.1	-577.5	-665.5	-517.7	-545	-762.3	-1105	-716.3	-758.8	-1091
-585.9	-622.6	-925.5	-1347	-299.2	-316.9	-506.3	-556.2	-439.7	-469.2	-681.1	-992.2	-612.1	-654.1	-988.3
-486.7	-522.9	-823.1	-1243	-243.6	-259.8	-430.1	-458.1	-365.6	-393.4	-601.9	-867	-517.5	-553.3	-885.2
-391.9	-427.6	-724.9	-1139	-192.5	-209.6	-357.3	-372.6	-293.8	-321	-523.4	-734.3	-415.8	-456.4	-785.6
-301.7	-336.9	-630.3	-1022	-146.8	-163.2	-285.1	-293.2	-224.9	-251.8	-445.6	-602.9	-326.1	-364.9	-686.9
-216.5	-251.1	-538.6	-858.8	-105.9	-121.4	-217.3	-224.8	-160.2	-185.5	-365.9	-476	-244.6	-280.4	-588.3
-136.7	-169.5	-443.5	-661.3	-69.97	-64.53	-154.5	-167.4	-99.74	-122.2	-281.3	-254.6	-171.2	-203.8	-482.2
-65.89	-95.49	-335.8	-460.4	-37.27	-50.6	-101.6	-113.9	-43.34	-65.19	-183.3	-239.8	-104.3	-134.8	-364.4
-10.7	-28.45	-203.6	-266.6	-11.54	-21.96	-59.95	-66.79	-4.672	-14.94	-104.6	-133.5	-45.56	-72.41	-241.5
-0.01446	-0.528	-64.53	-92.6	-0.3213	-2.786	-25.35	-29.58	-0.00758	-0.0763	-26.91	-41.7	-4.207	-17.01	-125.3
-0.01222	-0.01361	-1.312	-3.025	0.0237	-0.02828	-3.59	-5.475	0.00702	0.04885	-0.2562	-0.7666	-0.01828	-0.1875	-28.68
-0.00135	0.02759	0.008025	-0.04073	0.03066	-0.00628	-0.05802	-0.1013	-0.02813	-0.02509	0.04195	-0.04982	-0.03134	-0.05289	-0.308
0.0132	-0.03607	-0.00272	0.02727	0.03518	0.0156	0.00568	0.02222	0.04426	0.00059	-0.04719	0.03815	-0.05291	-0.04969	0.03914
-0.02935	0.03428	-0.00914	-0.00313	0.03504	0.01899	0.01363	-0.02292	-0.0487	-0.01899	0.04045	-0.00379	-0.02875	0.02043	-0.05212

3	3	3	3	3	3	3	3	3	3	3	3	3
11, 10	11, 10	11, 10	11, 10	11, 10	11, 10	11, 10	11, 10	11, 10	11, 10	11, 10	11, 10	11, 10
200	200	200	200	200	400	400	400	400	1500	1500	1500	1500
20	30	30	30	30	20	20	20	20	50	50	50	50
300	400	400	400	400	500	500	500	500	0	0	0	0
Y	N	N	N	N	N	N	N	N	Y	Y	Y	Y
100%	0%	80%	80%	100%	0%	60%	80%	100%	0%	60%	80%	100%
-1680	-871.7	-900.4	-1146	-1523	-641	-663.5	-837.7	-1024	-729.3	-753	-971.6	-1275
-1573	-752.7	-781.1	-1025	-1402	-570	-693.2	-766.8	-940.1	-646.7	-670.8	-890.5	-1145
-1464	-638.5	-666.8	-910.2	-1284	-501.1	-524	-697.9	-863.2	-566.7	-590.6	-811.5	-1118
-1341	-529	-556.9	-796.9	-1170	-433.7	-456.3	-629.8	-771.3	-488.8	-512.7	-734.3	-1041
-1182	-423.8	-451.2	-688.3	-1055	-367.7	-390.2	-563	-691.9	-412.5	-436.6	-658.5	-960.5
-999.6	-323.1	-349.8	-583	-933.5	-303.2	-325.4	-496.9	-604.7	-338.6	-362.6	-584.1	-866.7
-811.3	-227.4	-253.3	-480.7	-790.5	-240.2	-262.2	-431.7	-511.6	-266.7	-290.6	-511.3	-757.7
-625.3	-137.8	-162.3	-378.2	-625	-179.2	-200.3	-365.6	-424.4	-197.1	-220.8	-437.1	-634.3
-447.5	-58.85	-80.56	-268.6	-441.1	-120.5	-140.7	-296.1	-336.6	-130.5	-153.3	-357.9	-501.3
-286.4	-4.916	-13.16	-147	-249.8	-66.06	-84.86	-220.3	-243.3	-69.61	-90.76	-267.4	-363.9
-150.1	-0.05168	-0.06005	-31.56	-76.03	-17.89	-31.94	-138.5	-154.8	-17.62	-32.8	-167.3	-226.5
-39.98	0.04684	0.03387	-0.1485	-1.058	-0.4496	-2.092	-56.95	-71.53	-0.4593	-2.144	-67.04	-98.21
-0.5741	-0.04671	-0.04798	0.0481	0.04798	0.04951	0.00561	-4.179	-9.715	-0.03603	0.01326	-5.207	-11.85
0.04519	0.01471	0.04927	-0.04641	-0.04832	0.01106	0.02063	-0.01673	-0.05895	-0.0608	0.05708	-2.65	-0.08165
-0.04989	0.01155	-0.02954	0.01067	0.01294	0.565	0.2853	-0.1223	0.05412	-0.5944	0.03035	-0.02936	0.05783

Wafer			4	4	4	4	4	4	4	4	4	4	4	4	4	4	4	4	4	4	4
Cell			7, 3	7, 3	7, 3	7, 3	7, 3	7, 3	7, 3	7, 3	7, 3	7, 3	7, 3	7, 3	7, 3	7, 3	7, 3	7, 3	7, 3	7, 3	7, 3
Diameter [um]			200	200	200	200	200	200	200	200	200	200	200	200	400	400	400	400	1500	1500	1500
Guard Ring [um]			20	20	20	20	20	20	20	20	30	30	30	30	20	20	20	20	50	50	50
Pixel Dist [um]			300	300	300	300	300	300	300	300	400	400	400	400	500	500	500	500	0	0	0
Metal Ring			N	N	N	N	Y	Y	Y	Y	N	N	N	N	N	N	N	N	Y	Y	Y
Illumination [%]			0%	60%	80%	100%	0%	60%	80%	100%	0%	60%	80%	100%	0%	60%	80%	100%	0%	60%	80%
Bias Voltage [V]		-15.00	-1354	-1384	-1473	-1455									-961 4	-1000	-1053	-1028			
		-14 50	-1018	-1051	-1127	-1111									-730.1	-763.3	-839.4	-821.7			
		-14.00	-710.9	-753.7	-831 1	-810.9									-517 7	-544	-604.3	-604.3			
		-13.50	-449.4	-487 3	-557.1	-541.4									-330.3	-345.9	-394.4	-405.1			
		-13.00	-258.5	-278.5	-324.4	-314.8									-200 5	-200.2	-214.5	-227.7			
		-12 50	-151 3	-153.1	-151.1	-141.2									-107.1	-103.4	-82.57	-105 4			
		-12.00	-69.27	-87.24	-102.9	-91 95	-12410	-12460	-12700	-12940					-41.55	-50.32	-60.16	-98.22			
		-11.50	-54.19	-70.58	-79.92	-73.47	-10850	-10910	-11150	-11390					-30.96	-37.7	-45 88	-84.61			
		-11.00	-41.31	-56.77	-62.1	-58.68	-9354	-9398	-9849	-9933					-22.58	-27.84	-35.2	-73 76			
		-10.50	-30.66	-44.57	-47.5	-47 08	-7932	-7986	-8255	-8561					-16.21	-20.34	-27.26	-65.38			
		-10.00	-21.91	-33.75	-35.84	-37.84	-6654	-6685	-7003	-7287	-35.9	-37.71	-41.8	-56.1	-11 36	-14.72	-21.44	-58.98	-7425	-7591	-19000
		-9.50					-5531	-5545	-5871	-6183	-31	-32.56	-35 9	-50					-6047	-6228	-14340
		-9.05					-4571	-4573	-4909	-5207	-27.4	-28.7	-31 7	-45 8					-4750	-4930	-5971
		-8.47					-3720	-3722	-4066	-4349	-23.7	-24.7808	-27.3	-41.8					-3605	-3758	-4678
		-7.89					-2966	-3002	-3328	-3578	-21	-21.9	-24.2	-38.5					-2599	-2734	-3565
		-7.50					-2321	-2353	-2681	-2920	-18.82	-19.48	-21.5	-35.6					-1784	-1911	-2635
		-7.00					-1779	-1814	-2147	-2344	-16.72	-17.48	-19.1	-32.9					-1177	-1289	-1918
		-6.46					-1337	-1374	-1689	-1850	-14.71	-15.5028	-17	-30.3					-738.7	-832.1	-1368
		-6.00					-977	-1014	-1303	-1438	-13	-13.85	-15.3	-28.1					-451.4	-529 6	-970 2
		-5.50					-697.7	-733.7	-974.3	-1089	-11.37	-12.14	-13.8	-26.1					-283.7	-327 3	-693.4
		-5.00					-483.6	-512.5	-712.8	-804.7	-9.75	-10.52	-12.3	-23.8					-211.1	-221.5	-498.6
		-4.51					-320.7	-346.5	-497	-571.5	-8.42	-9.08	-10.7381	-22.2					-162.1	-166 1	-371.9
		-4.00					-222.8	-228.2	-329.4	-389.6	-7.1	-7.6928	-9.47393	-20 5					-123.2	-126.7	-283.3
		-3.50					-170.4	-166.1	-209	-254.1	-5.84	-6.22	-8 3	-18.6							
		-3.00					-126.5	-122	-130.4	-160.4	-4.973	-5.063	-6.96	-16.7							
		-2.50									-3.84	-4.033	-5.865	-15 01							
		-2.00									-2.784	-3.06	-4.84	-13 24							
		-1 50									-1.757	-1.995	-3.34	-11.3							
		-1.00									-0.7186	-0.9749	-2.263	-9 723							
		-0.50									-0.1843	-0.3023	-1.809	-8.701							
		0.00									0.04135	-0.07548	1.851	5.689							
		0.50									0.3052	0.728	2.658	6.611							
Curve Fit	a		11.76166	11.14881	8.770258	8.853379					2.57E-02	2.95E-02	0.05806	0.100617							
	b		353.9111	329.4592	237.4741	240 1088					6.70E-02	0.119131	0.546536	1.382015							
	c		3529.401	3214.361	2059.25	2081 598					1.826956	1.824237	3.85923	9.477178							
	d		11830.63	10297.14	5557.607	5598.701					0.18952	0.284974	1.012613	0.922955							
2nd Derivative	e		70.58997	68.89287	52.82155	53.12027					0.154212	0.177134	0.34836	0.6037							
	b		707 8223	658.8183	474.8481	480.2176					0 133921	0 238261	1.093072	2.76403							
Max Gradient	Vbr		-10.0301	-9.85035	-8.02573	-9.04019					-0.86842	-1.34509	-3.13777	-4.57848							
Threshold Voltage Breakdown	Vbr																				

4	4	4	4	4	4	4	4	4	4	4	4	4	4	4	4	4	4	4	4	4	4	4
7, 3	10, 9	10, 9	10, 9	10, 9	10, 9	10, 9	10, 9	10, 9	10, 9	10, 9	10, 9	10, 9	10, 9	10, 9	10, 9	10, 8	10, 9	10, 9	10, 9	10, 8	10, 9	
1500	200	200	200	200	200	200	200	200	200	200	200	200	30	30	30	30	400	400	400	400	1500	1500	1500	1500
50	20	20	20	20	20	20	20	20	400	400	400	400	20	20	20	20	50	50	50	50				
0	300	300	300	300	300	300	300	300	500	500	500	500	0	0	0	0								
Y	N	N	N	N	Y	Y	Y	Y	N	N	N	N	N	N	N	N	0	0	0	0	Y	Y	Y	Y
100%	0%	80%	80%	100%	0%	60%	80%	100%	0%	60%	80%	100%	0%	60%	80%	100%	0%	60%	80%	100%	0%	60%	80%	100%
									-1823	-1846	-1960	-2084												
									-1554	-1575	-1685	-1777												
									-1295	-1315	-1419	-1498												
									-1046	-1084	-1184	-1230												
									-809.5	-827	-918.3	-969 3												
									-585.6	-602.6	-679 8	-716.1												
	-528.1	-556.5	-674 7	-724.9	-11560	-12080	-12400	-12610	-378.8	-391.6	-445 1	-469.7	-139.7	-143	-143.3	-146 7								
	-441.1	-467 7	-574.6	-620 2	-9395	-9767	-10090	-10.29	-220 5	-213.2	-233	-246.9	-88.95	-92.02	-96.37	-105								
	-355	-381.1	-475.9	-517.8	-7491	-7765	-8066	-8245	-108.2	-96 76	-84.09	-84 84	-44.78	-67.92	-79.23	-98.61								
	-279.4	-298.1	-380	-418.4	-5881	-6089	-6359	-6541	-5.406	-9.301	-10.03	-18.14	-34.84	-56.48	-65.05	-82.11								
-18980	-218.2	-224.8	-288 5	-323.1	-4555	-4657	-4945	-5116	-3.726	-7.145	-7.873	-15.75	-28	-45.96	-52.35	-67.35	-5587	-5630	-5860	-6168				
-14570	-171.3	-170.5	-204.6	-234.5	-3416	-3459	-3751	-3918					-18.48	-36 37	-41.46	-54.67	-4304	-4307	-4534	-4817				
-11370	-126.5	-124 8	-131.5	-155.6	-2471	-2490	-2815	-29700					-12 57	-27.83	-32	-44.53	-3206	-3211	-3456	-3690				
-5897	-64.01	-62.33	-75.98	-84.69	-1740	-1761	-2091	-2231					-7.21	-20.33	-24.15	-36.83	-2336	-2346	-2563	-2829				
-4656	-49.89	-48.82	-45.41	-62 61	-1173	-1195	-1567	-1651					-4.435	-14.38	-18	-31 3	-1840	-1669	-1880	-2095				
-3623	-31.37	-31.77	-31.35	-46.31	-775.8	-772.7	-1118	-1195					-2.653	-8.806	-13.26	-27.83	-1097	-1127	-1332	-1516				
-2784	-21.37	-21.98	-22.23	-35.8	-469.5	-466.7	-756.9	-784.9					-1.445	-5 808	-9.262	-25.6	-675.3	-708.6	-879.3	-1046				
-2149	-14 54	-15.18	-15.96	-28 47	-247	-236.5	-451.5	-487.4					-0.579	-3.755	-7.591	-24.21	-363.4	-393.6	-531.9	-666.9				
-1575	-9.758	-10.29	-11.32	-23.3	-166 1	-148 2	-237	-268.1					-0.39	-2.292	-6.367	-23.37	-199.2	-200.5	-285.5	-402.9				
-1337	-6.533	-6.876	-8.194	-19.81	-108 4	-93.97	-118	-138.3					-0.3068	-1 514	-5 724	-22.61	-126.7	-123.9	-149.5	-256 7				
-1097	-4.32	-4.518	-6.094	-17.32	-64.81	-53.74	-60.07	-68.97					-0.143	-0.7255	-5.256	-22.17	-69 66	-67 42	-79.75	-184.1				
-926 9																	-33.23	-31 2	-47.84	-148.5				
-805																	-13.96	-13.84	-34 4	-130 9				

Wafer	5	5	5	5	5	5	5	5	5	5	5	5	5	5	5	5	5	5	5	5	5	5
Cell	5, 7	5, 7	5, 7	5, 7	5, 7	5, 7	5, 7	5, 7	5, 7	5, 7	5, 7	5, 7	5, 7	5, 7	5, 7	5, 7	5, 7	5, 7	5, 7	5, 7	5, 7	5, 7
Diameter [um]	200	200	200	200	200	200	200	200	200	200	200	200	400	400	400	400	1500	1500	1500	1500	1500	1500
Guard Ring [um]	20	20	20	20	20	20	20	20	30	30	30	30	20	20	20	20	50	50	50	50	50	50
Pixel Dist [um]	300	300	300	200	300	500	500	500	400	400	400	400	500	500	500	500	0	0	0	0	0	0
Metal Ring	N	N	N	N	Y	Y	Y	Y	N	N	N	N	N	N	N	N	Y	Y	Y	Y	Y	Y
Illumination [%]	0%	60%	80%	100%	0%	60%	80%	100%	0%	60%	80%	160%	0%	60%	80%	100%	0%	80%	80%	80%	80%	80%
Bias Voltage [V]																						
-100.0		-10240	-10540	-10530	-13150																	
-99.0		-8888	-9171	-9184	-12050																	
-98.0		-7740	-8039	-8058	-10940																	
-97.0		-6561	-6869	-6905	-9715																	
-96.0		-5358	-5661	-5712	-8648																	
-95.0		-4146	-4441	-4517	-7586																	
-94.0		-2979	-3234	-3356	-6515																	
-93.0		-1821	2066	-2231	-5445																	
-92.0		-714.4	-1024	-1216	-4384																	
-91.0		-63.82	-125.8	-350.3	-3341																	
-90.0		-47.01	-57.7	-77.8	-2290																	
-89.0		-8.62	-17.4	-15.09	-1343																	
-88.0		0	-2.608	-7.211	-353.2																	
-87.0		0	0	-6.873	-156.8																	
-86.0		0	0	0	-34.52																	
-85.0																						
-84.0																						
-83.0																						
-82.0																						
-81.0																						
-80.0																						
-79.0																						
-78.0																						
-77.0																						
-76.0																						
-75.0																						
-74.0																						
-73.0																						
-72.0																						
-71.0																						
-70.0																						
-69.0																						
-68.0																						
-67.0																						
-66.0																						
-65.0																						
-64.0																						
-63.0																						
-62.0																						
-61.0																					-50490	0	0
-60.0																					-23240	-39190	0
-59.0																					-3193	-4604	-35630
-58.0																					-697.6	-1895	-3342
-57.0																					-196.1	-319.7	-1346
-56.0																					-104.1	-138.7	-512.7
-55.0																					-62.22	-75.8	-252.8
-54.0																					-34.57	-42.87	-161.8
-53.0																					-32.95	-39.42	-140
-52.0																					-31.7	-37.71	-134.4
-51.0																					-30.09	-36.47	-131.2
-50.0					-3116	-3170	-3394	-3212															
-49.0					-2119	-2176	-2422	-2310															
-48.0					-1193	-1254	-1543	-1547															
-47.0					-409.3	-504.3	-834.8	-940.6															
-46.0					-78.96	-62.91	-325.5	-494.1															
-45.0					-54.28	-52.71	-97.8	-182.9															
-44.0					-34.55	-32.55	-40.95	-77.51															
-43.0					-13.5	-12.42	-13.55	-29.16															
-42.0					-8.624	-8.832	-13	-27.8															
-41.0					-7.12	-8.23	-12.32	-26.77															
-40.0					-8.652	-8.762	-11.91	-25.96															
-39.0																							
-38.0																							
-37.0																							
-36.0																							
-35.0																							
-34.0																							
-33.0																							
-32.0																							
-31.0																							
-30.0																							
-29.0																							
-28.0																							
-27.0																							
-26.0																							
-25.0																							
-24.0																							
-23.0																							
-22.0																							
-21.0																							
-20.0																							
-19.0																							
-18.0																							
-17.0																							
-16.0																							
-15.0																							
-14.0																							
-13.0																							
-12.0																							
-11.0																							
-10.0																							
-9.0																							
-8.0																							
-7.0																							
-6.0																							
-5.0																							
-4.0																							
-3.0																							
-2.0																							
-1.0																							
0.0																							
1.0																							
2.0																							

5	5	5	5	5	5	5	5	5	5	5	5	5	5	5	5	5	5	5	5	5	5
5, 7	9, 10	9, 10	9, 10	9, 10	9, 10	9, 10	9, 10	9, 10	9, 10	9, 10	9, 10	9, 10	9, 10	9 10	9, 10	9, 10	9, 10	9 10	9, 10	9, 10	9, 10
1500	200	200	200	200	200	200	200	200	200	200	200	200	200	400	400	400	400	1500	1500	1500	1500
50	20	20	20	20	20	20	20	20	30	30	30	30	30	20	20	20	20	50	50	50	50
0	300	300	300	300	300	300	300	300	400	400	400	400	400	300	500	500	300	0	0	0	0
Y	N	N	N	N	Y	Y	Y	Y	N	N	N	N	N	N	N	N	N	Y	Y	Y	Y
100%	0%	60%	80%	100%	0%	60%	80%	100%	0%	60%	80%	100%	0%	60%	60%	100%	0%	80%	60%	100%	
					-5732	-5870	-5973	-5323													
					-4852	-4990	-5108	-4378													
					-3955	-4096	-4231	-3517													
					-3043	-3187	-3349	-2678													
					-2132	-2282	-2475	-1894													
0					-1257	-1417	-1654	-1163						-10240 14	-10540.65	-10550 12	-13253 91				
0					-365.5	-538 7	-860 7	-594						-8868 142	-8171 651	-9204 117	-12153.91				
-39630					-166 7	-187	-331 8	-291 6						-7740 142	-8039 851	-8079 117	-11043.91				
-4627					-119.6	-133 4	-186.9	-153 8						-6561 142	-8868 651	-6925 117	-9818.915				
-2457					-79.12	-83 66	-92.13	-78.55						-5358.142	-5661 651	-5732.117	-8751.915				
-1405					-40.31	-55.23	-58 99	-50						-4146 142	-4441 851	-4537 117	-7689 915	-3856	-5834	11560	-13050
-848 9														-2970 142	-3234 651	-3376 117	-6618.915	-1771	-3019	-5852	-6951
-532														-1821 142	-2066 651	-2251 117	-5548.915	-526 4	-1280	-3146	-4070
-360 9														-714.5417	-1024.651	-1236 117	-4487 815	-161 5	-336 1	-1460	-2207
-264.8														-83.9617	-126 4512	-370 4168	-3444 915	-97.51	-129.8	-488.7	-1143
-552.2														-47 1517	-58 35117	-98.0168	-2393.815	-54.2	-77.29	-210 9	-500.8
														-8 781704	-18 05117	-35.2066	-1446.915	-9 176	-29 39	-105 3	-379 7
														-0.3786	-3.259175	-27 3278	-457 1147	-8 436	-12 16	-48 31	-261 9
														-0.2841	-0 7186	-26 7898	-260 7147	-7.919	-11.22	-42 09	-232
														-0 1854	-0.6845	-23 4578	-138 4347	-7 442	-10 6	-40 35	-223.9
														-0 141704	-0.651176	-20 1168	-103 9147	-6.977	-10 12	-39 48	-219 9
														-0 139428	-0.647443	-19 82684	-102 8717				
														-0 134532	-0 643003	-19 53488	-101 6775				
														-0 131848	-0.640458	-19 27784	-100 6278				
														-0 12811	-0.638596	-19 0925	-99 44177				
														-0 125754	-0 632518	-18 93278	-98 49235				
														-0 120735	-0.628183	-18 67439	-97 17535				
														-0.11779	-0 624718	-18 41057	-96 00644				
														-0 113982	-0 620709	-19 24674	-95 02074				
														-0 111205	-0 617091	-17 99596	-93 86587				
														-0 106696	-0.612105	-17 69458	-92 7356				
														-0 103023	-0.609296	-17 43443	-91 43036				
														-0 101355	-0 606003	-17.26273	-90 4265				
														-0 096852	-0.600888	-16.98496	-89.22725				
														-0.092916	-0.598293	-16.83706	-88.04113				
														-0 08924	-0 58371	-16 54676	-86 9797				
														-0 087363	-0.590623	-16 38484	-85.87701				
														-0 082918	-0.586687	-18 15534	-84 77478				
														-0 079922	-0.581871	-15.84699	-83 66751				
														-0 075965	-0 578662	-15.81514	-82.37957				
														-0.072844	-0 574901	-15.30926	-81 43037				
														-0.06812	-0 571688	-15 14198	-80 17065				
														-0 064883	-0 566414	-14 90162	-78.06724				
														-0 062524	-0 563371	-14 69568	-77.86703				
														-0 058468	-0.559379	-14 45551	-76 86365				
														-0 055033	-0 555935	-14.23767	-75 77481				
														-0 051828	-0 55245	-13 9478	-74 48169				
														-0 048679	-0 548712	-13.74221	-73 42534				
														-0 045357	-0.54558	-13.51061	-72.24342				
														-0 041211	-0 540042	-13.27736	-71 08077				
														-0 038099	-0 536051	-13 04821	-70 08621				
														-0 033585	-0.533347	-12.85072	-68.88978				
														-0 030042	-0 529187	-12.5652	-67.80075				
														-0 027182	-0 529159	-12.31964	-66 5548				
														-0 024273	-0 521118	-12.10543	-65 46598				
														-0 01384	-0.5178	-11.89	-64 48				
														-0 01384	-0.5178	-11 68	-63.3				
														-0 01384	-0 5178	-11.54	-62 18				
														-0 01384	-0 5176	-11.26	-61 00				
														-0 01384	-0.5178	-11 1	-59 64				
														-0 01394	-0.5178	-10 92	-57 73				
														-0 01384	-0.5178	-10 62	-27 37				
														-0.01384	-0 6178	-9 642	-9.814				
														-0 01384	-0 5178	-3 105	-2.827				
														-0 01384	-0 5176	-0 6459	-0 5817				
														-0 01384	-0 01035	0 92591	-0 00968				
														-0 01384	0 8543	1.28	1 179				
														-0.01384	3.53	4 964	5.174				

6.7.3 Figures of Merit Analysis of Selected Photodiodes

The following are figures of merit calculation of selected photodiodes discussed in this research paper.

Cell:	**W1 C5,6 D1500,50,0,Y**
Breakdown Voltage:	-1.244 [V]
Dark Current (@ Vbr):	-38.7 [uA]
Gain (@ Vbr):	1513
Responsitivity (@ 600nm, 2V Bias):	0.199 [A/W]
NEP (@ Vbr):	0.000195 [W]

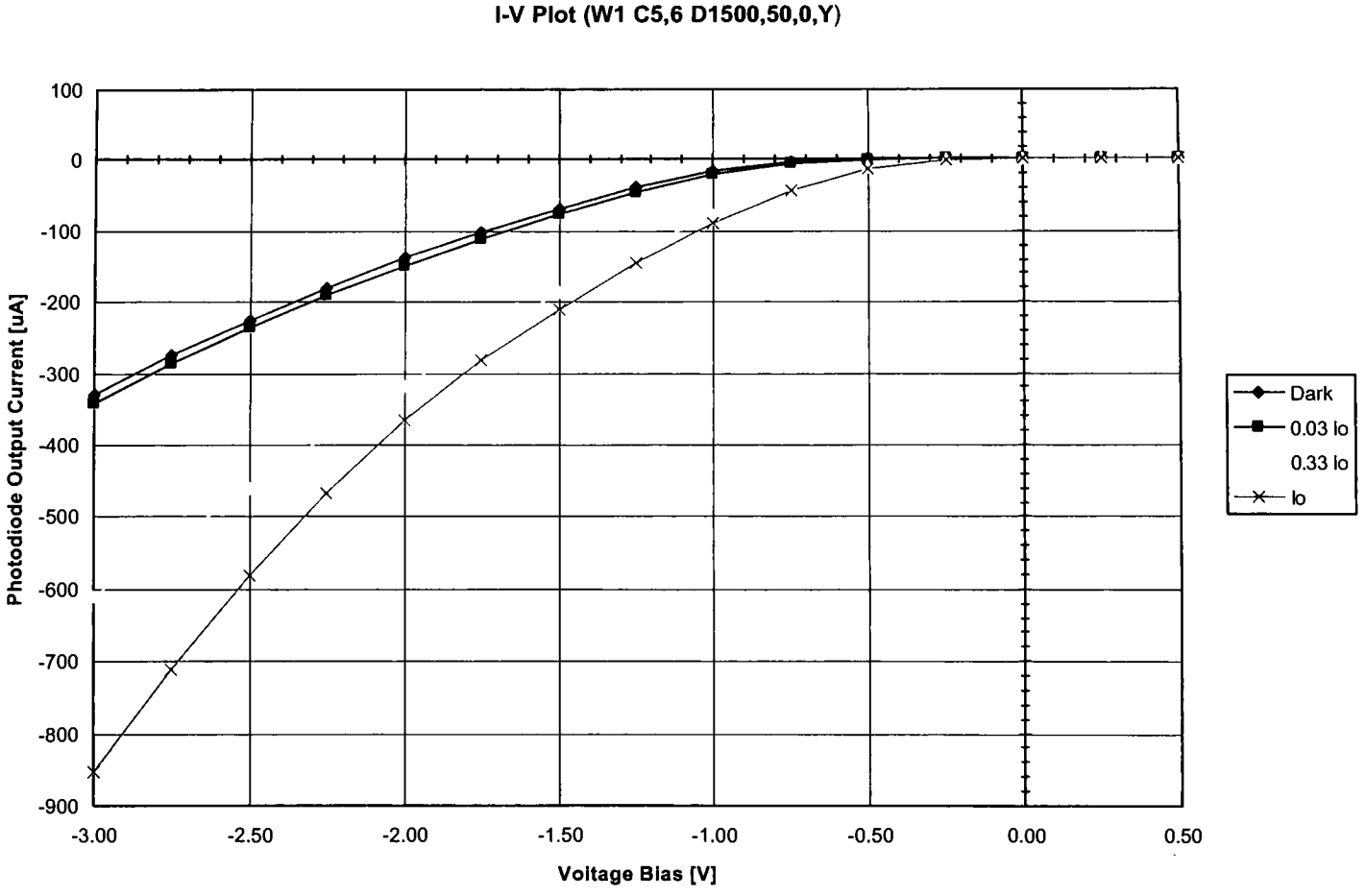
I-V Plot (W1 C5,6 D1500,50,0,Y)
Photodiode Output Current [uA]
100
0
-100
-200
-300
-400
-500
-600
-700
-800
-900
-3.00
-2.50
-2.00
-1.50
-1.00
-0.50
0.00
0.50
Voltage Bias [V]
Dark
0.03 Io
0.33 Io
Io

I-V Plot with Breakdown Voltage Interpolation Lines (W1 C5,6 D1500,50,0,Y)

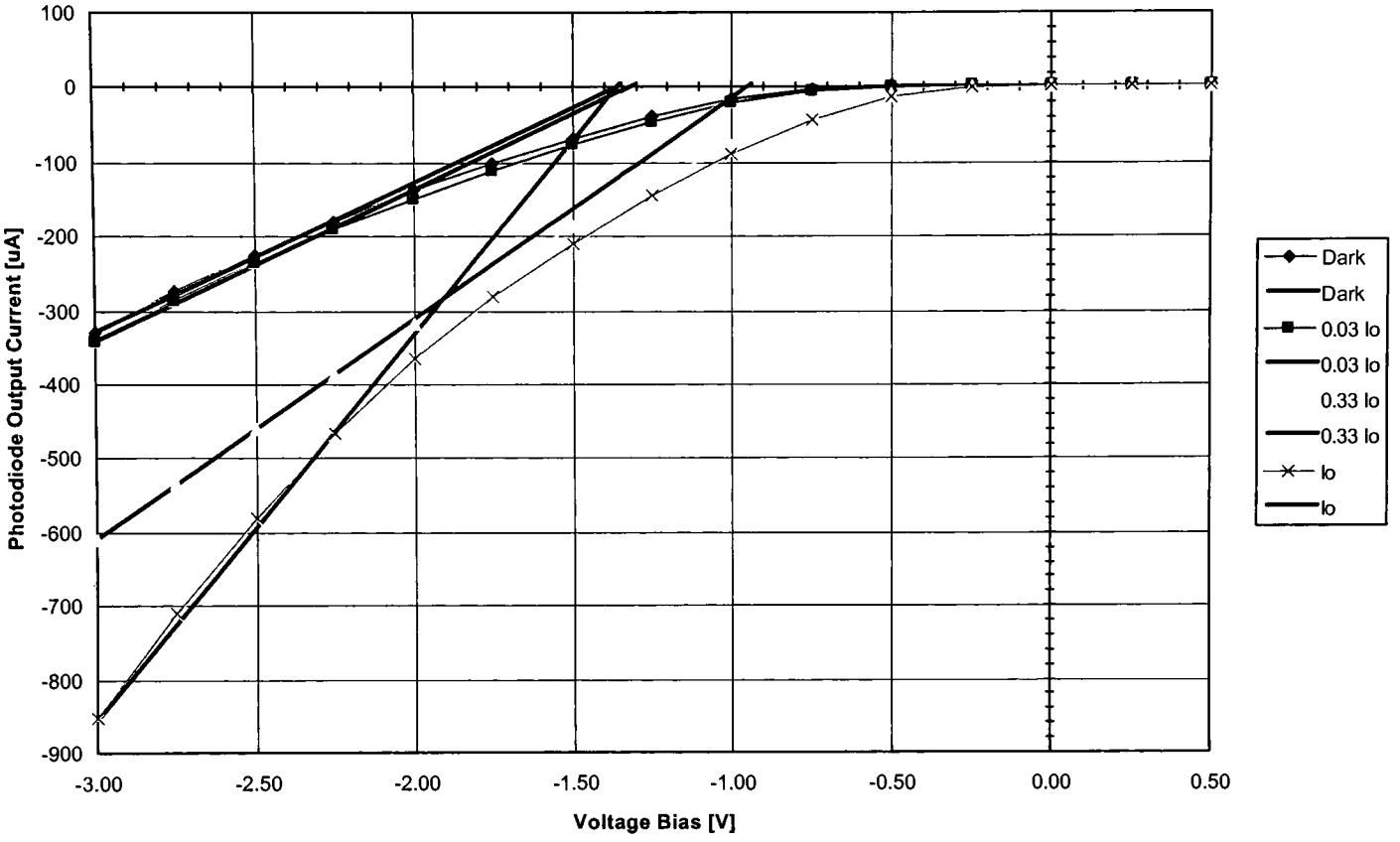

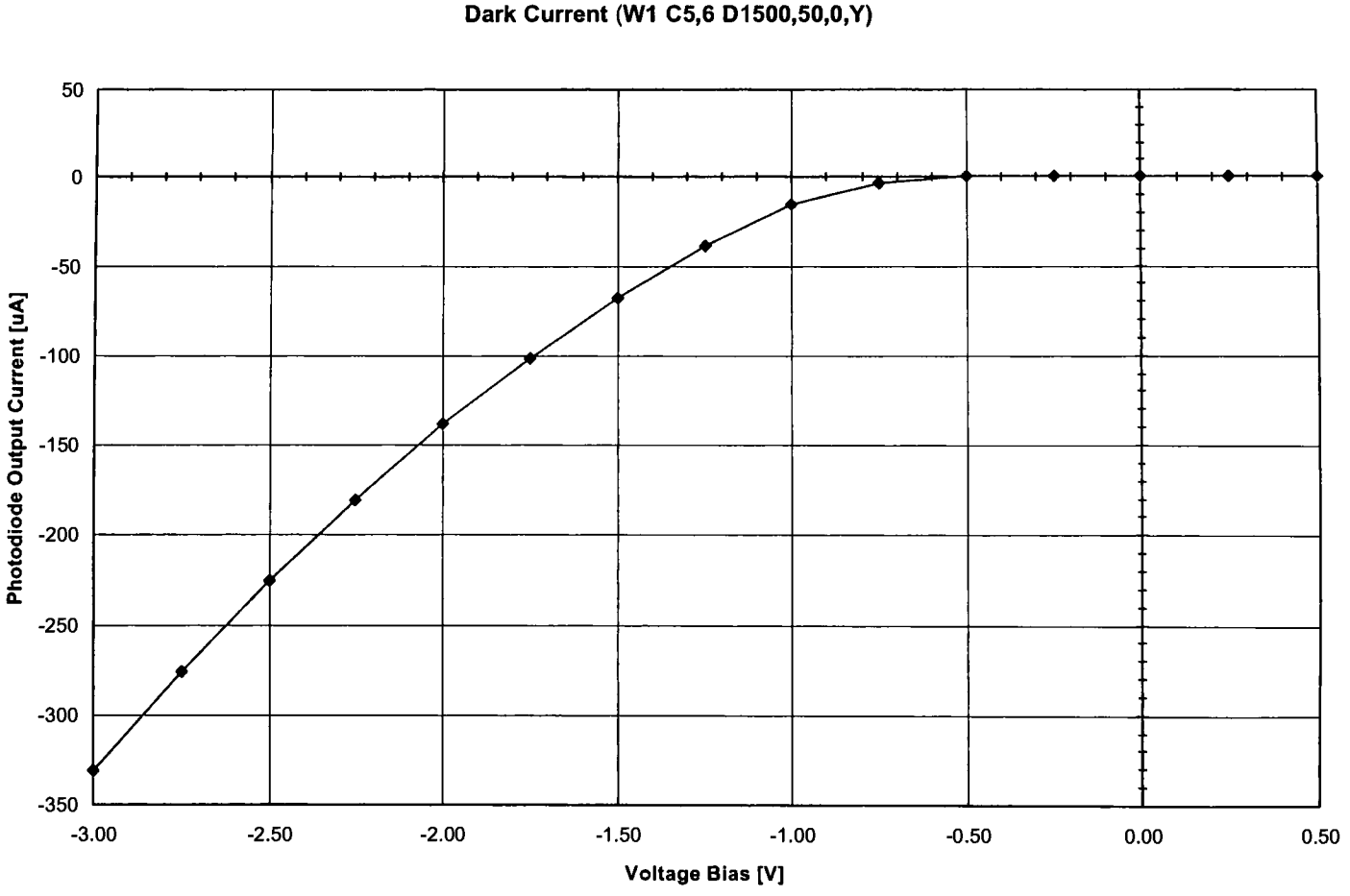
Dark Current (W1 C5,6 D1500,50,0,Y)
Photodiode Output Current [uA]
50
0
-50
-100
-150
-200
-250
-300
-350
-3.00
-2.50
-2.00
-1.50
-1.00
-0.50
0.00
0.50
Voltage Bias [V]

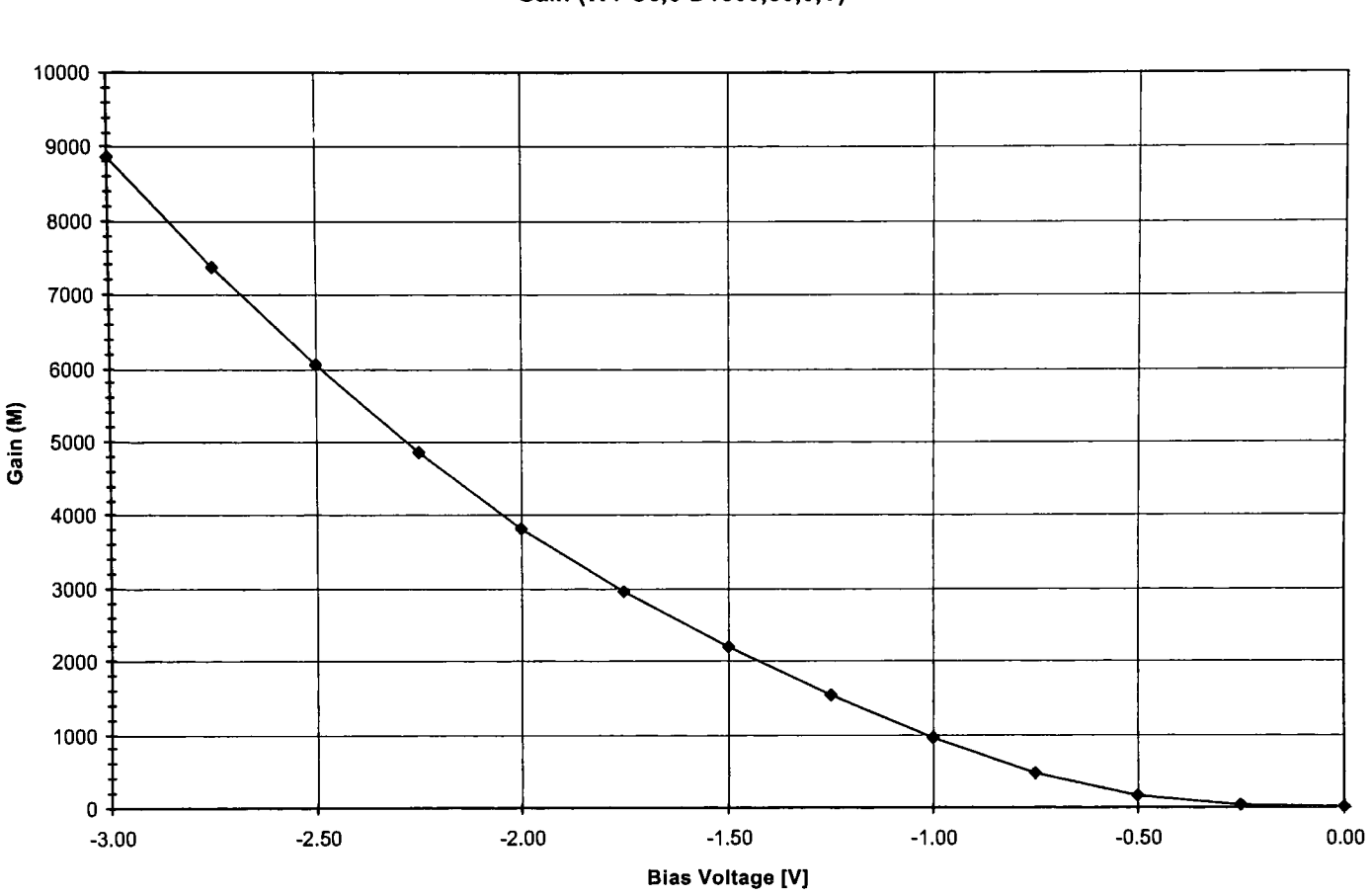
Gain (W1 C5,6 D1500,50,0,Y)
10000
9000
8000
7000
6000
5000
4000
3000
2000
1000
0
Gain (M)
-3.00
-2.50
-2.00
-1.50
-1.00
-0.50
0.00
Bias Voltage [V]

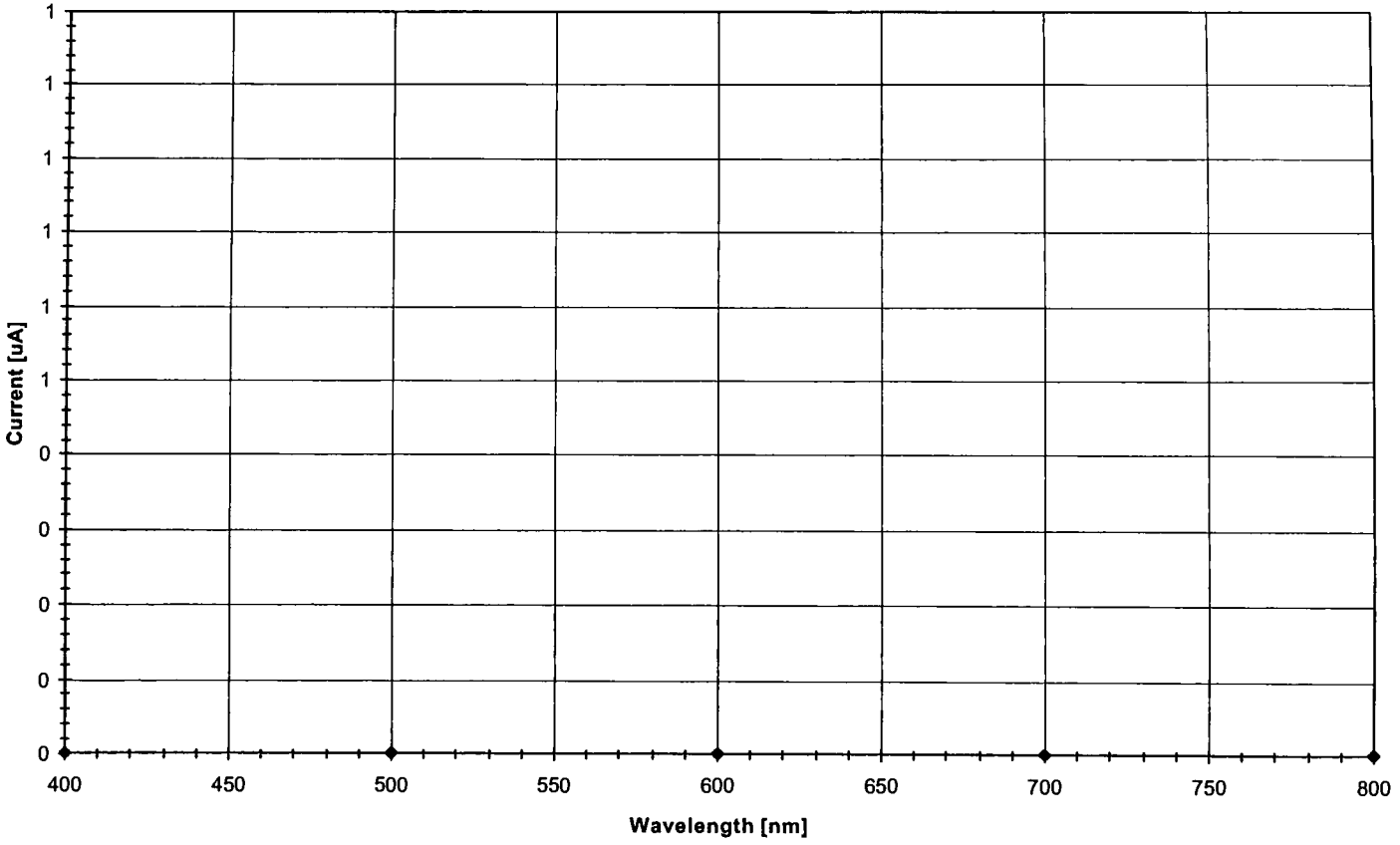
Current Output vs. Wavelength (W1 C5,6 D1500,50,0,Y)
Current [uA]
1
1
1
1
1
1
0
0
0
0
0
400
450
500
550
600
650
700
750
800
Wavelength [nm]

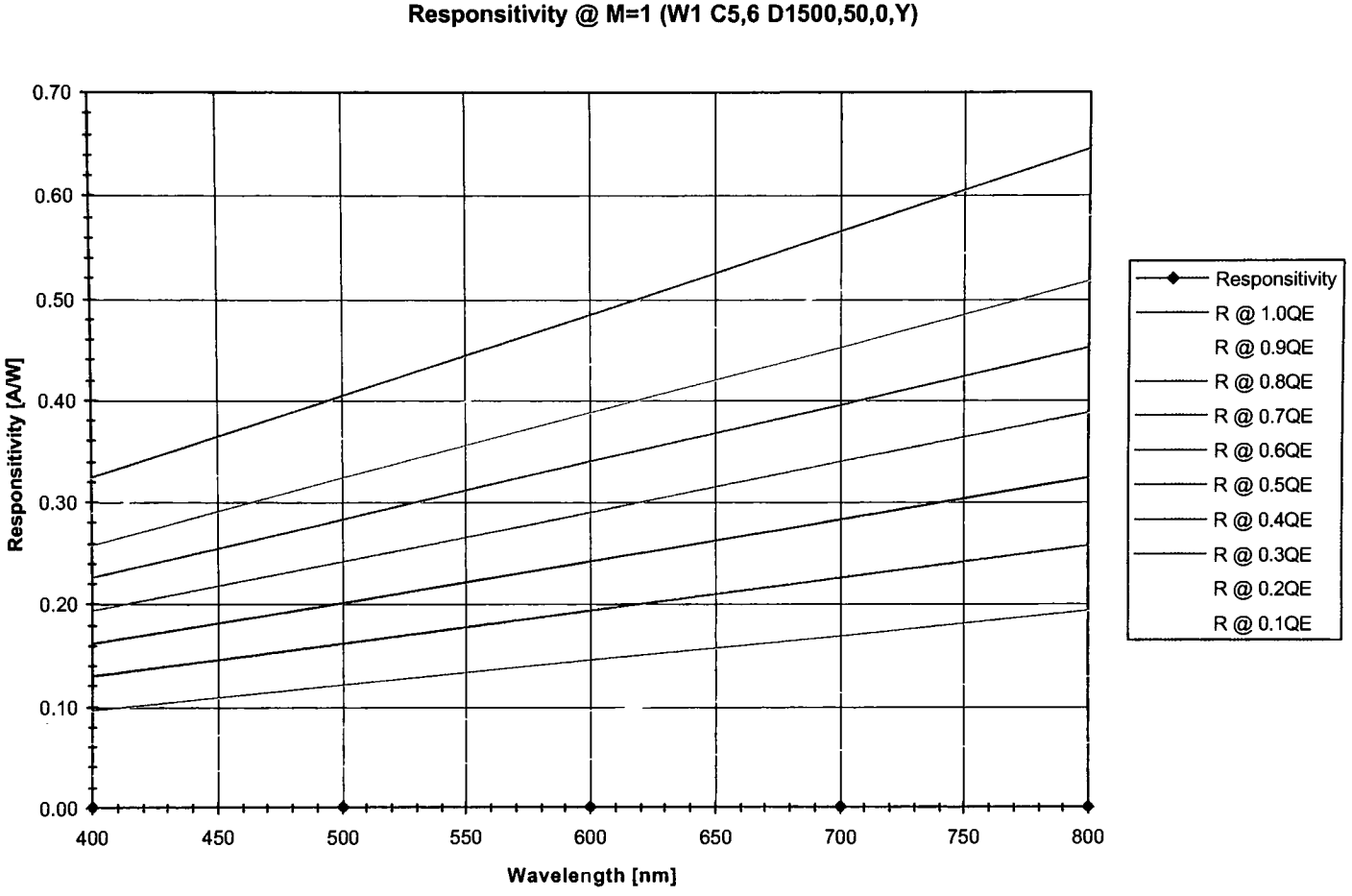
Responsitivity @ M=1 (W1 C5,6 D1500,50,0,Y)
0.70
0.60
0.50
0.40
0.30
0.20
0.10
0.00
Responsitivity [A/W]
400
450
500
550
600
650
700
750
800
Wavelength [nm]
Responsitivity
R @ 1.0QE
R @ 0.9QE
R @ 0.8QE
R @ 0.7QE
R @ 0.6QE
R @ 0.5QE
R @ 0.4QE
R @ 0.3QE
R @ 0.2QE
R @ 0.1QE

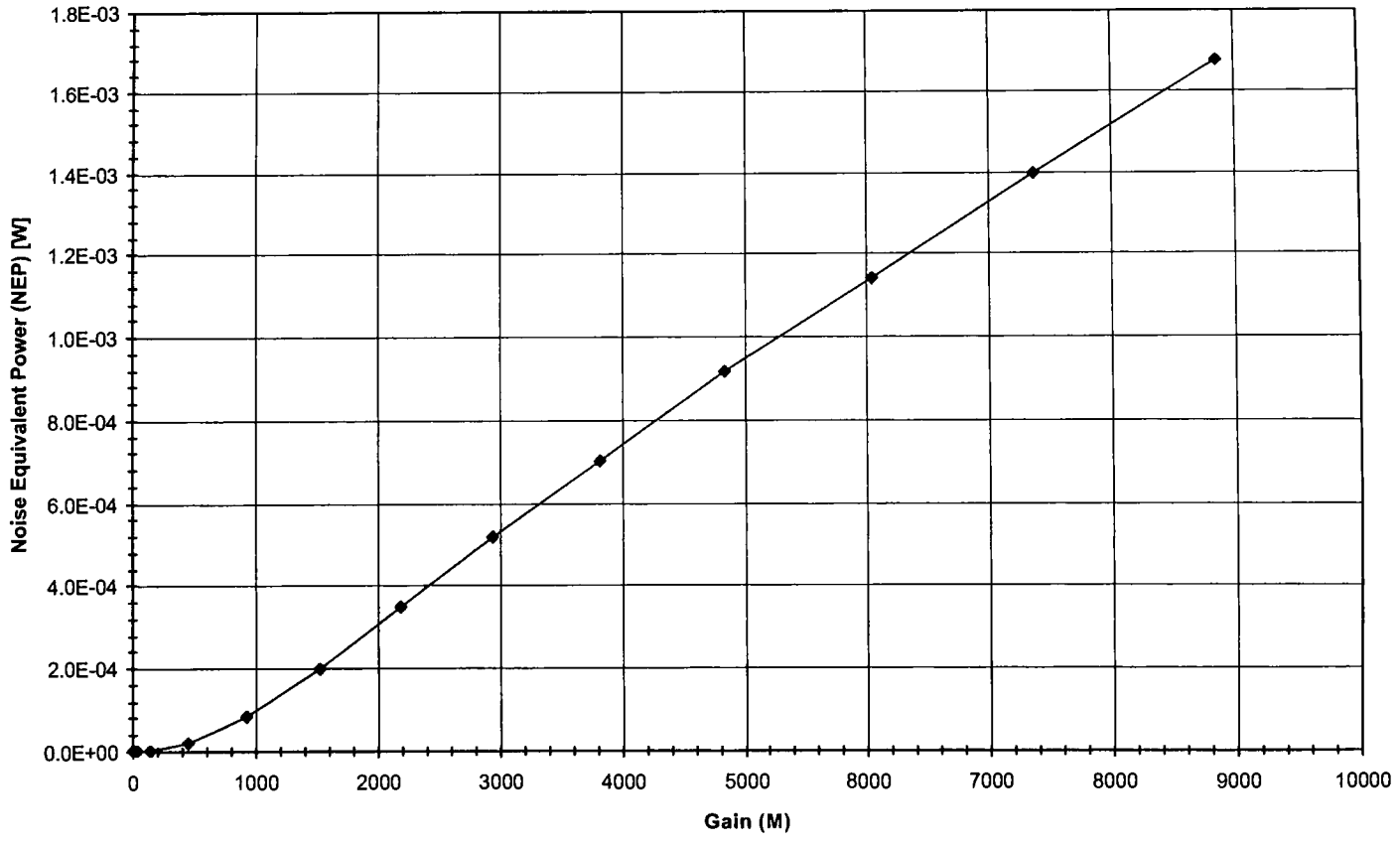
Noise Equivalent Power (NEP) (W1 C5,6 D1500,50,0,Y)
Noise Equivalent Power (NEP) [W]
1.8E-03
1.6E-03
1.4E-03
1.2E-03
1.0E-03
8.0E-04
6.0E-04
4.0E-04
2.0E-04
0.0E+00
0
1000
2000
3000
4000
5000
8000
7000
8000
9000
10000
Gain (M)

Wafer		1	1	1	1
Cell		5, 6	5, 6	5, 6	5, 6
Diameter [um]		1500	1500	1500	1500
Guard Ring [um]		50	50	50	50
Pixel Dist [um]		0	0	0	0
Metal Ring		Y	Y	Y	Y
Illumination [%]		Dark	0.03 Io	0.33 Io	Io
Bias Voltage [V]	*-3.00*	-331.9	-343.3	-610.8	-855.4
	-2.75	-276.4	-287.5	-535.6	-711.6
	-2.50	-226.2	-237.4	-460.9	-582.4
	-2.25	-181.8	-191.9	-387.6	-467.4
	-2.00	-139.1	-150.6	-317.6	-368.1
	-1.75	-102.4	-112.9	-250.1	-284.4
	-1.50	-69.19	-78.32	-187.1	-211.6
	-1.25	-39.24	-46.91	-129.1	-147.4
	-1.00	-16.07	-21.87	-77.7	-89.96
	-0.75	-3.657	-6.594	-36.33	-43.5
	-0.50	-0.188	-0.9371	-11.34	-14.02
	-0.25	-0.01516	0.02318	-2.021	-2.632
	0.00	-0.00445	-0.03432	-0.0167	0.0828
	0.25	-0.009	0.01149	-0.01705	0.03369
	0.50	0.01121	0.01576	-0.00152	-0.03434

MEASUREMENTS ARE DONE AT 600nm.

Wafer		1	1	1	1
Cell		5, 6	5, 6	5, 6	5, 6
Diameter [um]		1500	1500	1500	1500
Guard Ring [um]		50	50	50	50
Pixel Dist [um]		0	0	0	0
Metal Ring		Y	Y	Y	Y
Illumination [%]		Dark	0.03 Io	0.33 Io	Io
Bias Voltage [V]	*-3.00*	-331.9	-343.3	-610.8	-855.4
	-1.360	-0.822	-9.8492	-122.109	0.1592
	-1.356	-0.0212	-9.04232	-120.918	
	-1.311		0.03508	-107.521	
	-0.950			-0.044	

Curve Fit	a				
	b				
	c				
	d				
2nd Derivative	**a**				
	b				
Max Gradient	Vbr				
Threshold	Vbr				
Linear Trend	Vbr	-1.360	-1.356	-1.311	-0.950
Voltage Breakdown	Vbr	-1.244	-1.244	-1.244	-1.244

q =	1.60E-19	[C]
h =	6.63E-34	[J s]
c =	3.00E+08	[m/s]
wavel =	6.00E-07	[m]
v =	5.00E+14	[Hz]
Po @ 600r	4.86E-07	[W]
w =	**2.69E-06**	**[m]**
R @ 600nr	0.3538	[%]
a @ 600nr	3.75E+05	[1/m]
Ip =	9.65E-08	[A]

QE = 0.4104

Vbias [V]	Idark [A]	I [A]	*Inorm [A]*	*M*	*R @ 1 [A/V*	*NEP [W]*
-3.00	**-3.32E-04**	**-8.55E-04**	*9.65E-08*	*8862.437*	*0.1986*	*1.67E-03*
-2.75	**-2.76E-04**	**-7.12E-04**	*9.65E-08*	*7372.586*	*0.1986*	*1.39E-03*
-2.50	**-2.26E-04**	**-5.82E-04**	*9.65E-08*	*6034*	*0.1986*	*1.14E-03*
-2.25	**-1.82E-04**	**-4.67E-04**	*9.65E-08*	*4842.533*	*0.1986*	*9.15E-04*
-2.00	**-1.39E-04**	**-3.68E-04**	*9.65E-08*	*3813.728*	*0.1986*	*7.00E-04*
-1.75	**-1.02E-04**	**-2.84E-04**	*9.65E-08*	*2946.548*	*0.1986*	*5.16E-04*
-1.50	**-6.92E-05**	**-2.12E-04**	*9.65E-08*	*2192.298*	*0.1986*	*3.48E-04*
-1.25	**-3.92E-05**	**-1.47E-04**	*9.65E-08*	*1527.149*	*0.1986*	*1.98E-04*
-1.00	**-1.61E-05**	**-9.00E-05**	*9.65E-08*	*932.0374*	*0.1986*	*8.09E-05*
-0.75	**-3.66E-06**	**-4.35E-05**	*9.65E-08*	*450.6851*	*0.1986*	*1.84E-05*
-0.50	**-1.88E-07**	**-1.40E-05**	*9.65E-08*	*145.2553*	*0.1986*	*9.47E-07*
-0.25	**-1.52E-08**	**-2.63E-06**	*9.65E-08*	*27.26904*	*0.1986*	*7.63E-08*
0.00	**-4.45E-09**	**8.28E-08**	*9.65E-08*	*-0.857856*	*0.1986*	*2.24E-08*
0.25	**-9.00E-09**	**3.37E-08**	*9.65E-08*	*-0.349048*	*0.1986*	*4.53E-08*
0.50	**1.12E-08**	**-3.43E-08**	*9.65E-08*	*0.355782*	*0.1986*	*-5.64E-08*

q = 1.60E-19 [C]

h = 6.63E-34 [J s]

c = 3.00E+08 [m/s]

MEASUREMENTS ARE DONE AT -2V BIAS, FULL Io.

dark [A] = -2.07E-04

wavel [m]	wavel [nm]	R [%]	a [1/m]	w [m]	Po [W]	v [Hz]	Ip [A]	QE	I [A]	I [uA]	M		Responsiti	NEP [W]
4.00E-07	400	0.4888	8.98E+06	**2.69E-09**	1.73E-07	7.49E+14	2.85E-08	0.5112	**0.00E+00**	0.000		0.00	#DIV/0!	#DIV/0!
5.00E-07	500	0.3873	8.89E+05	**2.69E-09**	5.22E-07	6.00E+14	1.17E-07	0.5565	**0.00E+00**	0.000		0.00	#DIV/0!	#DIV/0!
6.00E-07	600	0.3538	3.75E+05	**2.69E-09**	4.86E-07	5.00E+14	9.65E-08	0.4104	**0.00E+00**	0.000		0.00	#DIV/0!	#DIV/0!
7.00E-07	700	0.3376	1.62E+05	**2.69E-09**	4.20E-08	4.28E+14	5.55E-09	0.2339	**0.00E+00**	0.000		0.00	#DIV/0!	#DIV/0!
8.00E-07	800	0.3278	6.40E+04	**2.69E-09**	1.60E-08	3.75E+14	1.1E-09	0.1062	**0.00E+00**	0.000		0.00	#DIV/0!	#DIV/0!

R @ 1.0QE	R @ 0.9QE	R @ 0.8QE	R @ 0.7QE	R @ 0.6QE	R @ 0.5QE	R @ 0.4QE	R @ 0.3QE	R @ 0.2QE	R @ 0.1QE
0.3226	0.2904	0.2581	0.2258	0.1936	0.1613	0.1290	0.0968	0.0645	0.0323
0.4033	0.3629	0.3226	0.2823	0.2420	0.2016	0.1613	0.1210	0.0807	0.0403
0.4839	0.4355	0.3871	0.3388	0.2904	0.2420	0.1936	0.1452	0.0968	0.0484
0.5646	0.5081	0.4517	0.3952	0.3388	0.2823	0.2258	0.1694	0.1129	0.0565
0.6452	0.5807	0.5162	0.4517	0.3871	0.3226	0.2581	0.1936	0.1290	0.0645

Cell:	W2 C6,8 C1500,50,0,Y
Breakdown Voltage:	-1.346 [V]
Dark Current (@ Vbr):	-73.8 [uA]
Gain (@ Vbr):	2413
Responsitivity (@ 600nm, 2V Bias):	0.199 [A/W]
NEP (@ Vbr):	0.000371 [W]

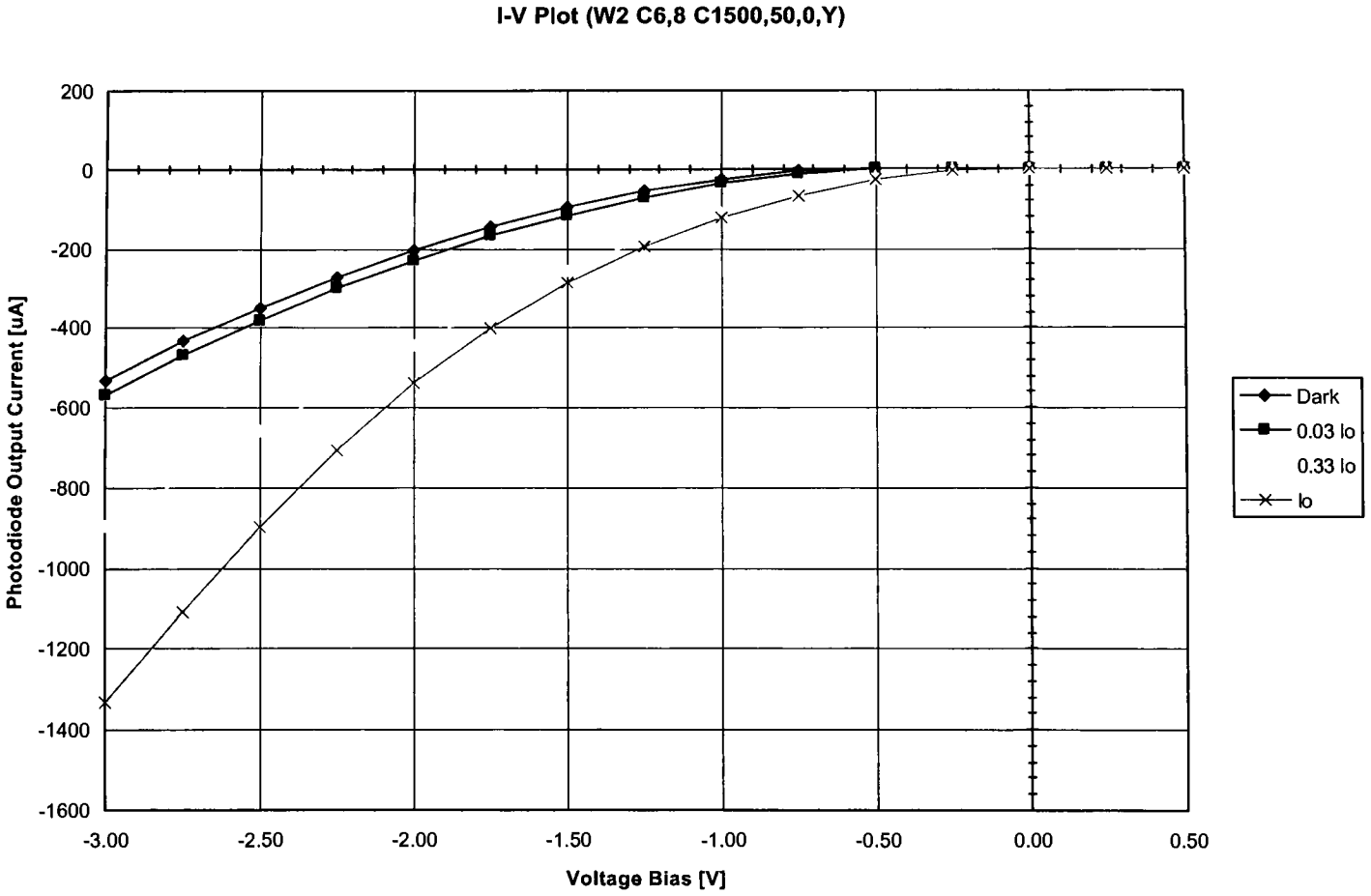
I-V Plot (W2 C6,8 C1500,50,0,Y)
200
0
-200
-400
-600
-800
-1000
-1200
-1400
-1600
Photodiode Output Current [uA]
-3.00
-2.50
-2.00
-1.50
-1.00
-0.50
0.00
0.50
Voltage Bias [V]
Dark
0.03 Io
0.33 Io
Io

I-V Plot with Breakdown Voltage Interpolation Lines (W2 C6,8 C1500,50,0,Y)

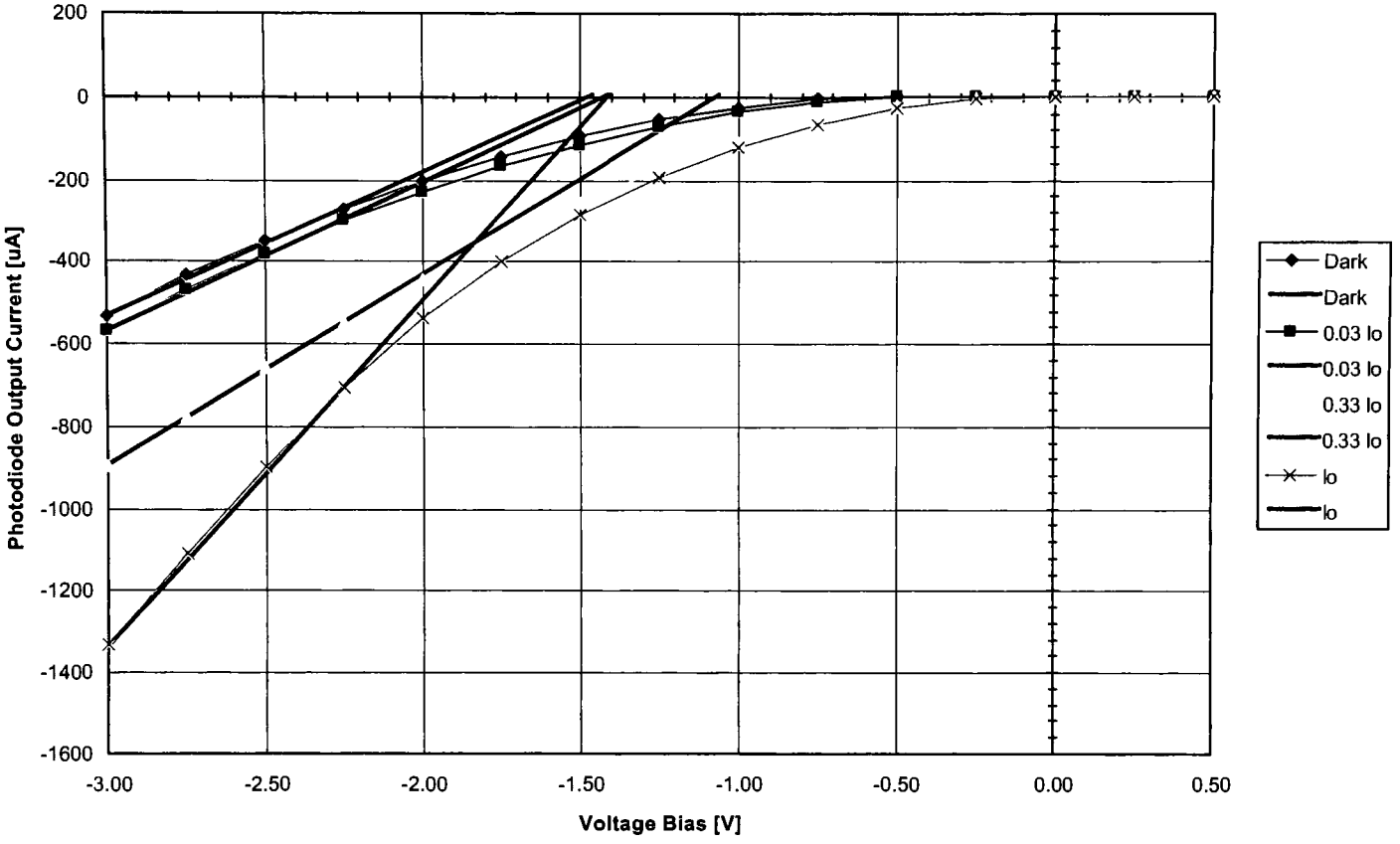

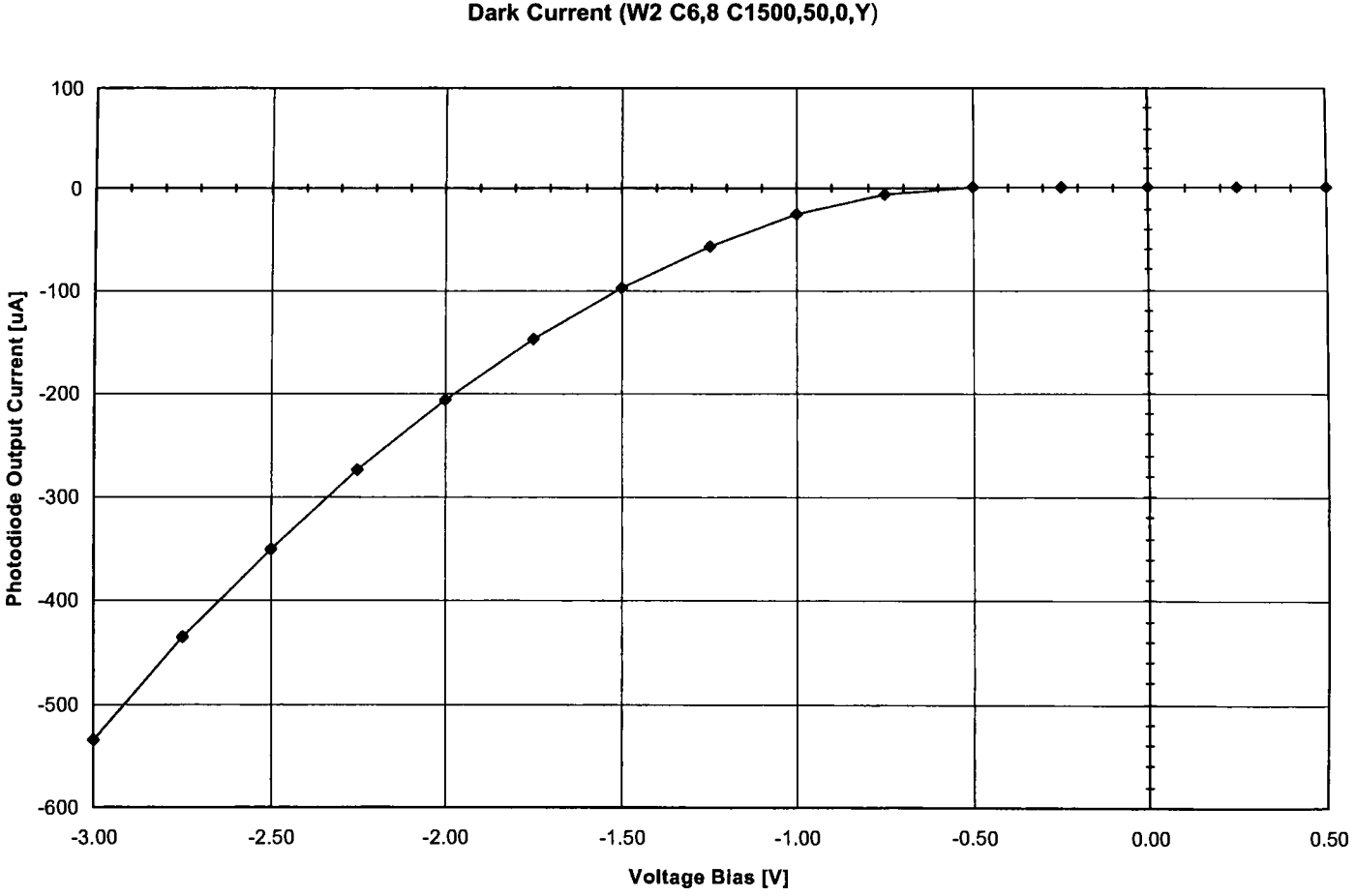
Dark Current (W2 C6,8 C1500,50,0,Y)
100
0
-100
-200
-300
-400
-500
-600
Photodiode Output Current [uA]
-3.00
-2.50
-2.00
-1.50
-1.00
-0.50
0.00
0.50
Voltage Bias [V]

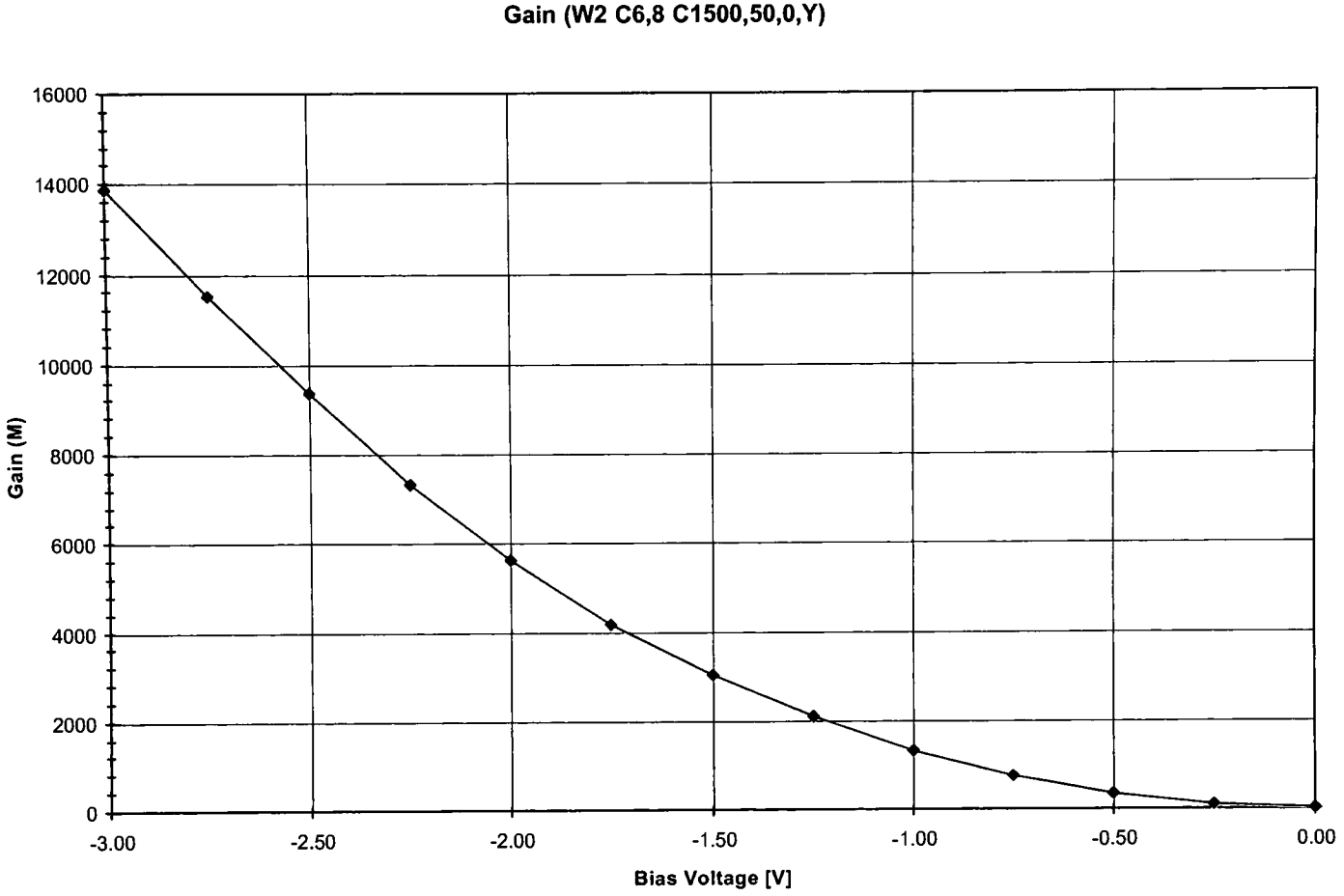
Gain (W2 C6,8 C1500,50,0,Y)
16000
14000
12000
10000
8000
6000
4000
2000
0
Gain (M)
-3.00
-2.50
-2.00
-1.50
-1.00
-0.50
0.00
Bias Voltage [V]

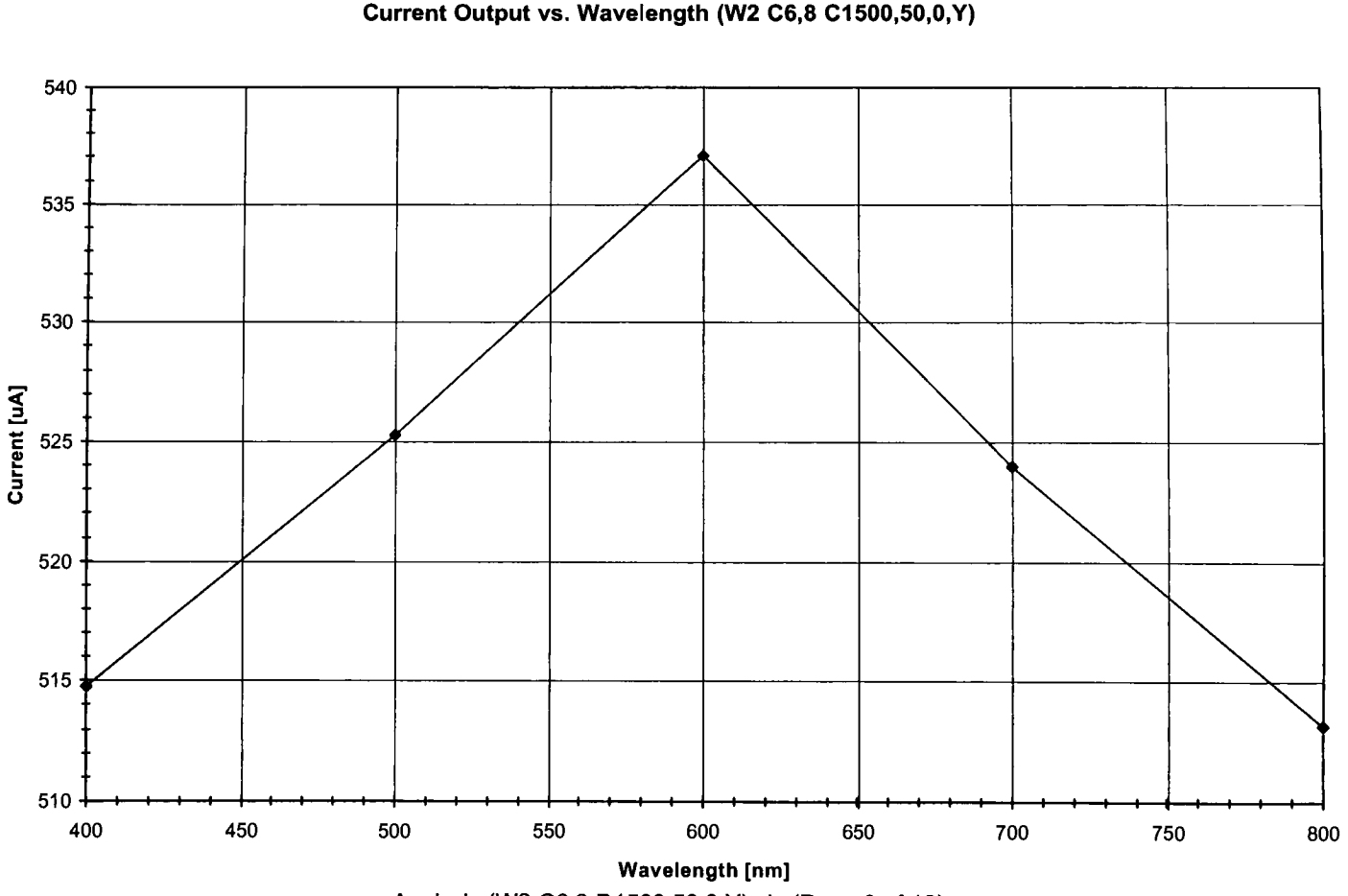
Current Output vs. Wavelength (W2 C6,8 C1500,50,0,Y)
Current [uA]
540
535
530
525
520
515
510
400
450
500
550
600
650
700
750
800
Wavelength [nm]

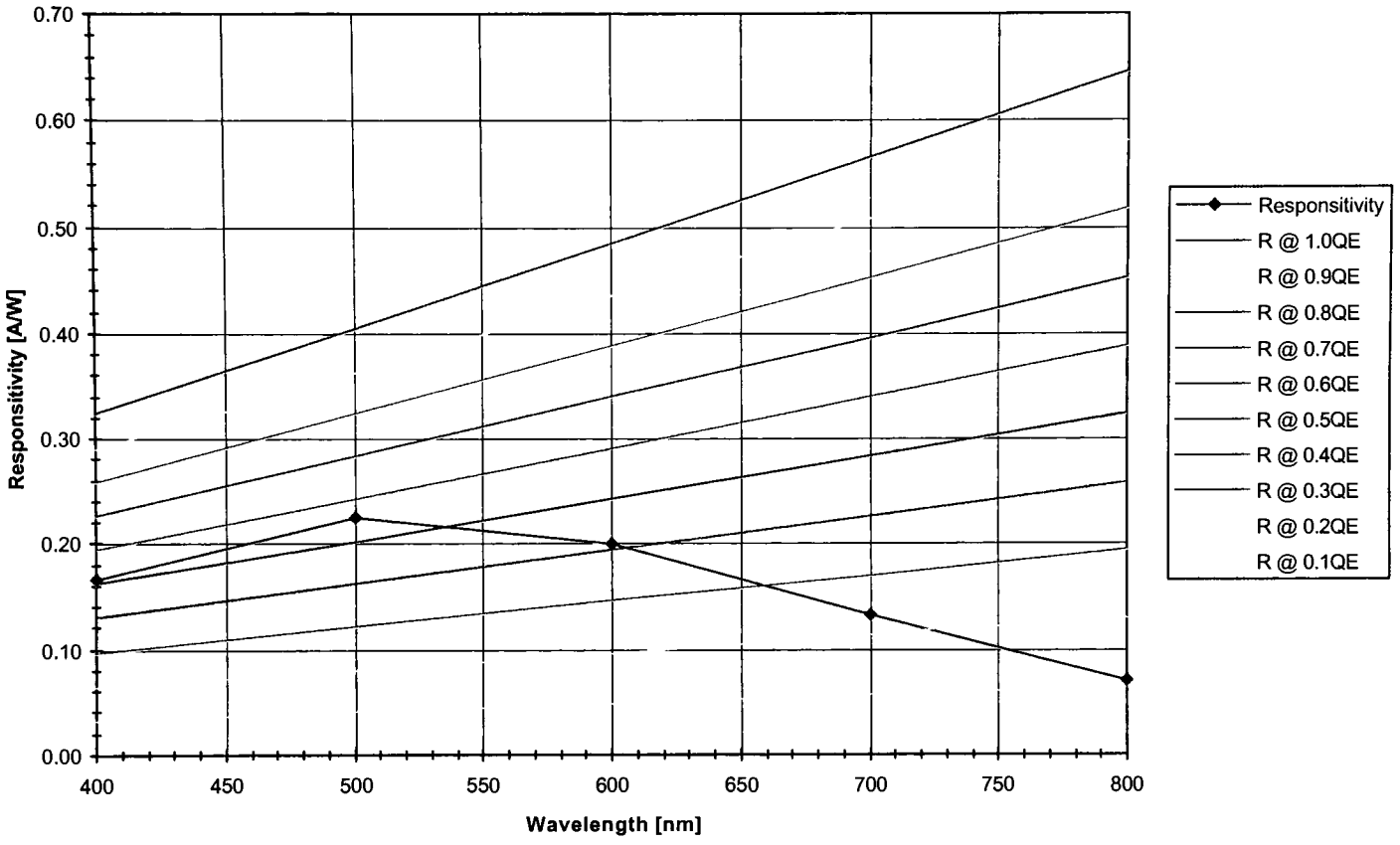
Responsitivity @ M=1 (W2 C6,8 C1500,50,0,Y)
0.70
0.60
0.50
0.40
0.30
0.20
0.10
0.00
Responsitivity [A/W]
400
450
500
550
600
650
700
750
800
Wavelength [nm]
Responsitivity
R @ 1.0QE
R @ 0.9QE
R @ 0.8QE
R @ 0.7QE
R @ 0.6QE
R @ 0.5QE
R @ 0.4QE
R @ 0.3QE
R @ 0.2QE
R @ 0.1QE

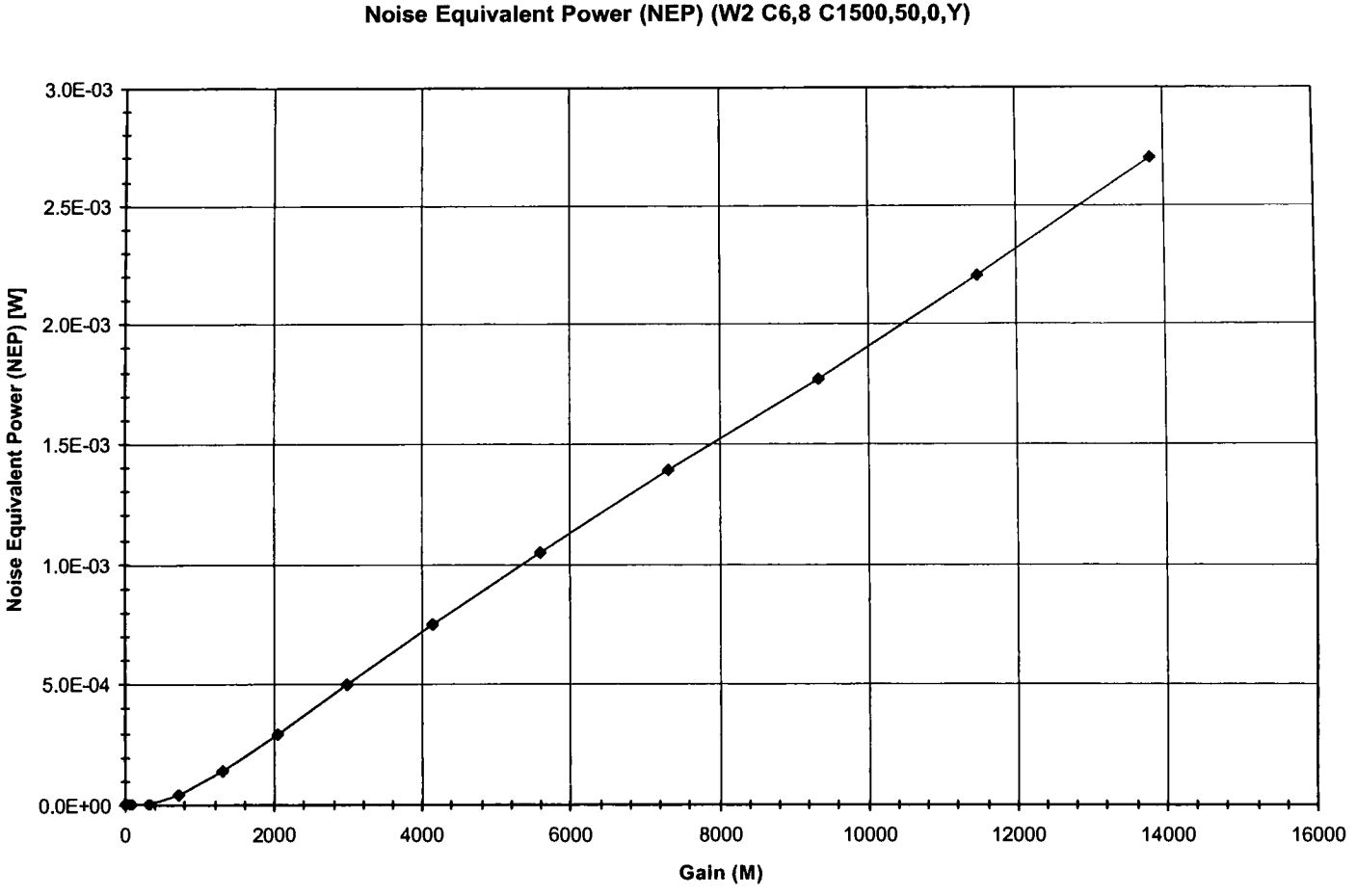
Noise Equivalent Power (NEP) (W2 C6,8 C1500,50,0,Y)
Noise Equivalent Power (NEP) [W]
3.0E-03
2.5E-03
2.0E-03
1.5E-03
1.0E-03
5.0E-04
0.0E+00
0
2000
4000
6000
8000
10000
12000
14000
16000
Gain (M)

Wafer		2	2	2	2
Cell		6, 8	6, 8	6, 6	6, 8
Diameter [um]		1500	1500	1500	1500
Guard Ring [um]		50	50	50	50
Pixel Dist [um]		0	0	0	0
Metal Ring		Y	Y	Y	Y
Illumination [%]		Dark	0.03 Io	0.33 Io	Io
Bias Voltage [V]	*-3.00*	-535.5	-573.2	-697.9	-1336
	-2.75	-436.5	-473.1	-777.5	-1110
	-2.50	-351.5	-382.8	-661	-900.8
	-2.25	-274.9	-303	-549.8	-706.9
	-2.00	-207.4	-232.5	-445.8	-540.5
	-1.75	-148.7	-170.6	-346.3	-400.9
	-1.50	-98.99	-117.6	-257	-286.8
	-1.25	-58.03	-72.86	-176.8	-196.1
	-1.00	-27.03	-37.69	-110.6	-125.5
	-0.75	-7.197	-13.53	-58.94	-69.58
	-0.50	-0.1097	-0.8969	-23.24	-30.07
	-0.25	-0.03668	-0.03785	-3.783	-6.599
	0.00	0.01462	0.01709	-0.01475	-0.08139
	0.25	-0.00971	-0.01285	0.002555	0.04026
	0.50	0.00502	-0.00071	-0.01521	-0.0094

MEASUREMENTS ARE DONE AT 600nm.

Wafer		2	2	2	2
Cell		6, 8	6, 8	6, 8	6, 8
Diameter [um]		1500	1500	1500	1500
Guard Ring [um]		50	50	50	50
Pixel Dist [um]		0	0	0	0
Metal Ring		Y	Y	Y	Y
Illumination [%]		Dark	0.03 Io	0.33 Io	Io
Bias Voltage [V]	*-3.00*	-535.5	-573.2	-897.9	-1336
	-1.472	0.16816	-17.5299	-186.189	-46.5192
	-1.423		0.12772	-163.437	-5.4278
	-1.417			-160.651	-0.3962
	-1.071			0.00328	

Curve Fit	a					
	b					
	c					
	d					
2nd Derivative	a					
	b					
Max Gradient	Vbr					
Threshold	Vbr					
Linear Trend	Vbr		-1.472	-1.423	-1.071	-1.417
Voltage Breakdown	Vbr		-1.346	-1.34575	-1.34575	-1.34575

q =	1.60E-19	[C]
h =	6.63E-34	[J s]
c =	3.00E+08	[m/s]
wavel =	6.00E-07	[m]
v =	5.00E+14	[Hz]
Po @ 600r	4.86E-07	[W]
w =	**2.69E-06**	**[m]**
R @ 600nr	0.3538	[%]
a @ 600nr	3.75E+05	[1/m]
Ip =	9.65E-08	[A]

QE = 0.4104

Vbias [V]	Idark [A]	I [A]	*Inorm [A]*	*M*	*R @ 1 [A/V*	*NEP [W]*
-3.00	**-5.36E-04**	**-1.34E-03**	*9.65E-08*	*13841.73*	*0.1986*	*2.70E-03*
-2.75	**-4.37E-04**	**-1.11E-03**	*9.65E-08*	*11500.24*	*0.1986*	*2.20E-03*
-2.50	**-3.52E-04**	**-9.01E-04**	*9.65E-08*	*9332.807*	*0.1986*	*1.77E-03*
-2.25	**-2.75E-04**	**-7.07E-04**	*9.65E-08*	*7323.891*	*0.1986*	*1.38E-03*
-2.00	**-2.07E-04**	**-5.41E-04**	*9.65E-08*	*5599.892*	*0.1986*	*1.04E-03*
-1.75	**-1.49E-04**	**-4.01E-04**	*9.65E-08*	*4153.555*	*0.1986*	*7.49E-04*
-1.50	**-9.90E-05**	**-2.89E-04**	*9.65E-08*	*2992.134*	*0.1986*	*4.98E-04*
-1.25	**-5.80E-05**	**-1.98E-04**	*9.65E-08*	*2052.43*	*0.1986*	*2.92E-04*
-1.00	**-2.70E-05**	**-1.26E-04**	*9.65E-08*	*1300.252*	*0.1986*	*1.36E-04*
-0.75	**-7.20E-06**	**-6.96E-05**	*9.65E-08*	*720.8889*	*0.1986*	*3.62E-05*
-0.50	**-1.10E-07**	**-3.01E-05**	*9.65E-08*	*311.5425*	*0.1986*	*5.52E-07*
-0.25	**-3.67E-08**	**-6.60E-06**	*9.65E-08*	*68.36944*	*0.1986*	*1.85E-07*
0.00	**1.48E-08**	**-8.14E-08**	*9.65E-08*	*0.843247*	*0.1986*	*-7.46E-08*
0.25	**-9.71E-09**	**4.03E-08**	*9.65E-08*	*-0.417117*	*0.1986*	*4.89E-08*
0.50	**5.02E-09**	**-9.40E-09**	*9.65E-08*	*0.097389*	*0.1986*	*-2.53E-08*

q = 1.60E-19 [C]
h = 6.63E-34 [J s]
c = 3.00E+08 [m/s]

MEASUREMENTS ARE DONE AT -2V BIAS, FULL Io.

dark [A] = -2.07E-04

wavel [m]	wavel [nm]	R [%]	a [1/m]	w [m]	Po [W]	v [Hz]	Ip [A]	QE	I [A]	I [uA]	M	Responsiti	NEP [W]
4.00E-07	400	0.4888	8.98E+06	**2.69E-09**	1.73E-07	7.49E+14	2.85E-08	0.5112	**5.15E-04**	514.700	18039.46	0.1649	-1.26E-03
5.00E-07	500	0.3873	8.89E+05	**2.69E-09**	5.22E-07	6.00E+14	1.17E-07	0.5565	**5.25E-04**	525.200	4482.79	0.2244	-9.24E-04
6.00E-07	600	0.3538	3.75E+05	**2.69E-09**	4.86E-07	5.00E+14	9.65E-08	0.4104	**5.37E-04**	537.000	5563.63	0.1986	-1.04E-03
7.00E-07	700	0.3376	1.62E+05	**2.69E-09**	4.20E-08	4.28E+14	5.55E-09	0.2339	**5.24E-04**	523.900	94473.31	0.1320	-1.57E-03
8.00E-07	800	0.3278	6.40E+04	**2.69E-09**	1.60E-08	3.75E+14	1.1E-09	0.1062	**5.13E-04**	513.100	467780.21	0.0686	-3.03E-03

R @ 1.0QE	R @ 0.9QE	R @ 0.8QE	R @ 0.7QE	R @ 0.6QE	R @ 0.5QE	R @ 0.4QE	R @ 0.3QE	R @ 0.2QE	R @ 0.1QE
0.3226	0.2904	0.2581	0.2258	0.1936	0.1613	0.1290	0.0968	0.0645	0.0323
0.4033	0.3629	0.3226	0.2823	0.2420	0.2016	0.1613	0.1210	0.0807	0.0403
0.4839	0.4355	0.3871	0.3388	0.2904	0.2420	0.1936	0.1452	0.0968	0.0464
0.5646	0.5081	0.4517	0.3952	0.3388	0.2823	0.2258	0.1694	0.1129	0.0565
0.6452	0.5807	0.5162	0.4517	0.3871	0.3226	0.2581	0.1936	0.1290	0.0645

Cell:	**W3 C11,10 D200,20,300,Y**
Breakdown Voltage:	-0.451 [V]
Dark Current (@ Vbr):	-3.4 [uA]
Gain (@ Vbr):	1332
Responsitivity (@ 600nm, 2V Bias):	0.199 [A/W]
NEP (@ Vbr):	1.7E-05 [W]

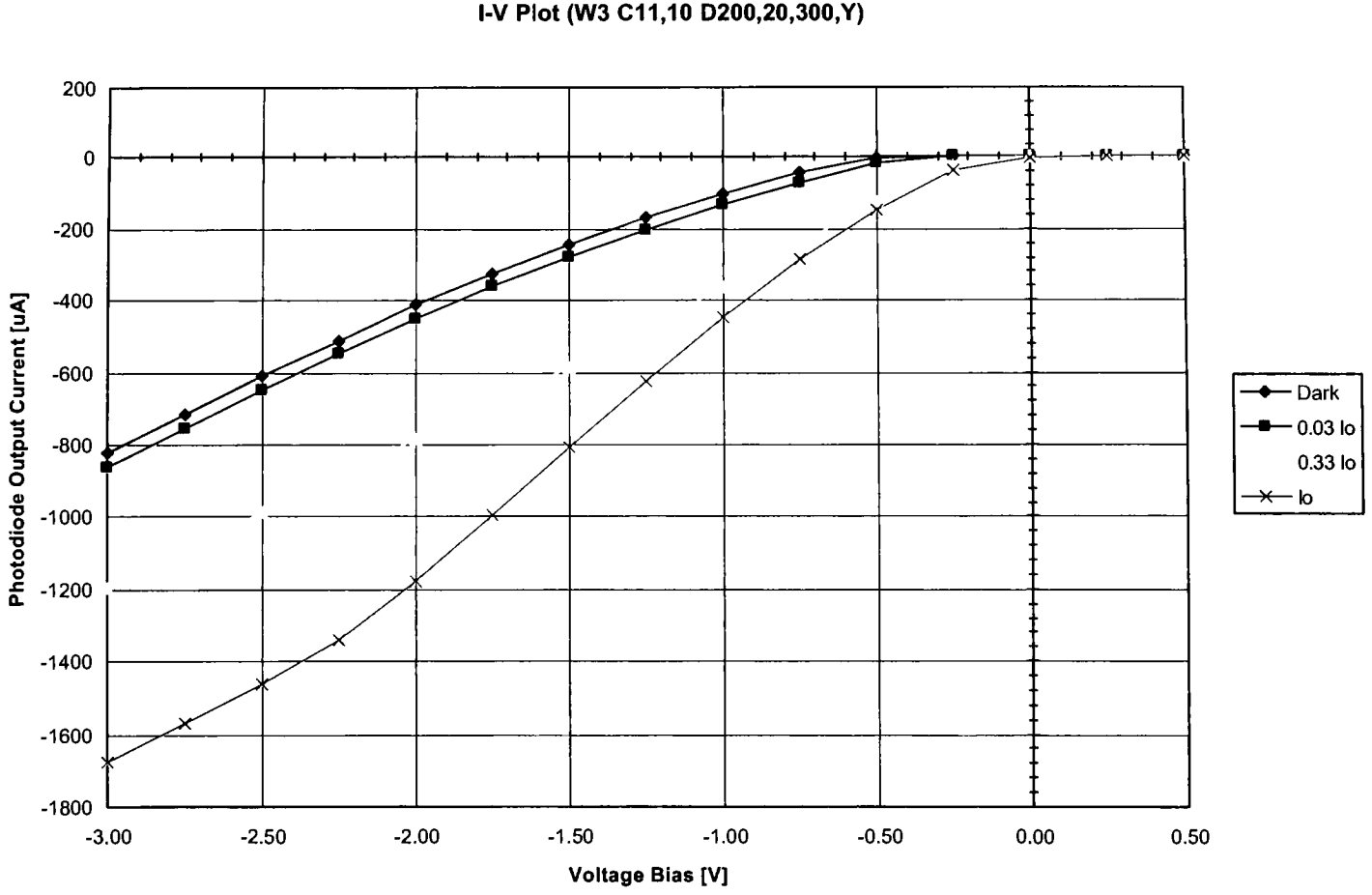
I-V Plot (W3 C11,10 D200,20,300,Y)
200
0
-200
-400
-600
-800
-1000
-1200
-1400
-1600
-1800
Photodiode Output Current [uA]
-3.00
-2.50
-2.00
-1.50
-1.00
-0.50
0.00
0.50
Voltage Bias [V]
Dark
0.03 Io
0.33 Io
Io

I-V Plot with Breakdown Voltage Interpolation Lines (W3 C11,10 D200,20,300,Y)

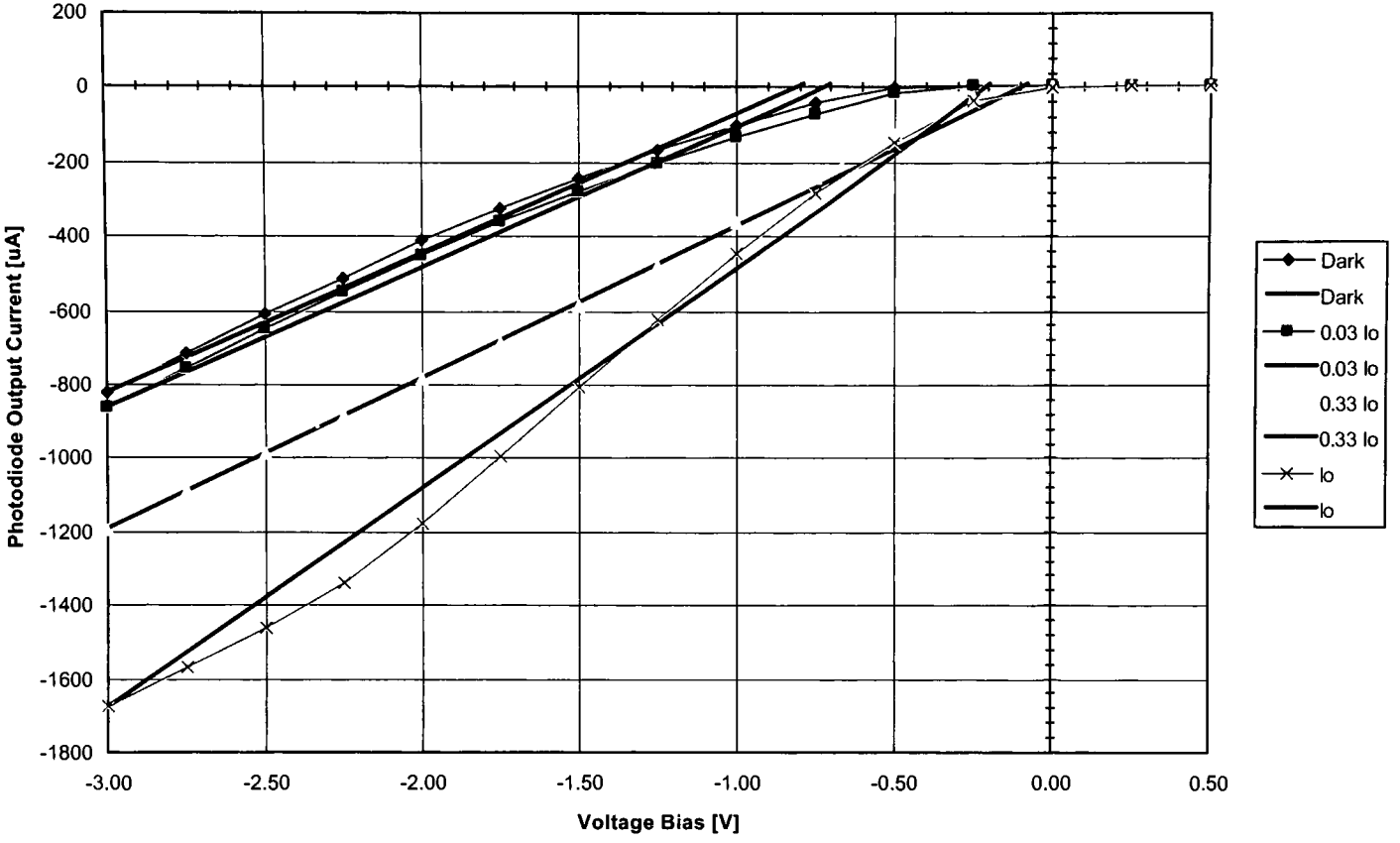

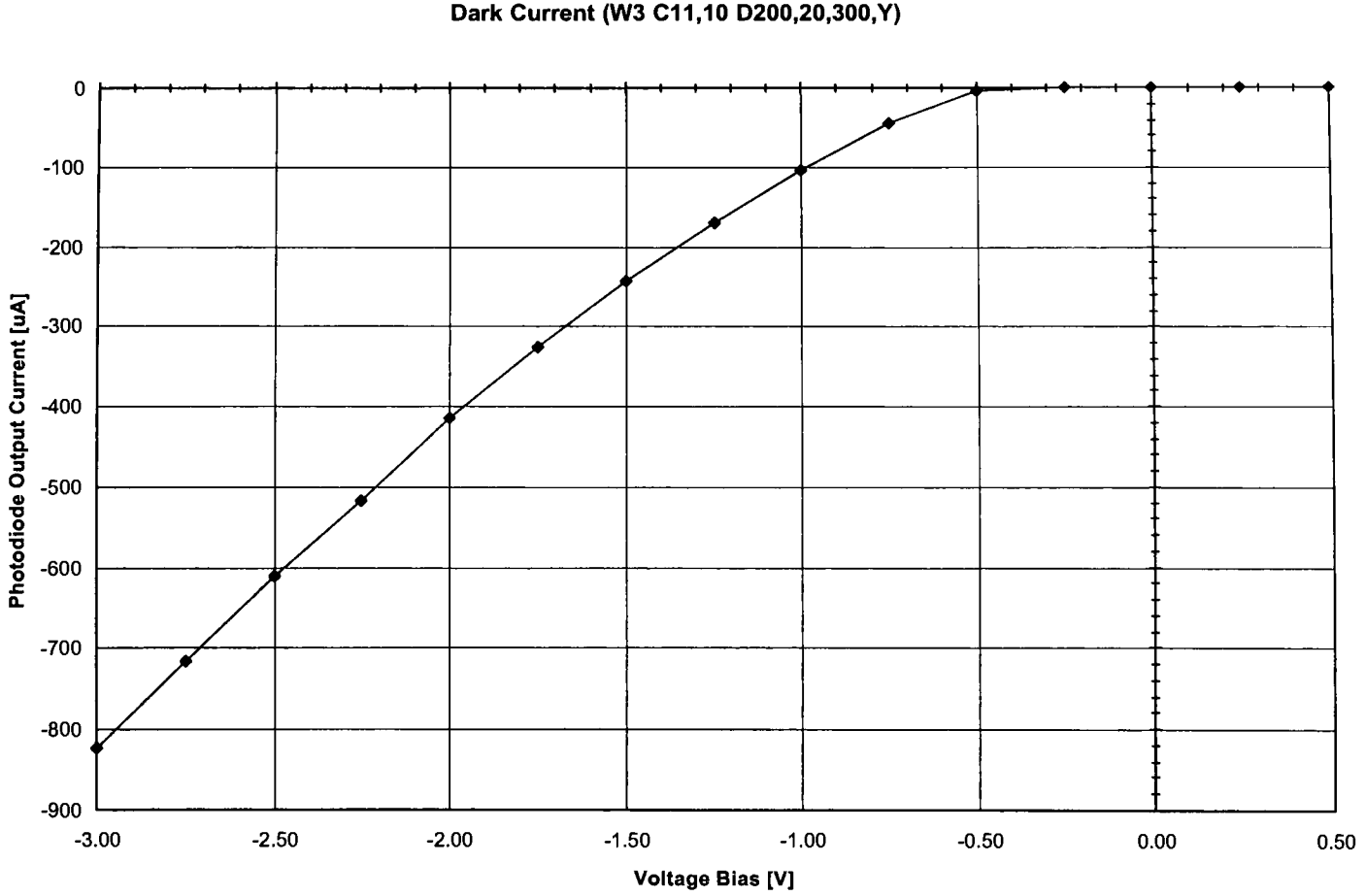
Dark Current (W3 C11,10 D200,20,300,Y)
Photodiode Output Current [uA]
0
-100
-200
-300
-400
-500
-600
-700
-800
-900
-3.00
-2.50
-2.00
-1.50
-1.00
-0.50
0.00
0.50
Voltage Bias [V]

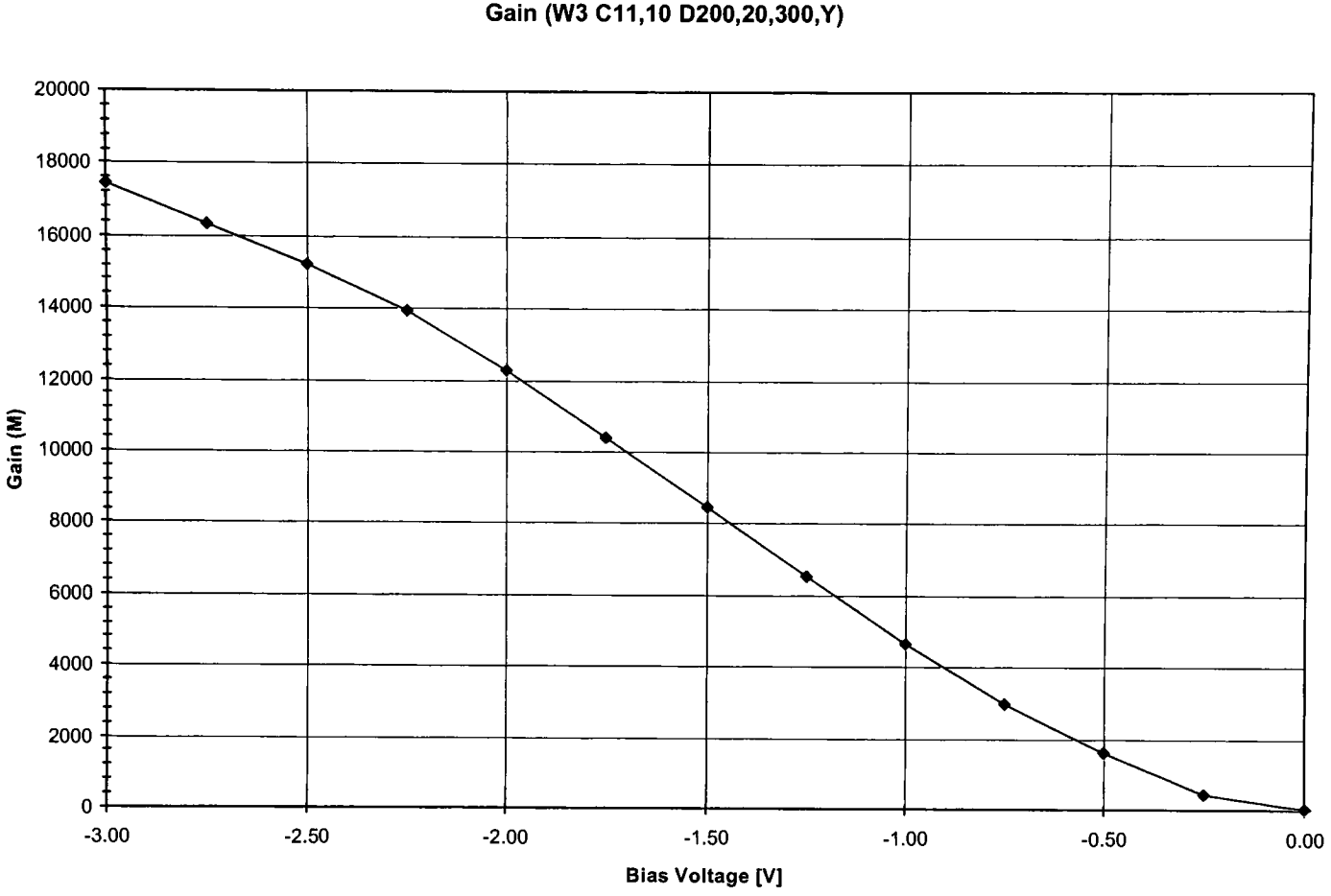
Gain (W3 C11,10 D200,20,300,Y)
20000
18000
16000
14000
12000
10000
8000
6000
4000
2000
0
Gain (M)
-3.00
-2.50
-2.00
-1.50
-1.00
-0.50
0.00
Bias Voltage [V]

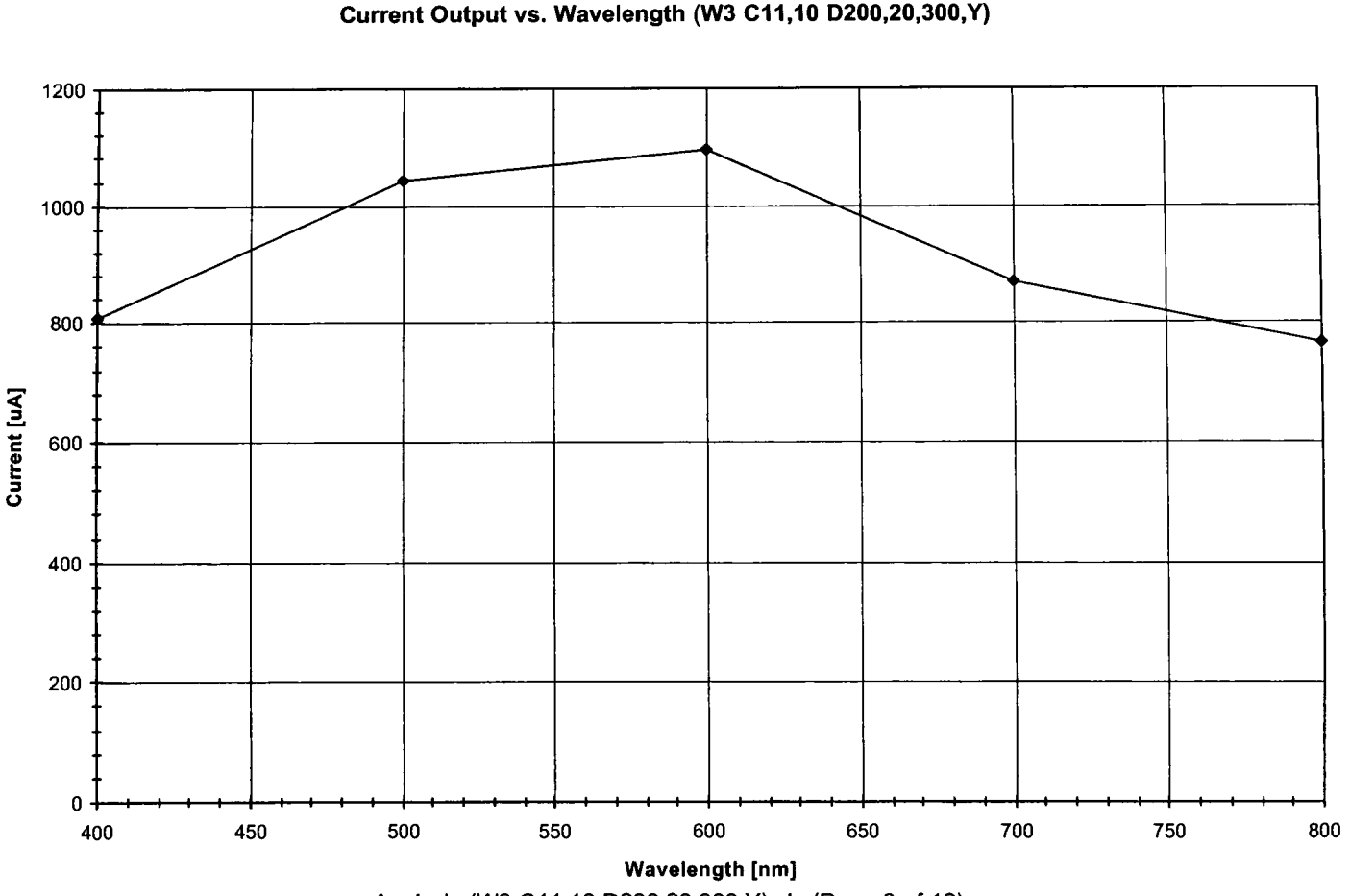
Current Output vs. Wavelength (W3 C11,10 D200,20,300,Y)
Current [uA]
1200
1000
800
600
400
200
0
400
450
500
550
600
650
700
750
800
Wavelength [nm]

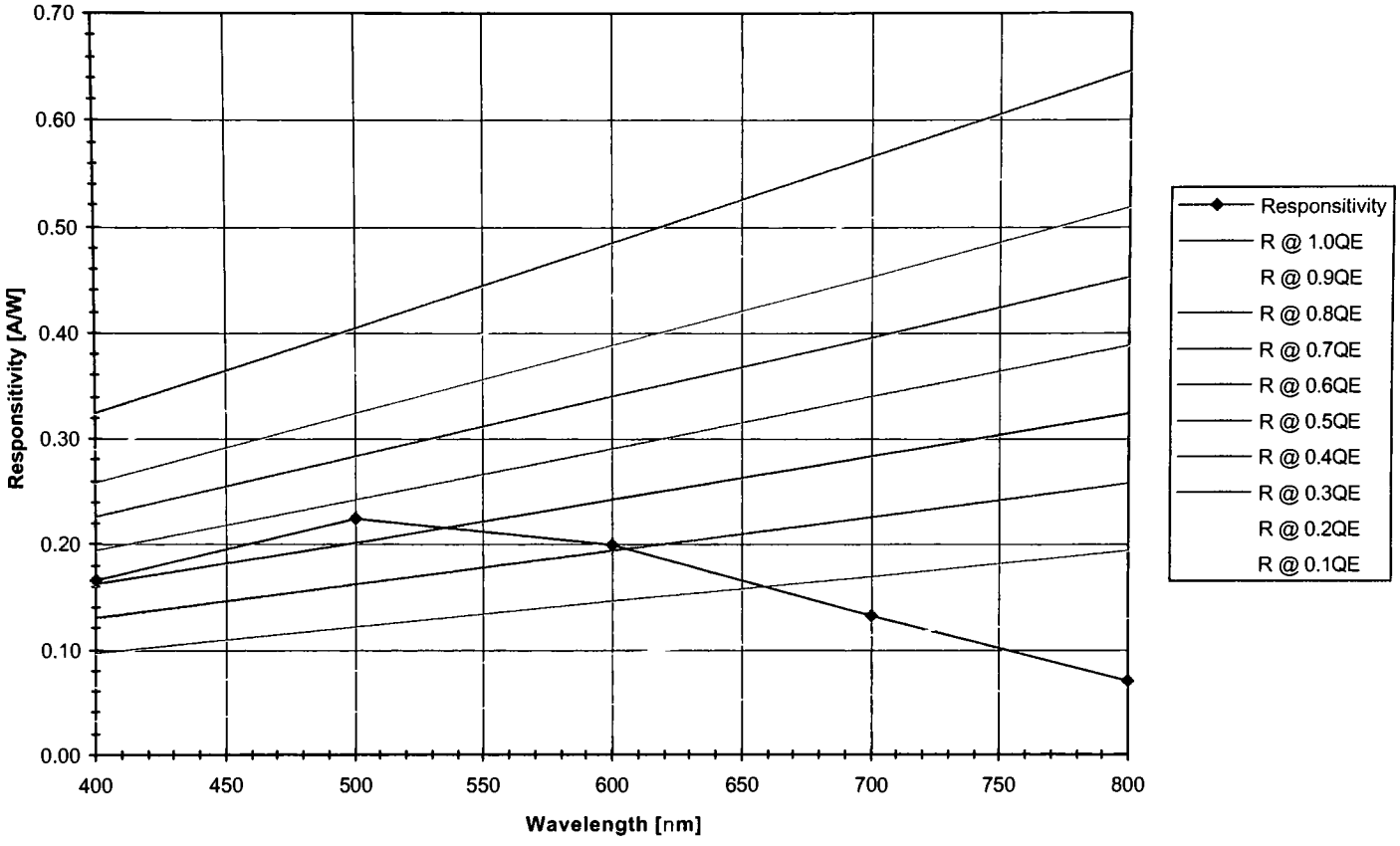
Responsitivity @ M=1 (W3 C11,10 D200,20,300,Y)
0.70
0.60
0.50
0.40
0.30
0.20
0.10
0.00
Responsitivity [A/W]
400
450
500
550
600
650
700
750
800
Wavelength [nm]
Responsitivity
R @ 1.0QE
R @ 0.9QE
R @ 0.8QE
R @ 0.7QE
R @ 0.6QE
R @ 0.5QE
R @ 0.4QE
R @ 0.3QE
R @ 0.2QE
R @ 0.1QE

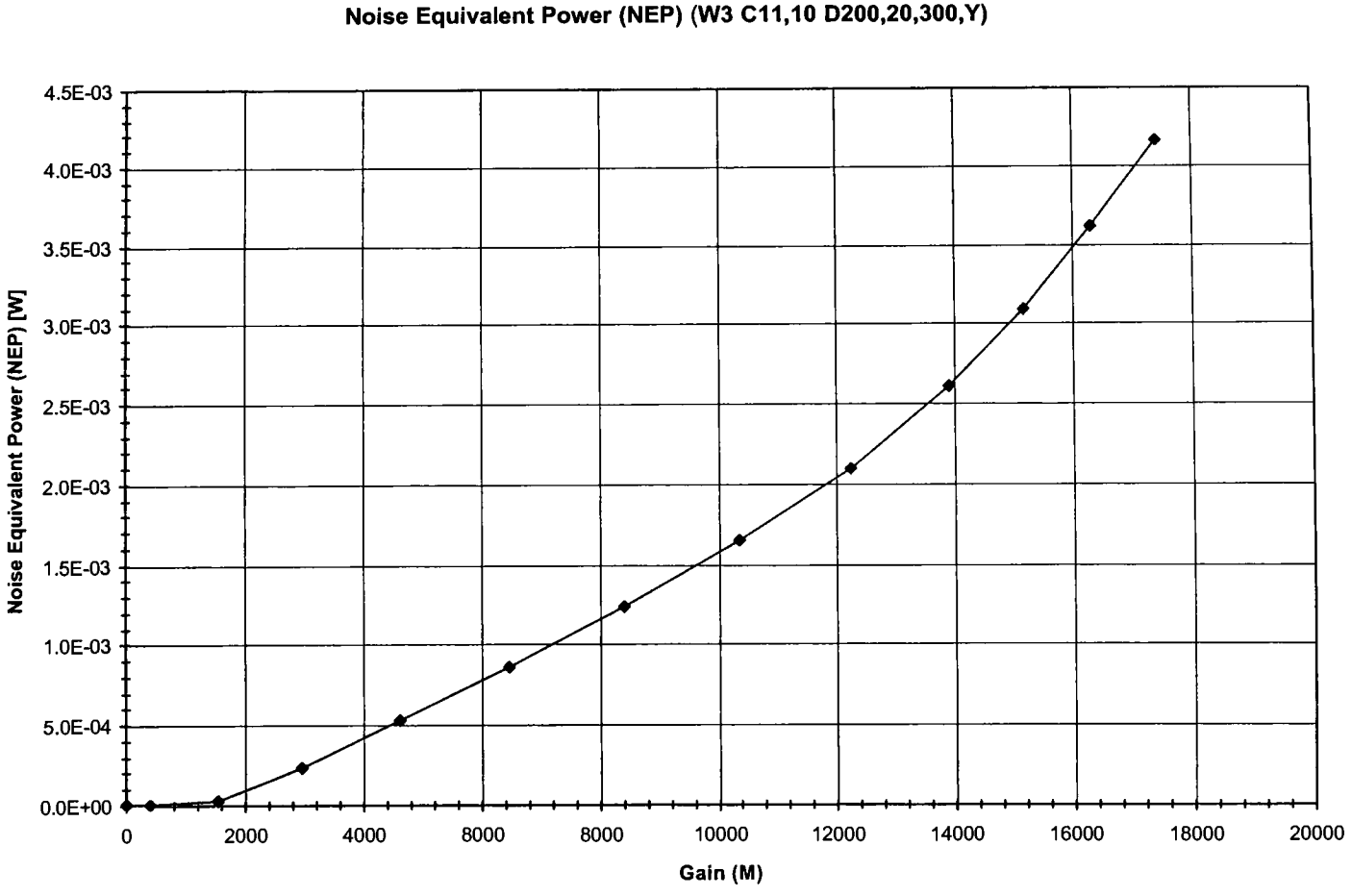
Noise Equivalent Power (NEP) (W3 C11,10 D200,20,300,Y)
Noise Equivalent Power (NEP) [W]
4.5E-03
4.0E-03
3.5E-03
3.0E-03
2.5E-03
2.0E-03
1.5E-03
1.0E-03
5.0E-04
0.0E+00
0
2000
4000
8000
8000
10000
12000
14000
16000
18000
20000
Gain (M)

Wafer		3	3	3	3
Cell		11, 10	11, 10	11, 10	11, 10
Diameter [um]		200	200	200	200
Guard Ring [um]		20	20	20	20
Pixel Dist [um]		300	300	300	300
Metal Ring		Y	Y	Y	Y
Illumination [%]		Dark	0.03 Io	0.33 Io	Io
Bias Voltage [V]	*-3.00*	-824.7	-866.9	-1198	-1680
	-2.75	-716.3	-758.8	-1091	-1573
	-2.50	-612.1	-654.1	-988.3	-1464
	-2.25	-517.5	-553.3	-885.2	-1341
	-2.00	-415.8	-456.4	-785.6	-1182
	-1.75	-326.1	-364.9	-886.9	-999.6
	-1.50	-244.6	-280.4	-588.3	-811.3
	-1.25	-171.2	-203.8	-482.2	-625.3
	-1.00	-104.3	-134.8	-364.4	-447.5
	-0.75	-45.56	-72.41	-241.5	-286.4
	-0.50	-4.207	-17.01	-125.3	-150.1
	-0.25	-0.01828	-0.1875	-28.68	-39.98
	0.00	-0.03134	-0.05289	-0.308	-0.5741
	0.25	-0.05291	-0.04969	0.03914	0.04519
	0.50	-0.02875	0.02043	-0.05212	-0.04989

MEASUREMENTS ARE DONE AT 600nm.

Wafer		3	3	3	3
Cell		11, 10	11, 10	11, 10	11, 10
Diameter [um]		200	200	200	200
Guard Ring [um]		20	20	20	20
Pixel Dist [um]		300	300	300	300
Metal Ring		Y	Y	Y	Y
Illumination [%]		Dark	0.03 Io	0.33 Io	Io
Bias Voltage [V]	*-3.00*	-824.7	-866.9	-1198	-1680
	-0.796	-0.04044	-31.0136	-291.177	-368.75
	-0.712		-0.05032	-256.685	-315.999
	-0.209			-50.1485	-0.11991
	-0.087			-0.05407	

Curve Fit	a					
	b					
	c					
	d					
2nd Derivative	a					
	b					
Max Gradient	Vbr					
Threshold	Vbr					
Linear Trend	Vbr		-0.796	-0.712	-0.087	-0.209
Voltage Breakdown	Vbr		-0.451	-0.451	-0.451	-0.451

q =	1.60E-19	[C]
h =	6.63E-34	[J s]
c =	3.00E+08	[m/s]
wavel =	6.00E-07	[m]
v =	5.00E+14	[Hz]
Po @ 600r	4.86E-07	[W]
w =	**2.69E-06**	**[m]**
R @ 600nr	0.3538	[%]
a @ 600nr	3.75E+05	[1/m]
Ip =	9.65E-08	[A]

QE = 0.4104

Vbias [V]	Idark [A]	I [A]	*Inorm [A]*	*M*	*R @ 1 [A/V*	*NEP [W]*
-3.00	-8.25E-04	-1.68E-03	*9.65E-08*	*17405.77*	*0.1986*	*4.15E-03*
-2.75	-7.16E-04	-1.57E-03	*9.65E-08*	*16297.19*	*0.1986*	*3.61E-03*
-2.50	-6.12E-04	-1.46E-03	*9.65E-08*	*15167.88*	*0.1986*	*3.08E-03*
-2.25	-5.18E-04	-1.34E-03	*9.65E-08*	*13893.53*	*0.1986*	*2.61E-03*
-2.00	-4.16E-04	-1.18E-03	*9.65E-08*	*12246.2*	*0.1986*	*2.09E-03*
-1.75	-3.26E-04	-1.00E-03	*9.65E-08*	*10356.43*	*0.1986*	*1.64E-03*
-1.50	-2.45E-04	-8.11E-04	*9.65E-08*	*8405.536*	*0.1986*	*1.23E-03*
-1.25	-1.71E-04	-6.25E-04	*9.65E-08*	*6478.468*	*0.1986*	*8.62E-04*
-1.00	-1.04E-04	-4.48E-04	*9.65E-08*	*4636.358*	*0.1986*	*5.25E-04*
-0.75	-4.56E-05	-2.86E-04	*9.65E-08*	*2967.269*	*0.1986*	*2.29E-04*
-0.50	-4.21E-06	-1.50E-04	*9.65E-08*	*1555.123*	*0.1986*	*2.12E-05*
-0.25	-1.83E-08	-4.00E-05	*9.65E-08*	*414.2158*	*0.1986*	*9.20E-08*
0.00	-3.13E-08	-5.74E-07	*9.65E-08*	*5.948007*	*0.1986*	*1.58E-07*
0.25	-5.29E-08	4.52E-08	*9.65E-08*	*-0.468194*	*0.1986*	*2.66E-07*
0.50	-2.88E-08	-4.99E-08	*9.65E-08*	*0.516889*	*0.1986*	*1.45E-07*

q = 1.60E-19 [C]
h = 6.83E-34 [J s]
c = 3.00E+08 [m/s]

MEASUREMENTS ARE DONE AT -2V BIAS, FULL Io.

dark [A] = -4.16E-04

wavel [m]	*wavel [nm]*	R [%]	a [1/m]	w [m]	Po [W]	*v [Hz]*	*Ip [A]*	*QE*	I [A]	*I [uA]*	*M*	*Responsiti*	*NEP [W]*
4.00E-07	*400*	*0.4888*	*8.98E+06*	**2.69E-09**	1.73E-07	*7.49E+14*	*2.85E-08*	*0.5112*	**8.06E-04**	*805.966*	*26247.96*	*0.1649*	*-2.52E-03*
5.00E-07	*500*	*0.3873*	*8.89E+05*	**2.69E-09**	*5.22E-07*	*6.00E+14*	*1.17E-07*	*0.5565*	**1.04E-03**	*1040.496*	*8881.04*	*0.2244*	*-1.85E-03*
6.00E-07	*600*	*0.3538*	*3.75E+05*	**2.69E-09**	*4.86E-07*	*5.00E+14*	*9.65E-08*	*0.4104*	***1.09E-03***	*1092.720*	*11321.21*	*0.1986*	*-2.09E-03*
7.00E-07	*700*	*0.3376*	*1.62E+05*	**2.69E-09**	*4.20E-08*	*4.28E+14*	*5.55E-09*	*0.2339*	**8.67E-04**	*867.120*	*156365.14*	*0.1320*	*-3.15E-03*
8.00E-07	*800*	*0.3278*	*6.40E+04*	**2.69E-09**	*1.60E-08*	*3.75E+14*	*1.1E-09*	*0.1062*	**7.65E-04**	*764.592*	*697059.07*	*0.0686*	*-6.07E-03*

R @ 1.0QI	*R @ 0.9QI*	*R @ 0.8QI*	*R @ 0.7QI*	*R @ 0.6QI*	*R @ 0.5QI*	*R @ 0.4QI*	*R @ 0.3QI*	*R @ 0.2QI*	*R @ 0.1QE*
0.3226	*0.2904*	*0.2581*	*0.2258*	*0.1936*	*0.1613*	*0.1290*	*0.0968*	*0.0645*	*0.0323*
0.4033	*0.3629*	*0.3226*	*0.2823*	*0.2420*	*0.2016*	*0.1613*	*0.1210*	*0.0807*	*0.0403*
0.4839	*0.4355*	*0.3871*	*0.3388*	*0.2904*	*0.2420*	*0.1936*	*0.1452*	*0.0968*	*0.0484*
0.5646	*0.5081*	*0.4517*	*0.3952*	*0.3388*	*0.2823*	*0.2258*	*0.1694*	*0.1129*	*0.0565*
0.6452	*0.5807*	*0.5162*	*0.4517*	*0.3871*	*0.3226*	*0.2581*	*0.1936*	*0.1290*	*0.0645*

Cell:	**W4 C7,3 D200,20,300,Y**
Breakdown Voltage:	-7.624 [V]
Dark Current (@ Vbr):	-2484 [uA]
Gain (@ Vbr):	22677
Responsitivity (@ 600nm):	0.2801 [A/W]
NEP (@ Vbr):	0.00887 [W]

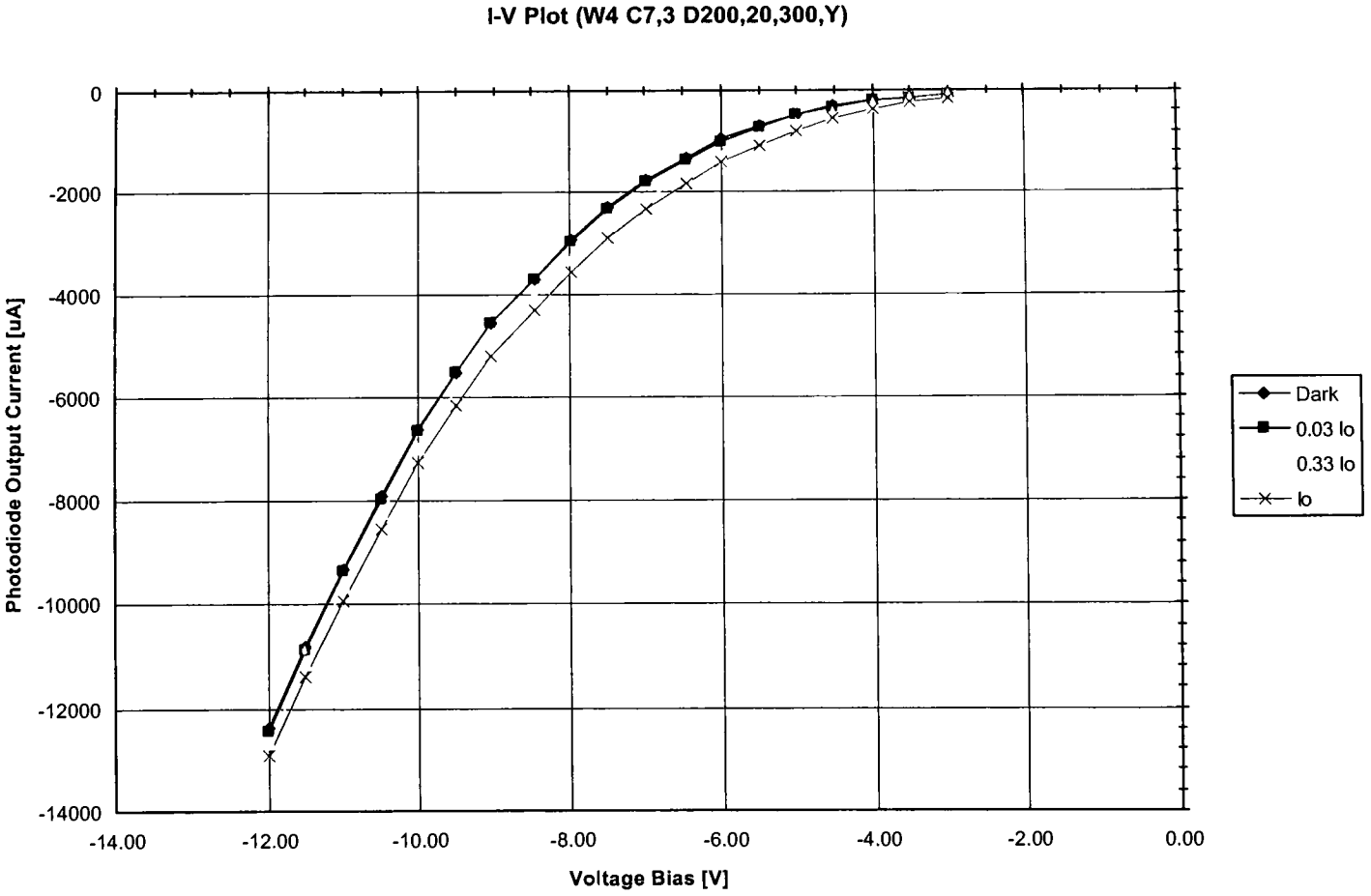
I-V Plot (W4 C7,3 D200,20,300,Y)
Photodiode Output Current [uA]
0
-2000
-4000
-6000
-8000
-10000
-12000
-14000
-14.00
-12.00
-10.00
-8.00
-6.00
-4.00
-2.00
0.00
Voltage Bias [V]
Dark
0.03 Io
0.33 Io
Io

I-V Plot with Breakdown Voltage Interpolation Lines (W4 C7,3 D200,20,300,Y)

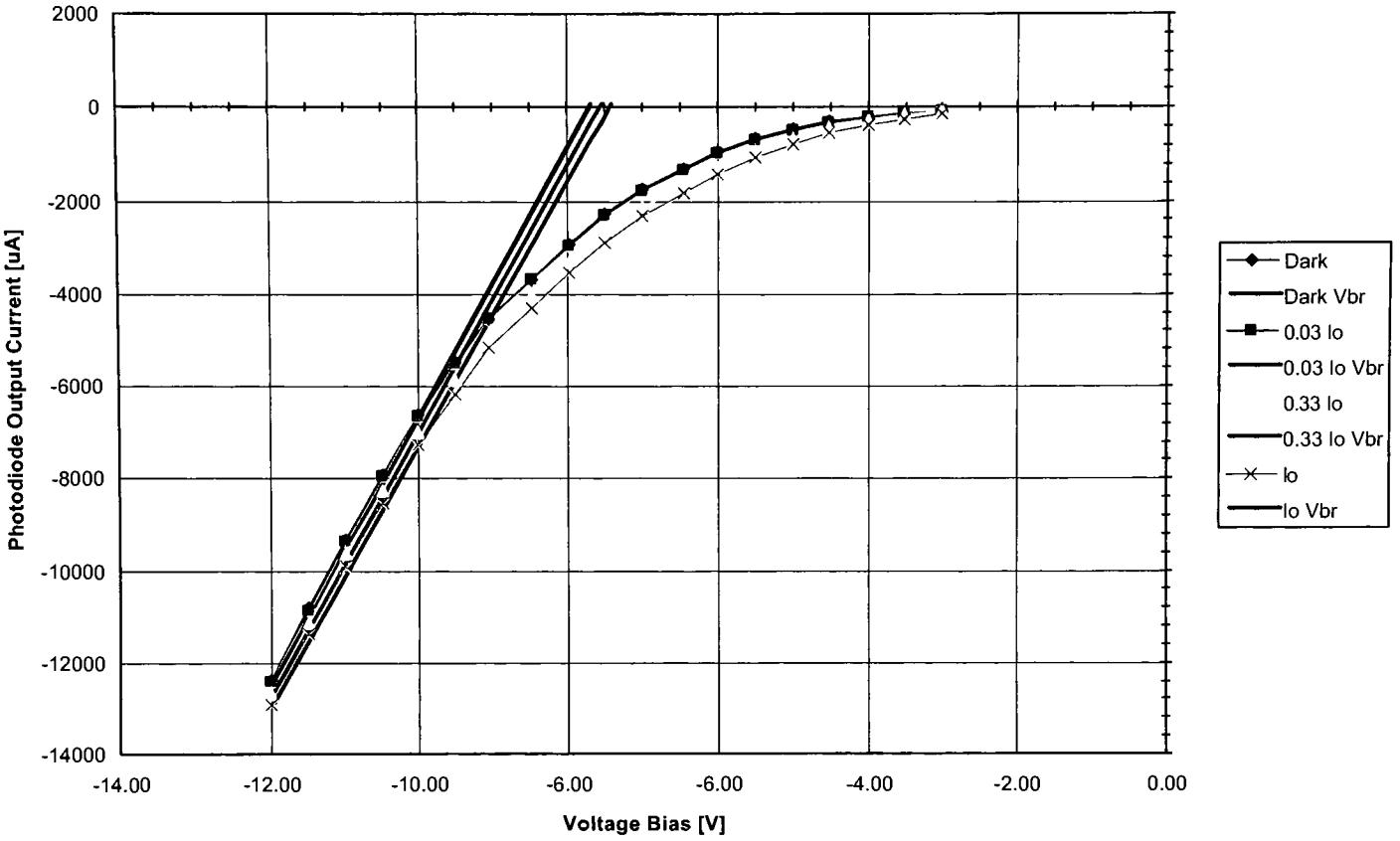

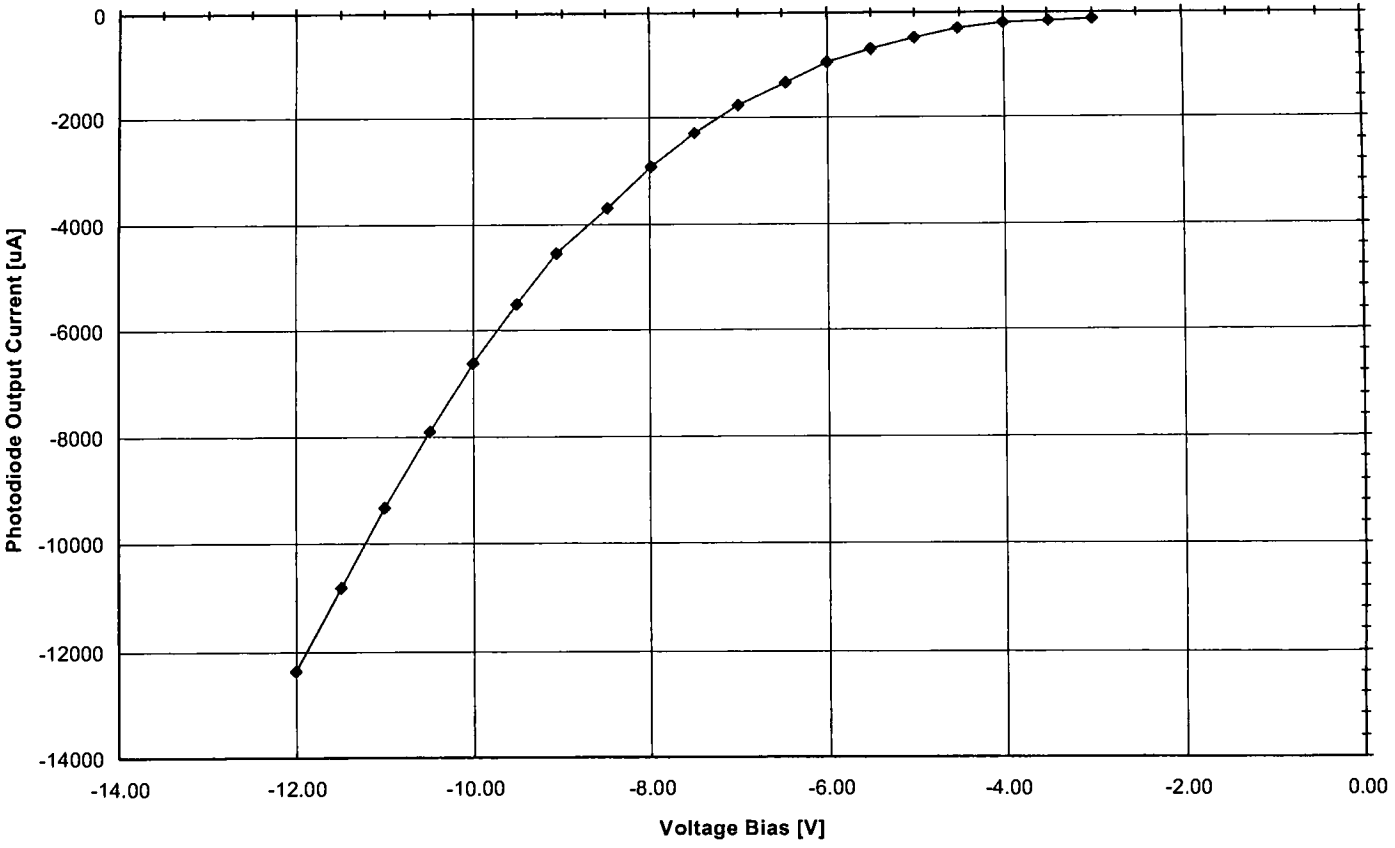
Dark Current (W4 C7,3 D200,20,300,Y)
Photodiode Output Current [uA]
0
-2000
-4000
-6000
-8000
-10000
-12000
-14000
-14.00
-12.00
-10.00
-8.00
-6.00
-4.00
-2.00
0.00
Voltage Bias [V]

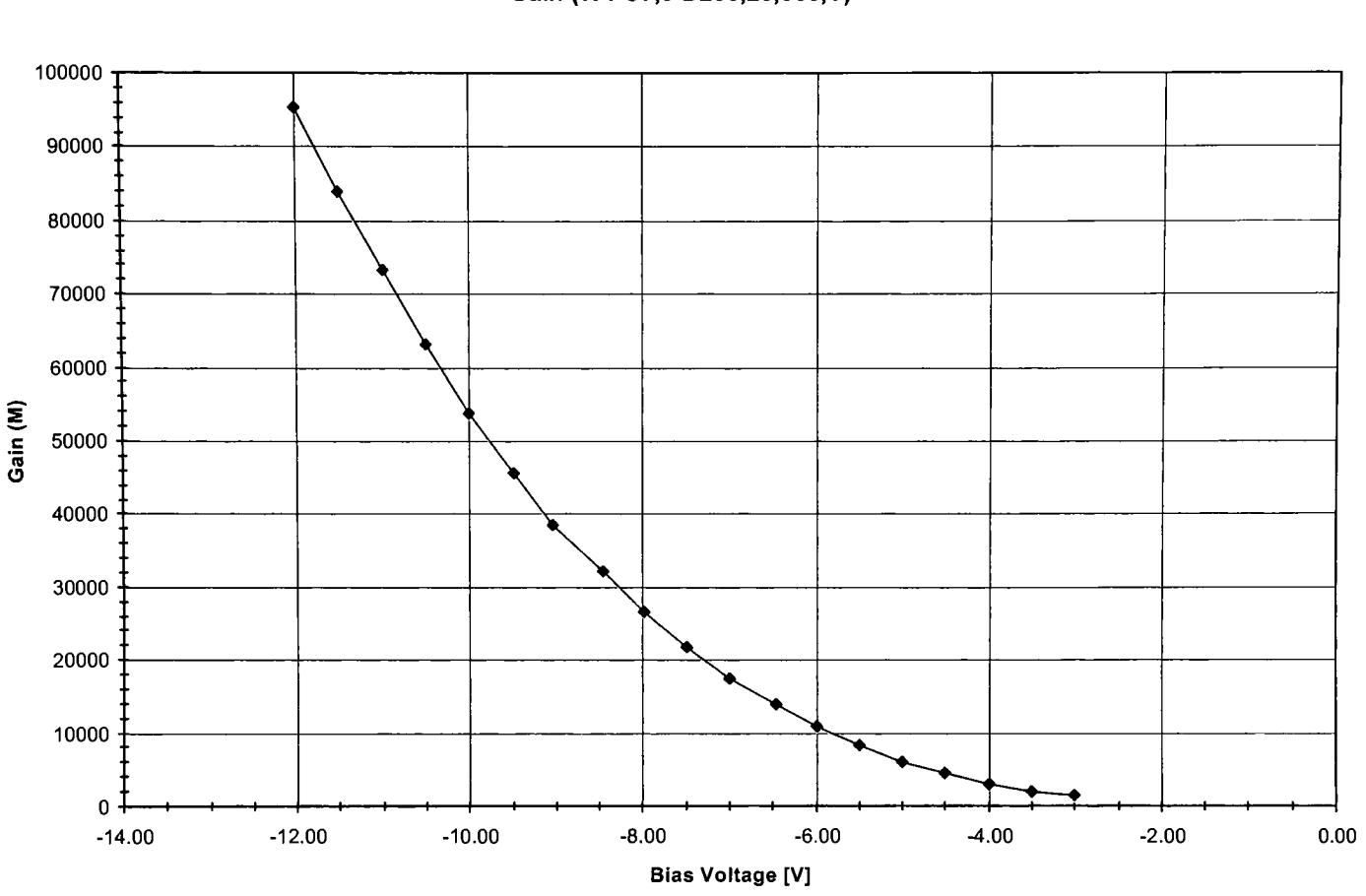
Gain (W4 C7,3 D200,20,300,Y)
100000
90000
80000
70000
60000
50000
40000
30000
20000
10000
0
Gain (M)
-14.00
-12.00
-10.00
-8.00
-6.00
-4.00
-2.00
0.00
Bias Voltage [V]

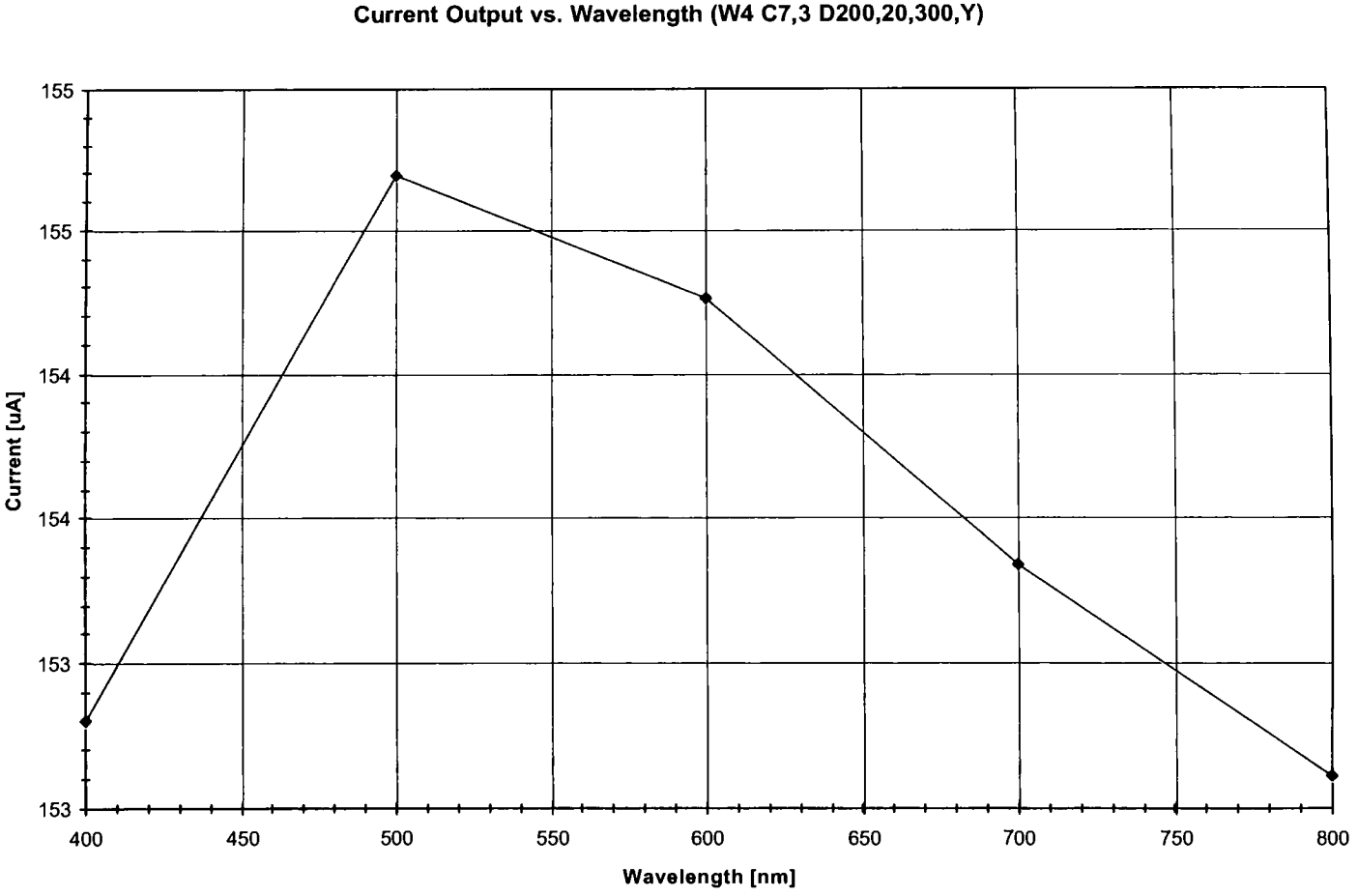
Current Output vs. Wavelength (W4 C7,3 D200,20,300,Y)
155
155
154
154
153
153
Current [uA]
400
450
500
550
600
650
700
750
800
Wavelength [nm]

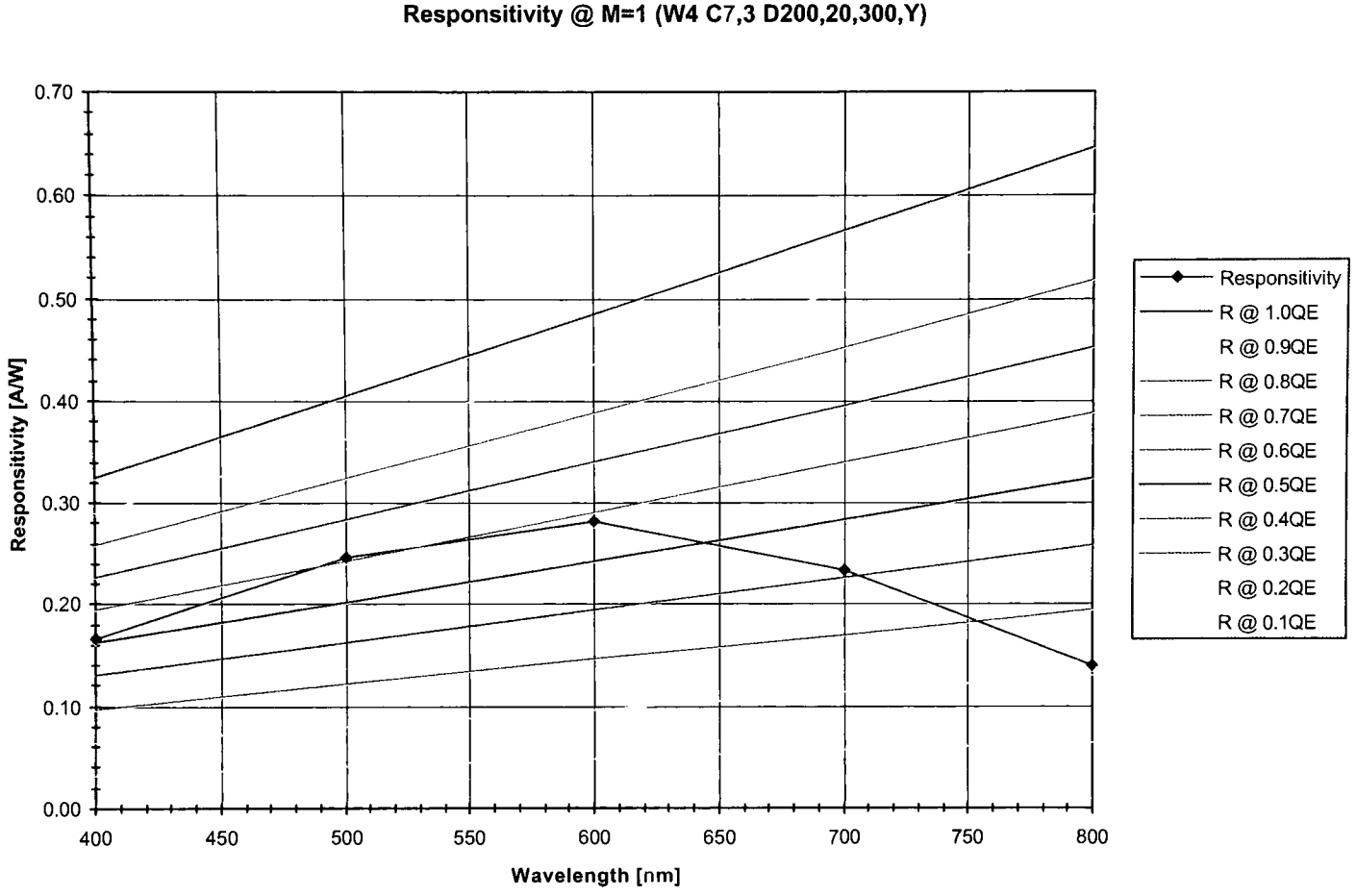
Responsitivity @ M=1 (W4 C7,3 D200,20,300,Y)
0.70
0.60
0.50
0.40
0.30
0.20
0.10
0.00
Responsitivity [A/W]
400
450
500
550
600
650
700
750
800
Wavelength [nm]
Responsitivity
R @ 1.0QE
R @ 0.9QE
R @ 0.8QE
R @ 0.7QE
R @ 0.6QE
R @ 0.5QE
R @ 0.4QE
R @ 0.3QE
R @ 0.2QE
R @ 0.1QE

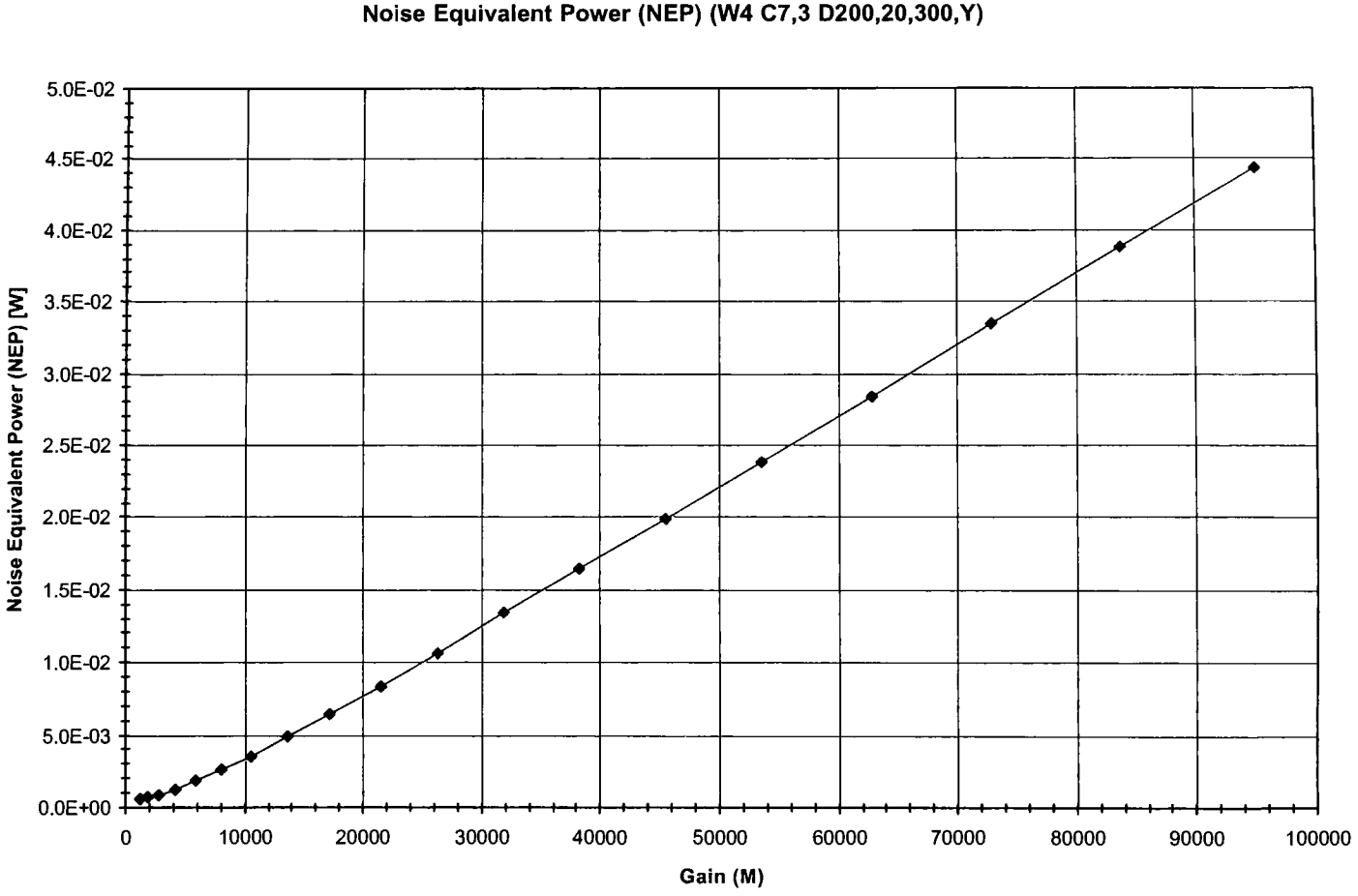
Noise Equivalent Power (NEP) (W4 C7,3 D200,20,300,Y)
Noise Equivalent Power (NEP) [W]
5.0E-02
4.5E-02
4.0E-02
3.5E-02
3.0E-02
2.5E-02
2.0E-02
1.5E-02
1.0E-02
5.0E-03
0.0E+00
0
10000
20000
30000
40000
50000
60000
70000
80000
90000
100000
Gain (M)

Wafer		4	4	4	4
Cell		7, 3	7, 3	7, 3	7, 3
Diameter [um]		200	200	200	200
Guard Ring [um]		20	20	20	20
Pixel Dist [um]		300	300	300	300
Metal Ring		Y	Y	Y	Y
Illumination [%]		Dark	0.03 Io	0.33 Io	Io
Bias Voltage [V]	*-12.00*	-12410	-12460	-12700	-12940
	-11.50	-10850	-10910	-11150	-11390
	-11.00	-9354	-9398	-9649	-9933
	-10.50	-7932	-7986	-8255	-8561
	-10.00	-6654	-6685	-7003	-7287
	-9.50	-5531	-5545	-5871	-6193
	-9.05	-4571	-4573	-4909	-5207
	-8.47	-3720	-3722	-4066	-4349
	-7.99	-2966	-3002	-3328	-3578
	-7.50	-2321	-2353	-2681	-2920
	-7.00	-1779	-1814	-2147	-2344
	-6.46	-1337	-1374	-1689	-1850
	-6.00	-977	-1014	-1303	-1438
	-5.50	-697.7	-733.7	-974.3	-1089
	-5.00	-483.6	-512.5	-712.8	-804.7
	-4.51	-320.7	-346.5	-497	-571.5
	-4.00	-222.8	-228.2	-329.4	-389.6
	-3.50	-170.4	-166.1	-209	-254.1
	-3.00	-126.5	-122	-130.4	-160.4

Wafer		4	4	4	4
Cell		7, 3	7, 3	7, 3	7, 3
Diameter [um]		200	200	200	200
Guard Ring [um]		30	30	30	30
Pixel Dist [um]		400	400	400	400
Metal Ring		N	N	N	N
Illumination [%]		Dark Vbr	0.03 Io Vbr	0.33 Io Vbr	Io Vbr
Bias Voltage [V]	*-12.00*	-12410	-12460	-12700	-12940
	-7.729	0.106	-18.9092	-403.936	-774.883
	-7.722		1.3544	-383.932	-755.094
	-7.588			-0.9864	-376.276
	-7.455				-0.285

Curve Fit	a				
	b				
	c				
	d				
2nd Derivative	a				
	b				
Max Gradient	Vbr				
Threshold	Vbr				
Linear Trend	Vbr	-7.729	-7.722	-7.588	-7.455
Voltage Breakdown	Vbr	-7.624	-7.624	-7.624	-7.624

q =	1.60E-19	[C]
h =	6.63E-34	[J s]
c =	3.00E+08	[m/s]
wavel =	6.00E-07	[m]
v =	5.00E+14	[Hz]
Po @ 600r	4.86E-07	[W]
w =	**6.02E-06**	**[m]**
R @ 600nr	0.3538	[%]
a @ 600nr	3.75E+05	[1/m]
Ip =	1.36E-07	[A]

QE = 0.5787

Vbias [V]	Idark [A]	I [A]	*Inorm [A]*	*M*	*R @ 1 [A/V*	*NEP [W]*
-12.00	-1.24E-02	-1.29E-02	*1.36E-07*	*95073.31*	*0.2801*	*4.43E-02*
-11.50	-1.09E-02	-1.14E-02	*1.36E-07*	*83685.09*	*0.2801*	*3.87E-02*
-11.00	-9.35E-03	-9.93E-03	*1.36E-07*	*72980.16*	*0.2801*	*3.34E-02*
-10.50	-7.93E-03	-8.56E-03	*1.36E-07*	*62899.74*	*0.2801*	*2.83E-02*
-10.00	-6.65E-03	-7.29E-03	*1.36E-07*	*53539.35*	*0.2801*	*2.38E-02*
-9.50	-5.53E-03	-6.19E-03	*1.36E-07*	*45501.47*	*0.2801*	*1.97E-02*
-9.05	-4.57E-03	-5.21E-03	*1.36E-07*	*38257.09*	*0.2801*	*1.63E-02*
-8.47	-3.72E-03	-4.35E-03	*1.36E-07*	*31953.16*	*0.2801*	*1.33E-02*
-7.99	-2.97E-03	-3.58E-03	*1.36E-07*	*26288.43*	*0.2801*	*1.06E-02*
-7.50	-2.32E-03	-2.92E-03	*1.36E-07*	*21453.95*	*0.2801*	*8.29E-03*
-7.00	-1.78E-03	-2.34E-03	*1.36E-07*	*17221.94*	*0.2801*	*6.35E-03*
-6.46	-1.34E-03	-1.85E-03	*1.36E-07*	*13592.4*	*0.2801*	*4.77E-03*
-6.00	-9.77E-04	-1.44E-03	*1.36E-07*	*10565.33*	*0.2801*	*3.49E-03*
-5.50	-6.98E-04	-1.09E-03	*1.36E-07*	*8001.147*	*0.2801*	*2.49E-03*
-5.00	-4.84E-04	-8.05E-04	*1.36E-07*	*5912.326*	*0.2801*	*1.73E-03*
-4.51	-3.21E-04	-5.72E-04	*1.36E-07*	*4198.949*	*0.2801*	*1.15E-03*
-4.00	-2.23E-04	-3.90E-04	*1.36E-07*	*2862.486*	*0.2801*	*7.96E-04*
-3.50	-1.70E-04	-2.54E-04	*1.36E-07*	*1866.934*	*0.2801*	*6.08E-04*
-3.00	-1.27E-04	-1.60E-04	*1.36E-07*	*1178.498*	*0.2801*	*4.52E-04*

q = 1.60E-19 [C]
h = 6.63E-34 [J s]
c = 3.00E+08 [m/s]

dark [A] = 2.48E-03

wavel [m]	wavel [nm]	R [%]	a [1/m]	w [m]	Po [W]	v [Hz]	Ip [A]	QE	I [A]	I [uA]	M	Responsiti	NEP [W]
4.00E-07	400	0.4888	8.98E+06	6.02E-09	1.73E-07	7.49E+14	2.85E-08	0.5112	1.53E-04	152.800	5355.41	0.1649	1.51E-02
5.00E-07	500	0.3873	8.89E+05	6.02E-09	5.22E-07	6.00E+14	1.28E-07	0.6098	1.55E-04	154.690	1205.03	0.2459	1.01E-02
6.00E-07	600	0.3538	3.75E+05	6.02E-09	4.86E-07	5.00E+14	1.36E-07	0.5787	1.54E-04	154.260	1133.39	0.2801	8.87E-03
7.00E-07	700	0.3376	1.62E+05	6.02E-09	4.20E-08	4.28E+14	9.79E-09	0.4128	1.53E-04	153.340	15666.31	0.2330	1.07E-02
8.00E-07	800	0.3278	6.40E+04	6.02E-09	1.60E-08	3.75E+14	2.22E-09	0.2150	1.53E-04	152.610	68739.69	0.1388	1.79E-02

R @ 1.0QE	R @ 0.9QE	R @ 0.8QE	R @ 0.7QE	R @ 0.6QE	R @ 0.5QE	R @ 0.4QE	R @ 0.3QE	R @ 0.2QE	R @ 0.1QE
0.3226	0.2904	0.2581	0.2258	0.1936	0.1613	0.1290	0.0968	0.0645	0.0323
0.4033	0.3629	0.3226	0.2823	0.2420	0.2016	0.1613	0.1210	0.0807	0.0403
0.4839	0.4355	0.3871	0.3388	0.2904	0.2420	0.1936	0.1452	0.0968	0.0484
0.5646	0.5081	0.4517	0.3952	0.3388	0.2823	0.2258	0.1694	0.1129	0.0565
0.6452	0.5807	0.5162	0.4517	0.3871	0.3226	0.2581	0.1936	0.1290	0.0645

Cell:	**W4 C7,3 D200,30,400,N**
Breakdown Voltage:	-5.2 [V]
Dark Current (@ Vbr):	-10.4 [uA]
Gain (@ Vbr):	188
Responsitivity (@ 600nm):	0.272 [A/W]
NEP (@ Vbr):	3.83E-05 [W]

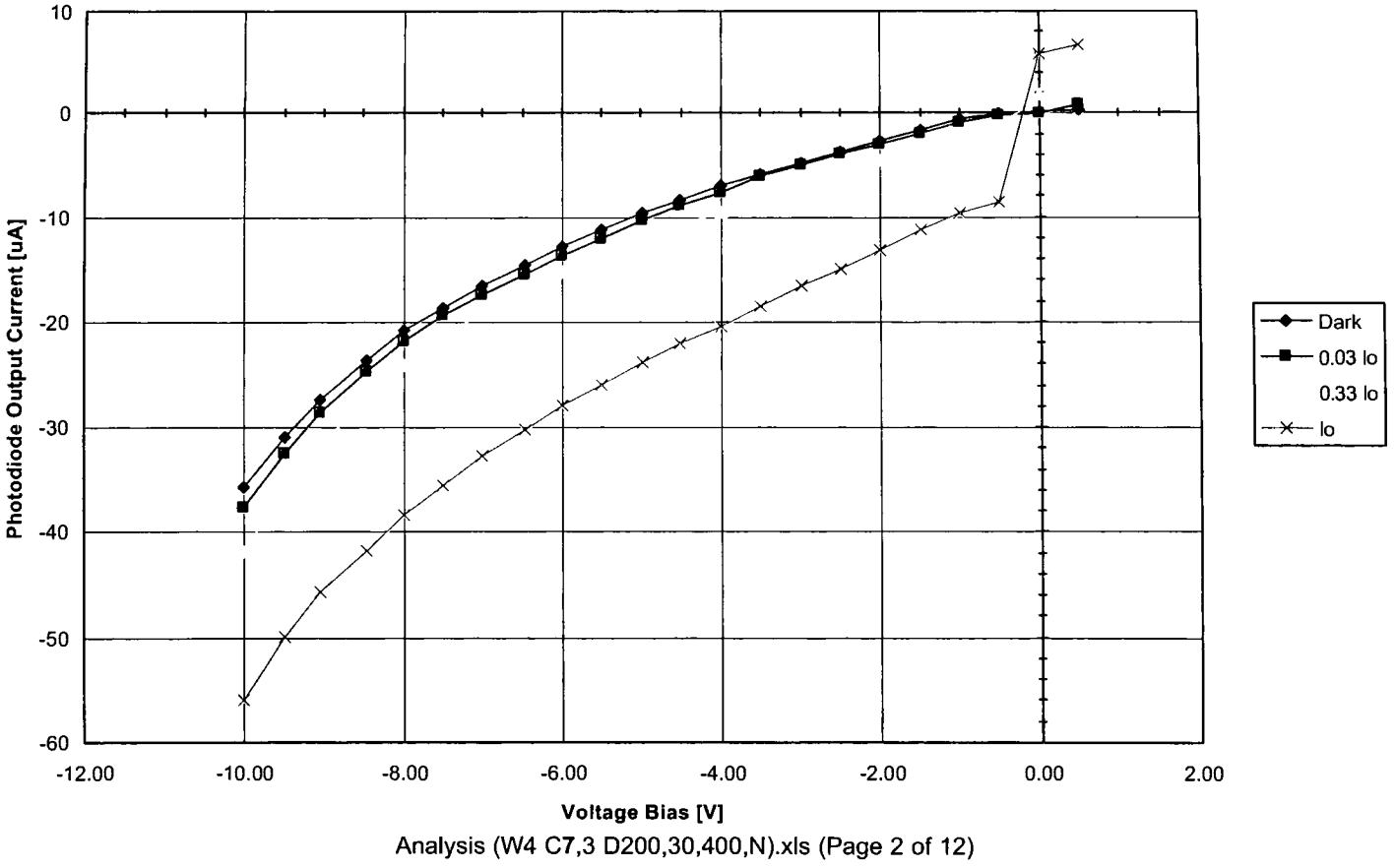
I-V Plot (W4 C7,3 D200,30,400,N)
Photodiode Output Current [uA]
10
0
-10
-20
-30
-40
-50
-60
-12.00
-10.00
-8.00
-6.00
-4.00
-2.00
0.00
2.00
Voltage Bias [V]
Dark
0.03 Io
0.33 Io
Io

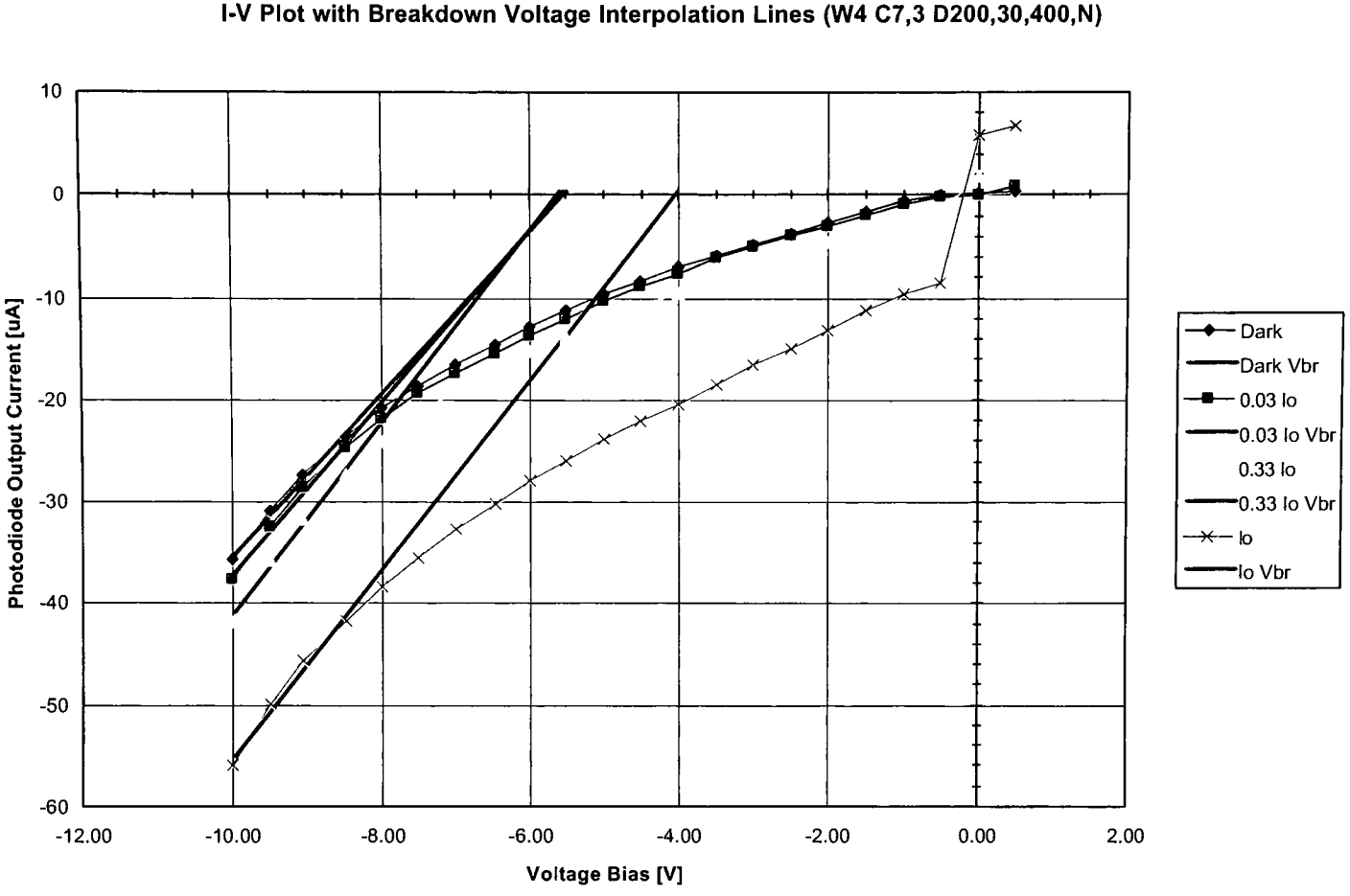
I-V Plot with Breakdown Voltage Interpolation Lines (W4 C7,3 D200,30,400,N)
Photodiode Output Current [uA]
10
0
-10
-20
-30
-40
-50
-60
-12.00
-10.00
-8.00
-6.00
-4.00
-2.00
0.00
2.00
Voltage Bias [V]
Dark
Dark Vbr
0.03 Io
0.03 Io Vbr
0.33 Io
0.33 Io Vbr
Io
Io Vbr

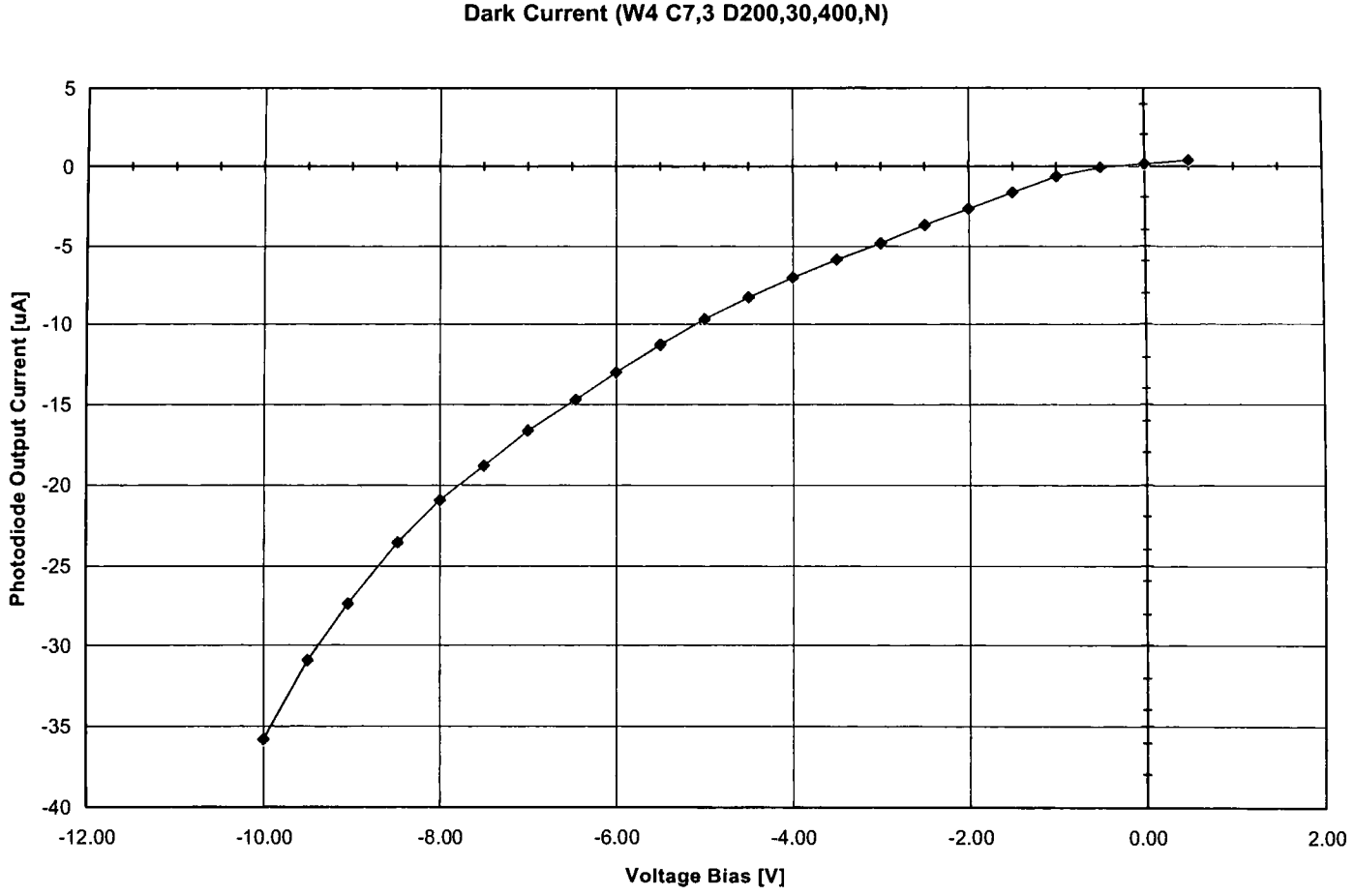
Dark Current (W4 C7,3 D200,30,400,N)
Photodiode Output Current [uA]
5
0
-5
-10
-15
-20
-25
-30
-35
-40
-12.00
-10.00
-8.00
-6.00
-4.00
-2.00
0.00
2.00
Voltage Bias [V]

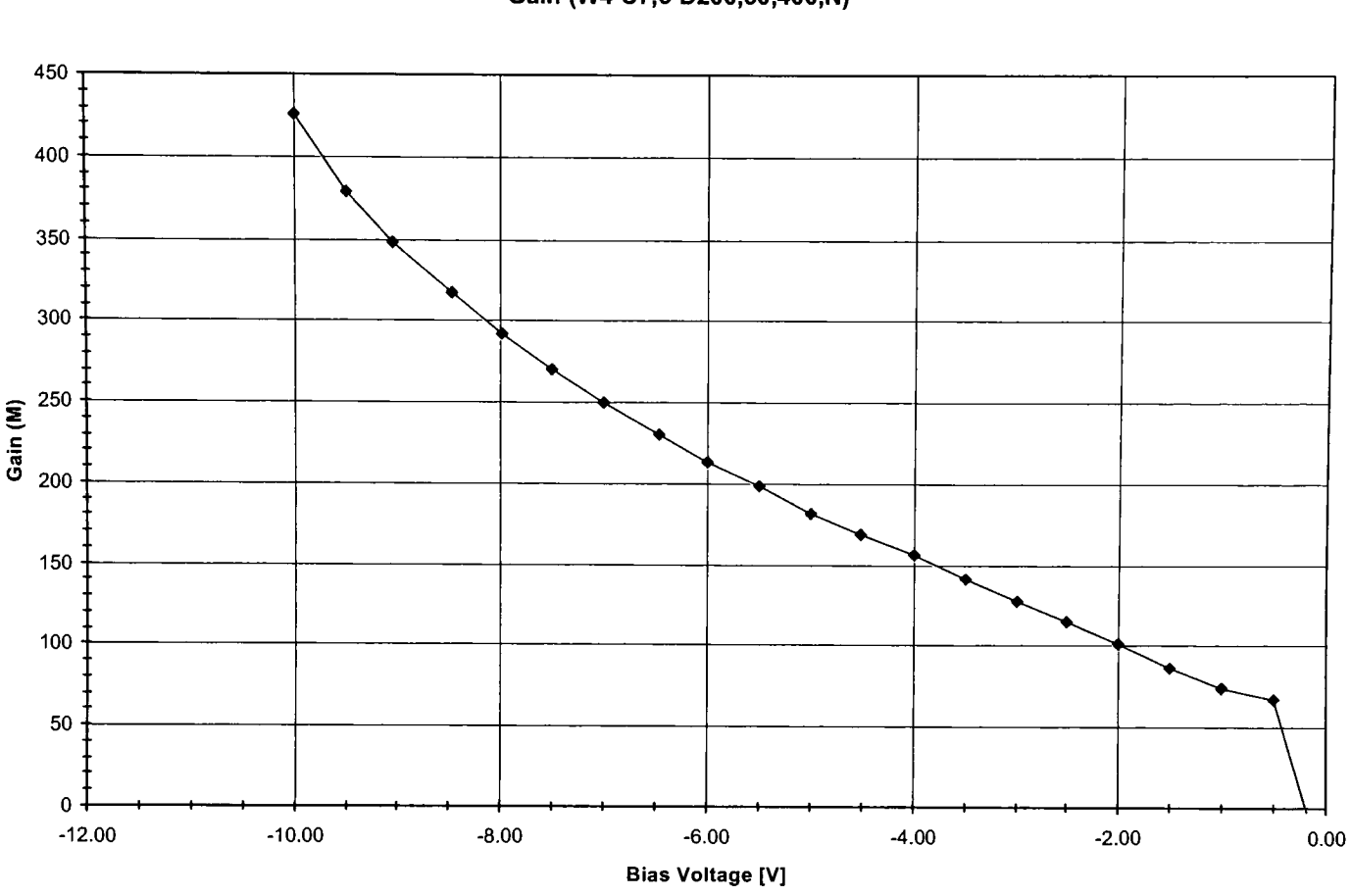
Gain (W4 C7,3 D200,30,400,N)
450
400
350
300
250
200
150
100
50
0
Gain (M)
-12.00
-10.00
-8.00
-6.00
-4.00
-2.00
0.00
Bias Voltage [V]

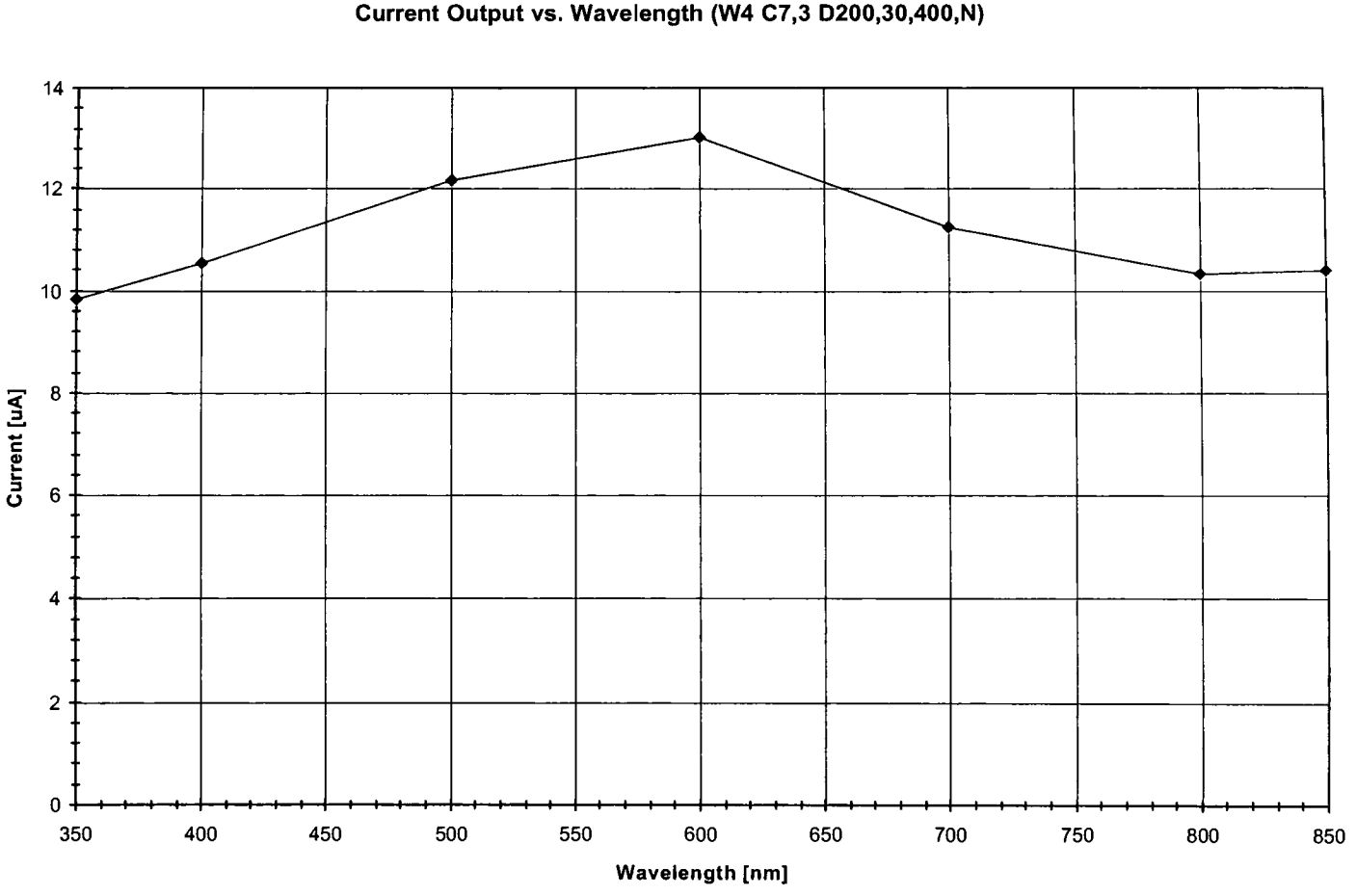
Current Output vs. Wavelength (W4 C7,3 D200,30,400,N)
Current [uA]
0
2
4
6
8
10
12
14
350
400
450
500
550
600
650
700
750
800
850
Wavelength [nm]

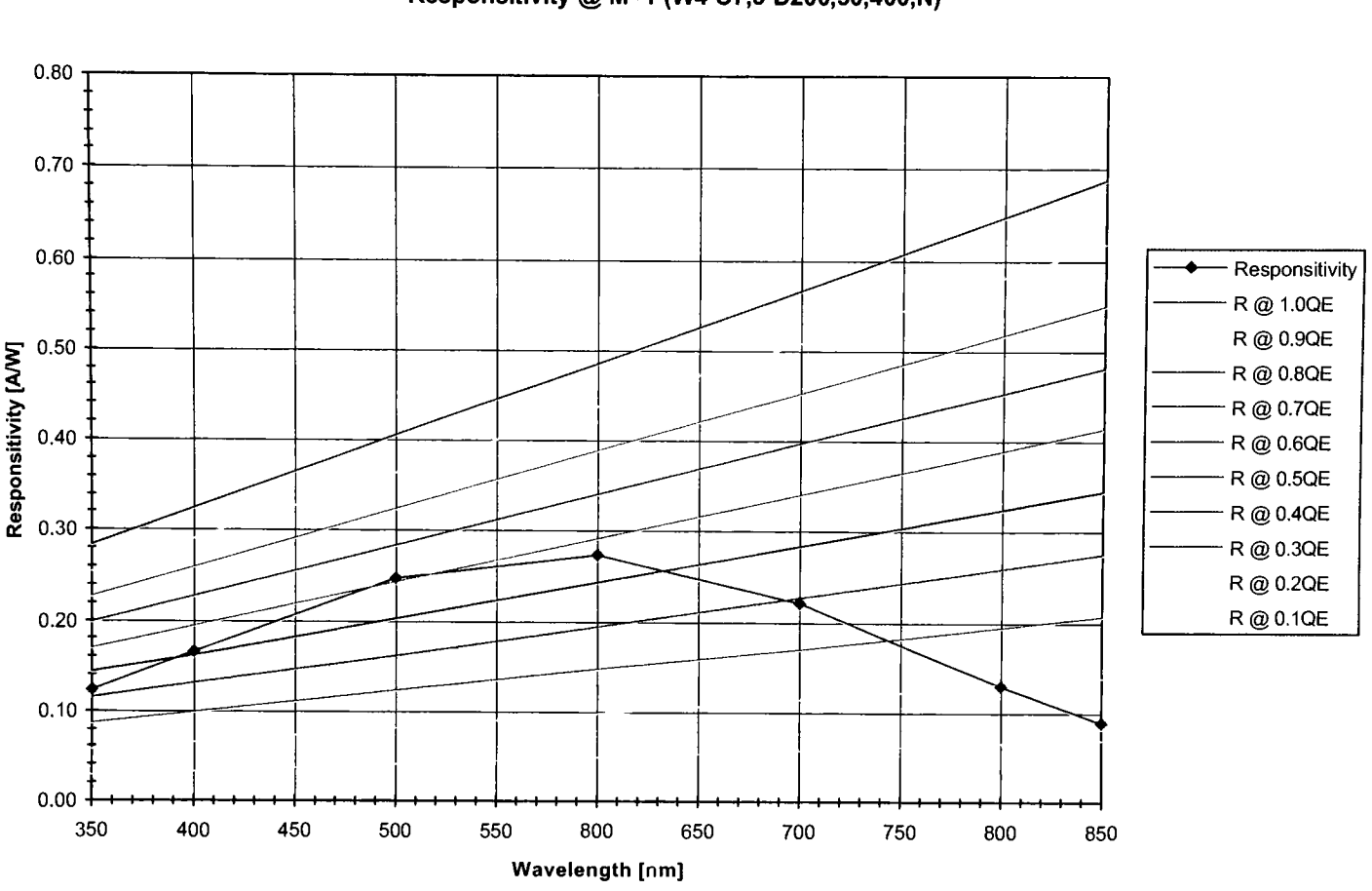
Responsitivity @ M=1 (W4 C7,3 D200,30,400,N)
Responsitivity [A/W]
0.80
0.70
0.60
0.50
0.40
0.30
0.20
0.10
0.00
350
400
450
500
550
800
650
700
750
800
850
Wavelength [nm]
Responsitivity
R @ 1.0QE
R @ 0.9QE
R @ 0.8QE
R @ 0.7QE
R @ 0.6QE
R @ 0.5QE
R @ 0.4QE
R @ 0.3QE
R @ 0.2QE
R @ 0.1QE

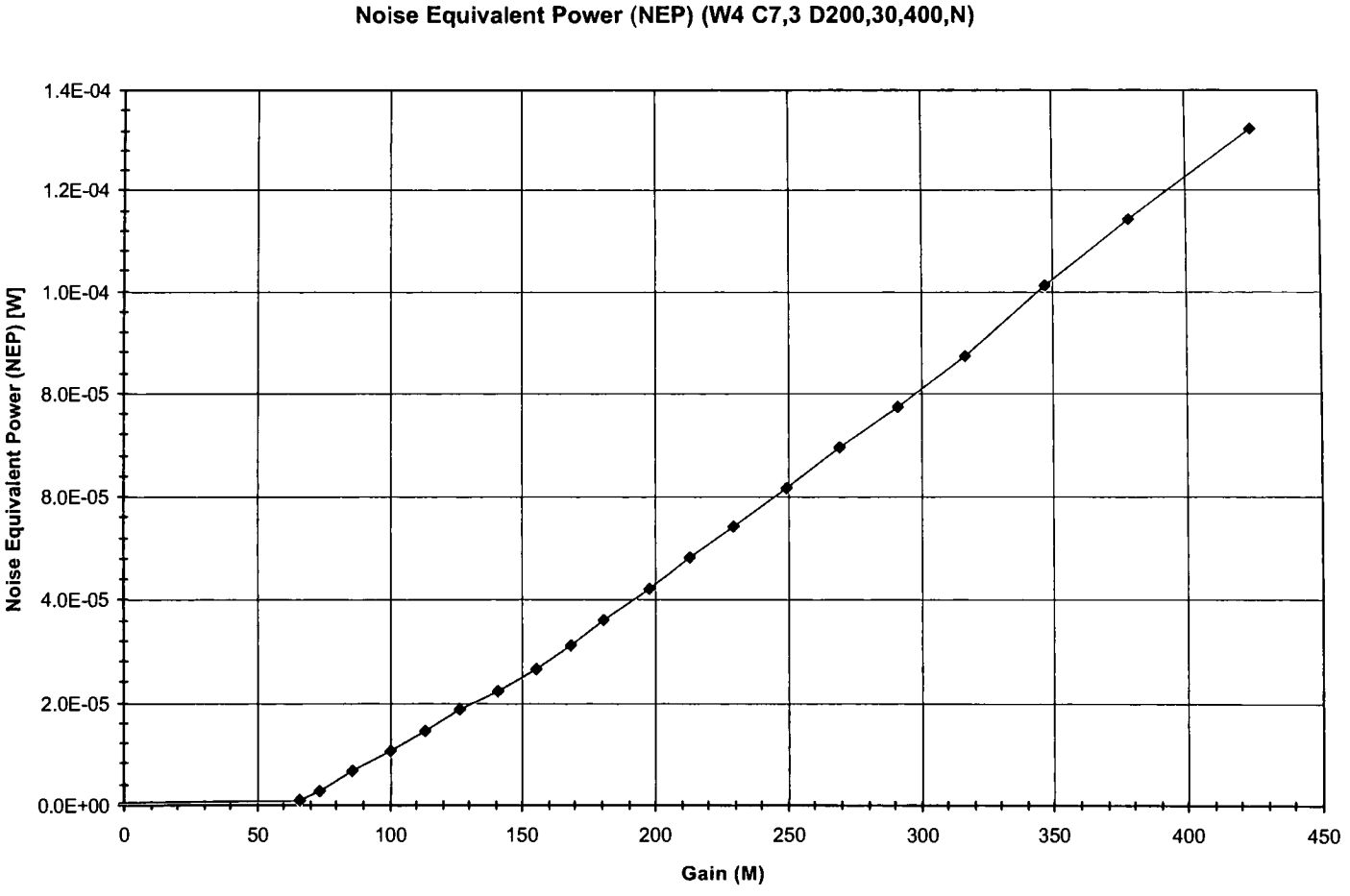
Noise Equivalent Power (NEP) (W4 C7,3 D200,30,400,N)
Noise Equivalent Power (NEP) [W]
1.4E-04
1.2E-04
1.0E-04
8.0E-05
8.0E-05
4.0E-05
2.0E-05
0.0E+00
0
50
100
150
200
250
300
350
400
450
Gain (M)

Wafer		4	4	4	4
Cell		7, 3	7, 3	7, 3	7, 3
Diameter [um]		200	200	200	200
Guard Ring [um]		30	30	30	30
Pixel Dist [um]		400	400	400	400
Metal Ring		N	N	N	N
Illumination [%]		Dark	0.03 Io	0.33 Io	Io
Bias Voltage [V]	*-10.00*	-35.9	-37.71	-41.8	-56.1
	-9.50	-31	-32.56	-35.9	-50
	-9.05	-27.4	-28.7	-31.7	-45.8
	-8.47	-23.7	-24.7808	-27.3	-41.8
	-7.99	-21	-21.9	-24.2	-38.5
	-7.50	-18.82	-19.48	-21.5	-35.6
	-7.00	-16.72	-17.48	-19.1	-32.9
	-6.46	-14.71	-15.5028	-17	-30.3
	-6.00	-13	-13.85	-15.3	-28.1
	-5.50	-11.37	-12.14	-13.8	-26.1
	-5.00	-9.75	-10.52	-12.3	-23.9
	-4.51	-8.42	-9.08	-10.7361	-22.2
	-4.00	-7.1	-7.6928	-9.47393	-20.5
	-3.50	-5.94	-6.22	-8.3	-18.6
	-3.00	-4.973	-5.063	-6.96	-16.7
	-2.50	-3.84	-4.033	-5.865	-15.01
	-2.00	-2.784	-3.06	-4.64	-13.24
	-1.50	-1.757	-1.995	-3.34	-11.3
	-1.00	-0.7186	-0.9749	-2.263	-9.723
	-0.50	-0.1643	-0.3023	-1.809	-8.701
	0.00	0.04135	-0.07548	1.851	5.689
	0.50	0.3052	0.728	2.658	6.611

Wafer		4	4	4	4
Cell		7, 3	7, 3	7, 3	7, 3
Diameter [um]		200	200	200	200
Guard Ring [um]		30	30	30	30
Pixel Dist [um]		400	400	400	400
Metal Ring		N	N	N	N
Illumination [%]		Dark Vbr	0.03 Io Vbr	0.33 Io Vbr	Io Vbr
Bias Voltage [V]	*-10.00*	-35.421	-37.218	-41.2	-55.354
	-5.63	-0.70091	-0.38555	-0.0004	-14.7206
	-5.59	-0.33455	0.003099		-14.2919
	-5.54	-0.00078			-13.9012
	-4.05				0.003171

Curve Fit	**a**	2.57E-02	2.95E-02	0.05806	0.100617
	b	6.70E-02	0.119131	0.546536	1.382015
	c	1.626956	1.924237	3.85923	9.477178
	d	0.18952	0.284974	1.012613	0.922955
2nd Derivative	**a**	0.154212	0.177134	0.34836	0.6037
	b	0.133921	0.238261	1.093072	2.76403
Max Gradient	Vbr	-0.86842	-1.34509	-3.13777	-4.57848
Threshold	Vbr				
Linear Trend	Vbr	-5.63	-5.59	-5.54	-4.048
Voltage Breakdown	Vbr	-5.2	-5.2	-5.2	-5.2

q = 1.80E-19 [C]

h = 8.83E-34 [J s]

c = 3.00E+08 [m/s]

dark [A] = 2.78E-08

wavel [m]	wavel [nm]	R [%]	a [1/m]	w [m]	Po [W]	v [Hz]	Ip [A]	QE	I [A]	I [uA]	M	Responsiti	NEP [W]
3.50E-07	350	0.5688	1.08E+08	5.42E-09	8.90E-08	8.57E+14	1.08E-08	0.4312	9.82E-06	9.824	906.82	0.1217	2.29E-05
4.00E-07	400	0.4888	8.98E+06	5.42E-09	1.73E-07	7.49E+14	2.85E-08	0.5112	1.05E-05	10.512	368.42	0.1849	1.69E-05
5.00E-07	500	0.3873	8.89E+05	5.42E-09	5.22E-07	6.00E+14	1.28E-07	0.6077	1.22E-05	12.165	95.09	0.2451	1.14E-05
8.00E-07	600	0.3538	3 75E+05	5.42E-09	4.88E-07	5.00E+14	1.32E-07	0.5615	1.30E-05	13.014	98.54	0.2717	1.02E-05
7.00E-07	700	0.3376	1.82E+05	5.42E-09	4.20E-08	4.28E+14	9.18E-09	0.3871	1.12E-05	11.240	1224.50	0.2186	1.27E-05
8.00E-07	800	0.3278	6.40E+04	5.42E-09	1.80E-08	3.75E+14	2.03E-09	0.1970	1.03E-05	10.318	5072.65	0.1271	2.19E-05
8.50E-07	850	0.3244	3.82E+04	5.42E-09	1.20E-08	3.53E+14	1.04E-09	0.1263	1.04E-05	10.376	9982.25	0.0866	3.21E-05

R @ 1.0QI	R @ 0.9QI	R @ 0.8QI	R @ 0.7QI	R @ 0.6QI	R @ 0.5QI	R @ 0.4QI	R @ 0.3QI	R @ 0.2QI	R @ 0.1QE
0.2823	0.2541	0.2258	0.1976	0.1694	0.1411	0.1129	0.0847	0.0585	0.0282
0.3226	0.2904	0.2581	0.2258	0.1936	0.1613	0.1290	0.0968	0.0645	0.0323
0.4033	0.3629	0.3226	0.2823	0.2420	0.2016	0.1813	0.1210	0.0807	0.0403
0.4839	0.4355	0.3871	0.3388	0.2904	0.2420	0.1936	0.1452	0.0988	0.0484
0.5646	0.5081	0.4517	0.3952	0.3388	0.2823	0.2258	0.1694	0.1129	0.0565
0.6452	0.5807	0.5162	0.4517	0.3871	0.3226	0.2581	0.1938	0.1290	0.0645
0.6856	0.6170	0.5485	0.4799	0.4113	0.3428	0.2742	0.2057	0.1371	0.0886

q =	1.60E-19	[C]
h =	6.63E-34	[J s]
c =	3.00E+08	[m/s]
wavel =	6.00E-07	[m]
v =	5.00E+14	[Hz]
Po @ 600r	4.86E-07	[W]
w =	5.42E-06	[m]
R @ 600nr	0.3538	[%]
a @ 600nr	3.75E+05	[1/m]
Ip =	1.32E-07	[A]

QE = 0.5615

Vbias [V]	Idark [A]	I [A]	*Inorm [A]*	*M*	*R @ 1 [A/V*	*NEP [W]*
-10.00	-3.59E-05	-5.61E-05	*1.32E-07*	*424.77*	*0.2717*	*1.32E-04*
-9.50	-3.10E-05	-5.00E-05	*1.32E-07*	*378.59*	*0.2717*	*1.14E-04*
-9.05	-2.74E-05	-4.58E-05	*1.32E-07*	*346.79*	*0.2717*	*1.01E-04*
-8.47	-2.37E-05	-4.18E-05	*1.32E-07*	*316.50*	*0.2717*	*8.72E-05*
-7.99	-2.10E-05	-3.85E-05	*1.32E-07*	*291.51*	*0.2717*	*7.73E-05*
-7.50	-1.88E-05	-3.56E-05	*1.32E-07*	*269.55*	*0.2717*	*6.93E-05*
-7.00	-1.67E-05	-3.29E-05	*1.32E-07*	*249.11*	*0.2717*	*6.15E-05*
-6.46	-1.47E-05	-3E-05	*1.32E-07*	*229.42*	*0.2717*	*5.41E-05*
-6.00	-1.30E-05	-2.8E-05	*1.32E-07*	*212.77*	*0.2717*	*4.78E-05*
-5.50	-1.14E-05	-2.6E-05	*1.32E-07*	*197.62*	*0.2717*	*4.18E-05*
-5.00	-9.75E-06	-2.4E-05	*1.32E-07*	*180.96*	*0.2717*	*3.59E-05*
-4.51	-8.42E-06	-2.2E-05	*1.32E-07*	*168.09*	*0.2717*	*3.10E-05*
-4.00	-7.10E-06	-2.1E-05	*1.32E-07*	*155.22*	*0.2717*	*2.61E-05*
-3.50	-5.94E-06	-1.9E-05	*1.32E-07*	*140.83*	*0.2717*	*2.19E-05*
-3.00	-4.97E-06	-1.7E-05	*1.32E-07*	*126.45*	*0.2717*	*1.83E-05*
-2.50	-3.84E-06	-1.5E-05	*1.32E-07*	*113.65*	*0.2717*	*1.41E-05*
-2.00	-2.78E-06	-1.3E-05	*1.32E-07*	*100.25*	*0.2717*	*1.02E-05*
-1.50	-1.76E-06	-1.1E-05	*1.32E-07*	*85.56*	*0.2717*	*6.47E-06*
-1.00	-7.19E-07	-9.7E-06	*1.32E-07*	*73.62*	*0.2717*	*2.64E-06*
-0.50	-1.64E-07	-8.7E-06	*1.32E-07*	*65.88*	*0.2717*	*6.05E-07*
0.00	4.14E-08	5.69E-06	*1.32E-07*	*-43.08*	*0.2717*	*-1.52E-07*
0.50	3.05E-07	6.61E-06	*1.32E-07*	*-50.06*	*0.2717*	*-1.12E-06*

Cell:	**W5 C9,10 D400,20,500,N**
Breakdown Voltage:	-50.43 [V]
Dark Current (@ Vbr):	-63 [uA]
Gain (@ Vbr):	19053
Responsitivity (@ 600nm, 2V Bias):	0.307 [A/W]
NEP (@ Vbr):	0.000205 [W]

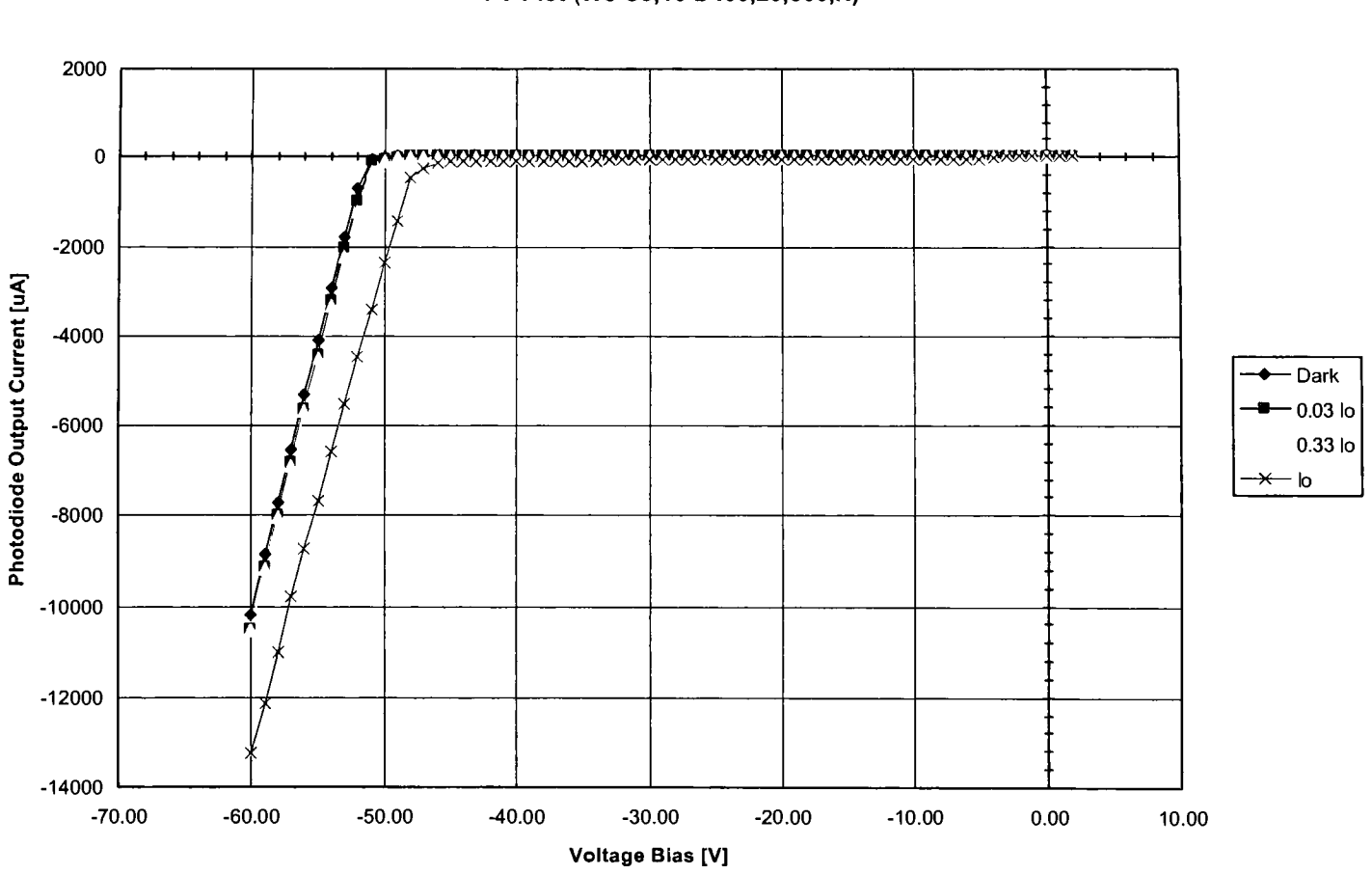
I-V Plot (W5 C9,10 D400,20,500,N)
Photodiode Output Current [uA]
2000
0
-2000
-4000
-6000
-8000
-10000
-12000
-14000
-70.00
-60.00
-50.00
-40.00
-30.00
-20.00
-10.00
0.00
10.00
Voltage Bias [V]
Dark
0.03 Io
0.33 Io
Io

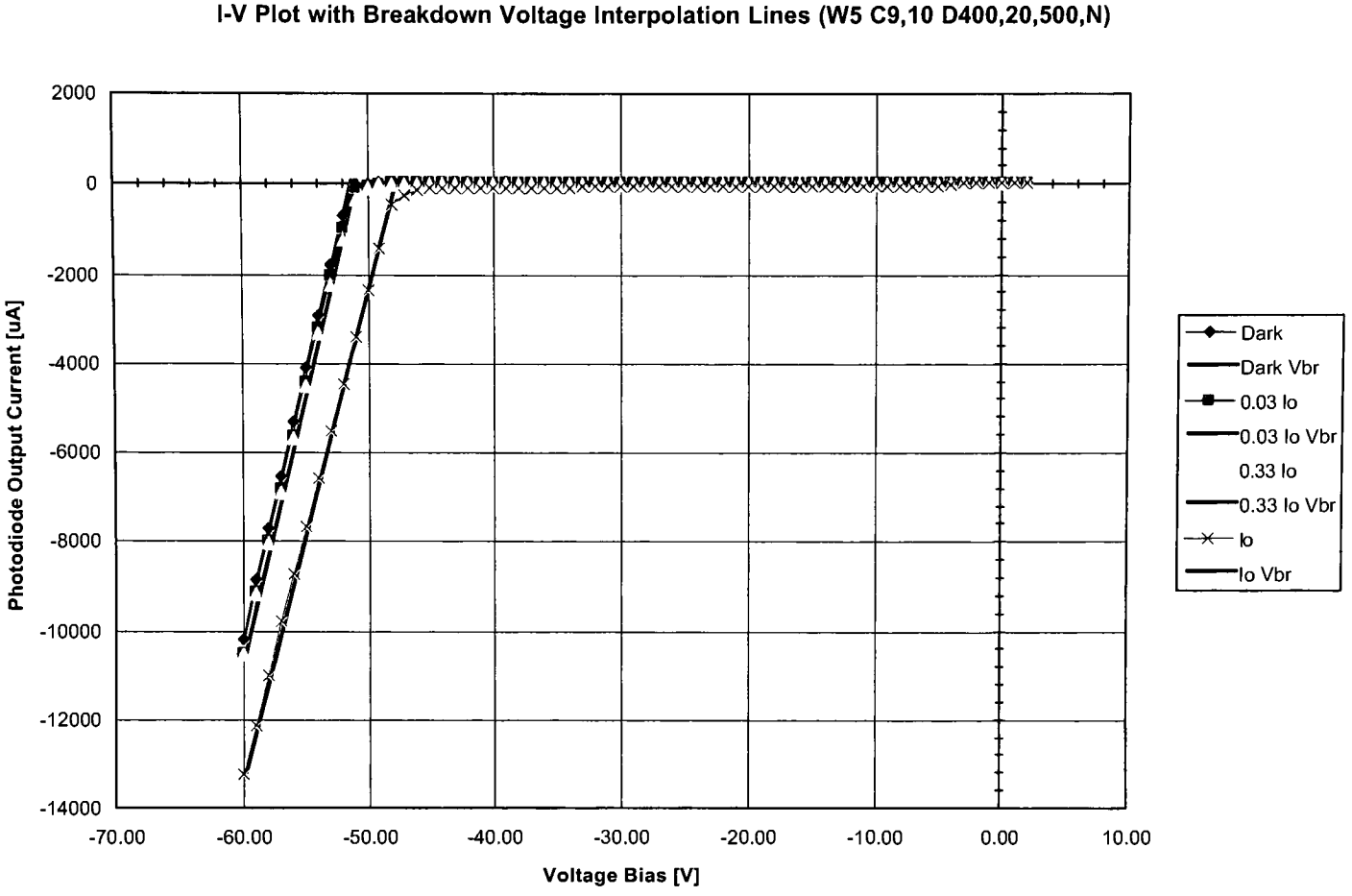
I-V Plot with Breakdown Voltage Interpolation Lines (W5 C9,10 D400,20,500,N)
Photodiode Output Current [uA]
2000
0
-2000
-4000
-6000
-8000
-10000
-12000
-14000
-70.00
-60.00
-50.00
-40.00
-30.00
-20.00
-10.00
0.00
10.00
Voltage Bias [V]
Dark
Dark Vbr
0.03 Io
0.03 Io Vbr
0.33 Io
0.33 Io Vbr
Io
Io Vbr

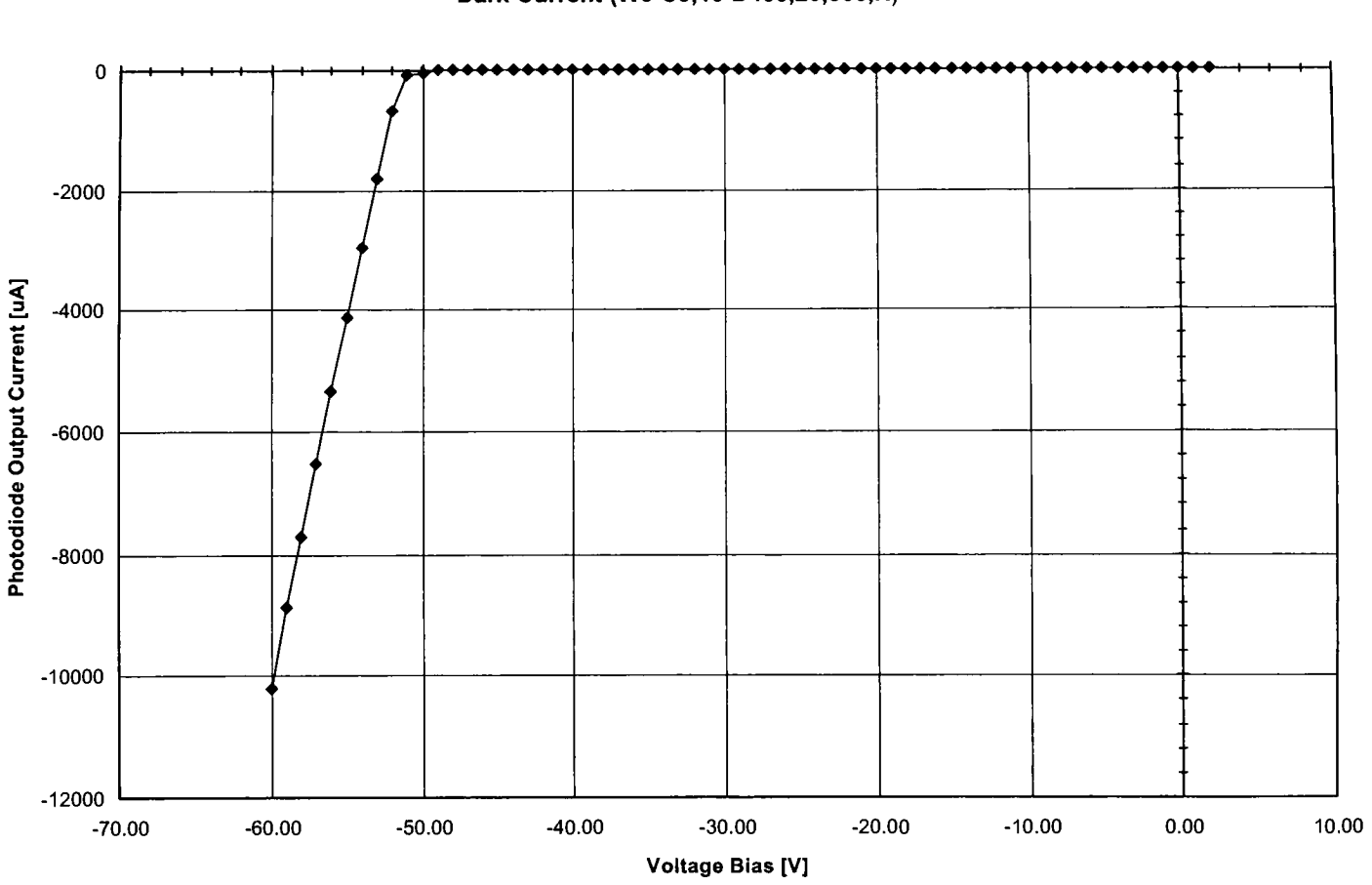
Dark Current (W5 C9,10 D400,20,500,N)
Photodiode Output Current [uA]
0
-2000
-4000
-6000
-8000
-10000
-12000
-70.00
-60.00
-50.00
-40.00
-30.00
-20.00
-10.00
0.00
10.00
Voltage Bias [V]

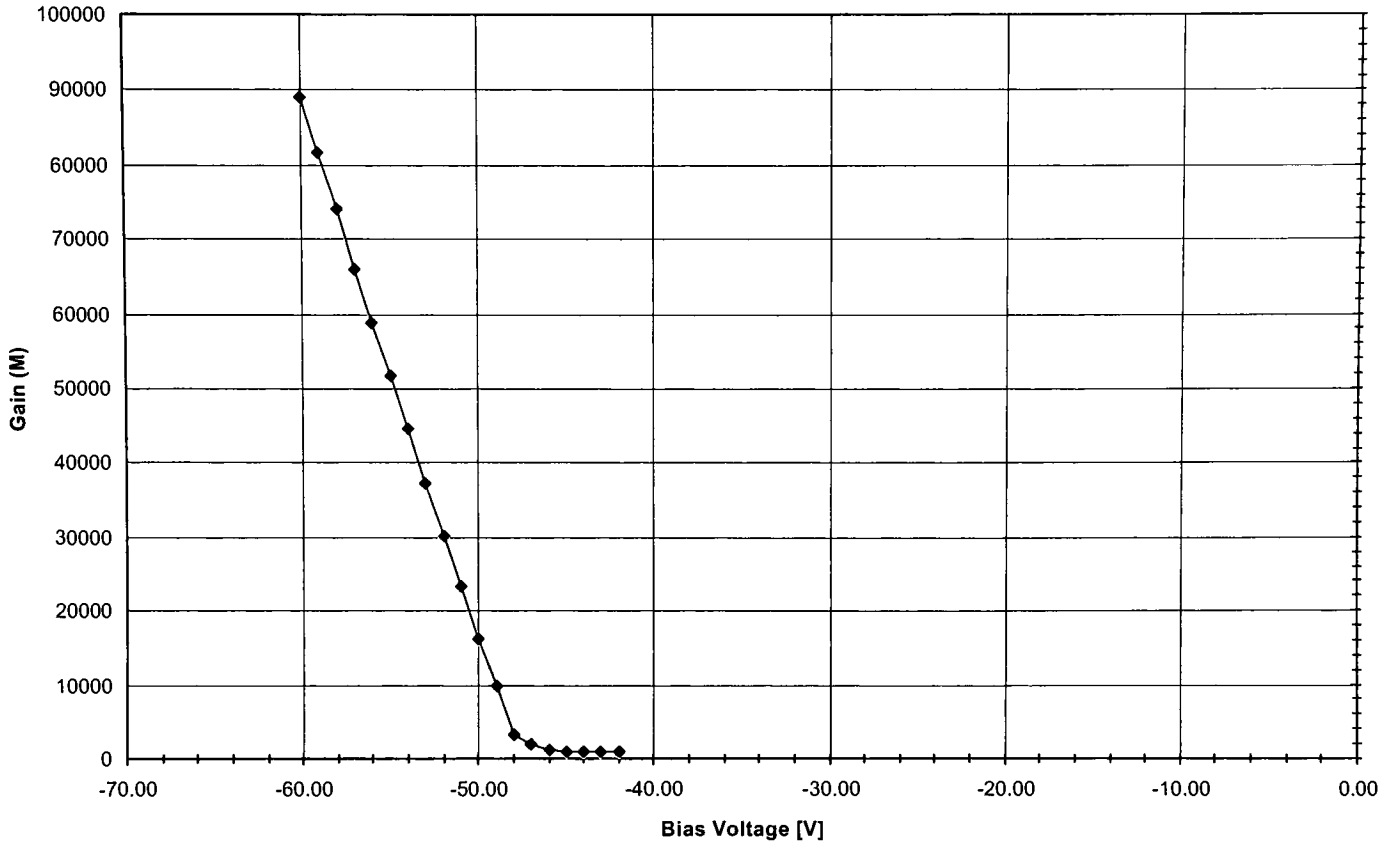
Gain (W5 C9,10 D400,20,500,N)
100000
90000
60000
70000
60000
50000
40000
30000
20000
10000
0
Gain (M)
-70.00
-60.00
-50.00
-40.00
-30.00
-20.00
-10.00
0.00
Bias Voltage [V]

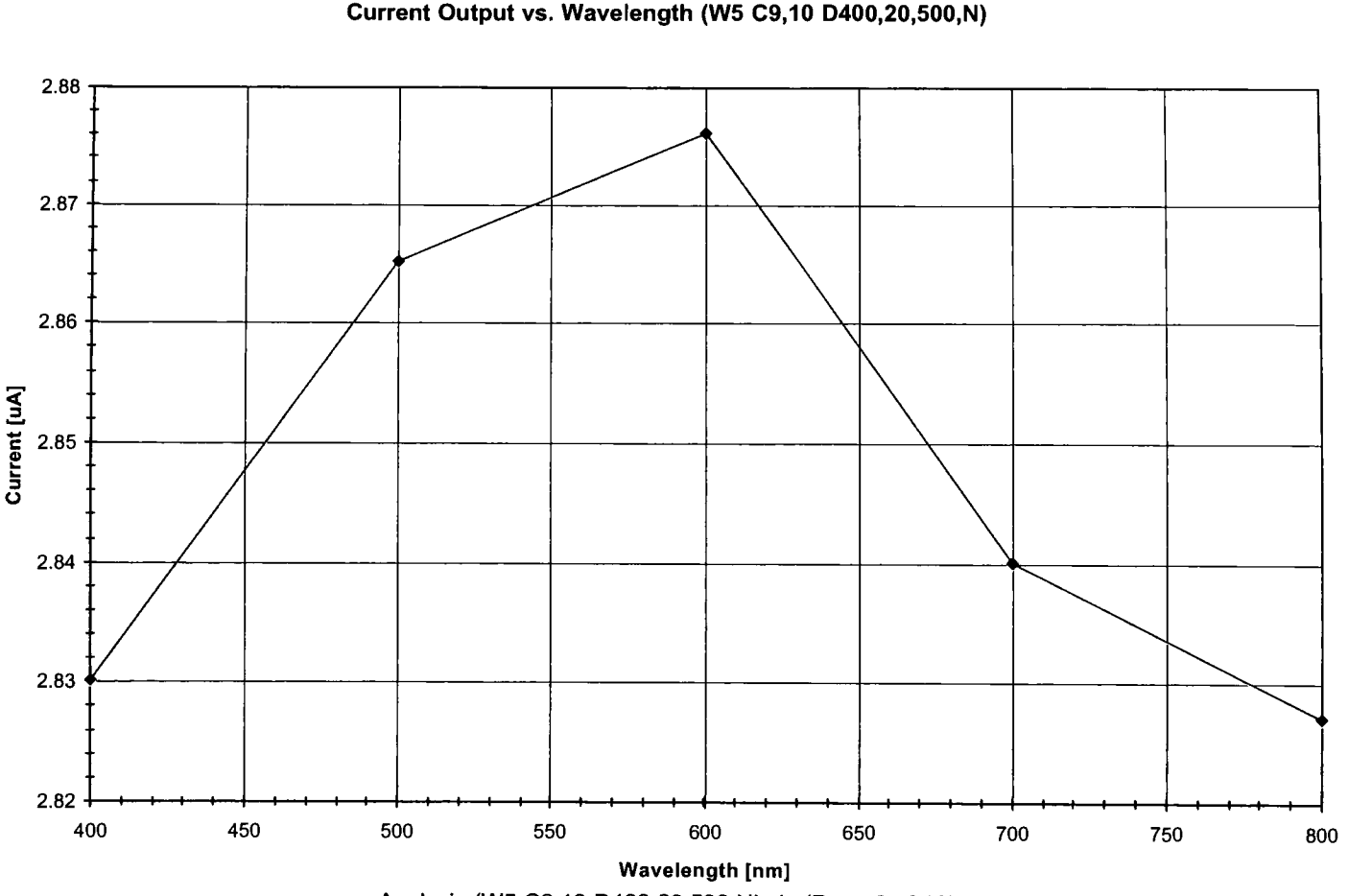
Current Output vs. Wavelength (W5 C9,10 D400,20,500,N)
2.88
2.87
2.86
2.85
2.84
2.83
2.82
Current [uA]
400
450
500
550
600
650
700
750
800
Wavelength [nm]

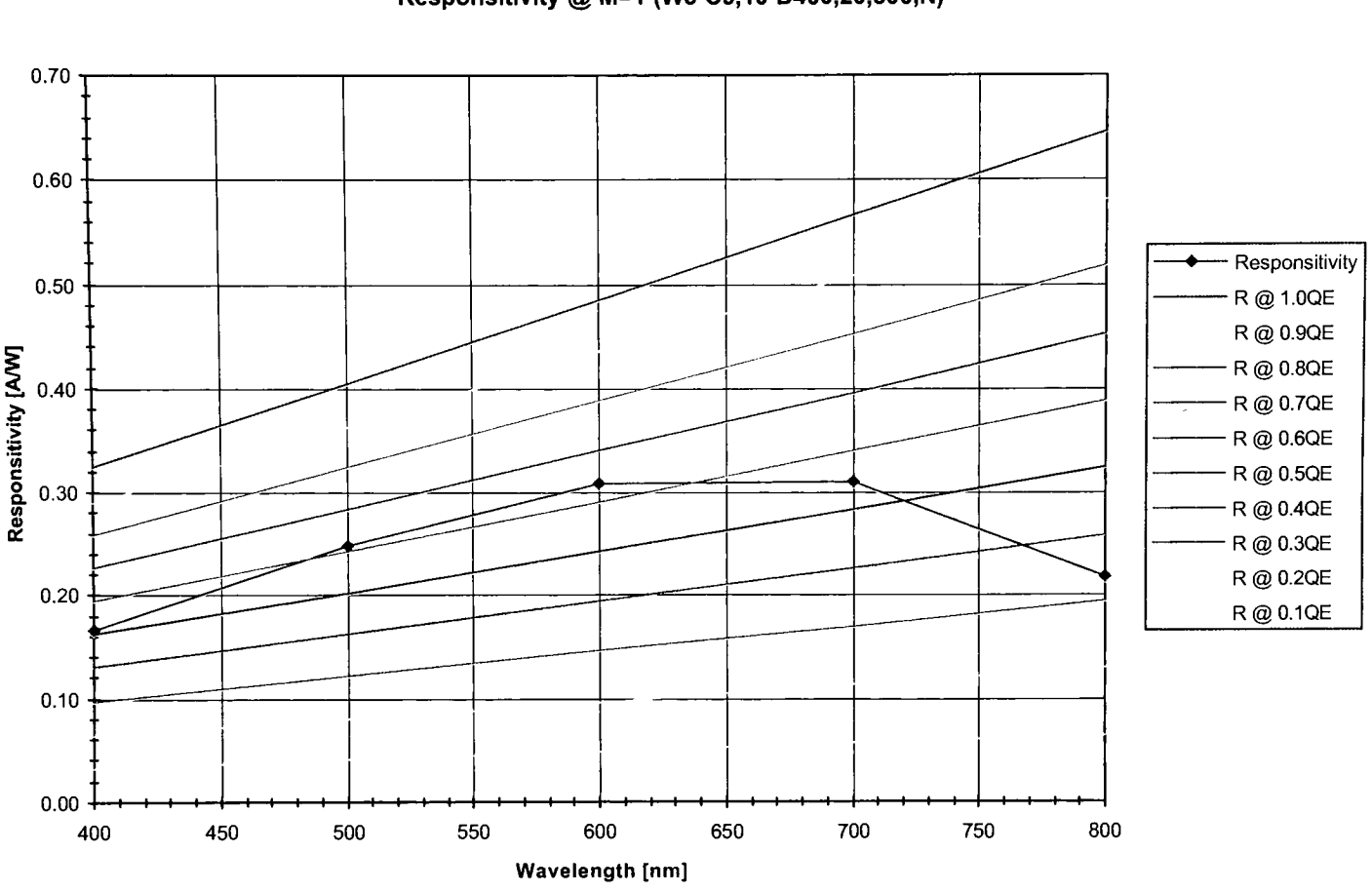
Responsitivity @ M=1 (W5 C9,10 D400,20,500,N)
Responsitivity [A/W]
0.70
0.60
0.50
0.40
0.30
0.20
0.10
0.00
400
450
500
550
600
650
700
750
800
Wavelength [nm]
Responsitivity
R @ 1.0QE
R @ 0.9QE
R @ 0.8QE
R @ 0.7QE
R @ 0.6QE
R @ 0.5QE
R @ 0.4QE
R @ 0.3QE
R @ 0.2QE
R @ 0.1QE

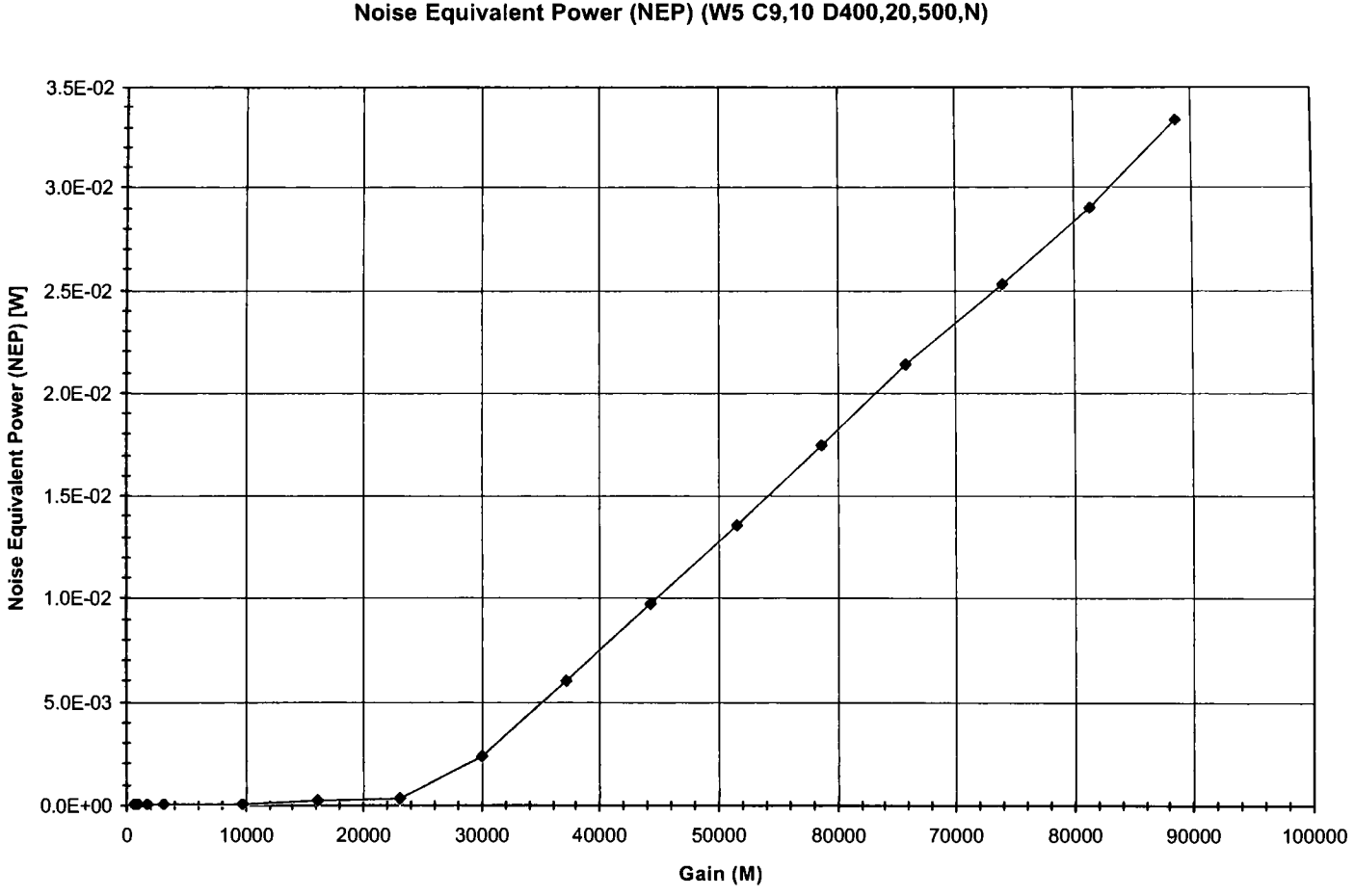
Noise Equivalent Power (NEP) (W5 C9,10 D400,20,500,N)
Noise Equivalent Power (NEP) [W]
3.5E-02
3.0E-02
2.5E-02
2.0E-02
1.5E-02
1.0E-02
5.0E-03
0.0E+00
0
10000
20000
30000
40000
50000
80000
70000
80000
90000
100000
Gain (M)

Wafer		4	4	4	4
Cell		7, 3	7, 3	7, 3	7, 3
Diameter [um]		300	200	200	200
Guard Ring [um]		20	20	20	20
Pixel Dist [um]		300	300	300	200
Metal Ring		Y	Y	Y	Y
Illumination [%]		Dark	0.03 Io	0 33 Io	Io
Bias Voltage [V]	-60.00	-10240 1	-10540.7	-10550 1	-13253 9
	-59 00	-8886 14	-9171.65	-9204.12	-12153.9
	-58.00	-7740.14	-8039.65	-8079 12	-11043.9
	-57 00	-6561 14	-6869.65	-6925.12	-9818.91
	-56 00	-5358.14	-5661.65	-5732.12	-8751.91
	-55 00	-4146 14	-4441.65	-4537.12	-7689.91
	-54 00	-2970.14	-3234.65	-3376.12	-6618.91
	-53 00	-1821.14	-2066 65	-2251.12	-5548.91
	-52.00	-714.542	-1024 65	-1236 12	-4487.91
	-51 00	-83 9617	-126 451	-370.417	-3444.91
	-50 00	-47.1517	-58.3512	-98.0168	-2393.91
	-49 00	-8.7617	-18.0512	-35.2068	-1446.91
	-48.00	-0.3786	-3.25917	-27 3278	-457 115
	-47.00	-0.2841	-0.7186	-26.7898	-260.715
	-46.00	-0.1854	-0.6845	-23 4578	-136.435
	-45.00	-0.1417	-0.65117	-20 1168	-103.915
	-44.00	-0.13843	-0.64744	-19.8268	-102.872
	-43 00	-0.13453	-0.6439	-19.5349	-101.677
	-42.00	-0.13185	-0.64046	-19.2776	-100.628
	-41	-0.12811	-0.6366	-19.0925	-99.4418
	-40	-0.12575	-0.63252	-18.9323	-98.4024
	-39	-0.12074	-0.62818	-18.6744	-97.1753
	-38	-0 11779	-0.62472	-18 4106	-96.0064
	-37	-0.11398	-0.62071	-18.2467	-95.0207
	-36	-0.1112	-0.61709	-17.996	-93.8659
	-35	-0.1067	-0.6121	-17.6946	-92.7356
	-34	-0 10302	-0.6093	-17.4344	-91 4304
	-33	-0.10136	-0 606	-17.2627	-90 4285
	-32	-0.09685	-0.60089	-16.886	-89.2212
	-31	-0.09292	-0.59829	-16.8371	-80.0411
	-30	-0.08924	-0.59371	-16.5468	-66 9797
	-29	-0.08736	-0.59082	-16.3648	-85 857
	-28	-0.08292	-0.58669	-16.1553	-84 7746
	-27	-0.07992	-0.58187	-15.647	-83.6675
	-26	-0.07599	-0.57886	-15.6151	-92.3796
	-25	-0.07284	-0.5749	-15.3093	-81.4304
	-24	-0.06812	-0.57168	-15.142	-80.1707
	-23	-0.06488	-0.56641	-14.9016	-79.0672
	-22	-0.06252	-0.56337	-14.6957	-77.667
	-21	-0.05847	-0.55938	-14.4555	-76.8637
	-20	-0.05503	-0.55593	-14.2377	-75.7746
	-19	-0.05183	-0.55245	-13.9478	-74 4817
	-18	-0.04868	-0.54871	-13.7422	-73 4253
	-17	-0.04536	-0.54558	-13.5106	-72.2434
	-16	-0.04121	-0.54004	-13.2774	-71 0608
	-15	-0.0381	-0.53605	-13.0482	-70.0862
	-14	-0.03356	-0.53335	-12.8507	-66 8868
	-13	-0.03004	-0.52919	-12.5652	-67.8008
	-12	-0.02718	-0.52616	-12.3196	-66.5548
	-11	-0.02427	-0.52112	-12.1054	-65.466
	-10	-0.01384	-0.5176	-11.99	-84 48
	-9	-0.01384	-0.5176	-11.68	-63.3
	-8	-0.01384	-0.5176	-11.54	-62.18
	-7	-0 01384	-0.5176	-11.26	-61.08
	-6	-0.01384	-0.5176	-11.1	-59.64
	-5	-0.01384	-0.5176	-10.92	-57.73
	-4	-0.01384	-0.5178	-10.62	-27.37
	-3	-0.01384	-0.5176	-9 642	-9.814
	-2	-0.01384	-0.5176	-3.105	-2.827
	-1	-0.01384	-0.5176	-0.6459	-0.5817
	0	-0.01384	-0.01035	0.02581	-0.00066
	1	-0.01384	0.8543	1.28	1.179
	2	-0.01384	3.53	4.684	5.174

MEASUREMENTS ARE DONE AT 600nm

Wafer		4	4	4	4
Cell		7, 3	7, 3	7, 3	7, 3
Diameter [um]		200	200	200	200
Guard Ring [um]		30	30	30	30
Pixel Dist [um]		400	400	400	400
Metal Ring		N	N	N	N
Illumination [%]		Dark Vbr	0.03 Io Vbr	0.33 Io Vbr	Io Vbr
Bias Voltage [V]	*-60.00*	-10240.1	-10540.7	-10550.1	-13253.9
	-51.470	-0.00952	-280.979	-490.077	-3844.69
	-51.234		0.05077	-214.973	-3585.55
	-51.050			0.00608	-3383.04
	-47.967				0.4208

Curve Fit	a				
	b				
	c				
	d				
2nd Derivative	a				
	b				
Max Gradient	Vbr				
Threshold	Vbr				
Linear Trend	Vbr	-51.470	-51.234	-51.050	-47.967
Voltage Breakdown	Vbr	-50.4303	-50.4303	-50.4303	-50.4303

q =	1 60E-19	|C|
h =	6 63E-34	|J s|
c =	3 00E+08	|m/s|
wavel =	5 00E-07	|m|
v =	5 00E+14	|Hz|
Po @ 600n	4 86E-07	|W|
w =	1 08E-05	|m|
R @ 600nm	0 3538	|%|
a @ 600nm	3 75E+05	|1/m|
Ip =	1 49E-07	|A|

QE = 0 6351

Vbias [V]	Idark [A]	I [A]	Inorm [A]	M	R @ I [A/W]	NEP [W]
-60.00	-1.02E-02	-1.33E-02	1 48E-07	88736 64	0 3073	3 33E-02
-59 00	-8.69E-03	-1.22E-02	1 49E-07	81372	0 3073	2 89E-02
-58.00	-7 74E-03	-1.10E-02	1 49E-07	73940 41	0 3073	2 52E-02
-57 00	-6 56E-03	-9 82E-03	1 49E-07	65730 88	0 3073	2 13E-02
-56.00	-5.36E-03	-8.75E-03	1 49E-07	58595 18	0 3073	1 74E-02
-55.00	-4 15E-03	-7 69E-03	1 49E-07	51484 95	0 3073	1 35E-02
-54.00	-2.97E-03	-6 62E-03	1 49E-07	44314 47	0 3073	8 66E-03
-53 00	-1 82E-03	-5.55E-03	1 49E-07	37150 69	0 3073	5 93E-03
-52.00	-7.15E-04	-4.49E-03	1 48E-07	30047 16	0 3073	2 32E-03
-51 00	-8 40E-05	-3 44E-03	1 49E-07	23064 14	0 3073	2 73E-04
-50.00	-4.72E-05	-2.39E-03	1 49E-07	16027 56	0 3073	1 53E-04
-49.00	-8.76E-06	-1 45E-03	1 48E-07	9687 277	0 3073	2 85E-05
-48.00	-3.79E-07	-4.57E-04	1 49E-07	3060 441	0 3073	1 23E-06
-47 00	-2 84E-07	-2.61E-04	1 49E-07	1745 518	0 3073	8 24E-07
-46 00	-1.85E-07	-1.38E-04	1 49E-07	926 8378	0 3073	6 03E-07
-45.00	-1 42E-07	-1 04E-04	1 49E-07	695 7221	0 3073	4 61E-07
-44.00	-1.39E-07	-1 03E-04	1 48E-07	668 7391	0 3073	4 54E-07
-43.00	-1.35E-07	-1.02E-04	1 49E-07	680 7436	0 3073	4 38E-07
-42.00	-1.32E-07	-1.01E-04	1 49E-07	673 7158	0 3073	4 29E-07
-41	-1.3E-07	-9.9E-05	1 49E-07	665 7752	0 3073	4 17E-07
-40	-1.3E-07	-9.8E-05	1 49E-07	658 8162	0 3073	4 09E-07
-39	-1.2E-07	-9.7E-05	1 49E-07	650 6013	0 3073	3 93E-07
-38	-1.2E-07	-9 6E-05	1 49E-07	642 7753	0 3073	3 83E-07
-37	-1.1E-07	-9.5E-05	1 49E-07	636 1758	0 3073	3 71E-07
-36	-1.1E-07	-9.4E-05	1 49E-07	628 4439	0 3073	3 62E-07
-35	-1.1E-07	-9.3E-05	1 48E-07	620 8766	0 3073	3 47E-07
-34	-1E-07	-9.1E-05	1 49E-07	612 1378	0 3073	3 35E-07
-33	-1E-07	-9E-05	1 49E-07	605 4303	0.3073	3 30E-07
-32	-9.7E-08	-8.9E-05	1 49E-07	597 3476	0 3073	3 15E-07
-31	-9.3E-08	-8.8E-05	1 49E-07	589 4465	0 3073	3 02E-07
-30	-8 9E-08	-8 7E-05	1 49E-07	582 3401	0 3073	2 90E-07
-29	-8.7E-08	-8.6E-05	1 49E-07	574 8236	0 3073	2 84E-07
-28	-8.3E-08	-8.5E-05	1 49E-07	567 5778	0 3073	2 70E-07
-27	-8E-08	-8.4E-05	1 49E-07	560 1648	0 3073	2 60E-07
-26	-7.6E-08	-8.2E-05	1 49E-07	551 5417	0.3073	2 47E-07
-25	-7.3E-08	-8.1E-05	1 49E-07	545 1867	0 3073	2 37E-07
-24	-6.8E-08	-8E-05	1 49E-07	536 7527	0.3073	2.22E-07
-23	-6.5E-08	-7.9E-05	1 49E-07	529 3652	0 3073	2 11E-07
-22	-6.3E-08	-7.8E-05	1 49E-07	521.3296	0 3073	2 03E-07
-21	-5.8E-08	-7.7E-05	1 48E-07	514 8118	0.3073	1 80E-07
-20	-5 5E-08	-7.6E-05	1 49E-07	507 322	0 3073	1 79E-07
-19	-5.2E-08	-7 4E-05	1 48E-07	498 6644	0 3073	1 68E-07
-18	-4.8E-08	-7.3E-05	1 49E-07	491 582	0.3073	1 58E-07
-17	-4.5E-08	-7.2E-05	1 48E-07	483 6788	0 3073	1 48E-07
-16	-4 1E-08	-7 1E-05	1 48E-07	475 7609	0 3073	1 34E-07
-15	-3 8E-08	-7E-05	1 49E-07	469 238	0 3073	1 24E-07
-14	-3 4E-08	-6.9E-05	1 48E-07	461 2257	0 3073	1 08E-07
-13	-3E-08	-6.8E-05	1 48E-07	453 8347	0 3073	9 78E-08
-12	-2 7E-08	-6 7E-05	1 48E-07	445 5828	0 3073	8 64E-08
-11	-2.4E-08	-6 5E-05	1 48E-07	438 3031	0 3073	7 80E-08
-10	-1.4E-08	-6 4E-05	1 48E-07	431 7018	0 3073	4 50E-08
-9	-1 4E-08	-6.3E-05	1 49E-07	423 8015	0 3073	4 50E-08
-8	-1 4E-08	-6.2E-05	1 49E-07	416 303	0 3073	4 50E-08
-7	-1.4E-08	-6 1E-05	1 48E-07	408 8384	0 3073	4 50E-08
-6	-1 4E-08	-6E-05	1 48E-07	399 2874	0 3073	4 50E-08
-5	-1 4E-08	-5.8E-05	1 49E-07	386 5097	0.3073	4 50E-08
-4	-1 4E-08	-2.7E-03	1 48E-07	183 2456	0.3073	4 50E-08
-3	-1 4E-08	-9.8E-06	1 48E-07	65 70598	0 3073	4 50E-08
-2	-1 4E-08	-2.8E-06	1 48E-07	18 92712	0.3073	4 50E-08
-1	-1 4E-08	-5.8E-07	1 48E-07	3 894555	0 3073	4 50E-08
0	-1 4E-08	-8.6E-10	1 48E-07	0 004418	0.3073	4 50E-08
1	-1 4E-08	1.18E-06	1 48E-07	-7 89355	0 3073	4 50E-08
2	-1 4E-08	5.17E-06	1 48E-07	-34 8406	0.3073	4 50E-08

q = 1.60E-19 [C]
h = 6.63E-34 [J s]
c = 3.00E+08 [m/s]

MEASUREMENTS ARE DONE AT -2V BIAS, FULL Io.

dark [A] = -6.30E-05

wavel [m]	wavel [nm]	R [%]	a [1/m]	w [m]	Po [W]	v [Hz]	Ip [A]	QE	I [A]	I [uA]	M	Responsiti	NEP [W]
4.00E-07	400	0.4888	8.98E+06	1.08E-08	1.73E-07	7.49E+14	2.85E-08	0.5112	2.83E-06	2.630	99.19	0.1649	-3.82E-04
5.00E-07	500	0.3873	8.89E+05	1.08E-08	5.22E-07	6.00E+14	1.29E-07	0.6127	2.87E-06	2.865	22.21	0.2471	-2.55E-04
6.00E-07	600	0.3538	3.75E+05	1.08E-08	4.86E-07	5.00E+14	1.49E-07	0.6351	2.88E-06	2.876	19.26	0.3073	-2.05E-04
7.00E-07	700	0.3376	1.62E+05	1.08E-08	4.20E-08	4.28E+14	1.3E-08	0.5478	2.84E-06	2.840	218.63	0.3093	-2.04E-04
8.00E-07	800	0.3278	6.40E+04	1.08E-08	1.80E-08	3.75E+14	3.47E-09	0.3361	2.83E-06	2.827	814.75	0.2169	-2.90E-04

R @ 1.0QE	R @ 0.9QE	R @ 0.8QE	R @ 0.7QE	R @ 0.6QE	R @ 0.5QE	R @ 0.4QE	R @ 0.3QE	R @ 0.2QE	R @ 0.1QE
0.3226	0.2904	0.2581	0.2258	0.1936	0.1613	0.1290	0.0968	0.0645	0.0323
0.4033	0.3629	0.3226	0.2823	0.2420	0.2016	0.1613	0.1210	0.0807	0.0403
0.4839	0.4355	0.3871	0.3388	0.2904	0.2420	0.1936	0.1452	0.0968	0.0484
0.5646	0.5081	0.4517	0.3952	0.3388	0.2823	0.2258	0.1694	0.1129	0.0565
0.6452	0.5807	0.5162	0.4517	0.3871	0.3226	0.2581	0.1936	0.1290	0.0645

6.7.4 Raw Crosstalk Data

The following graphs are the raw crosstalk test results of the APD arrays. Only arrays exhibiting promising data were tested for crosstalk.

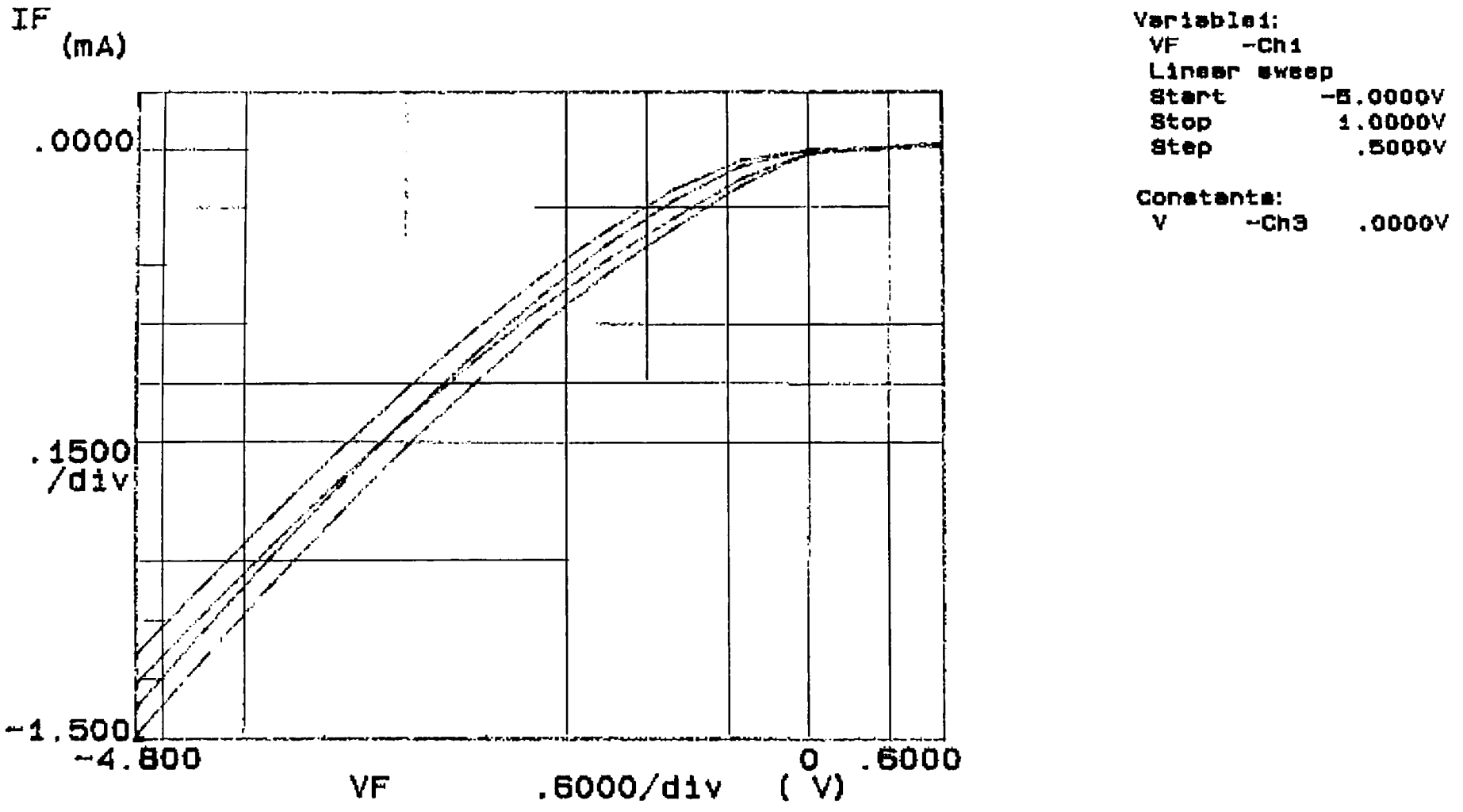
****** GRAPHICS PLOT ******
W1 C11, 10 D400 20, 750, N L1, 4
IF
(mA)
.0000
.1500
/div
-1.500
-4.800
0
.6000
VF
.6000/div
(V)
Variable1:
VF -Ch1
Linear sweep
Start -5.0000V
Stop 1.0000V
Step .5000V
Constants:
V -Ch3 .0000V

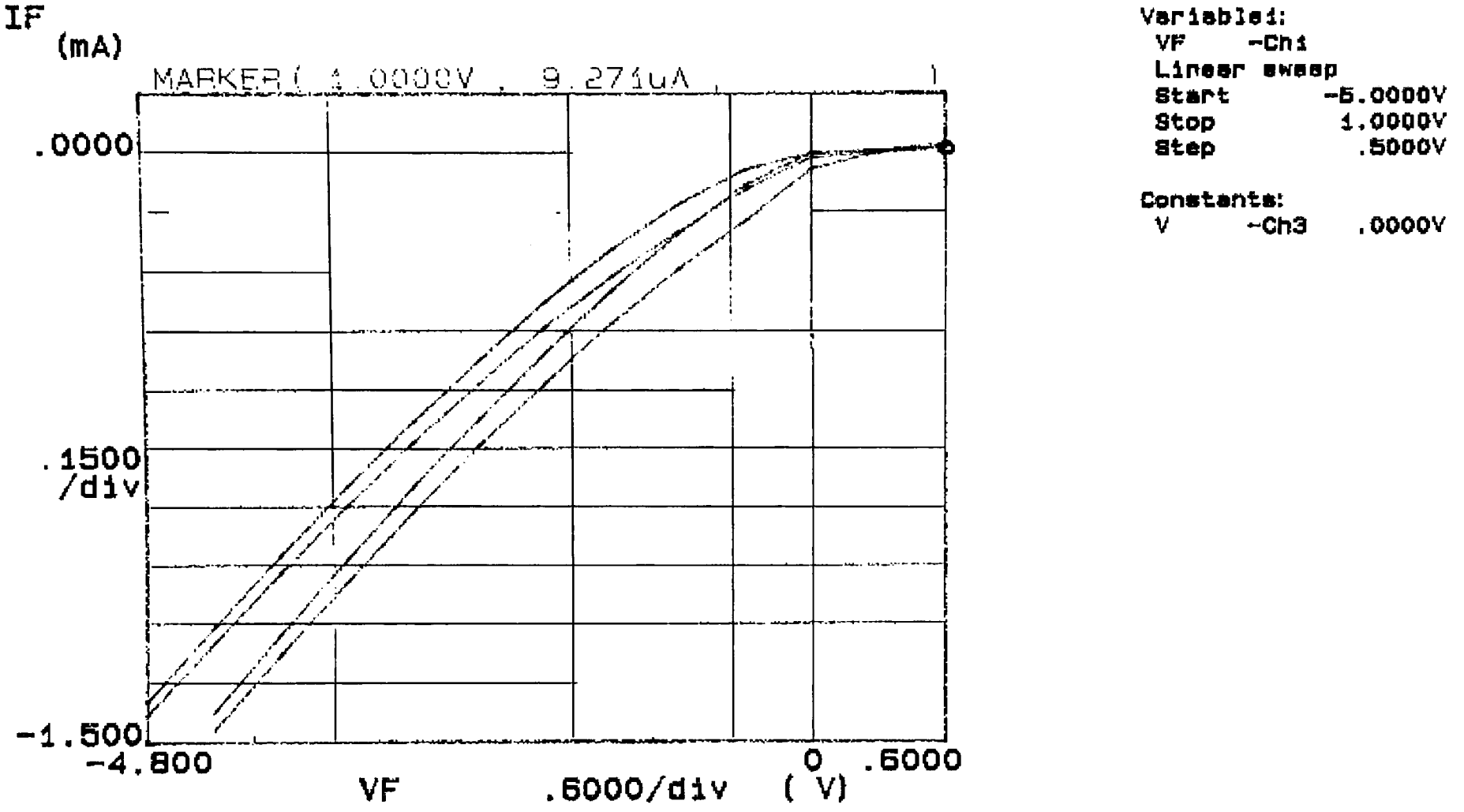
****** GRAPHICS PLOT ******
W1 C11,10 D400,20.750,N L2,4
IF
(mA)
MARKER(1.0000V , 9.271uA)
.0000
.1500
/div
-1.500
-4.800
0
.6000
VF .6000/div (V)
Variable1:
VF -Ch1
Linear sweep
Start -5.0000V
Stop 1.0000V
Step .5000V
Constants:
V -Ch3 .0000V

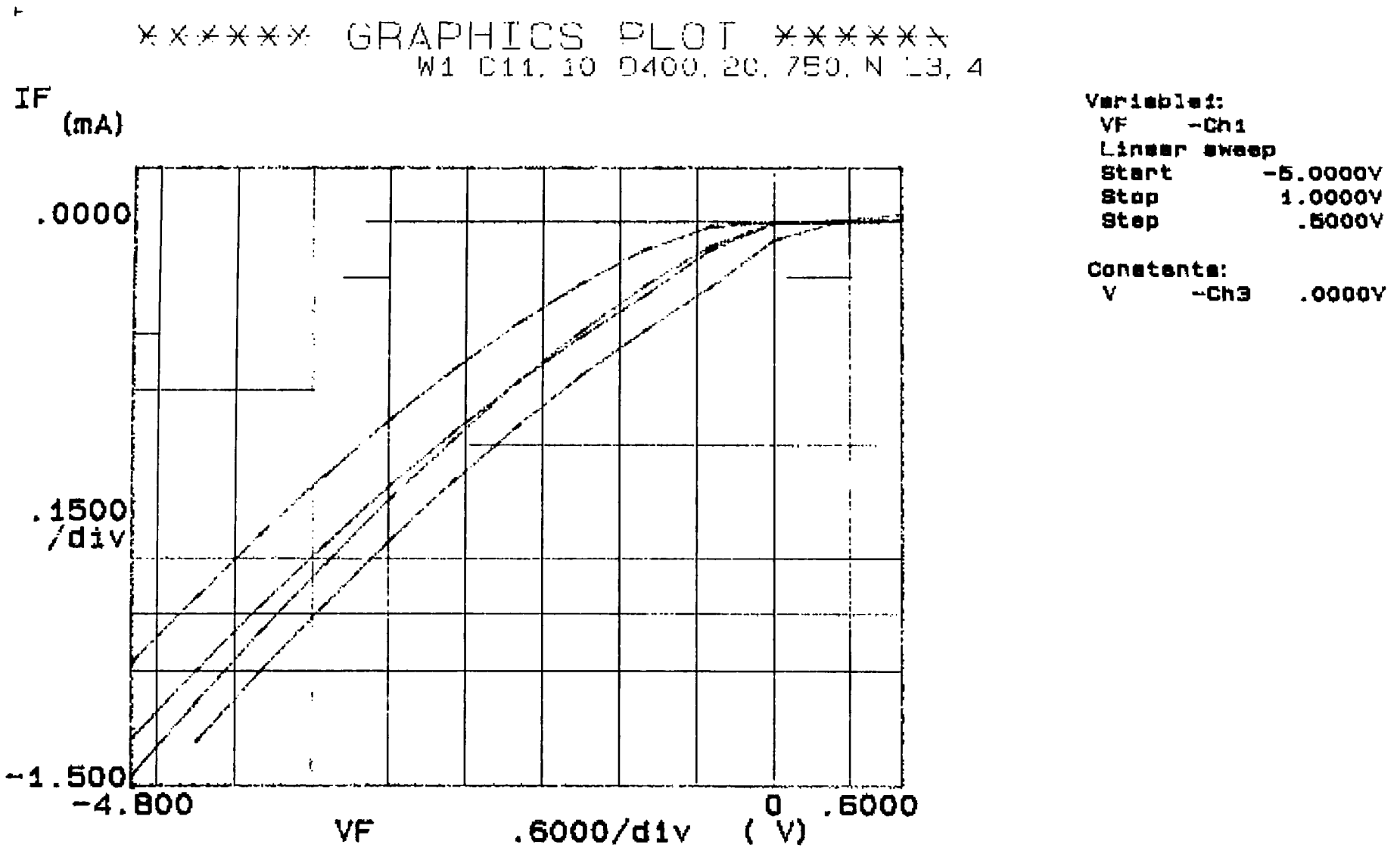
****** GRAPHICS PLOT ******
W1 C11, 10 D400, 20, 750, N L3, 4
IF
(mA)
.0000
.1500
/div
-1.500
-4.800
0
.6000
VF
.6000/div
(V)
Variable1:
VF -Ch1
Linear sweep
Start -5.0000V
Stop 1.0000V
Step .6000V
Constants:
V -Ch3 .0000V

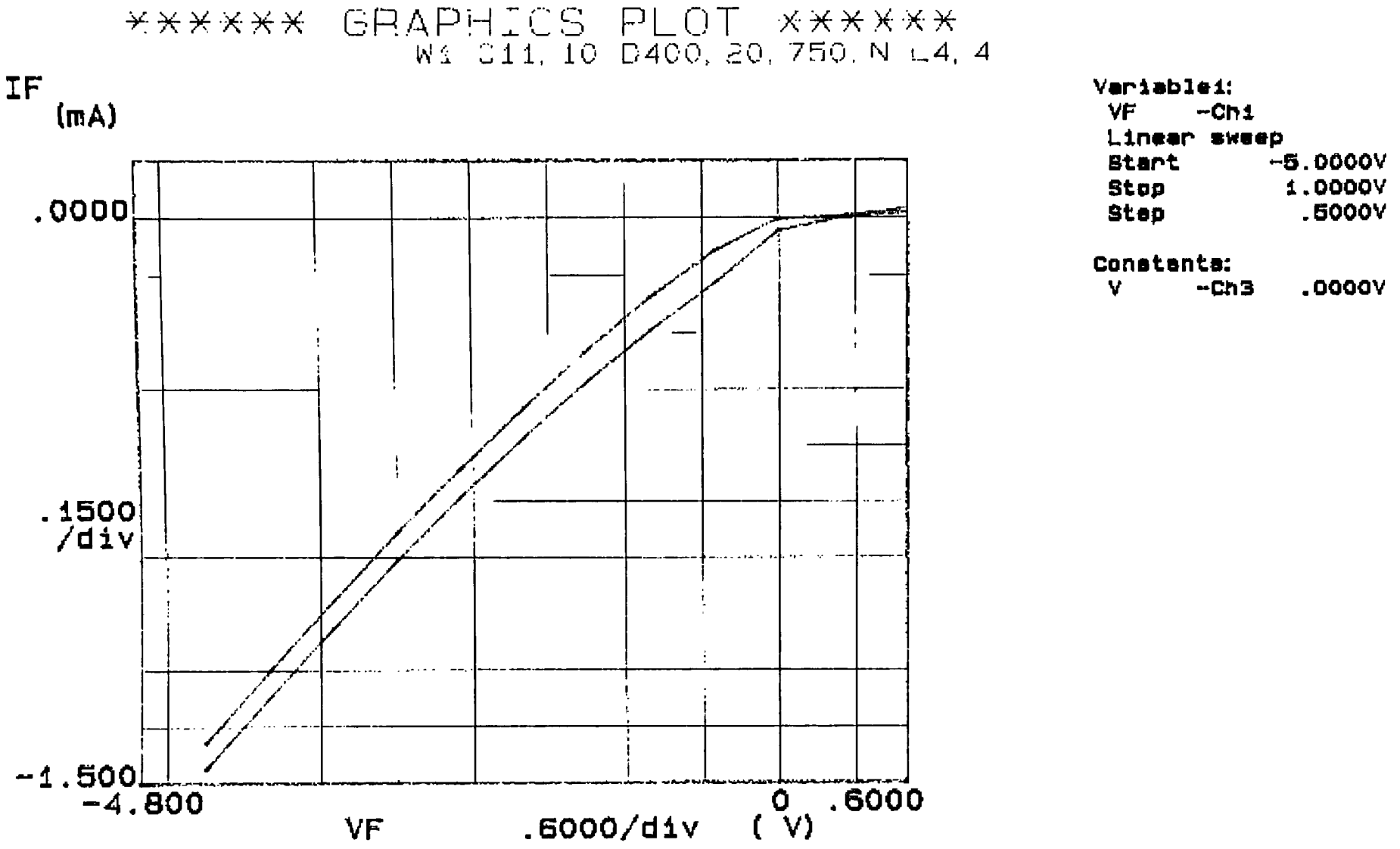
****** GRAPHICS PLOT ******
W1 S11, 10 D400, 20, 750, N L4, 4
IF
(mA)
.0000
.1500
/div
-1.500
-4.800
0
.6000
VF
.6000/div
(V)
Variable1:
VF -Ch1
Linear sweep
Start -5.0000V
Stop 1.0000V
Step .5000V
Constants:
V -Ch3 .0000V

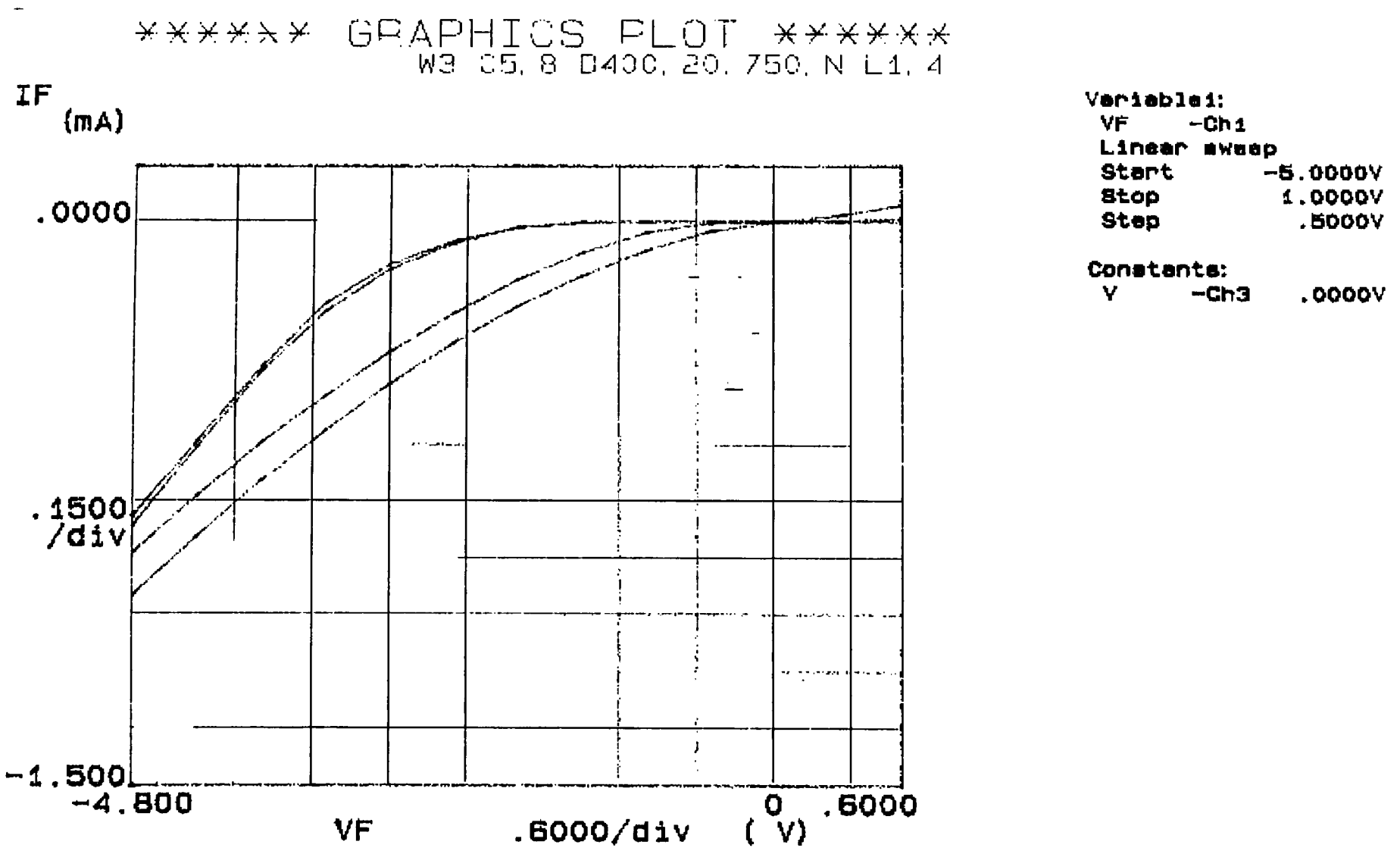
****** GRAPHICS PLOT ******
W3 C5, 8 D40C, 20, 750, N L1, 4
IF
(mA)
.0000
.1500
/div
-1.500
-4.800
0
.6000
VF
.6000/div
(V)
Variable1:
VF -Ch1
Linear sweep
Start -5.0000V
Stop 1.0000V
Step .5000V
Constants:
V -Ch3 .0000V

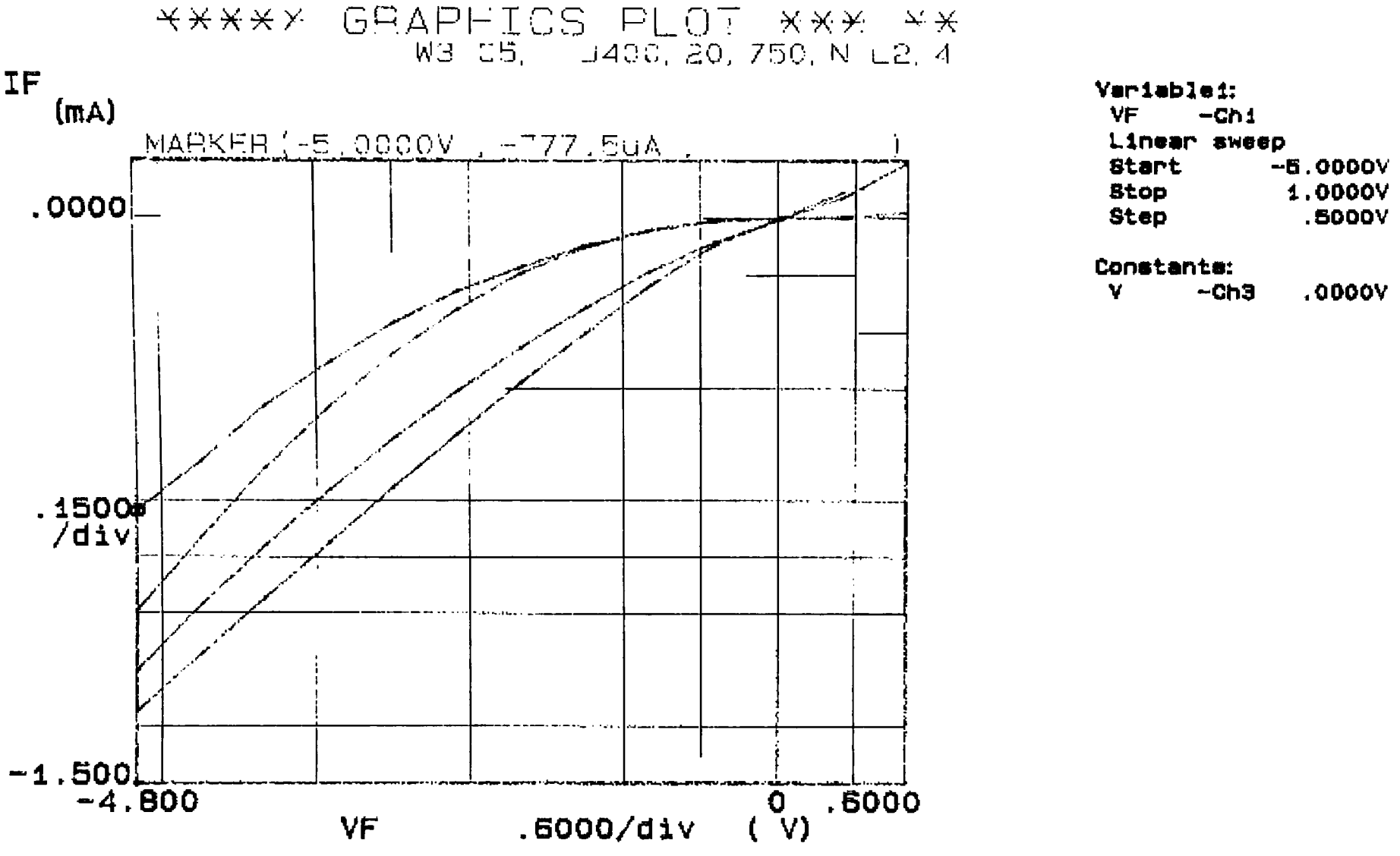
***** GRAPHICS PLOT *** **
W3 C5, J400, 20, 750, N L2, 4
IF
(mA)
MARKER (-5.0000V , -777.5uA ,
.0000
.1500
/div
-1.500
-4.800
0
.6000
VF .6000/div (V)
Variable1:
VF -Ch1
Linear sweep
Start -5.0000V
Stop 1.0000V
Step .5000V
Constants:
V -Ch3 .0000V

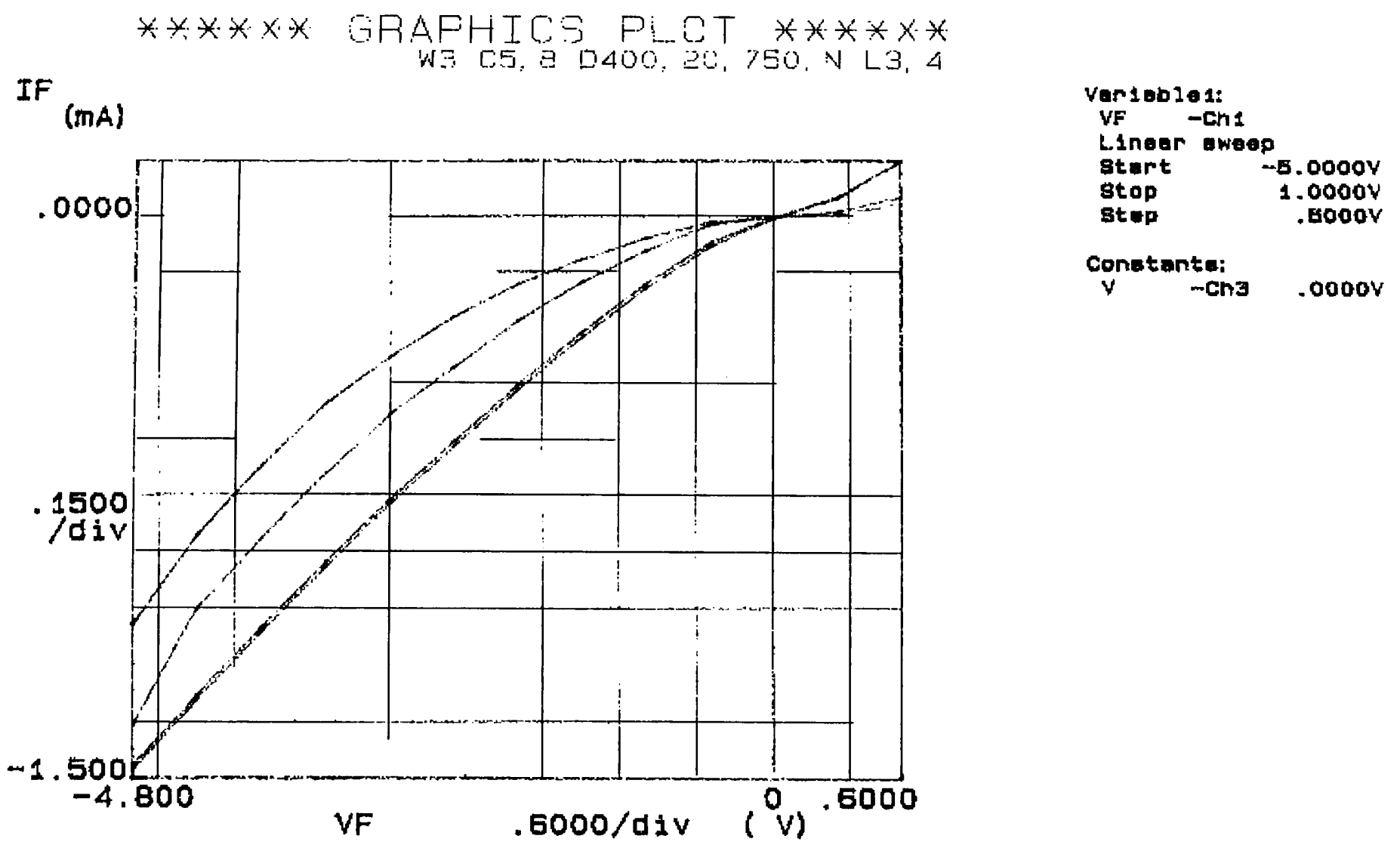
****** GRAPHICS PLOT ******
W3 C5, 8 D400, 20, 750, N L3, 4
IF
(mA)
.0000
.1500
/div
-1.500
-4.800
0
.6000
VF
.6000/div
(V)
Variable1:
VF -Ch1
Linear sweep
Start -5.0000V
Stop 1.0000V
Step .6000V
Constants:
V -Ch3 .0000V

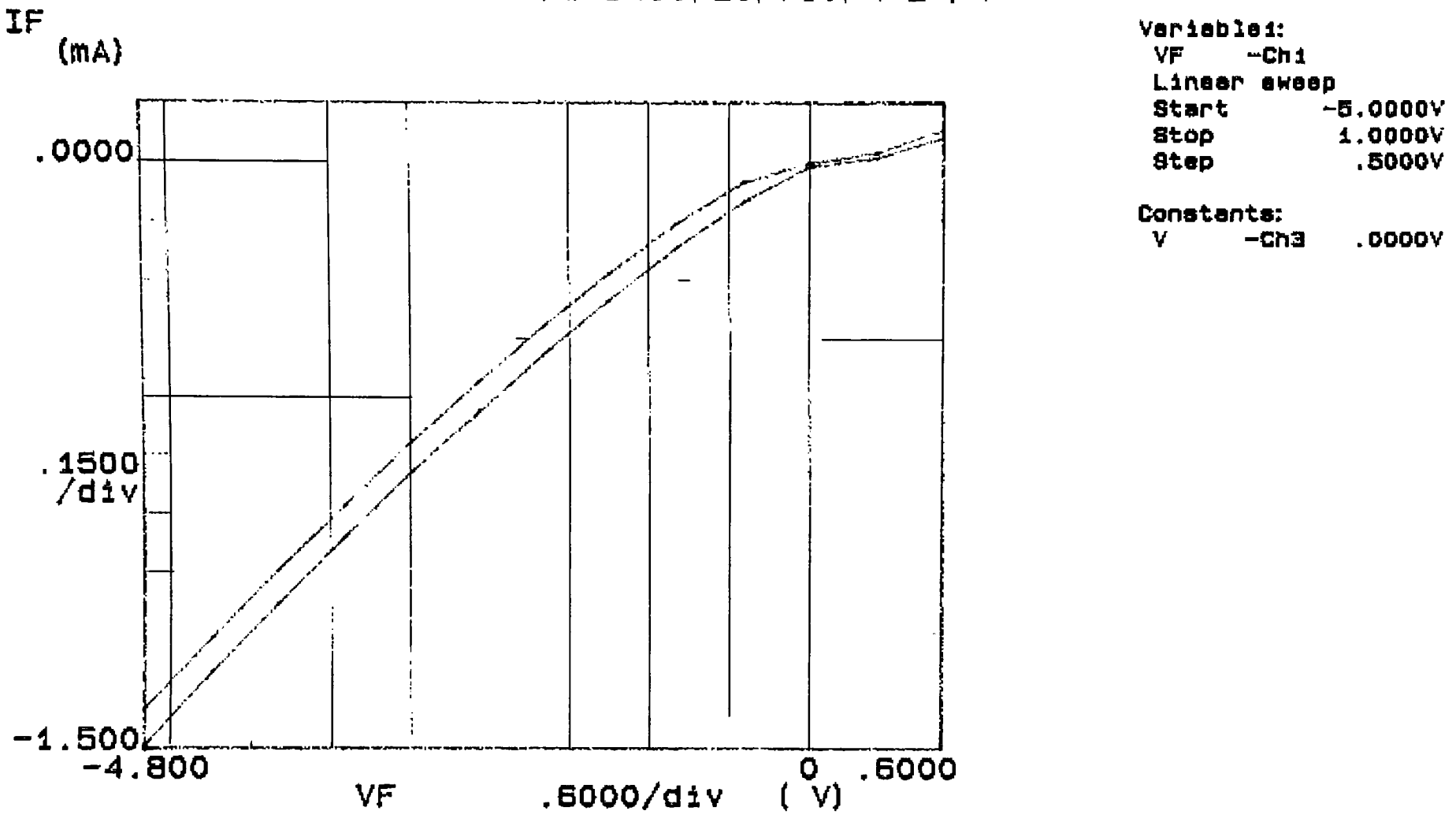
****** GRAPHICS PLOT ******
W3 C5.9 9400,20,750,N L4,4
IF
(mA)
.0000
.1500
/div
-1.500
-4.800
0
.6000
VF
.6000/div
(V)
Variable1:
VF -Ch1
Linear sweep
Start -5.0000V
Stop 1.0000V
Step .5000V
Constants:
V -Ch3 .0000V

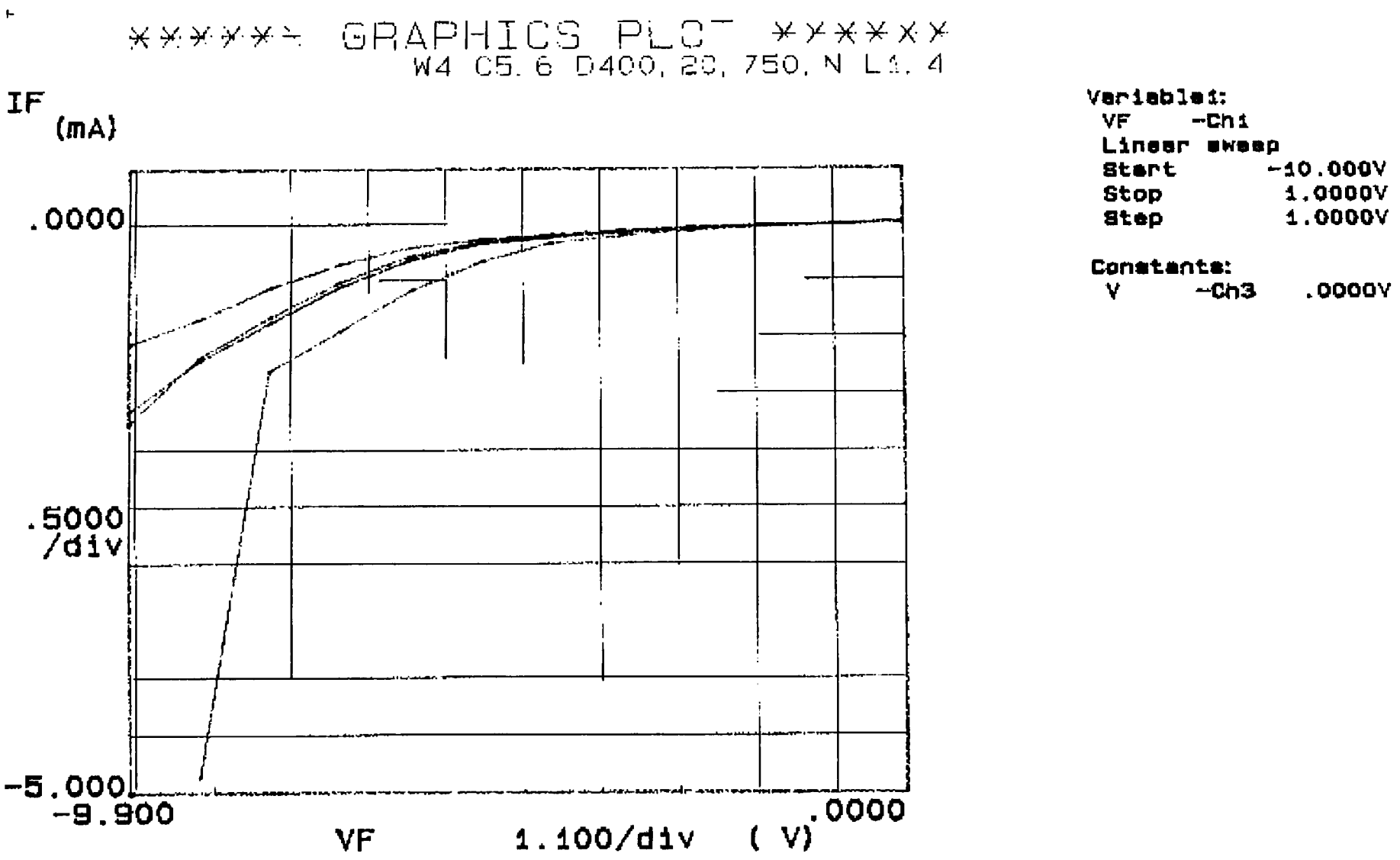
****** GRAPHICS PLOT ******
W4 C5.6 D400,20,750,N L1,4
IF
(mA)
.0000
.5000
/div
-5.000
-9.900
.0000
VF
1.100/div
(V)
Variable1:
VF -Ch1
Linear sweep
Start -10.000V
Stop 1.0000V
Step 1.0000V
Constants:
V -Ch3 .0000V

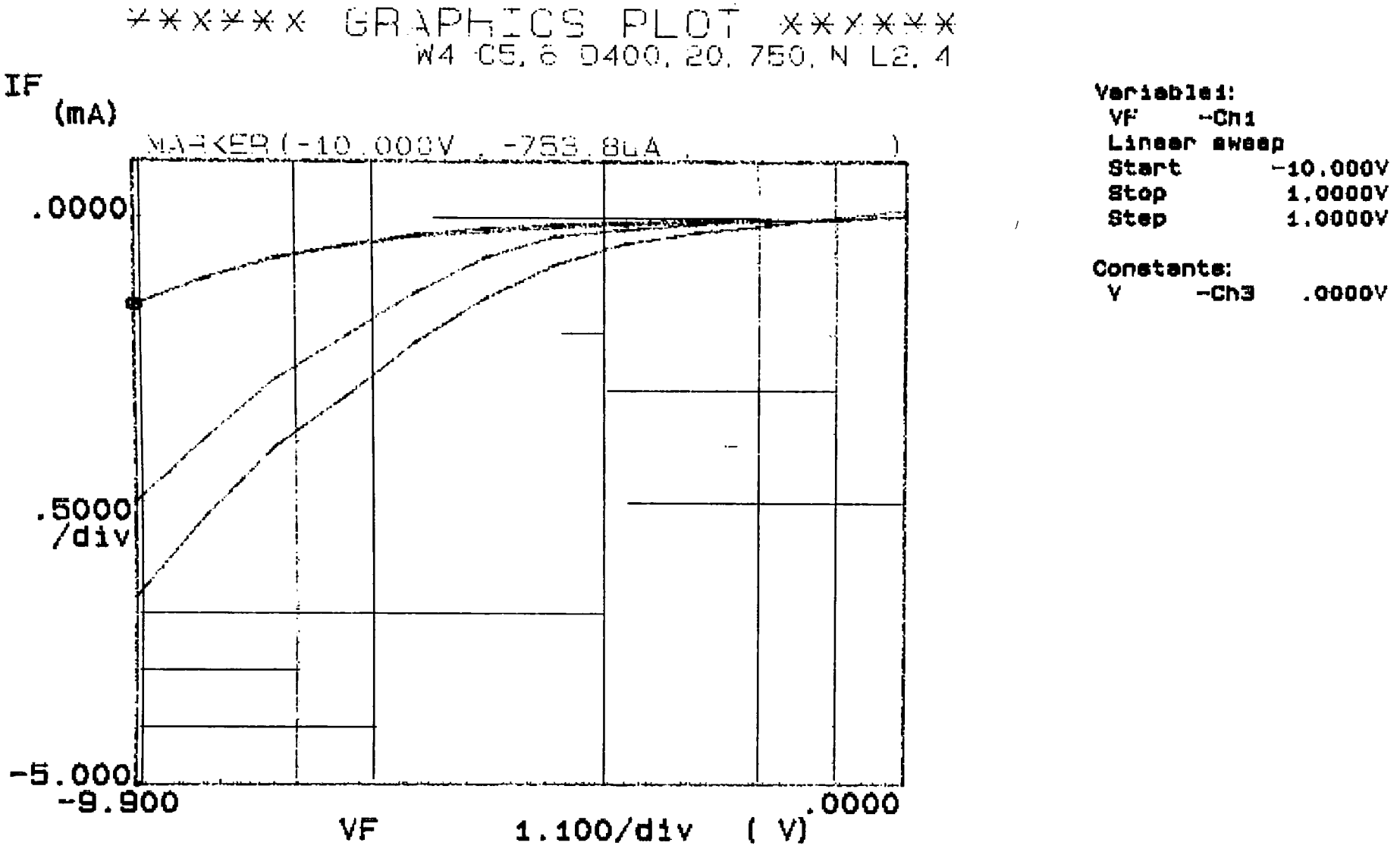
****** GRAPHICS PLOT ******
W4 C5,6 D400,20,750,N L2,4
IF
(mA)
MARKER(-10.000V , -753.8uA)
.0000
.5000
/div
-5.000
-9.900
.0000
VF
1.100/div
(V)
Variable1:
VF -Ch1
Linear sweep
Start -10.000V
Stop 1.0000V
Step 1.0000V
Constants:
V -Ch3 .0000V

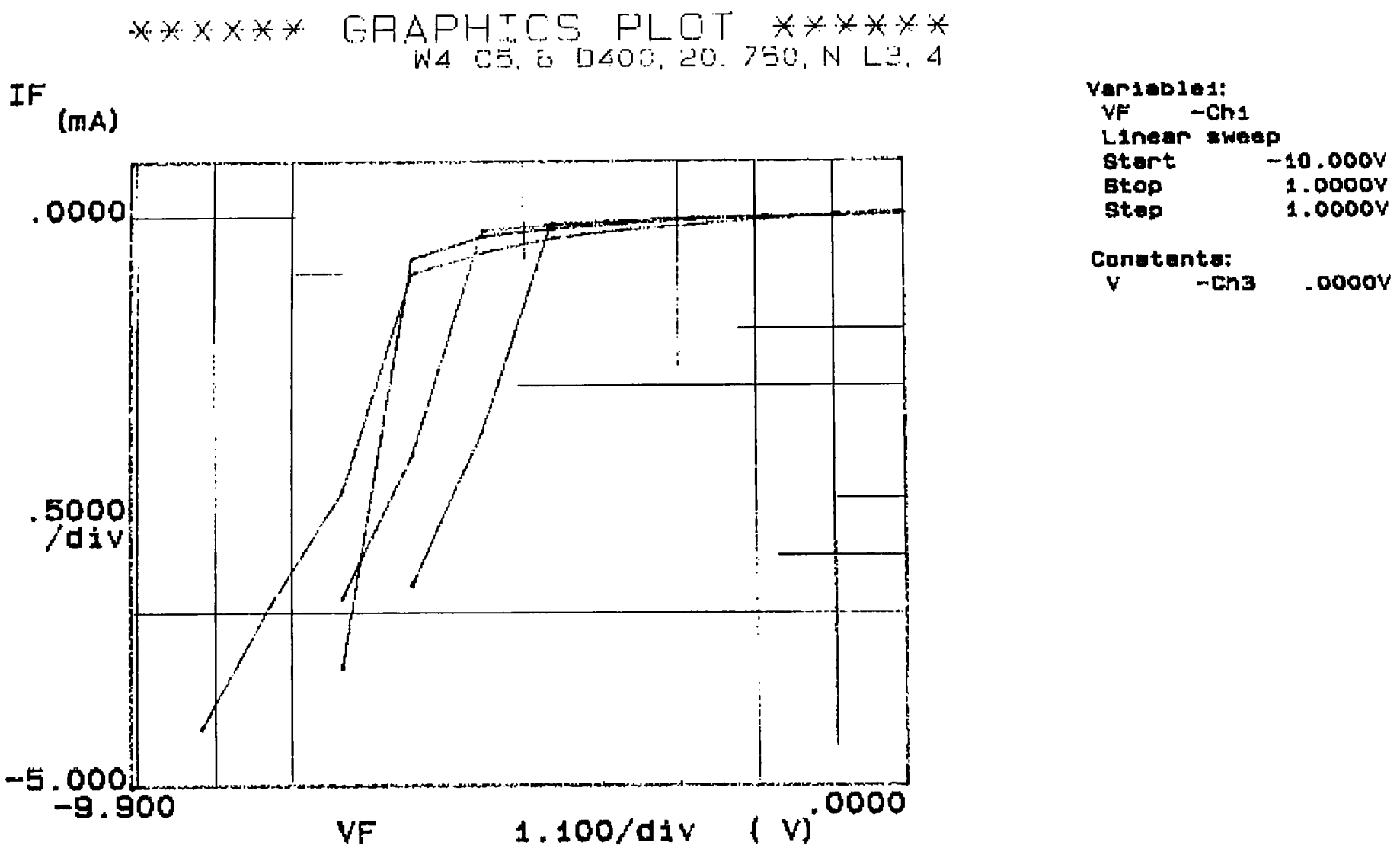
****** GRAPHICS PLOT ******
W4 C5, 6 D400, 20, 750, N L2, 4
IF
(mA)
.0000
.5000
/div
-5.000
-9.900
.0000
VF
1.100/div
(V)
Variable1:
VF -Ch1
Linear sweep
Start -10.000V
Stop 1.0000V
Step 1.0000V
Constants:
V -Ch3 .0000V

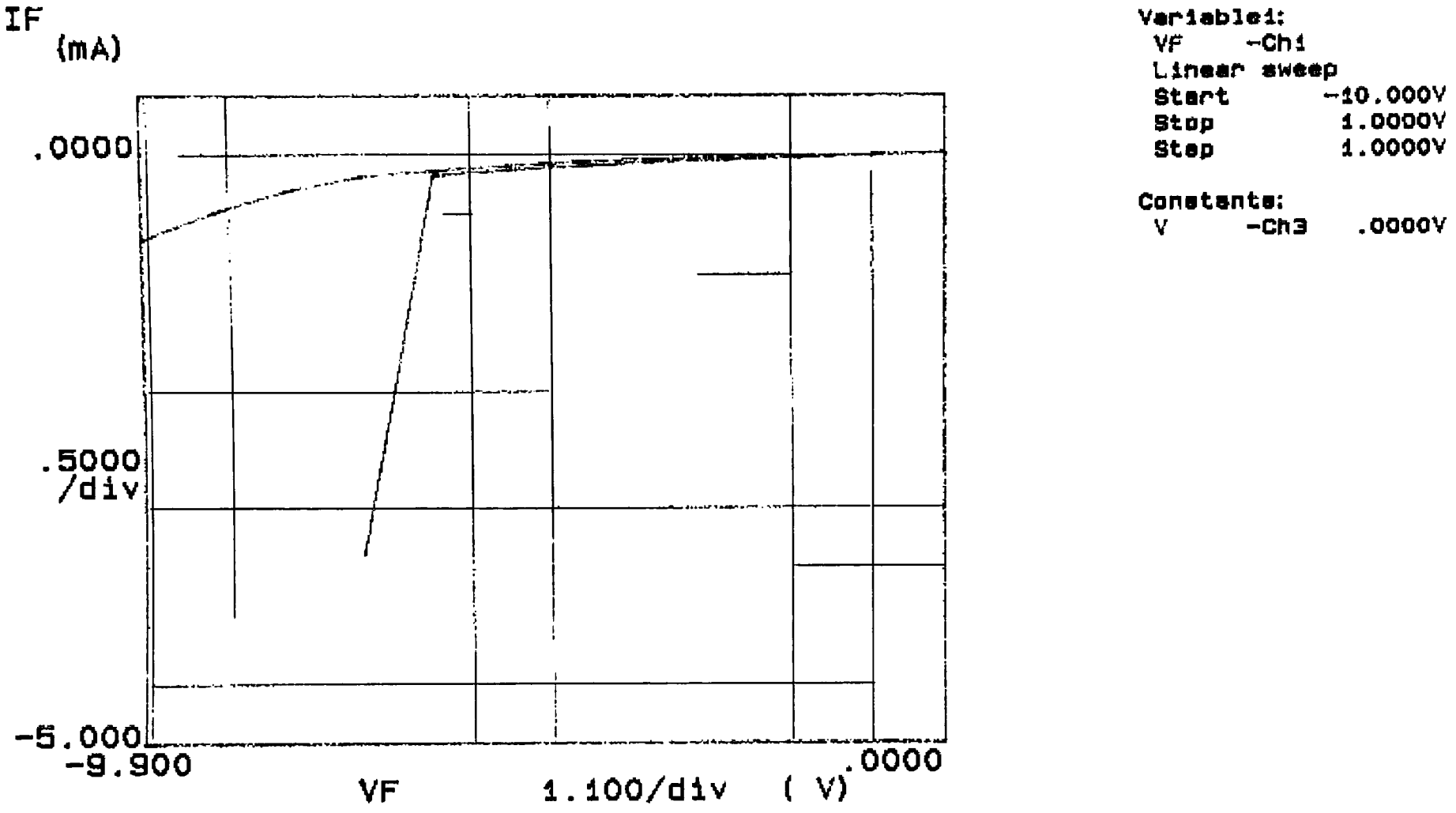

Variable1:
VF -Ch1
Linear sweep
Start -10.000V
Stop 1.0000V
Step 1.0000V

Constante:
V -Ch3 .0000V

6.7.5 Crosstalk Analysis of Selected Photodiodes

The following are crosstalk calculations of selected APD arrays.

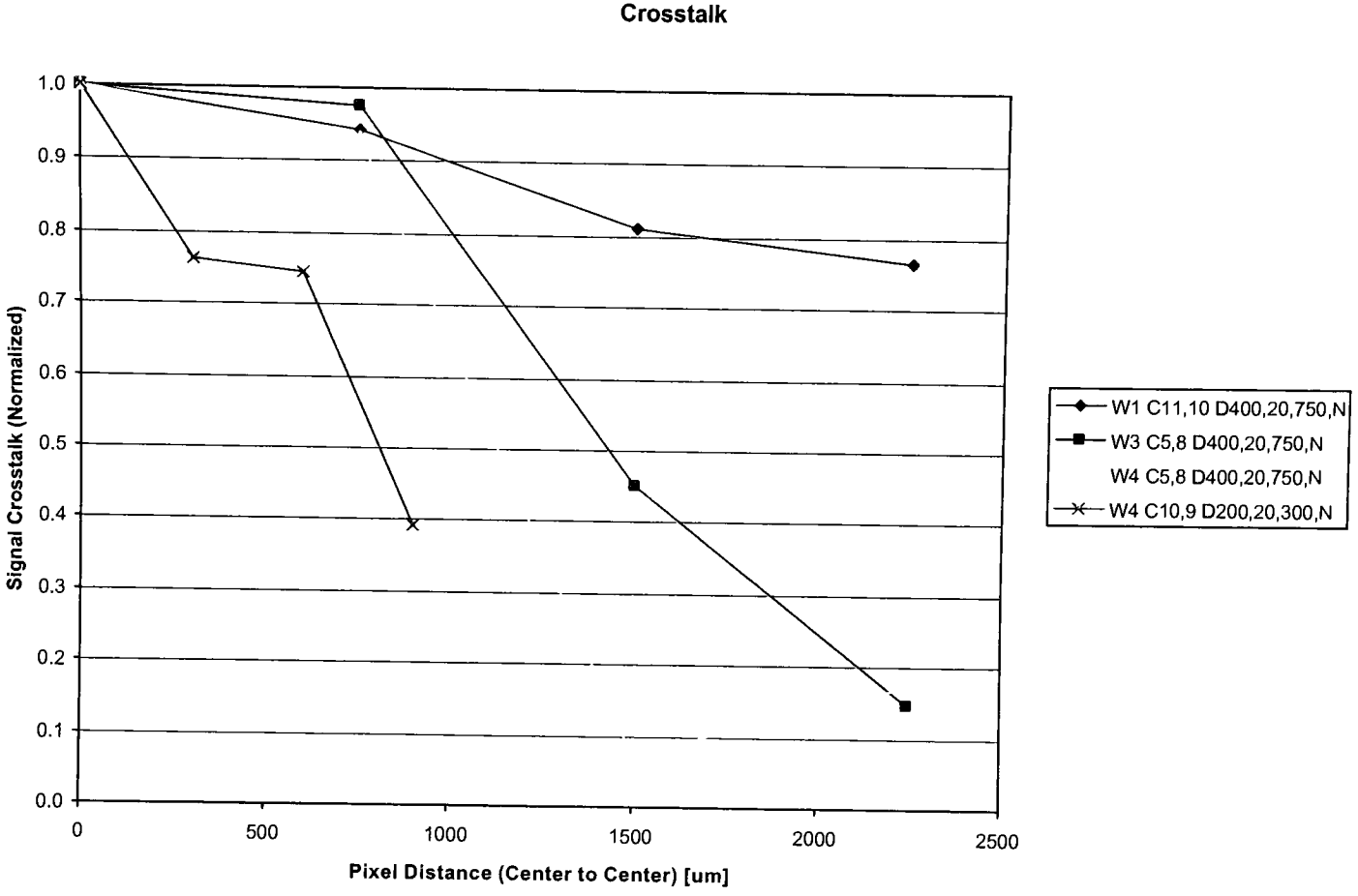
Crosstalk
Signal Crosstalk (Normalized)
1.0
0.9
0.8
0.7
0.6
0.5
0.4
0.3
0.2
0.1
0.0
0
500
1000
1500
2000
2500
Pixel Distance (Center to Center) [um]
W1 C11,10 D400,20,750,N
W3 C5,8 D400,20,750,N
W4 C5,8 D400,20,750,N
W4 C10,9 D200,20,300,N

Die: **W1 C11,10 D400,20,750,N**

Vbias: -3.0 [V]

Distance	P4 Off	P4 On	Signal Cr	Signal Crosstalk (Normalized)
0	-718.95	-907.5	1.262257	1
750	-718.95	-854.9	1.189095	0.942039
1500	-718.95	-734.8	1.022046	0.809697
2250	-718.95	-693.1	0.964045	0.763747

Die: **W3 C5,8 D400,20,750,N**

Vbias: -3.0 [V]

Distance	P4 Off	P4 On	Signal Cr	Signal Crosstalk (Normalized)
0	-470.575	-794.7	1.688785	1
750	-470.575	-774.4	1.645646	0.974456
1500	-470.575	-357.5	0.759709	0.449855
2250	-470.575	-114.6	0.243532	0.144205

Die: **W4 C5,6 D400,20,750,N**

Vbias: -9.0 [V]

Distance	P4 Off	P4 On	Signal Cr	Signal Crosstalk (Normalized)
0	-807.9	-7112	8.80307	1
750	-807.9	-6619	8.192846	0.930681
1500	-807.9	-519.6	0.643149	0.07306
2250	-807.9	-1208	1.495235	0.169854

Die: **W4 C10,9 D200,20,300,N**

Vbias: -9.0 [V]

Distance	P4 Off	P4 On	Signal Cr	Signal Crosstalk (Normalized)
0	-191.1	-398.9	2.087389	1
300	-191.1	-303.96	1.590581	0.761995
600	-191.1	-297	1.55416	0.744548
900	-191.1	-155.6	0.814233	0.390073

7. Bibliography

Cheung, N., "EECS143 Lecture #7", University of California Berkeley, 2003

Cova, S., Ghiono, M., Lacaita, A., Samori, C., and Zappa, F., "Avalanche Photodiodes and Quenching Circuits for Single-Photon Detection", Applied Optics, April 1996, Vol. 35, No. 12, p. 1956

Forrest, S.R., DiDomenico, Jr., M., Smith, R.G., and Stocker, H.J., "Evidence for tunneling in reverse-biased III-IV photodetector diodes", Applied Physics Letters, 1980, Vol. 36, p. 580

Kruger, A., "Photodiode Responsitivity", http://www.chipcenter.com/eexpert/akruger/akruger040.html, 2002

Laifer, E. and Gilad, E., "Zener Diode", http://www.hait.ac.il/staff/vagner/zener/content.html, 2002

MacGregor, A., "Silicon Avalanche Photodiodes for Low-Light, High-Speed Systems", Photonics Spectra, February 1991, p. 139

Matsushima, Y., Moda, Y., Kushiro, Y., Seki, N., and Akiba, S., Electronics Letters, 1984, Vol. 20, p. 235

McIntyre, R.J., "Multiplication Noise in Uniform Avalanche Diodes", IEEE Trans. on Electron Devices, January 1966, Vol. ED-13, No. 1, p. 164

McKay, K. and Chynoweth, A., "Photon Emission from Avalanche Breakdown in Silicon", Physics Review, May 1956, Vol. 102, No. 2, p. 369

Mitsubishi, "PD8042, PD8932 Datasheet", Mitsubishi Laser Diodes, November 1997

Pierret, R., "Semiconductor Device Fundamentals", Addison-Wesley Publishing Company, March 1996, p. 355

Proudfoot, C.N., "Handbook of Photographic Science and Engineering", IS&T, 1997, p. 127

Ridley, B.K., "Factors Affecting Impact Ionisation in Multilayer Avalanche Photodiodes", IEE Proceedings, June 1985, Vol. 132, No. J3, p. 177

Schroder, D.K., "Semiconductor Material and Device Characterization", John Wiley & Sons, 1990

Sze, S.M., "Physics of Semiconductor Devices, 2nd. Edition", John Wiley & Sons, 1981

Torres, M., Sandoval, M., and Lush, P., "EE3329 Study Guide", http://www.ece.utep.edu/courses/ee3329/ee3329/Studyguide/, 2002

Webb, P.P. and McIntyre, R. J., "Multi-Element Reachthrough Avalanche Photodiodes", IEEE Trans. on Electron Devices, September 1984, Vol. ED-31, No. 9, p. 1206

Wêgrzecka, I., Wêgrzecki, M., Grynglas, M., Bar, J., Uszyñski, A., Grodecki, R., Grabiec, P., Krzemiñski, S., and Budzyñski, T., "Design and properties of silicon avalanche photodiodes", Opto-electronics Review, 2004, Vol. 12, p. 95

Wolf, S. and Tauber, R.N., "Silicon Processing for the VLSI Era", Lattice Press, 1986, Vol. 1, p. 289

Zappa, F., "Solid-state single-photon detectors", Optical Engineering, April 1996, Vol. 35, No. 4, p. 938

Zeghbroeck, B.V., "Principles of Semiconductor Devices", http://ece-www.colorado.edu/~bart/book/, 2001